An Integrated Control System for Heating and Indoor Climate Applications

Tahersima, Fatemeh

Publication date:
2012

Document Version
Early version, also known as pre-print

Fatemeh Tahersima

An Integrated Control System for Heating and Indoor Climate Applications

An Integrated Control System for Heating and Indoor Climate Applications
Ph.D. thesis

ISBN: xxx-xx-xxxxx-xx-x
September 2012

Contents

Preface

This thesis, in form of a collection of papers, is submitted in partial fulfillment of the requirements for obtaining the Doctor of Philosophy degree in Automation & Control, at the Department of Electronic Systems, Aalborg University, Denmark.

The work has been carried out from September 2009 to September 2012, under supervision of Professor Jakob Stoustrup and Associate Professor Henrik Rasmussen.

The PhD project was defined as one of the work packages of an extensive university project called *Strategic Research Center on Zero Emission Building (ZEB)*. ZEB was partly funded by EUDP (Energy Technology Development and Demonstration Program in Denmark) and carried out as cooperation between Aalborg University, Danish Technical University, Danish Technological Institute, Saint-Gobain Isover A/S, Danfoss A/S, Dansk Byggeri, Velux A/S ans Dong Energy A/S.

Acknowledgments

I would like to express my gratitude to all people who helped me direct or indirectly in the course of the past three years and created an enjoyable peaceful working environment in Section of Automation and Control at Aalborg University.

I am especially thankful to my great academic advisors, Professor Jakob Stoustrup and Associate Professor Henrik Rasmussen with whom I experienced three years of inspirations and constructive technical discussions. A perfect combination of control theory and profound knowledge of control applications that I benefited a lot during this project.

I would like to express my gratitude to my industrial advisors Peter C. Andersen, Klaus L. Nielsen, and Peter G. Nielsen for their technical cooperation and facilitation. Thanks to *Danfoss A/S* and *Strategic Research Center for Zero Energy Buildings* that initiated this PhD project and partially financed it. Special thanks also to Peter Svendsen, Lars Hansen, Søren Østergaard Jensen, and Christian H. Christiansen in *Technological Institute* for their collaboration and patience in setting-up the experimental setup and during several months of running experiments.

I am always indebted to my dear parents and my beloved husband, Soroush whose encouragement, love and life-long genuine-companionship made this achievement possible.

Maryam
September 2012, Aalborg, Denmark

Abstract

Low temperature hydronic heating and cooling systems connected to renewable energy sources have gained more attention in the recent decades. This is due to the growing public awareness of the adverse environmental impacts of energy generation using fossil fuel. Radiant hydronic sub-floor heating pipes and radiator panels are two examples of such systems that have reputation of improving the quality of indoor thermal comfort compared to forced-air heating or cooling units. Specifically, a radiant water-based sub-floor heating system is usually combined with low temperature heat sources, among which geothermal heat pump, solar driven heat pumps and the other types are categorized as renewable or renewable energy sources.

In the present study, we investigated modeling and control of hydronic heat emitters integrated with a ground-source heat pump. Optimization of the system performance in terms of energy efficiency, associated energy cost and occupants' thermal comfort is the main objective to be fulfilled via design of an integrated controller. We also proposed control strategies to manage energy consumption of the building to turn domestic heat demands into a flexible load in the smart electricity grid.

We developed a simulation infrastructure for computer-based testing of the developed control methodologies. As the basis for components modeling, dynamical modeling of hydronic radiators controlled by thermostatic radiator valves is studied thoroughly. We have shown via analytical studies that a simply designed gain scheduling controller will overcome the well know instability problem of radiators which usually occurs in low heat demand conditions. We dealt with the problem as a dilemma between stability and performance. Since, controller parameters can be chosen such that the radiator works stable in the entire operation region, as a result the performance will become deteriorated during the cold season. To overcome the dilemma, an adaptive controller is designed analytically which satisfies both performance and stability at all operating points. The studied radiator model is further adapted to the modeling of the sub-floor heating system.

In order to minimize the electric power consumption of the integrated heating system, a novel hypothesis is proposed and further investigated via experimental and simulation studies. The idea is to minimize the forward temperature of hot water in order to maximize the heat pump's efficiency and by this means reduce the power consumption of the heat pump. The hypothesis is that such an optimal point coincides with saturation of at least one of the subsystems control valves. The idea is implemented experimentally using simple PI and on/off controllers on a real test setup i.e. a multiple room detached house in Copenhagen; the hypothesis is further investigated by designing a hierarchical control structure which uses model predictive controller (MPC) at the top level orchestrating single control loops at the lower level of control hierarchy. MPC is specifically chosen in order to embed measured exogenous disturbances e.g. comfort profile, weather forecast

and electricity price signals. Incorporation of the latter knowledge in the decision making enables the domestic energy consumer to act as a flexible load in the smart electrical grid to regain balance.

Synopsis

Synopsis Lavtemperatur hydroniske varme-og kølesystemer, forbundet med vedvarende energikilder har fået mere opmærksomhed på grund af den voksende offentlige bevidsthed om de negative miljøpåvirkninger fra energiproduktion ved hjælp af fossilt brændsel. Udstrlende hydrauliske varmerør under gulve og radiator paneler er to sådanne systemer, der har ry for at forbedre kvaliteten af indendørs termisk komfort sammenlignet med tvungen-luft varme-eller køleanlæg. Specifikt er et udstrålende vandbaseret sub-gulvvarmeanlæg en passende løsning, der skal kombineres med lavtemperatur varmekilder, blandt hvilke jordvarme pumper, soldrevne varmepumper og de andre typer er kategoriseret som helt eller delvist vedvarende energikilder.

I den foreliggende undersøgelse undersøgte vi modellering og styring af hydrauliske varmeafgivere integreret med en jord-varmepumpe. Optimering af systemet i form af energieffektivitet, energimæssig omkostningsminimering og beboernes termisk komfort er det vigtigste mål for den integrerede controller. Vi har også konstrueret kontrolstrategier til at styre energiforbruget i bygningen, således at varmebehovet udgør en fleksibel belastning i det intelligente elnet.

Som grundlag for komponenters modellering er dynamiske modeller af vandbårne radiatorer, der styres af termostatiske radiatorventiler, studeret grundigt. Vi har vist via analytisk undersøgelse, at en enkelt designet gain-scheduling regulator vil overvinde det velkendte ustabilitet problem af radiatorer, som normalt opstår under betingelser med lave varmebehov. Problemet behandles som et dilemma mellem stabilitet og ydeevne, da de forringede resultater ville opstå som følge af at vælge regulator parametre konservativt for at holde det i den stabile region i den kolde årstid. For at overvinde det dilemma, er en adaptiv regulering designet analytisk som tilfredsstiller både ydelse og stabilitet i hele operation somrdet. Den studerede radiator model er yderligere tilpasset til modellering af gulvvarmesystemet.

For at minimere det elektriske effektforbrug af det integrerede varmesystem, er en hidtil uprøvet hypotese foreslået, og yderligere undersøgt ved hjælp af forsøg og simulerede undersøgelser. Ideen er at minimere massen af fremløbstemperatur for at maksimere varmepumpens virkningsgrad og herved reducere effektforbruget af varmepumpen. Hypotesen er, at sådan et optimalt punkt falder sammen med mætningen af i det mindste et af delsystemernes reguleringsventil. Ideen er implementeret eksperimentelt ved hjælp af simple PI og on / off-controllere på et rigtigt test setup, dvs et flerværelses parcelhus i København. Den hypotese undersøges yderligere ved at designe en hierarkisk kontrolstruktur, som anvender model prædiktiv regulering (MPC) på øverste niveau som orkestrering af de lokale lukkede sløjfer på det lavere niveau af reguleringshierarkiet. MPC er specifikt valgt for at integrere målte eksterne forstyrrelser: f.eks komfort profil, vejrudsigt og elpris signaler. Sidstnævnte oplysninger giver private energiforbrugere po-

tentielt mulighed for at tilbyde en fleksibel belastning som middel til at genvinde balancen i elnettet.

List of Figures

List of Tables

1 | Introduction

1.1 Motivation: Integration of Building Services Systems

There are increasing interests in energy conservation and using renewable resources for power generation in both residential and commercial sectors. Adverse environmental impacts of using fossil fuel and shortages of theses supplies in few decades are pushing the global trend toward using renewable energy resources to turn them into the prime source of energy in the near future. Strategic Research Center on Zero Energy Building (ZEB) is a Danish research center established in 2009 at Aalborg University with the aim of developing new integrated low energy building solutions entirely based on extensive energy savings and renewable energy supplies [AU12a]. The research is divided into three Work Packages (WP) focusing on either component, system or concept, see Fig. 1.1 [AU12b]. This PhD thesis is meant to cover the first task out of the four in WP2 which deals with intelligent control of integrated building services systems in residential scale.

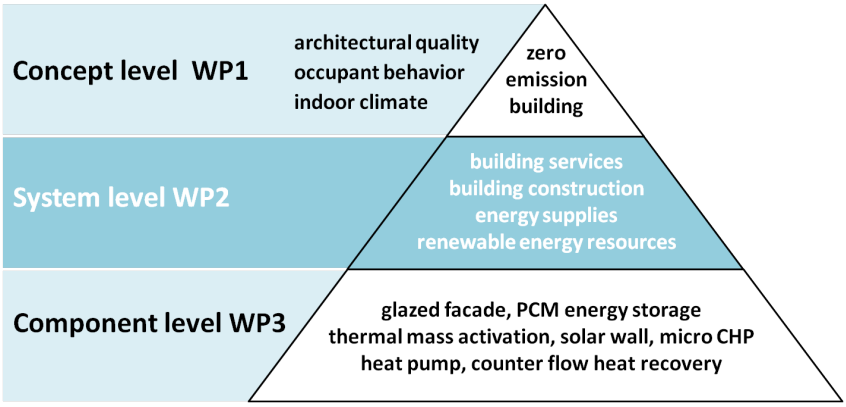

Figure 1.1: ZEB work packages

- **WP3** is dedicated and limited to development of intelligent building components as parts of the building construction and envelope system that are actively used for transfer and storage of heat, light, water and air.
- Development of integrated control strategies of the building services, renewable energy and other energy supplies, building construction and envelope systems is

the focus of **WP2**. Developments of new building services and renewable resources are limited to integration and control. A key aspect in development of new control strategies is the *real-life* testing possibility on a residential detached house, Energy Flex House which is developed by Technological Institute (TI) in Copenhagen, Denmark.

- The technical solutions of **WP2** and **WP3** will form the basis for development of new building concepts in **WP1**. Besides application of new technical solutions, the research of WP1 also focus on defining the future context of the building concepts including energy supply scenarios, user perspectives and behavior, architecture and indoor climate.

The center collaborates closely with the industry to deliver the necessary basis for long-term sustainable development in construction. The other academic and industrial partners of the research center are the Technical University of Denmark, Danish Technological Institute, Danfoss A/S, Velux A/S, Saint Gobain Isover A/S, and The Danish Construction Association, the section of aluminum facades.

The overall objective of WP2 is to rationally combine the building services systems with the construction, envelope and energy sources to reach an optimal environmental performance. Different levels of system integration and performance analysis for realization of the WP2 objectives are illustrated in Fig. 1.2. All the subsystems that are studied in separate PhD researches within WP2 are shown, among them those concerned in the present study are highlighted.

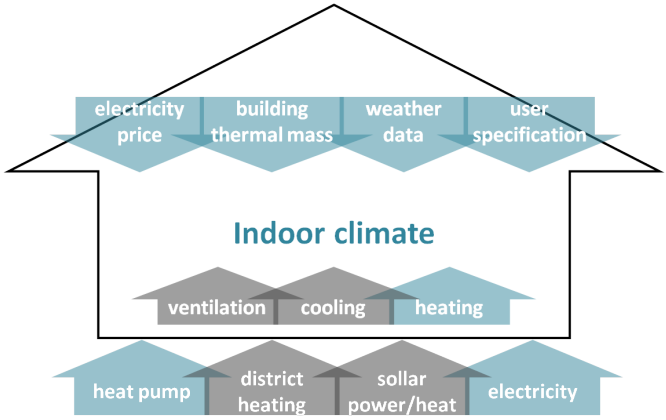

Figure 1.2: ZEB work package II. The highlighted blocks in blue compose the application of the thesis.

As depicted in Fig. 1.2, a combination of different Heating Ventilation and Air Conditioning (HVAC) subsystems might be available in a building to offer a perfect thermal comfort to the residents that directly influences their productivity and thermal satisfaction. HVAC subsystems have been regulated independently in the conventional control setups in spite of the strong cross correlation that might cause thermal dissatisfaction, performance degradation of the whole system and as a result energy inefficiency. The HVAC subsystems that condition the same space have to work in harmony with each other and

also with the specific building envelop system in order to preserve balance between energy consumption and thermal comfort. This goal is feasible via an integrated control strategy which takes into consideration all the influential dynamics and disturbances.

In this study, a combination of hydorinc heating systems with a heat pump that supplies hot water to the heating emitters are studied. Knowledge about weather data, electricity price, user preferences and the building thermal mass storage are included in the controller design procedure. In the following, a general overview of a hierarchical control system for indoor climate control is presented which provides the basis for the controller design in the thesis.

1.2 Indoor Climate Control Hierarchy

As discussed previously, a variety of subsystems might incorporate in the indoor climate conditioning. The participating subsystems, by their nature, might be competing, conflicting and/or complementing in combination with each other. For instance, two heating emitters that heat up a single zone (a space with the same temperature set point) would often compete, leading to a situation where one emitter is working almost always while the other seldom. Ventilation and a heating emitter in the same zone are examples of two conflicting subsystems. A heat source and a heat emitter are complementing while they can be controlled in two independent fashions, the interactions can not be ignored for the sake of stability and performance. Bearing in mind these interactions, buildings are multi-time scaled, complex multi-input multi-output systems with various exogenous disturbances. The closed loop performance of a such system is highly affected by the choice of a proper control structure.

Control of buildings indoor climate with many interacting subsystems by a centralized controller could be difficult due to the required inherent computational complexity, robustness and reliability problems [Sca09]. On the other hand, a distributed controller which distributes the regulation responsibility among partially linked control agents has great reliability and stability advantages. Although the resulting performance using a distributed control scheme might be suboptimal compared to the centralized approach, the alleviated computational complexity, higher reliability and stability are of great importance. In a distributed regime, fault diagnosis is much easier and the fault distribution through the whole system is less probable while it is usually the case for centralized controllers in a faulty situation.

A variety of distributed control structures have been developed over the past forty years for large scale complex systems, among them are decentralized, distributed (with exchange of information among local regulators) and hierarchical control structures [Sca09, Sil91, FBB$^+$80, HS94, MDT70]. Hierarchical controllers are very popular in the building systems control application.

A hierarchical control structure for plantwide optimization is customized for the application of building indoor climate control in Fig. 1.3. The overview shows a three-layer hierarchical control structure and the relevant information exchange corresponding to the building indoor climate control for energy and heating cost efficiency. The schematic is a modification of Fig. 1.1 in [Den10] i.e. based on a general framework introduced in [Sca09]. Relevant subsystems and layers of control hierarchy that we investigated in the thesis are highlighted in blue.

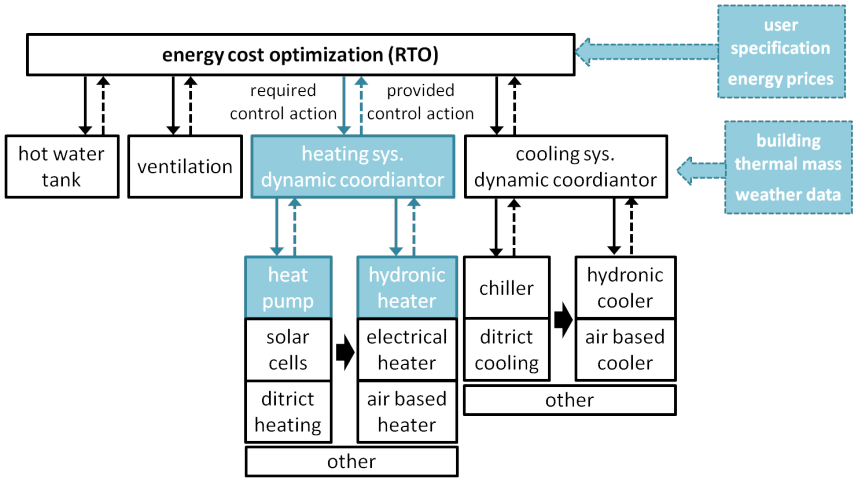

Figure 1.3: Vision of the overall climate control hierarchy. Focus of the thesis is highlighted in blue.

In the general setup, thermostatic controllers of heating/cooling emitters, at the component level, regulate a single zone's temperature, CO_2 or humidity. A specific energy source at this level is also controlled to supply the demanded heat/cool to the whole building. The upper level control agent generates top-down set point signals for the thermal comfort and the building energy demand to the corresponding local units such that both heat demands and energy optimization are fulfilled.

The dynamic optimal controller at the intermediate level provides the setpoint signals to the local units by solving a receding horizon optimization problem. The main objective of this controller is to minimize the energy consumption by optimizing the energy source performance via integration to the thermal emitters. Consideration of the building thermal mass and the weather data, in a receding horizon fashion, are essential for an acceptable performance especially when the building thermal mass is huge. Building thermal mass refers to the thermal capacity of the building mass structure, the large amount of heat/cool which can be stored in the building concrete floor, envelope and/or insulated water tanks. Heat can be buffered when it is cheap and available to be used later on when the power is expensive and less available. Weather data in the form of instantaneous measurements could be beneficial for feed forwarding control actions. However, foreseen weather data could be of great advantage for the controller to forecast heat demand and schedule for load shifting toward an optimal performance. The bottom-up information on constraints and performance and the top-down cost oriented signals on the heat/cool/ventilation demands incorporate into the decision making process.

Real time thermal demand signals are generated at the top level by solving an static or dynamic real time optimization (RTO) problem. RTO determines the thermal demand for the down stream units based on user thermal preferences and energy prices. This controller makes decisions basically on activating cooling or heating, produces economic thermal demand signal such that it meets the user specifications, and also controls directly the ventilation and the hot water tank.

Among the possible control architectures for the purpose of system integration, the chosen structure is flexible in terms of adding new subsystems to the component level. The goal of such control architecture is to encapsulate the specific properties and functionality of individual controllers at the actuators level toward a more generic interface with the intermediate level. The challenge is to describe the lower level subsystem properties such as saturation levels and dynamic ranges using a generic protocol that suits all lower level controllers [Den10]. Such generic interface links any newly added subsystem to the relevant intermediate level controller. The latter optimizes performance of the system in terms of minimum energy consumption and maintaining thermal comfort; The top level controller is responsible for integration of the building to the electricity grid. This design also prevents conflicting control actions for instance running both cooling and heating at the same time which wasts the energy and wears out the actuators due to fast switchings. Competing scenarios also can be considered and prevented by the intermediate coordinators.

Focus of the thesis at the component level is only on the heating systems, specifically on hydronic floor heating and hydronic radiators controlled by thermostatic radiator valves (TRV) that are combined with a heat pump. The upper levels, however, are merged in order to prevent model mismatch concerns between RTO and MPC as discussed further in the subsequent sections.

1.3 State of the Art of the Control System Structure

Deciding about the control system structure is an indispensable phase in design of any control system. In its simplest form, it consists of choosing what to measure and what to manipulate, and how to associate them to each other in a *pairing* process. Choice of the measured and manipulated variables depends on availability of suitable instruments and final control elements. In many cases, direct measurement or actuation is not possible due to technological or economical barriers. In such cases, target measurement variables are inferred from auxiliary measurements and intermediate calculations, e.g. static mapping. In this context, there are a number of classical strategies that specifically deal with situations in which either direct measurement or control is not possible or feasible: for instance the hot water flow rate is a variable whose measurement is costly and thus is estimated instead. These strategies make the building blocks of larger control system architectures and are reviewed in the sequel.

1.3.1 Classical Compounds

Classical control methods are still popular in industrial control applications. These classical components have been dominantly used in indoor climate control for regulating temperature, humidity and other influential factors on the residents' thermal comfort. We also employed proportional integral (PI)-based controllers as the basic building blocks of the control structure. An adaptive PI controller is designed for regulation of flow rate passing through radiator valves. Some of the classical control components are reviewed.

1.3.1.1 Feedforward Control

In most existing solutions, feed-forward control is used in combination with simple SISO feedback loops. It could be implemented when an extra measured variable is available. Actuation will be provided by the actuator of the SISO feedback loop. In other words, the simplest case of a feed-forward feedback system consists of two measuring devices and one actuator. The extra measurement comes from a known source of input disturbance that cannot be prevented, yet is measurable. For example, ambient temperature inevitably affects indoor heating control systems, but if it is measured while influencing the system, *proactive* action can be taken to compensate its *anticipated effect* on the main measured output. Fig. 1.4 illustrates a simple feedback loop and addition of the feed-forward path.

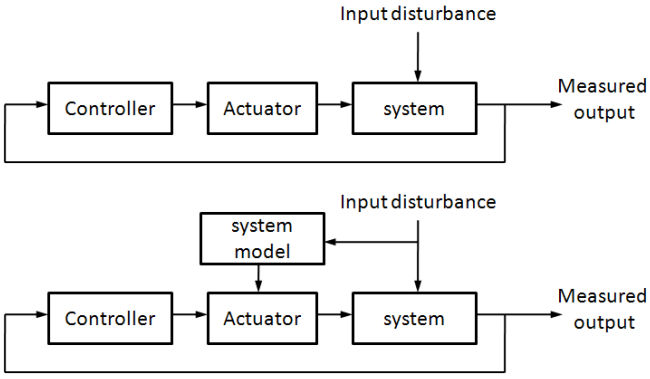

Figure 1.4: Addition of feed-forward path to a SISO feedback loop

An effective feed-forward design is the one that can accurately anticipate the effect of the measured disturbance on the measured output. Therefore, it is highly dependent on accuracy of the plant model. The feed-forward path simply tries to synthesize the effect of the measured disturbance on the measured output. Then it utilizes the actuator such that the disturbance effect is canceled out by subtraction. Therefore, although model accuracy is vital in usefulness of the feed-forward path, an improper design will not result in catastrophic results such as instability. In worst case, it adds a constrained error that can be compensated by the feedback loop. This has made feed-forward a popular control strategy wherever feasible.

One of the application examples of this method is adjusting forward temperature of hot water in a building hydronic distribution circuit. The ambient temperature is feed forwarded to the relevant controller of the hot water supplier. We have compared the proposed method of this thesis with the feed-forward control i.e. the commonly applied method to hot water temperature regulation of heat pumps.

1.3.1.2 Cascade Control

Another strategy that uses one or more extra measurement signals, or equivalently utilizes only one actuator with the data provided by more than one sensor is cascade control. Unlike feed-forward, in cascade control all of the measured signals are wired out from the process itself. Neither of them is fed from exogenous inputs. The philosophy is

however similar to feed-forward control in sense of devising a proactive action on the most important measured variable. Cascade control finds application in processes with large time lags and slow dynamics which have measurable intermediate process variables between a desired setpoint and the output measured variable. Extra measurements come from those intermediate variables which give an indication of how things are going on inside the process. By monitoring these intermediate points and correcting control action on the single actuator situated in the beginning of the process chain, it is possible to have a tighter control on the main measured output at the end of the chain. In absence of intermediate variables, effects of the control signal are only revealed when it influences the output measurement at the end of the chain. Fig. 1.5 illustrates addition of extra measurements to make a cascaded structure.

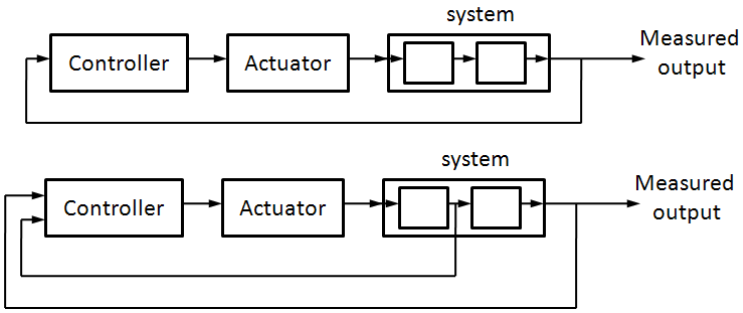

Figure 1.5: Addition of extra measurements to a SISO feedback loop to make a cascade loop

Since cascade control is implemented by feedback paths, design of the preventive actions is not critically dependent on accuracy of the plant model. However, contradicting control actions should be avoided. As an example, use of integrators to eliminate steady state error in intermediate measurements is a typical mistake because it can result in saturated control signals which try to overcome each other. At the end, only control performance of the output measured variable is important and the auxiliary variables need not to follow a specific setpoint. Last but not least, cascade control is most useful when the intermediate probes are evenly divided alongside of the time-lags of the process under control. If there is only a fast dynamic between the intermediate point and the output measured variable, there is not much to do because the effect of the current control signal affects the output variable shortly after being evaluated at the intermediate point.

A system of sub-floor heating pipes casted into a heavy concrete floor is an example of such systems that benefits from cascade control strategy greatly as studied in [Den10]. Part of the thesis addresses the difficulty of controlling indoor temperature using a heavy sub-floor heating system with long time lags. It proposes to use a cascade control with the inner loop controlling the estimated concrete temperature. The results show a much better performance controlling based on only room temperature measurement.

1.3.1.3 Split-range, Mid-range, & Ratio Control

After studying structures that enjoy more measurements than actuations, it is time to look into the other side: one measurement signal and two or more actuations mainly due to insufficiency of the control action provided only by one actuator. Also, it could be due to the system specific structure: for instance, in the case study of the thesis, indoor temperature is controlled by two manipulation variable i.e. the flow rate and temperature of hot water passing through the hydronic heat emitters.

In practice, some actuators are limited to provide a unilateral control action. For example, a heater can only heat and not cool. Therefore, if a temperature control system needs both cooling and heating, two different actuators are needed. In controller design, special attention is required for the area that one actuator is deactivated and the other one is started. Use of dead-zone in order to prevent conflicting action is a typical solution which adds nonlinearity to the system. In another scenario, the actuators are similar, but are different in size or capacity. An example could be flow control with two parallel valves of different capacities. While the larger valve provides the major portion of the flow, *fine tuning* is done by the smaller valve. In such cases, the fine tuning actuator is paired with the measured variable and the coarse tuning actuator uses the control signal of the fine tuning element as its measured variable. The objective of the coarse tuning element is guaranteeing effectiveness of the fine tuning element by preventing it from being saturated. This could be done via optimization either by treating the control signal of the fine tuning element as an objective function with its zero cost associated to the mid-range of the fine tuning element, or by constraining the control signal between minimum and maximum values and implementing a constrained optimization. Another case is where neither of the actuators can directly affect the measured variable, but their combination can. A typical example is where the measured variable represents concentration of a material in a mixing process. In such cases, the *ratio* between two control signals affects the measured variable. Hence, use of two separate physical actuators is necessary.

1.3.1.4 Selector & Override Control

This section is not about different number of sensors or actuators. Instead, it introduces different control logics which can be activated based on operating conditions of the system. Such logics are originated from safety requirements of control systems. Although safety control systems is the subject of recent standardization in automation industries under *safety instrumented systems (SIS)*, and usually require dedicated measuring and actuating elements to guarantee a quantified level of availability in terms of *safety integrity level (SIL)*, classical approaches consist of *selecting* between different sets of control algorithms based on the measured values or *overriding* the normal control commands in abnormal or emergency situations.

1.3.2 More Complex Architectures

When it comes to combining various elements in control systems with linear and nonlinear models to build up large systems for fulfilling some overall performance criteria, *implementation* in automation industry is much ahead of *analysis* among scientists. While high-tech industries like aviation that enjoy exact and accurate modeling benefit most from control theories, process control contains many elements that are simple in action

but complex in modeling which void many control theories, especially theories of linear systems. Therefore, in the following, we will introduce the industrial concept, namely *The Automation Pyramid*, followed by three different academic interpretations of different implementation architectures. Lack of an integrated analysis tool or method is notable when it comes to complex interconnected systems.

1.3.2.1 The Automation Pyramid

The automation pyramid or the Purdue Reference Model (PRM), introduces a hierarchical architecture for the overall control system within process industries. It was originated in 1980s and was the basis for standardization of manufacturing and production management from field level dealing with sensors and actuators to enterprise level where managerial decisions are taken. Fig. 1.6 shows a typical representation of the automation pyramid.

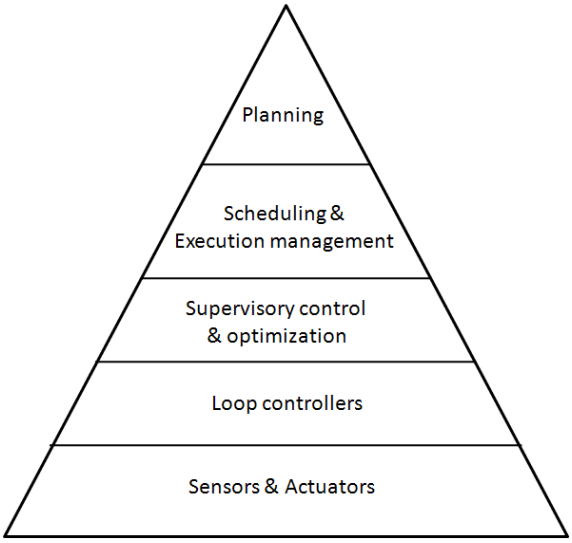

Figure 1.6: The automation pyramid

The top level, *Enterprise Resource Planning (ERP)* is mostly fed by data from the market of the associated industry. For example, in petrochemical industries price of different products could lead into change of production plans to maximize profit and stabilize the market. Change of production plan, requires scheduling new activities and executing some operations. Such activities are usually done with software packages that are said to comprise the *Manufacturing Execution System (MES)* level of the automation pyramid.

The most interesting layers for control design are the three lower layers. The lowest layer is basically the set of chosen measuring and actuating devices besides the signaling method which refers to the wiring or the industrial network which is utilized to transmit data between field level equipments, including sensors, actuators, and controllers. The second lowest layer comprises of field level controllers. They collect data from sensors and send commands to actuators. Field level controllers can be physically placed in a

central location or distributed in different places. A combination of both is quite usual. Orchestrating of field level controllers is done in the supervisory control level which monitors performance measures for individual controllers and can change effective parameters of controllers including individual setpoints. Supervisory control systems interact with the MES layer by preparing compact performance reports and accepting high-level commands. The main point in the hierarchical structure of the automation pyramid is the unavailability of components of a layer to other components which cannot be placed in the neighboring layer. For example, a supervisory control system does not directly control an individual actuator. In other words, levels of authority are separated in the automation pyramid. Note that a supervisory control system, in context of the automation pyramid, is different from a computer control system which is connected to remote I/O via a high bandwidth field-bus. Such a system is categorized as field level controller. In the following, a formal classification of different architectures in the two lowest levels is offered. Although the classification can be found in the literature of control theory, it is clearly originated from the concept of the automation pyramid.

1.3.2.2 Decentralized Control Systems

When different field-level controllers operate independently, a decentralized control system is formed. Data from a sensor can be reported and used in more than one controller unit, but each actuating element is linked to one of the controllers. Each controller unit in this architecture seeks its own individual performance measure. Careful design is essential to prevent contradicting actions or scenarios which lead to waste of energy or even damage to asset or personnel.

A decentralized control architecture is shown in Fig. 1.7. Two subsystems in the figure are S_1 and S_2 with states, input and output variables (x_1, u_1, y_1) and (x_2, u_2, y_2) respectively. Interactions between the two subsystems are caused by mutual effects of the internal states. Subsystems have to be defined such that interaction between them are weak, and by this mean the design of individual controllers would be trivial. In contrary, a strong interaction between different input, output or state pairs can prevent achieving stability and/or performance [Sca09].

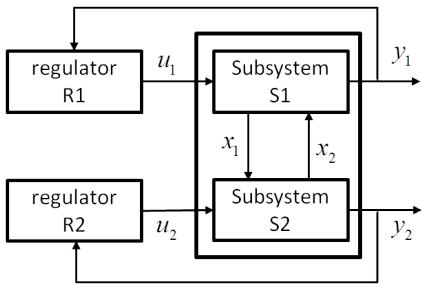

Figure 1.7: Decentralized control [Sca09]

1.3.2.3 Distributed Control Systems

If data is transmitted between individual controllers in order to have a coherent operation, distributed control architecture is implemented. In practice if the controllers are physically separated, data transfer is done via the supervisory control layer and a coordinating algorithm.

Data transfer between two regulators in Fig. 1.8 could be input or state types. If the exchanged data is the state or system evolution in the case of predictive controllers, any local regulator needs to know the dynamics of the subsystem directly controlled. However, if future control actions are transmitted each regulator have to know the dynamics of all the subsystems. In any case, the transmission protocols have a major impact on the achievable performance [Sca09].

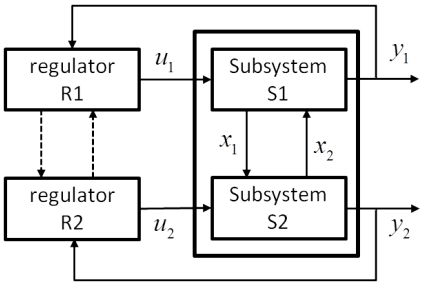

Figure 1.8: Distributed control [Sca09]

1.3.2.4 Hierarchical Control Systems

Hierarchical control is a direct adoption from the automation pyramid. Separation between the supervisory high-level control and sensors and actuators by the layers of local controllers is a key property of hierarchical control systems. Another characteristic is the difference in size and frequency of the transferred data between: 1) field-level instruments and field-level controllers, and 2) field-level controllers and supervisory controllers. While the former requires low cycle times with lots of small data packets sent from sensors to controllers and sent to actuators from controllers, the latter usually employs less frequently data transmission among controllers with more data-rich transmissions. This is in accordance with the general data transmission in the automation pyramid which follows a pattern of simple more frequent data in lower layers and complex less frequent data in higher layers.

Two hierarchical control structures are shown in Fig. 1.9. In the two-level structure, a coordinator integrate the local controllers placed at a lower level. Design of this coordinator has been addressed widely in the literature [MDT70, FBB+80]. In the left structure, the overall system is composed of two subsystems with some interacting variables. The three-layer system in the right figure, inherently has a hierarchical structure [MDT70]. The highest layer of the hierarchy usually corresponds to a dynamical system with slow dynamics. This layer feeds the immediate lower layer by the setpoint signals that is computed based on the received control inputs from the lower layers.

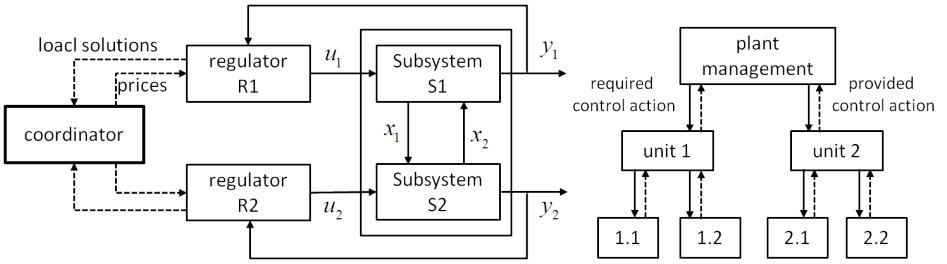

Figure 1.9: Distributed control [Sca09]

The conventional hierarchical control structure shown in Fig. 1.10 is widely used in the process industry for plantwide optimization, see e.g. [QB03, SEM04]. At the higher layer, Real Time Optimization (RTO) is performed to compute the optimal operating conditions with respect to a performance index representing an economic criterion. At this stage, a detailed, although static, physical nonlinear model of the system is used. At the lower layer a simpler linear dynamic model of the same system that is derived often by means of identification experiments is used to design a regulator with MPC, guaranteeing that the target values transmitted from the higher layer are attained. Also, the lower level can transmit bottom-up information on constraints and performance. The regulators (PI-PID) at the lowest layer control the actuators, so that they make reference to the actuators' models while conceptually, the two higher levels make reference to the plantwide optimization problem [Sca09].

We, in this thesis, have employed a similar structure to meet both performance optimization and energy cost minimization. However, we have combined the RTO layer with the systemwise controller MPC in a single block in order to avoid model mismatches. The new control block is termed as *Economic MPC* in the literature which we describe in the sequel.

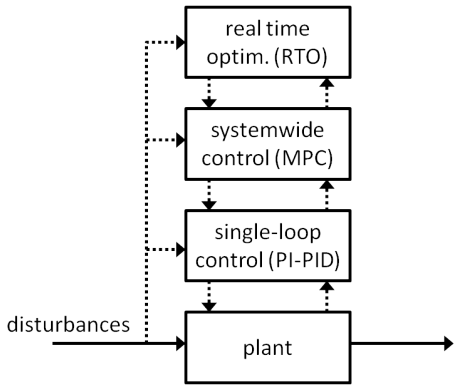

Figure 1.10: A representation of hierarchical structure for systemwide control and optimization.

1.3.2.5 Economic Optimization

The dominant approach in many industrial applications is to use a similar hierarchical setup as depicted in Fig. 1.10 in which the plant's economic optimization is decomposed into two levels. The first layer performs a steady-state optimization and decides the plant's economic operating conditions i.e. setpoints. This part is usually referred to as Real Time Optimization (RTO) layer that sends the setpoints to the lower layer which performs a dynamic optimization [RA09]. At this layer, a form of model predictive control (MPC) is used guarantying that the target values determined by the RTO will be attained [Sca09]. This layer can also provide bottom-up system information on constraints and performance to the upper RTO level.

One of the main problems of the RTO/MPC structure addressed in the literature is generation of unreachable setpoints by RTO. This is due to inconsistency between the models used at the two levels. Different methods are discussed in [RR99] for resolving the inconsistency problems and finding reachable targets that are as close as possible to those found by RTO. Two main disadvantages that [Eng07] points out are: 1) models in the two layers are not fully matched, particularly, they might have different steady-state gains [BBM00, CP83, SGP02]; 2) Time scales of the two layers are different, in principle because the optimization layer works in steady state [CP83].

Some issues have to be considered in the design of the RTO module even though it is based on a static model of the process. First, the static model have to be updated periodically to deal with new operating conditions and disturbances. Second, the two models in the static and in the dynamic layer have to be coherent, see [YT04]. Third, the decided optimal targets for the input/outputs have to be feasible by the MPC and as close as possible to the optimal setpoints. Some related literatures in finding the reachable setpoint have addressed in [RR99, RBJ$^+$08, RA09].

A performance measure is introduced by [FM96, ZF00] for RTO to compare its profit in theory and practice. Three types of losses are considered in the criteria i.e. 1) loss in transient time while system evolves toward a steady state, 2) loss due to model mismatch errors and 3) stochastic measurement errors. [ZTdGO02] describes an approach for mixing the two nonlinear steady-state optimization and MPC control into one economic MPC formulation. There are an increasing need for mixing the two levels of hierarchy by emerging market-driven economy which demands just-in-time production for being competitive [BBM00].

A dynamic real time optimization (D-RTO) technique is proposed in [HAM00]. Instead of a steady-state optimization, a dynamic optimization over a fixed horizon is performed to specify a reference trajectory that is followed by a simpler linear model at the lower level. This enables the system to work with a faster sampling rate. Still, an additional disturbance model is required in the linear dynamic model to resolve inconsistency with the optimization layer. An improvement revision of the approach is proposed by [KM07].

Disadvantages of RTO/MPC are criticized in many studies and resolutions or substitutions to the structure are proposed. A self-optimizing control i.e. based on conventional feedback control structure is suggested in [Sko00]. [ASS08] proposes a coordinator MPC where MPC coordinates local capacities of all units. [SP04] discusses integrating of process design, process control and process operability, and by this mean deal with the process economics.

As pointed out before, the dynamic MPC layer can be mixed with the RTO level to optimize the process economics directly [RA09]. We start by introducing the general case of MPC with a convex stage cost formulation based on [RM09, Ros03]. The stage cost is improved step by step until we give formulation for an economic MPC.

In the remaining part of this section, we briefly introduce the general case of MPC and economic MPC.

1.3.3 Model Predictive Control

This section is written mainly based on [RM09].

1.3.3.1 Linear Models

The general case of MPC with a convex stage cost and a linear model is considered. The linear time invariant system model is:

$$x^+ = Ax + Bu \tag{1.1}$$

$x \in \mathbb{R}^n$, $u \in \mathbb{R}^m$. The cost function $L(x,u)$ is strictly convex and nonnegative. It vanishes only at the setpoint, $L(x_{sp}, u_{sp}) = 0$. The cost function has a standard quadratic form as follows:

$$L(x,u) = 1/2\left(|x - x_{sp}|_Q^2 + |u - u_{sp}|_R^2 + |u(j+1) - u(j)|_S^2\right) \quad Q > 0, R, S \geq 0 \tag{1.2}$$

In the above cost function, at least one of $R, S > 0$. The system can be put in the standard LQR form by augmenting the state $\tilde{x} = [x(k)\ u(k-1)]$ [RR99]. This MPC is termed as sp-MPC in [RM09]. Also, input constraints form a nonempty polytope in $\mathbb{R}^m$

$$\mathbb{U} = \{u | Hu \leq h\} \tag{1.3}$$

The optimal steady state $(x^\star, u^\star)$, is the solution to the following optimization problem

$$min_{x,u} L(x,u) \quad subject\,to: \ x^+ = Ax + Bu \ \ u \in \mathbb{U} \tag{1.4}$$

The standard MPC in which the optimal steady-state is chosen as the center of the cost function is termed as tar-MPC.

1.3.3.2 Terminal Constraint MPC

Now, we consider the case in which terminal constraint $x(N) = x^\star$ is added to the controller. The following cost function holds:

$$V(x, u(i)_{i=0}^{N-1}) = \sum_{k=0}^{N-1} L(x(k), u(k)) \quad subject\,to: \ x^+ = Ax + Bu, \ \ x(0) = x_0 \tag{1.5}$$

For notational simplicity, we define $\mathbf{u} = \{u(i)_{i=0}^{N-1}\}$. The MPC control problem looks like:

$$min_u V(x, \mathbf{u}) \;\; subject\, to: \; x(N) = x^\star \;\; \mathbf{u} \in \mathbb{U} \tag{1.6}$$

The optimal input sequence is denoted as:

$$\mathbf{u}^0(x) = \{u^0(0, x), u^0(1, x), ..., u^0(N-1, x)\} \tag{1.7}$$

The MPC feedback law is the first move of this optimal sequence, which we denote as $u^0(x) = u^0(0, x)$. The optimal cost is denoted by $V^0(x)$. The closed loop system is given by:

$$x^+ = Ax + Bu^0(x) \tag{1.8}$$

By adding the terminal constraint, we lose the decreasing cost property, however this does not mean loosing asymptotic stability. An stability theorem for MPC with terminal constraint has been established by Rawlings in [RBJ$^+$08].

1.3.3.3 Economic MPC Versus Tracking MPC

An *economic MPC* addresses a cost function $L(x, u)$ for which other points (x, u) might exist that $L(x, u) < L(x^\star, u^\star)$ and satisfies system constraints except for the steady state constraints [DAR11].

There are many Lyapunov based stability theorems in the literature for *tracking MPC*. Proof of asymptotic stability of an economic MPC is addressed in [RBJ$^+$08] for the linear, stabilizable model with strictly convex quadratic cost and an unreachable setpoint. However, it does not find a Lyapunov function. In the technical note [DAR11], a Lyapunov function admits the stability properties of a class of MPC schemes that use an economic cost function. The functions $f(.)$ and $L(.)$ are assumed to be Lipschitz continuous on a specified admissible set. Also two forms of system controllability are the main assumptions that are required for the proof of stability: *Weak Controllability* and *Strong Duality of Steady-State Problem* [RBJ$^+$08].

1.4 Research Objectives

As mentioned earlier in this chapter, the focus of this study is designing a hierarchical control structure which maintains some optimization criteria motivated by indoor climate control of a building. The application is a residential detached house with multiple rooms, each room equipped with a hydronic heater i.e. floor heating or a hydronic radiator. An electrically-driven ground-source heat pump (GHP) supplies the system with hot water. The objectives to be maintained by the proposed model-based multi-layer controller are as follows:

- Stable stand alone local controllers for the system components that follow corresponding setpoints. This way, the whole control structure can be fitted to the existing commercial thermostats by only configuring interfaces to the intermediate level.

- System integration to acquire an optimal performance of the entire building system such that individual subsystems function at their optimal operating regions that depend on the thermal mass of the individual building and the weather condition. The minimized energy consumption is the result of the system optimal performance achieved by the intermediate level controller.
- Minimizing the energy cost as the immediate outcome of minimizing the energy consumption and foremost by proposing the building as a flexible load to the electricity grid. The building thermal mass is a heat buffer with a large storage potential which can contribute to the grid balancing issues based on the economic incentives that the electricity market offers to end-users.

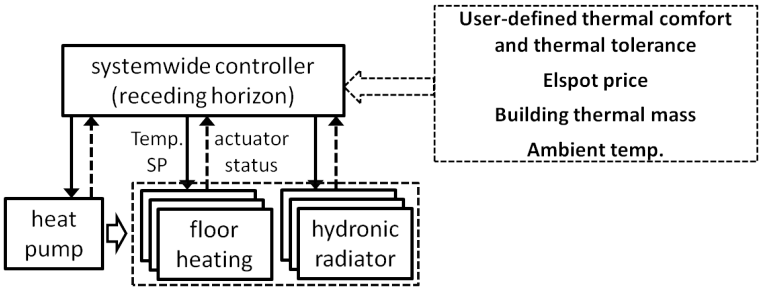

Figure 1.11: Schematic overview of the system control hierarchy.

We have proposed a two-layer hierarchical controller with single loops of PI controllers at the lowest level and a model based predictive controller at the top level to fulfill the aforementioned objectives. Instead of a separate real-time optimization module as shown in Fig. 1.3, we merged the two top levels by designating a MPC such that both energy and associated costs are minimized. Development of the proposed control structure, see Fig. 1.11 involves both numerical simulations and real-life experiments. Precise dynamical models of the subsystems were derived for simulation based studies and reduced order models for the purpose of controller design. The building thermal mass was modeled and verified using real experimental data.

At the top level, MPC modifies the user-specified thermal comfort temperature profile based on the user thermal tolerance degree and the Elspot price, that is a list of provisional price values for the next 24 hours given by the power utility provider. It generates setpoints for forward temperature of hot water and room temperature also using forecast of ambient temperature and dynamical models of building HVAC components. local controllers at the lowest level follow the corresponding setpoints.

1.5 Contributions and Publications

The contributions of the thesis falls in three areas that are motivated by the aforementioned objectives. A summary of tackled problems, proposed solutions and the relevant publications are listed in the following.

- **A solution to stability/performance dilemma of TRV controlled hydronic radiators:**
  Radiators are usually designed and regulated to meet high heat demands of the cold season. The large closed loop gain as a result of this specific design usually causes oscillations in the radiator flow and consequently in the room temperature in low heat demand seasons. The instability can be avoided by recalibration of thermostatic valves to reduce the closed loop gain, though in cost of an inferior performance during cold weather.
  The proposed solution is a gain scheduled controller for flow regulation instead of the conventionally used proportional (P) or proportional-integral (PI) controllers with fixed design parameters. The other influencing parameters i.e. the water temperature and pressure are centrally controlled for the entire building and can not be regulated in favor of only radiators, assuming that other HVAC systems might be available in the system. The gain scheduled controller is designed in a systematic fashion based on an analytically developed Linear Parameter Varying (LPV) model of the radiator's dissipated heat.
  The radiator modeling and control related publications are:

  - *Thermal Analysis of an HVAC System with TRV Controlled Hydronic Radiator*. IEEE Conference on Automation Science and Engineering, August 2010.
  - *Stability Performance Dilemma in Hydronic Radiators with TRV*. IEEE Conference on Control Applications, September 2011.
  - *Eliminating Oscillations in TRV-Controlled Hydronic Radiators*. IEEE Conference on Decision and Control, December 2011.
  - *An Analytical Solution for Stability-Performance Dilemma of TRV-Controlled Hydronic Radiators*. Submitted for Journal Publication, January 2012.

- **Energy minimization of a central heating system with hydronic heaters and geothermal heat pump:**
  The research question of this part is: How to integrate the Ground-source Heat Pump (GHP) with the heaters to achieve optimal performance in terms of minimum energy consumption, whilst satisfying comfort constraints?
  The proposed hypothesis is that the optimal feed temperature happens when at least one actuator works with full capacity. The rationale behind the hypothesis is heuristic: Electricity for heating purposes is mostly consumed by the heat pump's compressor. The latter would be minimized if the heat pump's Coefficient of Performance (COP) increases. COP is inversely related to the temperature gap between condenser and evaporator sides. Minimizing this gap is doable by reducing the condenser temperature or equivalently the feed water temperature to the building. The feed temperature can be reduced to the extent that the most demanding zone of the building can still meet the corresponding thermal comfort, in other words the relevant actuator works very close to its saturation limit for example the floor heating valve is almost fully open.
  An optimization problem in a receding horizon scheme is formulated to seek the proposed optimal operating point.
  Related publications are:

  - *Optimal Power Consumption in a Central Heating System with Geothermal Heat pump*. 18^{th} IFAC World Congress, September 2010.
  - *Energy Minimizing Controller for a Residential Central Heating System with Hydronic Floor Heating and a Heat Pump*. Submitted for Journal Publications, September 2012.

- **Contribution of buildings to smart grid control:**
  Research questions of this section are: How and to what extent, domestic heating systems can be helpful in regaining power balance in a smart grid? How much reduction in electricity bill would be achieved by load shifting based on power price? The idea is to deviate power consumption of the heat pump from its optimal value, to compensate power imbalances in the grid. Heating systems could be forced to consume energy, i.e. storing it in heat buffers when there is a power surplus in the grid; and be prevented from using power, in case of power shortage. It is shown that the large heat capacity of the concrete floor alleviates undesired temperature fluctuations. Therefore, incorporating it as an efficient heat buffer is a viable remedy for smart grid temporary imbalances. From residents' perspective, they can avoid high electricity bills by deferring their daily power consumption without loss of thermal comfort.
  The energy cost minimizing related publications are:

  - *Contribution of Domestic Heating Systems to Smart Grid Control*. IEEE Conference on Decision and Control. December 2011.
  - *Economic COP Optimization of a Heat Pump with Hierarchical Model Predictive Control*. Accepted in: IEEE Conference in Decision and Control , December 2012.

1.6 Outline of the Thesis

Having explained the motivation, problem statement and research objectives, it is time to outline the structure of the thesis. The thesis is structured according to the contributions in components modeling, energy and cost minimizing controller for the entire system, and finally real-life experimental results and validations.

The central heating system is described in Chapter 2.We proceed to the radiator modeling and control in Chapter 3. The well known dilemma between stability and performance for TRV-controlled radiators is investigated. Modeling of the system components i.e. the building thermal mass, radiators, and thermostatic valves are presented which provide a simulation infrastructure for testing and development of control methods. A short literature review precede development of the LPV model and relevant analysis of radiator partial differential equations. Gain scheduled controller design and simulations are presented shortly in this chapter with reference to the publications for details [TSR12a].

In Chapter 4 the optimal control problem for the cost and energy minimization is formulated. Dynamical models of the floor heating and heat pump are given. The proposed hypothesis for systemwide optimization and the model predictive problem formulation proceed state of the art for chosen methodologies. Both simulation and experimental results confirm the optimization hypothesis, improvement of the indoor climate and the electricity bill reduction to a significant amount.

The thesis is continued with Chapter 5 that summarizes the carried out works for solving the economic indoor climate control of the building. This chapter gives the reader an overview of the methods without going into details. The thesis is concluded in Chapter 6. It gives conclusions and recommendations for future works related to the building energy management and indoor climate control.

It is worth mentioning that although the thesis is presented as a collection of papers, the body of the thesis is written in a way such that the reader can read it seamlessly from the beginning to the end without really requiring interrupting and referring to appendices for further details. This is provided to facilitate reading of the thesis and has inevitably forced the author to replicate blocks of text and figures from the articles in the body of the thesis. All symbols and subscripts are locally introduced at the end of each chapter.

2 | System Description

Energy saving for the sake of sustainability and reduction of greenhouse gases is a global commitment to be partly fulfilled via design of efficient control solutions. The building sector is identified as providing the largest potential for CO_2 reduction by 2020. It is the hypothesis that through development of new integrated low energy building solutions and technologies entirely based on extensive energy savings and renewable energy supplies, the zero emission building solutions can be developed.

In this thesis, we investigate the potential energy savings in residential buildings achieved only by integration and performance improvement of the HVAC subsystems control. This improvement in terms of desired thermal comfort, energy efficiency and reduction of energy prices are to be obtained by design of advanced control architectures that integrate the entire HVAC subsystems with the building mass structure.

In this chapter, we described the specific building application and components of the building HVAC system. The test facility is described i.e. a real scale residential building to which we applied the proposed control methods.

2.1 Hydronic Central Heating System

The system consists of a detached residential building equipped with an electrically driven heat pump as the only heat source which is connected to a network of sub-floor heating pipes and radiators. Figure 2.1 depicts a schematic overview of all the heating loops. Obviously, the number of heating emitters could be extended by increasing the number of rooms in the building, although it is an assumption that each room is conditioned by either a circuit of sub-floor heating pipes or a hydronic radiator. By this, the competing situation when more than one heater heat up a single temperature zone is prevented, thus not considered in the controller design in the subsequent chapters.

The circulation pump in the distribution circuit is controlled to maintain a constant differential pressure across all three parallel branches of the rooms' pipe grids. Exogenous disturbances affecting the system are a profile of user-defined comfort temperature, solar radiation through glazing, the power price signal and the measured and/or predicted ambient temperature. Actuation facilities for disturbance rejection and set-point tracking of the space temperature are dissipated heat from radiators and floor heating pipes to the rooms. We have not considered the influence of ventilation or wind speed on the indoor climate variations, nor the window shadings for controlling direct sunlight through windows.

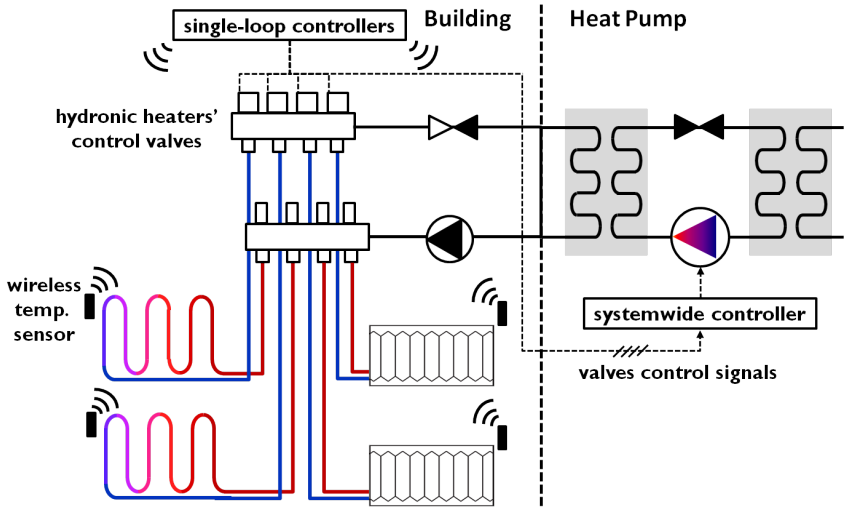

Figure 2.1: Schematic of the HVAC subsystems.

2.2 Building Model

2.2.1 Related Literature

A comprehensive building model can serve as a useful tool in selection of insulation materials, different building services, analyzing energy management and control strategies and several other purposes. Two main approaches might be used for building dynamical and steady state modelings. The conventional approach is to use knowledge of the physical building characteristics and subsystems to find a deterministic model. Grey box modeling is an alternative approach when building performance data and statistical methods are also exploited.

Various deterministic approaches have been addressed in the literature [TMAR05, ASS90, HU99]. [ASS90] has proposed a methodology to make a unified approach for building thermal control, analysis and energy calculations. In the latter work, Laplace transfer functions of the building and HVAC systems are achieved using thermal network models that include both distributed and lumped elements e.g. thermal mass and room air thermal capacitance respectively. In another approach, [HU99] developed a computationally efficient building thermal model which is appropriate for controller design purposes. In the latter paper, a simple lumped capacitance model analogous to an RC electrical circuit for a commercial building is used. By simulating the first and second order linear models in Simulink, [HU99] have reported that there is no tangible advantage of using higher order models in short term simulations.

The alternative approach, grey box modeling, is to use building measurement data with inferential and statistical methods for system identification. A grey box modeling approach is used in [MH95] and [AMH98] to derive a simple stochastic continuous-time model based on both experimental data and the building physical characteristics. Other methods based on experimental data include: utilizing pseudo-random binary sequences

of the input to derive the heat dynamics [LPP82], and employing an inverse grey box thermal network model for transient building load prediction [BC02]. According to [XFD08] the main drawback of this approach is that it requires a significant amount of training data and the estimated parameters may not always reflect a specific physical behavior to give a rational perception. However, [AMH98] and [FVLA02] identify parameters of a continuous-time model directly which is formulated as a system of stochastic differential equations. Therefore, the parameters have direct physical interpretation.

There are two main differences between the grey box modeling and the traditional deterministic approach in particular, as argued in [MH95]. Firstly, the deterministic approach only uses knowledge about the building physical characteristics, while the grey box approach identifies the model structure using both the building physical knowledge and performance data. Secondly, the deterministic approach has a deterministic framework but the grey box approach has a stochastic framework, potentially resulting in a suitable parameterization. That is usually a difficult task with the first approach [AMH98].

Here, in this study we took the grey box modeling approach where the structure of the building, HVAC components and heat inputs are formed based on the building physical knowledge and thermodynamics. The relevant parameters are derived based on the specific building performance data.

2.2.2 Building Thermal Capacitance Model

In this section formulation of a continuous-time simple model that describes variations of the room air temperature is described. The total model of the heat transfer is usually formulated based on heat diffusion equations for the heat conduction through walls, heat convection and radiation from indoor surfaces to the air. In a commonly used simplification the entire heat capacity of a the materials is concentrated in a single heat-storage medium [MH95, Ada68]. This storage medium is analogous to a capacitance element in an electric circuit. Equivalent heat transfer coefficients between different nodes i.e. room air and surfaces can also be modeled as resistors. The circuit will be completed by adding current and voltage sources analogous with heat emitters and dependent temperature nodes. An analogous electric circuit to the building thermal network is suggested in Fig.2.2. This model has been frequently used in the literature for modeling of both residential and commercial buildings [AJKS+85, HU99, KH04].

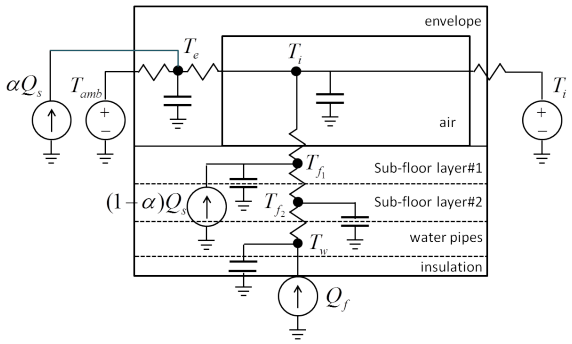

Figure 2.2: Analogous electric circuit to the building thermal network.

The state space equations which govern a single room's dynamics are derived in the following. The validity of similar linear state space models has been widely investigated in the researches. The energy balance equations are formulated based on five main thermal masses: air, 2 layers of concrete sub-floors, the water influent in the floor heating pipes and external envelope i.e. walls, ceiling and glazing.

$$
\begin{aligned}
C_i\dot{T}_i &= B_{ie}(T_{e_i} - T_i) + B_{ij}(T_j - T_i) + B_{if}(T_{f1_i} - T_i) + Q_{rad} \\
C_e\dot{T}_{e_i} &= B_{ie}(T_i - T_{e_i}) + B_{ae}(T_{amb} - T_{e_i}) + \alpha Q_s \\
C_{f_i}\dot{T}_{f1_i} &= B_{if}(T_i - T_{f1_i}) + B_{ff}(T_{f2_i} - T_{f1_i}) + (1-\alpha)Q_s \\
C_{f_i}\dot{T}_{f2_i} &= B_{ff}(T_{f1_i} - T_{f2_i}) + B_{fw}(T_{w_i} - T_{f2_i}) \\
C_{w_i}\dot{T}_{w_i} &= B_{fw}(T_{f2_i} - T_{w_i}) + c_w q_i(T_{forward} - T_{r_i})
\end{aligned}
\tag{2.1}
$$

in which i and j are indices of two adjacent rooms. B represents the equivalent convection/conduction heat transfer coefficient between two connected nodes. For instance, B_{fw} is the conduction heat transfer coefficient between a concrete sub-floor layer and floor heating pipes that are at temperature T_w. C stands for a mass thermal capacitance. Indices e, f, w represent envelope, floor and water respectively. Heating sources are solar radiation through glazing that is absorbed partially by walls, αQ_s and floor, $(1-\alpha)Q_s$ and dissipated to the space, dissipated heat by the radiator, Q_{rad} and floor heating, $Q_f = c_w q_i(T_{forward} - T_{r_i})$. $T_{forward}$ is the water forward temperature and T_{r_i} is the water return temperature. In the equations, heat transfer to the ground is eliminated due to having thick layers of insulation beneath the concrete sub-floor. Please find a description of all symbols in Table 2.1.

Envelops, room air and each layer of concrete floor are assumed to be at uniform temperature, i.e. no temperature gradient is considered in any of them. Thermal capacitance of partitioning walls that separate two adjacent zones (rooms) are negligible compared to the external walls; therefore they are not considered as capacitance elements in the model. The concrete sub-floor is sectioned for a better approximation of temperature distribution from water pipes upward to the floor surface. More layers give more accurate temperature distribution, however higher precision is not required for the main purpose of current thesis i.e. design of controllers. Both fast and slow dynamics are very well simulated by using this five node model.

The fifth-order model (2.1) is the most comprehensive version that we used in this PhD study for simulation purposes. Other reduced order models has been used in different papers with different assumptions for control purposes. In the last publication [TSR12b] a two node model is used and verified based on the experimental results. This second order model of a room shows very good conformity with the test data. Parameters of the 2-node model were estimated and validated using experimental data and further used in the simulations of that paper. However, the parameters values in other publications [TSR11c, TSR11b, TSR11a, TSMR11, TSR12a, TSRM12] were adopted and adjusted according to the typical experimental and standard values of a low-energy building [ASH90].

2.3 Test Facility: Energy Flex House

The case study is a low energy demonstration building located in Copenhagen, Denmark. The building is built to provide test facilities for development and test of energy efficient

control solutions, renewable energy sources and new facade technologies [Ins]. Built in 2009, Energy Flex House (EFH) lab is an uninhabited test facility examining the interplay of various floor types, outer walls and technical installations, Fig. 2.3.

Figure 2.3: Energy Flex House is a low energy building built basically for testing, developing and demonstrating innovative energy efficient solutions.

The system consists of three separate heat zones i.e. rooms. Each room has a separate grid of sub-floor PEX pipes embedded into a thick layer of concrete, in a serpentine pattern with a center-to-center distance of 100 mm. The mass flow rate through the three parallel pipe branches through individual rooms is not the same due to different hydraulic resistances. The flow is regulated by a multiple-rate circulating pump to around 32, 22 and 20 l/h through the pipes of the rooms#1,2 and 3 respectively. The average U-value of the building envelope of the reference room, including 1.6 m^2 of windows, is $0.2W/m^2/K$. A Schematic diagram of the closed loop heating system is shown in Fig. 2.4.

The three rooms in the above schematic have the same sizes, each having a triple-glazed window which faces south in rooms#1 and 2, and faces north in room#3. Being in the north hemisphere, rooms#1 and 2 receive solar radiation through windows and have high solar heat gains.

There are other spaces adjacent to the aforementioned rooms i.e. a room adjacent to room#3, a corridor between southern and northern rooms and two bathrooms. Each space has its own sub-floor heating pipe grid that was disconnected from the main manifold in the course of experiments. The building has two floors with the lab located in the ground floor. The measurement and control are limited to the three separated rooms in the ground floor that receive negligible heat gain from the adjacent and above spaces. It is because, those spaces were disconnected from the heat source in the course of experiments.

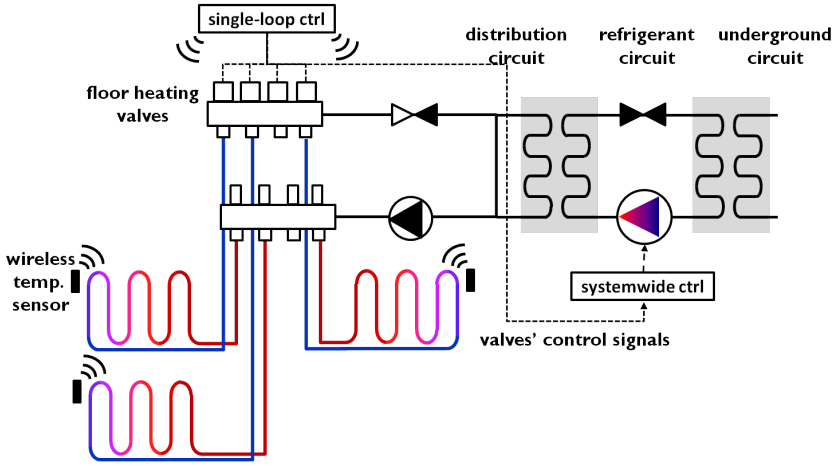

Figure 2.4: A schematic diagram of the piping system of Flex House (case study).

2.4 Nomenclature

Table 2.1: Symbols and Subscripts

Nomenclature	
B	heat transfer coefficient between two nodes in an electric circuit $(kJ/s°\mathrm{K})$
C	thermal capacitance $(J/kg\,°\mathrm{C})$
c_w	water specific heat $(J/kg\,°\mathrm{C})$
Q	heat (W)
q	water flow rate in floor heating (kg/sec)
T	temperature $(°\mathrm{C})$
Subscripts	
amb	ambient
e	envelope
f	floor (with i index corresponding to room#i
f_i	floor of the ith room
i, j	room numbers
$forward$	forward temperature of water
r	return temperature of water
rad	radiator
s	solar
w	water

3 Stability-Performance of TRV-Controlled Hydronic Radiators

3.1 Background and Objectives

Room-by-room zoning, especially in residential buildings, is usually selected to maintain rooms at different temperatures; also, to maintain room temperature variations on a regular basis. In many cases, this is feasible by adjusting the flow rate through the emitters serving each room. Panel radiators equipped with thermostatic radiator valves and piped using a manifold distribution system facilitates room-by-room zoning of a building at minimal price [Cal09].

Hydronic radiators controlled by TRVs provide good comfort under normal operating conditions. Thermal analysis of the experimental results of a renovated villa in Denmark, built before 1950, has demonstrated that energy savings near 50% were achieved by mounting TRVs on all radiators and fortifying thermal envelope insulation [STBH05]. Also, various studies are conducted worldwide to conclude that radiant heating consumes less energy compared to that used by a forced air heating system [DC98, CRW00, HH00].

TRVs are usually designed for treating the high heat demand situations; Alternatively, radiators or the circulation pump are over dimensioned that result in a large closed-loop gain in low heat demand conditions. This large loop gain usually brings about inefficiency in low heat demand seasons [Rat87]. In low heat demand situation, due to a small mass flow rate, loop gain increases. As a result, oscillations in the room temperature and the radiator flow usually occurs. Besides discomfort, oscillations decrease the life time of the actuators and increase maintenance costs. This problem is addressed in [APSB04] for a central heating system with gas-expansion based TRVs. It is proposed to control the differential pressure across the TRV by estimating the valve position to keep it in a suitable operating area.

We studied this problem as a dilemma of stability/performance. The dilemma arises when TRV is regulated by a linear controller with time invariant parameters. A high loop gain and long time constant are the main reasons of this phenomenon. In contrary, selecting a smaller controller gain to handle the instability situation, will result in a poor performance of radiator when the heat demand is high. The objectives of this chapter is:

1. Proposing an adaptive controller that satisfies both stability and high performance

in entire operating region. The purpose is to design a stable stand-alone controller for radiators as an element of the entire application (see the list 1.11).

2. Parameters of the proposed controller are to be determined systematically based on the operating point, such that it is easily implementable in practice.

In this study, we dealt with a battery-powered TRV that is driven by a stepper motor. It has been investigated via simulations that a Proportional Integral (PI) controller with fixed parameters will fail satisfying both performance and stability through the entire operating region of the radiator, see Fig. 3.1 and 3.2. In either scenarios a PI controller is tuned using Ziegler-Nichols step response method [ÅH95], for a specific weather condition .

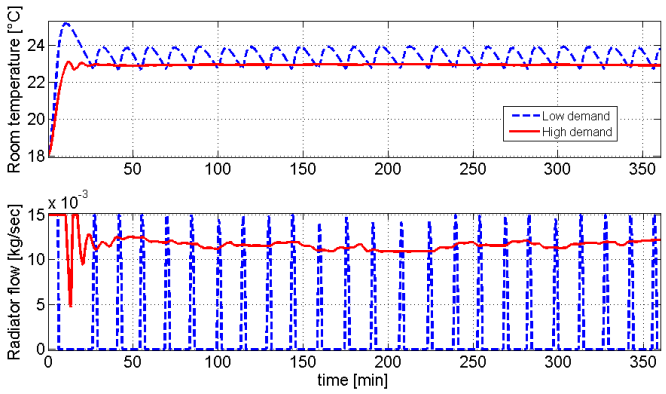

Figure 3.1: Performance of a controller that is designed to suit the high demand condition is shown in both low and high heat demand weather conditions.

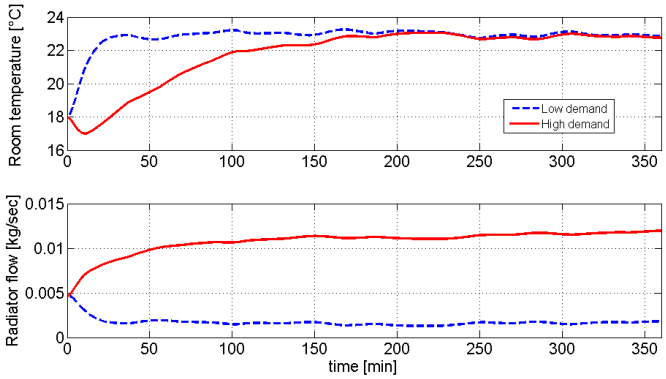

Figure 3.2: Performance of a controller that is designed to suit the low demand condition is shown in both low and high heat demand weather conditions.

In this study we assumed that a constant pressure drop across the radiators valves is maintained using a multiple-rate circulation pump, unlike [APSB04] that regulates pump speed to maintain a proper loop gain all year around. Instead, we assumed that flow

control of individual radiators is feasible by accurate adjustments of the valves' opening made by the embedded stepper motor.

We designed a gain scheduled controller based on a proposed linear parameter varying model. The model is parameterized based on the operating flow rate, room temperature and radiator specifications. The parameters are derived according to the proposed analytic solution for the heat dissipated by the radiator. It is shown via simulations that the designed controller based on the proposed linear parameter varying (LPV) model performs excellent and remains stable in the whole operating conditions.

A thorough understanding of the radiator dynamics will enhance investigations and analysis of the instability problem. [Han97] gives a thorough review of the hydronic circuit components modeling. For instance, it represents the static one exponent and two exponent models of radiators which was mainly based on [Web70, Bec72, JPSØ79]. We have used the dynamical version of the one exponent model in our simulations mainly based on the model proposed originally in [PG85] i.e. based on partial differential equations. In [XFD08] two model structures for describing the radiator dynamics are discussed: the discrete element and lumped models. A combination of both models is used in the latter study; the return water temperature is calculated based on the first model and the mean water temperature of radiator based on the lumped model to determine the heat power to the space.

We have formulated the radiator dynamics in two ways. Firstly, it has been treated as a distributed system in order to analyze the radiator dissipated heat as presented in [XFD08]. Using the resulted analytical solution of the heat power, the radiator model is approximated by a lumped system that is simple enough for control design purposes. By the lumped model reduced the computational costs by solving an Ordinary Differential Equation (ODE) at a few points instead of solving a full Partial Differential Equation (PDE).

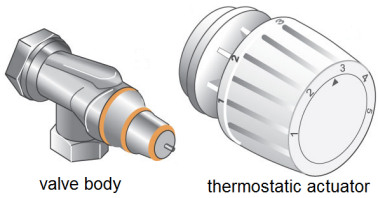

Figure 3.3: Thermostatic radiator valves comprise two parts: a valve body and an electric/non-electric valve operator.

A radiator thermostatic valve is to regulate the flow rate through the radiator and by this mean, the room temperature. TRV is composed of two parts Fig. 3.3: a valve body and an electric/non-electric thermostatic operator. Four thermostatic valve types are studied in [Gam74]. It was concluded that the gas expansion-based type is the most advantageous one, with 0 dead-time and the time constant of 15 minutes. However, we have studied a modern type of TRV with a stepper motor that adjusts the valve opening fairly precisely and quickly and is energized by a battery. With the new TRV, stem position of the valve is predictable, making it possible to estimate the flow mass if we assume a constant pressure drop across the valve.

3.2 Problem Statement

The case study of this chapter is a room heated by a hydronic radiator equipped with a thermostatic valve. A central heating system with multiple radiator circuits equipped with TRVs is demonstrated in Fig. 3.4. Disturbances that excite the system are the ambient temperature and solar radiations.

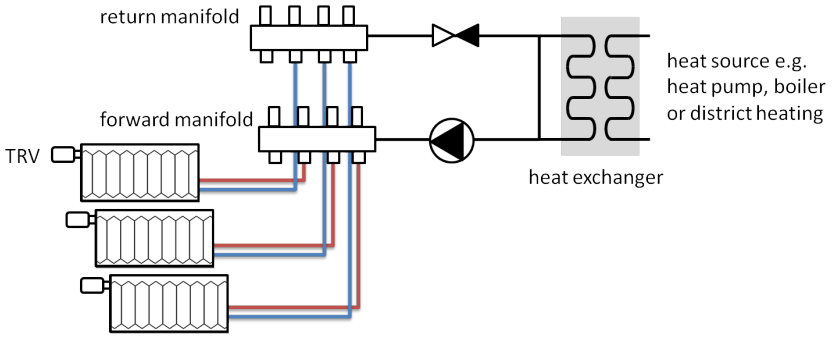

Figure 3.4: Schematic of the radiator hydraulic circuit.

The dilemma between stability and performance arises when the TRV is controlled by a fixed linear controller. To deal with the dilemma, a gain scheduled controller is proposed which is designed based on a proposed LPV model of radiator. Parameters of the LPV model are developed in a closed form as a function of the system operating point and the radiator specific dimensioning characteristics. The block diagram of the system, shown in Fig. 3.5, illustrates the closed loop control system. It is worth stating that the chosen values of all parameters are in accordance with the typical experimental and standard values.

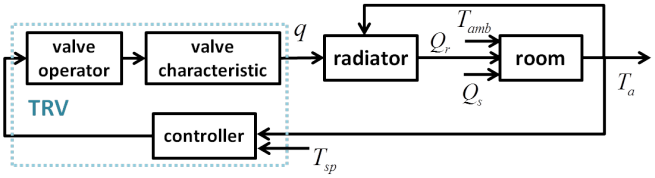

Figure 3.5: Closed loop control system of the room and radiator.

In the subsequent sections, firstly a one exponent model is introduced for describing the radiator dynamics and further used in the simulations. Based on the step response of the radiator, we concluded that the entire system can be modeled by a second order transfer function. In order to develop this second order model systematically, step response of the radiator is formed as a Partial Differential Equation (PDE). We solved the PDE analytically and derived the parameters of an LPV model for radiator. The developed second-order LPV model is further used for design of a gain-scheduled controller.

3.3 Component Modeling

3.3.1 Discrete-Element Model of a Panel Radiator

Radiator is modeled as a lumped system with N elements in series Fig. 3.6. The nth section temperature is given by, [Han97]:

$$\frac{C_r}{N}\dot{T}_n = c_w q(T_{n-1} - T_n) - \frac{B_r}{N}(T_n - T_a) \tag{3.1}$$

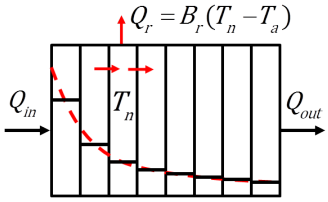

Figure 3.6: A discrete element model of radiator. Input and output heat flux, through the sections and dissipated to the space are shown by arrows.

in which C_r is the heat capacity of water and radiator material, T_n is the temperature of the radiator's nth section area and $n = 1, 2, \ldots, N$. The temperature of the radiator ending points are inlet temperature: $T_0 = T_{in}$, and return temperature: $T_N = T_{out}$. T_a represents the room air temperature. In this formulation, we assumed that a section's surface and the passing influent water are at the same temperature. Besides, heat transfer from radiator surface is assumed to be only via convection. We have also assumed that heat is transferred between two sections only by mass transport, implying that convective heat transfer is neglected. B_r represents the radiator equivalent heat transfer coefficient which is defined based on one exponent formula, [Han97] in the following:

$$B_r = \frac{\Phi_0}{{\Delta T_{m,0}}^{n_1}}(T_n - T_a)^{n_1 - 1} \tag{3.2}$$

in which Φ_0 is the radiator nominal power in nominal condition which is $T_{in,0} = 90°C$, $T_{out,0} = 70°C$ and $T_a = 20°C$. $\Delta T_{m,0}$ expresses the mean temperature difference which is defined generally as follows:

$$\Delta T_m = \frac{T_{in} - T_{out}}{2} - T_a \tag{3.3}$$

in nominal condition. The exponent n_1 is usually around 1.3, [Han97]. In such a case, we can approximate the non-fixed, nonlinear term in B_r with a constant between 2.5 and 3.2 for a wide enough range of temperature values. Picking 2.8 as the approximation value would result in:

$$B_r = 2.8 \times \frac{\Phi_0}{{\Delta T_{m,0}}^{1.3}} \tag{3.4}$$

Heat dissipation to the room by the radiator can be described as:

$$Q_r = \sum_{n=1}^{N} B_r(T_n - T_a) \tag{3.5}$$

3.3.2 Room Model

Heat balance equations of the room is governed by the following lumped model [HU99]:

$$\begin{aligned} C_a\dot{T}_a &= B_{ae}(T_e - T_a) + B_{af}(T_f - T_a) + Q_r \\ C_e\dot{T}_e &= B_{ae}(T_a - T_e) + B_{ae}(T_{amb} - T_e) + \alpha Q_s \\ C_f\dot{T}_f &= B_{af}(T_a - T_f) + (1-\alpha)Q_s \end{aligned} \tag{3.6}$$

in which T_e represents the envelop temperature, T_f the temperature of the concrete floor and T_a the room air temperature. Q_r is the radiator's dissipated heat to the room. Q_s is the solar radiation through glazing that is absorbed partially by envelope and floor surfaces. Each of the envelops, floor and room air masses are considered as single lumps with uniform temperature distribution.

3.3.3 Thermostatic Radiator Valves

TRVs that facilitate room-by-room zoning in a building are mainly designed in two types: electrically or non-electrically driven thermostatic operators. The thermostatic head is called the valve actuator. Two examples of electrically powered actuator types are *heat motor* and *synchronous motor* actuators. The first actuator moves the valve's shaft linearly by expansion of a wax compound within an expandable chamber and heated by an electrically powered resistor. It drives the valve fully open in two to three minutes after the power is applied. Actuation time of the motorized thermostatic head is much less i.e. two to three seconds. A gear assembly coupled to the synchronous motor rotates the valve shaft makes the flow modulating possible. The first type is an on/off zone valve intended to operate in either its fully open or close position.

One of the most popular thermostatic heads do not need electricity to operate the zoning hardware. The mechanical force required to move the valve shaft is generated by expansion of either a wax compound or gas sealed within the operator. The generated pressure pushes a spring-loaded shaft toward closing the valves opening, thus reducing the influent flow. See Fig. 3.7 for a cross section of a non-electric TRV.

The pressure drop across the valves are maintained constant by a multiple-rate circulation pump. Therefore, the flow rate depends only on the valve opening and the specific valve design characteristics. In the study, we used a specific plug&seat valve Fig.3.8 with the following relationship between the passing flow rate q and the valve opening degree δ:

$$q = -3.4 \times 10^{-4}\delta^2 + 0.75\delta \tag{3.7}$$

This nonlinear relationship does not interfere with the controller design by adding up more nonlinearity to the radiator dynamical equations. The above equation is used only

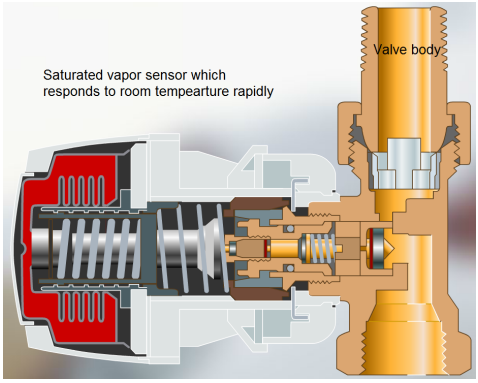

Figure 3.7: The thermostatic head of a gas expansion based actuator. The source of figure: [Dan12b].

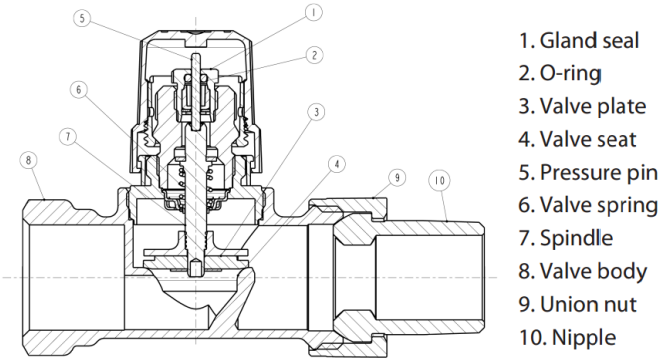

Figure 3.8: Cross section of a specific valve characterized by 3.7. The source of figure: [Dan12a].

for translating flow and opening degree to each other when the desired flow is determined by the controller. Also, flow is not measured directly, but is estimated using the known opening percentage and differential pressure drop across the valve.

Flow estimation in a stepper-motor driven valve was formulated based on the valve opening. However, in a gas/wax expansion based TRV, flow rate can be estimated using temperature deviation of the medium in the actuator chamber and the temperature set value determined by consumer's behavior. The relationship can be obtained based on the characteristic curves of a specific valve gained from the test according to the CEN EN215 standard [sta04], with a pressure drop across the valve at 0.1 bar [XFD08].

3.3.4 Control Oriented Models

For the control design purposes, the relationship between the room air temperature and the radiator output heat can be well approximated by a 1^{st} order transfer function as

follows:

$$\frac{T_a}{Q_r}(s) = \frac{K_a}{1+\tau_a s} \tag{3.8}$$

Parameters τ_a and K_a can be identified simply via a step response test.

Step response simulations and experiments confirm a first order transfer function between the output heat and the input flow rate of the radiator at a specific operating point as follows:

$$\frac{Q_r}{q}(s) = \frac{K_r}{1+\tau_r s} \tag{3.9}$$

Parameters of the above model are formulated in the next section based on a closed-form solution for the radiator dissipated heat, $Qr(t, q, T_a)$.

3.4 Transient-Time Analysis of the Radiator PDE

To develop the map, $Q_r(t, q, T_a)$, a step flow is applied to the radiator, i.e. changing the flow rate from q_0 to q_1, at a constant differential pressure across the valve. Propagating with the speed of sound, the flow shift is seen in a fraction of a second all along the radiator. Hence, flow is regarded as a static parameter for $t > 0$, compared to the sections' temperature which vary in a slow pace compared to the flow change.

Consider a small radiator section Δx with depth d and height h as shown in Fig. 3.9. The temperature of incoming flow to this section is $T(x)$, while the outgoing flow is at $T(x+\Delta x)\,^{\circ}C$. The temperature is considered to be the same as $T(x)$ throughout a single partition.

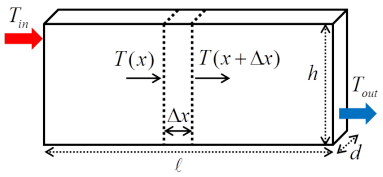

Figure 3.9: A radiator section area with the heat transfer equation governed by (9). Entering flow to the section is at the temperature $T(x)$ and the leaving flow is at $T(x+\Delta x)$. The section temperature is also assumed to be at $T(x)$.

The corresponding section heat balance equation is given as follows:

$$qc_w\left(T(x) - T(x+\Delta x)\right) + B_r\frac{\Delta x}{\ell}\left(T_a - T(x)\right) = C_r\frac{\Delta x}{\ell}\frac{\partial T(x)}{\partial t} \tag{3.10}$$

in which $q = q_0$ at $t = 0$ and $q = q_1$ for $t > 0$. C_r is the heat capacity of water and the radiator material defined as: $C_r = c_w\rho_w V_w$. Dividing both sides of (3.10) by Δx and letting $\Delta x \to 0$, we have:

$$-qc_w\frac{\partial T(x,t)}{\partial x} + \frac{B_r}{\ell}\left(T_a - T(x,t)\right) = \frac{C_r}{\ell}\frac{\partial T(x,t)}{\partial t} \tag{3.11}$$

with boundary conditions:

$$T(0,t) = T_{in} \tag{3.12a}$$

$$T(\ell, 0^-) = T_{out,0} \tag{3.12b}$$

$$T(\ell, \infty) = T_{out,1} \tag{3.12c}$$

in which T_{in} is the constant temperature of supply water, $T_{out,0}$ and $T_{out,1}$ are return water temperatures corresponding to q_0 and q_1 respectively. The first solution candidate would be a separable solution like $T(x,t) = T(t) \times X(x)$. Substituting it into (3.11), gives:

$$T(0,t) = c_1 e^{k_1 t} + c_2 \tag{3.13}$$

which implies a contradiction according to 3.12a.

Before proceeding to solve the full PDE (3.11), we need to find the two boundary conditions $T_{out,0}$ and $T_{out,1}$. For this purpose, the steady state form of (3.11) is needed:

$$-qc_w \frac{dT(x)}{dx} + \frac{B_r}{\ell}\left(T_a - T(x)\right) = 0 \tag{3.14}$$

which can be written as:

$$\frac{dT(x)}{dx} + \frac{\beta}{\gamma} T(x) = T_a \tag{3.15}$$

with constants $\beta = \frac{B_r}{C_r}$ and $\gamma = \frac{qc_w\ell}{C_r}$.
Therefore, the steady state temperature, $T(x,t)|_{t\to\infty}$ will be achieved as:

$$T(x) = c_1 e^{-\frac{\beta}{\gamma}x} + c_0 \tag{3.16}$$

at a specific flow rate q. Substituting the above equation in (3.15) gives $c_0 = T_a$. Knowing $T(0) = T_{in}$, c_1 is also found. Finally $T(x)$ looks like:

$$T(x) = (T_{in} - T_a)e^{-\frac{\beta}{\gamma}x} + T_a \tag{3.17}$$

Therefor the two boundary conditions are:

$$\begin{aligned} T_{out,0} &= (T_{in} - T_a)e^{-\frac{\beta}{\gamma_0}x} + T_a \\ T_{out,1} &= (T_{in} - T_a)e^{-\frac{\beta}{\gamma_1}x} + T_a \end{aligned} \tag{3.18}$$

with γ_0 and γ_1 corresponding to the flow rates q_0 and q_1.

Next, we solve (3.11) for $T(x,t)$ in frequency domain. Taking Laplace transform of this equation will give:

$$-qc_w \frac{\partial \tilde{T}(x,s)}{\partial x} + \frac{B_r}{\ell}\left(\frac{T_a}{s} - \tilde{T}(x,s)\right) = \frac{C_r}{\ell}\left(s\tilde{T}(x,s) - T(x,0)\right) \tag{3.19}$$

which is simplified to:

$$\frac{\partial \tilde{T}(x,s)}{\partial x} + \frac{s+\beta}{\gamma}\tilde{T}(x,s) = \frac{\beta}{\gamma}\frac{T_a}{s} + \frac{1}{\gamma}T(x,0) \tag{3.20}$$

with $T(x,0)$ computed based on (3.17) when $q = q_0$:

$$T(x,0) = (T_{in} - T_a)e^{-\frac{\beta}{\gamma_0}x} + T_a \tag{3.21}$$

and boundary conditions:

$$\tilde{T}(0,s) = \frac{T_{in}}{s} \tag{3.22}$$

with $\beta = \frac{B_r}{C_r}$, $\gamma_0 = \frac{q_0 c_w \ell}{C_r}$ and $\gamma_1 = \frac{q_1 c_w \ell}{C_r}$. The solution to the above differential equation comes out of inspection as follows:

$$\begin{aligned}
\tilde{T}(x,s) &= c_1 e^{-\frac{\beta}{\gamma_0}x} + c_2 e^{-\frac{s+\beta}{\gamma_1}x} + c_0 \\
c_0 &= \frac{T_a}{s} \\
c_1 &= \frac{T_{in} - T_a}{s + \beta(1 - \frac{\gamma_1}{\gamma_0})} \\
c_2 &= \frac{T_{in}}{s} - c_0 - c_1
\end{aligned} \tag{3.23}$$

The time response is obtained via taking inverse Laplace transform of the above frequency response. It is shown in the following:

$$\begin{aligned}
T(x,t) = (T_{in} - T_a)e^{-\beta t - \frac{\beta}{\gamma_0}(x - \gamma_1 t)} \left(u(t) - u(t - \frac{x}{\gamma_1}) \right) \\
+ (T_{in} - T_a)e^{-\frac{\beta}{\gamma_1}x} u(t - \frac{x}{\gamma_1})
\end{aligned} \tag{3.24}$$

in which $u(t)$ is a *unit step function*.

We, however, are interested in the radiator output heat $Q_r(t)$ to find K_r and τ_r in (3.9). It is defined as:

$$Q_r(t) = \int_0^\ell \frac{B_r}{\ell} \left(T(x,t) - T_a \right) \, dx \tag{3.25}$$

Taking time derivative of the above equation gives:

$$\frac{dQ_r(t)}{dt} = \int_0^\ell \frac{B_r}{\ell} \frac{\partial T(x,t)}{\partial t} \, dx \tag{3.26}$$

and rewriting the result using (3.11):

$$\begin{aligned}
\frac{dQ_r}{dt} &= \int_0^\ell \beta \left(-q c_w \frac{\partial T(x,t)}{\partial x} + \frac{B_r}{\ell} \left(T_a - T(x,t) \right) \right) dx \\
&= \beta q c_w (T_{in} - T_{out}(t)) - \beta Q_r(t)
\end{aligned} \tag{3.27}$$

which turns into the following differential equation:

$$\frac{dQ_r(t)}{dt} + \beta Q_r(t) = \beta q c_w \left(T_{in} - T_{out}(t) \right) \tag{3.28}$$

$$T_{out}(t) = T(\ell, t)$$

in which $T(\ell, t)$ is obtained using (3.25). The solution to the above first order differential equation via inspection is:

$$\begin{aligned} Q_r(t) = {} & Q(0)e^{-\beta t} + c_w q(T_{in} - T_a)(1 - e^{-\beta t}) + \\ & + \frac{c_w q(T_{in} - T_a)\gamma_0}{\gamma_1} e^{-\beta t}\left(e^{-\frac{\beta}{\gamma_0}\ell} - e^{-\frac{\beta}{\gamma_0}(\ell - \gamma_1 t)}\right) - \\ & - c_w q(T_{in} - T_a)e^{-\beta t}\left(\frac{\gamma_0}{\gamma_1}(1 - e^{-\frac{\beta}{\gamma_0}(\ell-\gamma_1 t)}) - (1 - e^{-\frac{\beta}{\gamma_1}(\ell-\gamma_1 t)})\right) u(t - \frac{\ell}{\gamma_1}) \end{aligned} \tag{3.29}$$

The process of deriving the precise step response is completed here. An approximate solution is firstly derived in [TSR11a] based on the intuition achieved in [TSR11c]. The final precise solution is given finally in [TSR12a] where we found the precise closed-form map from the operating point to the radiator dissipated heat i.e. $Q(t, q, T_a)$. q and T_a are respectively the hot water flow rate through the radiator and the room temperature.

In the next section, we utilize the derived formula to extract the required gain and time constant for the approximation LPV model.

3.5 Radiator LPV Model

Parameters K_r and τ_r of the radiator LPV model (3.9), are derived based on the best first order fit to the step response of the radiator dissipated heat (3.29). Using the tangent to $Q_r(t)$ at $t = 0^+$, we obtained the time constant. Equating the slope of the tangent at $t = 0^+$ with the first derivative of:

$$Q_{r,app}(t) = Q_r(t_\infty) + (Q_r(t_{0^-}) - Q_r(t_\infty))e^{-\frac{t}{\tau_r}} \tag{3.30}$$

i.e. the first order approximation of $Q(t)$. It gives:

$$\tau_r = \frac{Q_r(t_\infty) - Q_r(t_{0^-})}{q_1 c_w \beta (T_{in} - T_a)(\frac{\gamma_0}{\gamma_1} - 1)} \tag{3.31}$$

Steady state gain is also obtained as follows:

$$K_r = \frac{Q_r(t_\infty) - Q_r(t_{0^-})}{q_1}$$

in which $Q_r(t_\infty)$ and $Q_r(t_{0^-})$ are the dissipated heat by the radiator in steady state corresponding to the flow rates q_1 and q_0 respectively.

These two parameters depend also on room temperature and supply water temperature. However, we have assumed a constant feed water temperature for the heating system. Therefore, variations of K_r and τ_r against a number of flow rates and room temperatures are shown in the following figure. Room temperature varies between 5 and 25 $^\circ C$ and flow rate changes between the minimum and the maximum flow rates i.e. 0 and 360 $\frac{kg}{h}$.

In Fig.3.10, no variation of time constant against room temperature is recognized. However, the small signal gain decreases with an increase in the room temperature which

seems rational. There is also a slight deviation between the simulation and the analytic results of the time constant. This is due to the first order approximation of $Q(t)$ in calculation of the time constant. In simulations, the time constant is taken as the time when 0.63 of the final value is met while in calculations, it is derived based on the tangent to $Q(t)$ and its first order approximation.

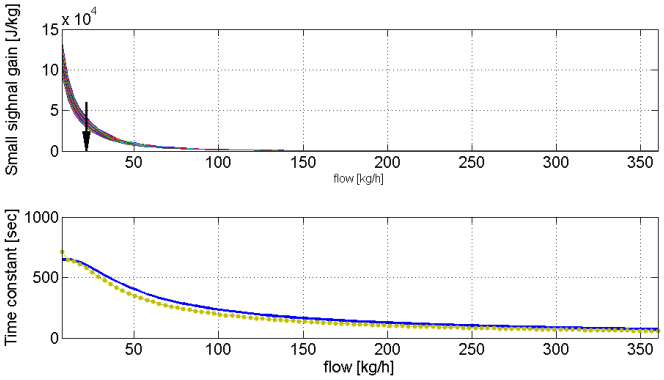

Figure 3.10: K_r and τ_r deviations against flow rate and room temperature variations. The direction of air temperature increase is shown via an arrow. The results are shown for both simulation (dotted) and analytic (solid) results. Comparing the result of analytic solution with simulation, the system gain is the same throughout all operating points, however there is marginal variations in the system time constant. This is due to employing the best 1^{st} order fit of $Q(t)$.

In the next section, we will design a gain scheduling controller based on the developed radiator LPV model.

3.6 Gain-Scheduled Controller

In the previous section, we developed a linear parameter varying model of the radiator instead of the high-order nonlinear model (3.1). To control the system, among various possible control structures, a gain scheduling approach is selected which is a very useful technique for reducing the effects of parameter variations [ÅW08].

The term of flow adaptation, here, is chosen to further emphasize on the operating point-dependent controller. The main idea of designing an adaptive controller is to transform the system (3.9) to one which is independent of the operating point. The controller is designed for the new transformed system which is a linear time invariant (LTI) system. The block diagram of this controller is shown in Fig. 3.11.

The function g is chosen in a way to cancel out the variable dynamics of the radiator and to place a pole instead in a desired position. The desired position corresponds to the high flow rate or high demand condition. In this situation, the radiator has the fastest dynamic. Therefore, the simplest candidate for the linear transfer function g is a phase-lead structure, as follows:

$$g(K_r, \tau_r) = \frac{K_{hd}}{K_r} \frac{\tau_r s + 1}{\tau_{hd} s + 1} \tag{3.32}$$

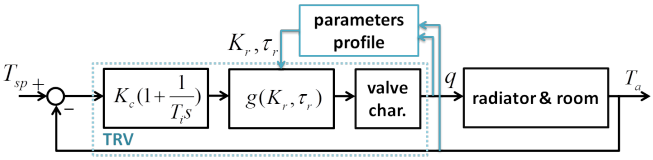

Figure 3.11: Block diagram of the closed loop system with linear transformation.

in which K_{hd} and τ_{hd} correspond to the gain and time constant of radiator in the *high demand* situation when the flow rate is about maximum. Consequently, the transformed system would behave always similar to the high demand situation. By choosing high demand as the desired situation, we give the closed loop system the incentive to place the dominant poles as far as possible from the imaginary axis, and as a result as fast as possible.

The controller of the transformed Linear Time Invariant (LTI) system is, therefore, a fixed PI controller. The rationale for choosing a PI controller is to track a step reference with zero steady state error. Parameters of this controller is calculated based on the Ziegler-Nichols step response method [ÅH95]. To this end, the transformed second order control-oriented model i.e.

$$\frac{T_a}{q} = \frac{K_a K_r}{(1+\tau_a s)(1+\tau_r s)} \tag{3.33}$$

is approximated by a first-order system with a time delay as follows:

$$\frac{T_a}{q}(s) \quad = \quad \frac{k}{1+\tau s} e^{-Ls} \tag{3.34}$$

The time delay and time constant of the above model can be found easily by looking into the time response of the second-order model (3.33) to a unit step input q. The step response is derived and shown in the following:

$$T_a(t) = K_{hd} K_a (1 + \frac{\tau_{hd}}{\tau_a - \tau_{hd}} e^{\frac{-t}{\tau_{hd}}} + \frac{\tau_a}{\tau_{hd} - \tau_a} e^{\frac{-t}{\tau_a}}) q(t) \tag{3.35}$$

in which $q(t) = u(t)$ is the unit step input.

The apparent time constant and time delay are calculated based on the time when 0.63 and 0.05 of the final value of T_a is achieved, respectively. The positive solution of the following equation gives the time delay when $\chi = 0.05$ and the time constant when $\chi = 0.63$.

$$(2-\chi)t^2 - 2\chi(\tau_{hd} + \tau_a)t^2 - 4\chi\tau_{hd}\tau_a = 0 \tag{3.36}$$

The nonnegative solution of the above equation for each χ gives τ and L. Consequently, PI parameters comes out of the Ziegler-Nichols step response method. The parameters are the integration time $T_i = 3L$ and proportional gain $K_c = \frac{0.9}{a}$ with $a = k\frac{L}{T}$ and DC gain $k = K_{hd} \times K_a$.

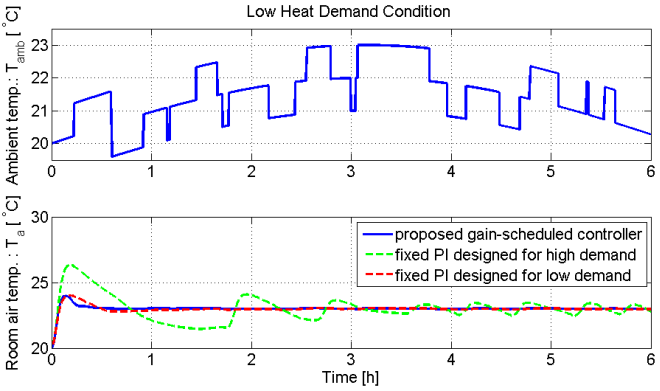

Figure 3.12: (Top) ambient temperature, (bottom) room temperature for three controllers. The results of simulation with flow adaptive controller together with two fixed PI controllers are shown. The PI controller designed for the high demand situation encounters instability in the low heat demand condition.

3.7 Simulation Results

The proposed flow-adaptive controller is designed for the case study described earlier in Sec. 3.2. The controller is applied to simulation models of room and radiator i.e (3.6) and (3.1). Parameter values used in simulations are listed in Table 3.1. PI controller parameters are obtained as $K_c = 0.01$ and $T_i = 400$. Ambient temperature is considered as the only source of disturbance for the system. In a partly cloudy weather condition, the effect of intermittent sunshine is modeled by a fluctuating outdoor temperature. A random binary signal is added to a sinusoid with the period of 12 hours to model the ambient temperature.

Simulation results with the designed controller and the corresponding ambient temperature are depicted in Fig. 3.12 and Fig.3.13. The results are compared to the case with fixed PI controllers designed for both high and low heat demand conditions.

The simulation results of the proposed control structure show significant improvement in the system performance and stability compared to the fixed PI controller.

3.8 Symbols and Parameters Amounts

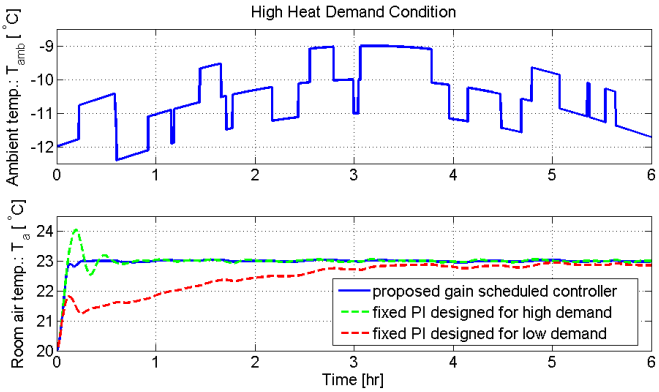

Figure 3.13: (Top) ambient temperature, (bottom) room temperature for three controllers. The results of the simulation with flow adaptive controller together with two fixed PI controllers are shown. The PI controller designed for the low demand condition is very slow for the high demand situation.

Table 3.1: Parameters Amounts

Room Parameters		Radiator Parameters	
A_e	$56\ m^2$	A_r	$1.5\ m^2$
A_f	$20\ m^2$	C_r	$3.1 \times 10^4\ \frac{J}{°C}$
C_a	$5.93 \times 10^4\ \frac{J}{°C}$	c_w	$4186.8\ \frac{J}{kg\,°C}$
C_e	$5 \times 10^4\ \frac{J}{°C}$	N	45
C_f	$1.1 \times 10^4\ \frac{J}{°C}$	n_1	1.3
U_e	$1.2\ \frac{W}{m^2\,°C}$	q_{max}	$0.015\ \frac{kg}{s}$
U_f	$1.1\ \frac{W}{m^2\,°C}$	T_s	$70\ °C$
		V	$5\ \ell$

Table 3.2: Symbols and Subscripts

Nomenclature	
B	heat transfer coefficient between two nodes in an electric circuit $(kJ/s^{\circ}\mathrm{K})$
C	thermal capacitance $(J/kg\,^{\circ}\mathrm{C})$
c_w	water specific heat $(J/kg\,^{\circ}\mathrm{C})$
B_r	equivalent heat transfer coefficient of radiator
K	gain parameter of a first order control oriented model
L	time delay
N	number of the radiator sections
n	number of a specific element of radiator
Q	dissipated heat (W)
q	water flow rate (kg/sec)
T	temperature $(^{\circ}\mathrm{C})$
Φ_0	radiator nominal power
δ	opening degree of the valve
τ	time constant parameter of a first order control oriented model
Subscripts	
a	room air temperature
amb	ambient
e	envelope
f	floor surface
hd	high demand
in	temperature of the influent water to the radiator
out	return temperature of water
r	radiator
s	solar
sp	setpoint

4 Energy and Cost Minimizing Controller for the Central Heating System

4.1 Background and Objectives

Thermal comfort is the prime requisite for a building HVAC system that directly influences the productivity and thermal satisfactory of the occupants. Fortifying buildings' insulations have cut down the heating associated energy costs on one hand, but increased demands for sophisticated control solutions because of the more need for ventilation and direct sunlight control on the other hand. Dwelling's HVAC services have to work in harmony with the specific building envelop system in order to preserve balance between energy consumption and thermal comfort. This is feasible via an integrated control strategy which takes into account all the influencing dynamics on the indoor climate.

A cost efficient energy management is the other main concern for both electric power consumers and producers. A cut down in the electricity bill is subject to load scheduling according to power availability. The more available the power is the less expensive it would be sold by the electricity market. On the other hand, load shifting will contribute to regaining balance between power supply and demand in the grid. Continuously increasing emergence of green power, produced by renewable resources, generally makes the grid more prone to grid imbalances [MK10]. Regaining balance in the grid requires that the power consumption by the storage devices e.g. electric vehicles, heat tanks and other heat/cool buffers for instance the building thermal mass can be adjusted to utilize surplus of cheap power efficiently.

The purposes of this chapter is to propose an indoor climate controller that minimizes the energy consumption and its associated cost. The structure have to be fitted to the current infrastructure of the HVAC systems with single loop thermostatic controllers at the lowest level.

This chapter presents an integrated framework for energy and cost optimization of the specified hydronic heating system, see Fig. 1.11. We optimized the heat pump's efficiency by minimizing the supply temperature and shifting the power consumption according to variations of the ambient temperature. The principal idea of the optimization method is developed first in [TSR11b] and tested via experiments that is documented in [TSR12b]. Optimization of electricity price is also feasible by load shifting. This is maintained by incorporating the concrete floor as a heat reservoir to store heat, [TSMR11,

TSRM12]. By deferring daily power consumption from price-peak times to off-peak periods, residents can cut down electricity bills. According to [Jen11], approximately half of the economic potential for saving in annual electricity bills, can be achieved by postponing power consumption in each day for a couple of hours.

In the subsequent sections, we described the function of each subsystem and their models in Section 4.2. A two-layer hierarchical controller and formulation of the optimization problem is introduced for the purpose of energy minimization in Section 4.3. A cost minimizing MPC formulation is proposed in Section 4.3.6. Section 4.4 presents the simulation results for different scenarios and purposes. Finally, in Section 4.5, we reported the test results that serve as a proof of concept for the optimization hypothesis.

4.2 System Overview and Subsystems Modeling

The entire system is illustrated formerly in Chapter 2, please see Fig. 2.1. In the next two sub-sections we introduce modeling of floor heating and heat pump systems and give a background on their modeling and control methods.

4.2.1 Hydronic Radiant Floor Heating

Hydronic radiant floor heating systems have been used in Europe for decades in domestic, commercial and industrial applications [Lei91]. Its popularity in Europe increased by standardizing the plastic pipes for floor heating in late 1970s, especially in Switzerland, Austria, Germany and Scandinavian countries [Ole02]. The mainly used plastic pipes are PEX-types, today. Its popularity is partly due to the higher level of comfort that such systems provide compared to conventional 100% forced air heating systems, not to mention in a noise-free operation. Much of the interest in hydronic floor heating systems stems from the reduced energy consumption [HHK95] to be about 30% as suggested by [Buc89]. According to [Ole83] a floor heating system can reach the same level of operative temperature at a lower air temperature compared to the air-forced heating system. This will result in a lower ventilation heat loss in buildings with high ventilation rates.

A floor heating system, typically consists of a circulation pump that maintains the required flow of heated water to a network of sub-floor pipes embedded into the concrete floors of the heated rooms. Each room has a separate Pulse Width Modulation (PWM) valve controller which adjusts the valve's opening, and by this mean regulates the room temperature. Dissipated heat power depends both on the flow rate and the water temperature. The latter is adjusted by a separate controller, which regulates the heat source temperature. Hot water could be supplied by an oil furnace, district heating network or a heat pump. Minimizing the forward temperature decreases the heat loss in the pipe lines and increases the efficiency of the heat exchangers. Especially, the heat pump's efficiency increases by reducing the temperature of the condenser side i.e. the forward temperature.

Spite of the very promising features of the floor heating, for instance the thermal comfort sensation of a warm floor surface, the low temperature supply water or the potential load flexibility, it reacts very slowly to the heat demand signals. The long response time of the floor heating could arise thermal dissatisfaction. Specifically when a disturbance influences the indoor climate with a dynamic much faster than that of a Concrete Floor Heating (CFH), regaining thermal satisfaction only by using CFH could be troublesome. Fortunately, this problem can be resolved by a suitable controller design. There are many

investigations in the literature which address this issue; [TLT07] proposes a cascaded controller with the inner loop controlling the sub-floor temperature and the outer loop controlling the heated room temperature. The sub-floor temperature is estimated based on measurements of the room and the return water temperature and the distributed model of the concrete sub-floor. The conclusion was that the concrete temperature was controlled in a fast and precise way without overshoot or exceeding the floor temperature limitations. A new algorithm for Generalized Predictive Controller (GPC) is described in [Che02] and applied to a radiant floor heating system. A simulation study compares GPC with on-off and PI which confirms a superior performance of GPC in terms of response speed, minimum offset and on-off cycling frequency.

However, all of the above mentioned methods potentially mitigate the influence of the predicted/forecast disturbances, for instance foreseen outdoor temperature and wind, solar radiation, future heat demands or occupants' activities. On the contrary, unexpected disturbances e.g. opening/closing a door or window or unpredicted indoor activities can not be eased by the proposed control schemes. One approach to reduce thermal dissatisfaction is to employ other heating/ventilation/cooling facilities in combination with the floor heating. However, this idea does not fall into the scope of this PhD study and is postponed to future investigations.

In this project, we use the traditional PI controller as a room temperature controller while ruling the set-point temperature by an external loop to the PI controller. In the external loop a MPC makes decision about setpoint temperature based on the user-specified comfort level, measurement of the room temperature, the flow rate, the available building model and disturbance measurements/predictions. This way, the impact of the predicted disturbances are eliminated to a very good extent.

4.2.1.1 Dynamical Model

The considered floor heating has a serpentine piping with the pipes embedded into a heavy concrete sub-floor as shown in Fig. 4.1. Heat flux from pipes exterior is considered only upward. Employing a similar modeling as radiator, the distributed lump model is governed by:

$$C_n\dot{T}_n = c_w q(T_{n-1} - T_n) + B_n(T_{f_2} - T_n) \tag{4.1}$$

with T_n as the nth section's temperature and T_{f_2}, the immediate layer of concrete above the floor heating pipes which is assumed the same all over the sub floor. Distribution of lumped elements are considered to be alongside the pipe. Heat propagation from the pipes exterior surface is considered to be only upward toward the floor surface. We have also assumed that heat is transferred between two sections only by mass transport, implying that convective heat transfer is neglected. Another assumption is that the pipes material and water are at the same temperature. Neglecting the thermal resistance of the pipe, heat transfer coefficient, B_n would only depend on thermal conductivity of concrete, i.e. $B_n = U_{f_2}A_n$ in which A_n is the effective area of the nth section of the concrete slab just above the corresponding pipe section. U values are selected based on thickness and composition of concrete floor layers, [ASH90].

An important assumption in the above modeling is that a uniform temperature is assumed all over a concrete layer. Although this is a very simplifying assumption, it turned

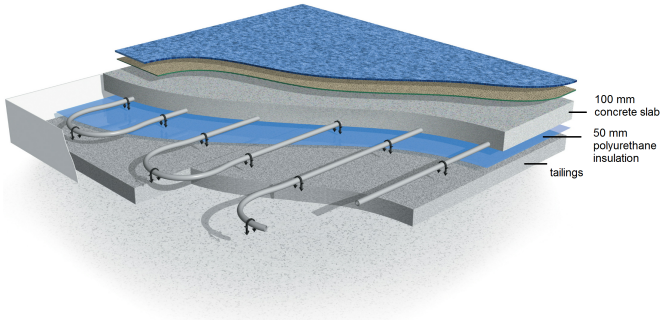

Figure 4.1: Serpentine hydronic floor heating pipes casted in a concrete slab sub-floor [Bui12].

out to be precise enough to provide a benchmark for simulations in order to test the developed control solutions.

Heat transfer from the pipes exterior to the sub-floor concrete layer just above the pipes is achieved by integration over all the sections' heat transfer i.e.:

$$Q_{fh} = \sum_{n=1}^{N} B_n(T_n - T_{f_2}) \tag{4.2}$$

The employed simulation model for floor heating is inspired by a similar radiator model addressed in [Han97] and the floor heating model proposed in [HHW95].

Floor heating valve has an on-off thermal wax actuator. This actuator is controlled by pulse width modulation signal in practice. However, the actuation time of this wax actuators is far less than the floor heating time constant by a fraction of 360. Therefore, without loss of generality, we designed a floor heating controller in continuous time.

4.2.1.2 Control Oriented Model

A low-order, yet sufficiently accurate model of the floor heating dissipated heat is presented for the purpose of controller design. A single loop controller is designed for maintaining the room's setpoint by means of regulating the flow of hot water in the floor heating pipes.

A room's temperature pertains to the dissipated heat by floor heating via a 3^{rd} order transfer function which can be approximated with a first order transfer function which is sufficient for control purposes. The transfer function between the floor heating output and the hot water flow is:

$$\frac{Q_{fh}}{q_{fh}}(s) = \frac{k_{fh}}{1 + \tau_{fh}s} e^{-\tau_d s} \tag{4.3}$$

Constants k_{fh}, τ_{fh} depend on the hot water forward temperature. However, this dependency does not cause significant variations in the parameters, thus we assumed constant parameters. The relationship between room temperature and the flow rate also can be stated as a reduced order model as given in the following:

$$\frac{T_i}{q_{fh}}(s) = \frac{k_i}{(1+\tau_i s)(1+\tau_{fh} s)} e^{-\tau_d s} \tag{4.4}$$

T_i represents room#i temperature, k_i and τ_i the time constant and equivalent gain of the system.

4.2.2 Geothermal Heat Pump

Renewable energy sources have gained more attention recently due to a surge for energy savings and the quest for mitigation of global warming. Most of these resources are intrinsically low temperature make it difficult to fit into old building infrastructures that have huge thermal losses. However, they potentially provide a good thermal comfort to well insulated building spaces. Design of the heating emitters have to be matched with the low-temperature nature of these resources. A heat pump is an ideal heat source to combine with radiant floor heating systems as the water temperature have to never exceed a certain limit in order to prevent damages to the floor-surface covering in high temperatures.

According to the Environmental Protection Agency (EPA), Ground-source Heat Pump (GHP) systems are one of the most energy efficient, environmentally clean, and cost-effective space conditioning systems available. About 70% of the energy used by a GHP system is from a renewable energy source i.e. the ground. High efficiency GHP systems are on average 48% more efficient than gas furnaces, 75% more efficient than oil furnaces, and 43% more efficient when in the cooling mode [LZH93]. However, a recent study which is conducted in the UK has argued that heat pumps have higher environmental impacts than gas boilers due to the use of electricity [GA12] with a higher impact by air source heat pumps (AHP) compared to GHPs and water source heat pumps.

A heat pump uses the same mechanical principles as a refrigerator and transfers the heat from a cooler medium, e.g. the ambient air, shallow ground or water to the building which is at a higher temperature. An electrically driven heat pump can generate 3-4 kWh of heat from 1 kWh of electricity for driving the heat pump's compressor. A geothermal heat pump system is shown in Fig. 4.2. There are typically two hydronic and one refrigerant circuits interconnected through two heat exchangers. These are: 1) the underground buried brine-filled – mixture of water and anti-freeze – pipes with a small circulating pump; 2) the refrigerant-filled circuit, equipped with an expansion valve and driven by a compressor which is called heat pump; and 3) a hot water tank that supplies the hot water to the indoor under-surface grid of pipes with another small circulation pump which distributes heat to the concrete floor of the building, or to the radiators [SH02, MAB04].

The underground temperature is fairly constant during several days and slowly varies with an annual pattern. This slow dynamic is due to the huge capacity of the ground and is an advantage to the air-source heat pump with the brine pipes exposed to the ambient air. The higher temperature at the evaporator side of the refrigerant circuit potentially increases the heat pump's Coefficient of Performance (COP) in the cold season. It is also an advantage in the warm season when heat pump works in reverse to cool down the building; because underground temperature is cooler than the ambient air in summer. Therefore, we specifically focus on geothermal-type heat pumps and assume a constant brine temperature all over the cold season.

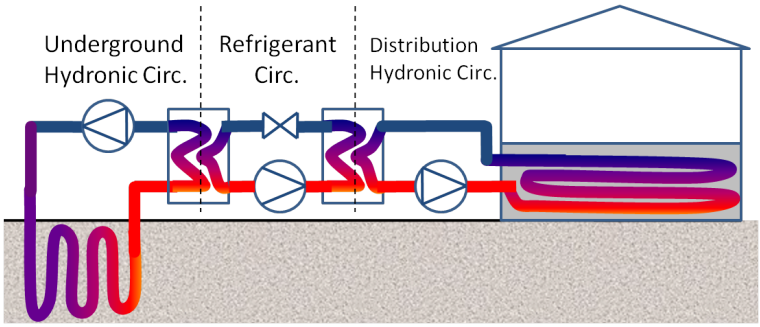

Figure 4.2: An under-floor heating system with a geothermal heat pump.

Annual performance of a GHP is generally higher than an AHP. An experimental-simulation study conducted in Johannesburg, South Africa by [SM01] shows an annual improvement of 14% in a GHP's COP compared to that of an AHP. Especially the improvement at low ambient air temperatures turned out to be more than 20%. However, the efficiency improvements are subject to both the depth of the boreholes of GHP and also the local annual temperature variations. In a different study, [KHP10] shows that a combination of solar collectors and the GHP could increase the annual efficiency of the heat pump, because the net annual heat extraction from the ground is reduced by recharging the boreholes from solar heat.

The COP of a heat pump is a function of temperature lift i.e. the temperature difference between the heat source and the output temperature of the heat pump. In the ideal condition, COP is determined solely by the condensation temperature and the temperature lift (condensation-evaporation temperature) [RET05]. The ratio between the actual and the ideal COP is defined as the *Carnot Efficiency* which varies between 0.3 to 0.5 for small electric heat pumps and 0.5 to 0.7 for large, very efficient electric heat pump systems [RSIT07]. Operating performance of the heat over the season or year is called seasonal/annual performance factor (SPF). It is defined as the ratio of delivered heat to the overall energy supplied over the season/year [WA03]. The vendor of a heat pump usually indicates the actual COP variations in the heat pump's data sheet. Solar assisted heat pumps have recently been of great interests and benefits as they boost the heat pump efficiency by decreasing the temperature lift between evaporator and condenser [ALPV08, CA11]

4.2.2.1 Dynamical Model

The heat pump's dynamic is much faster than the fastest dynamic in the building. Therefore, we consider it as a static system. The relationship between the transferred heat from the condenser to the water in the distribution circuit, Q_b, and the heat pump's electrical work, W_c, is given by:

$$W_c = \frac{Q_b}{\eta_{cop}} \tag{4.5}$$

with η_{COP} representing the coefficient of performance. This term depends on the temperature difference between the evaporator i.e. brine water temperature, and the condenser

i.e. floor heating supply temperature. COP as a manufacturer parameter is usually documented in the heat pump data sheet. We have used a COP curve, see Fig. 4.3 based on the statistical data given in [Hee11]. The aforementioned models comprise the plant's simulation model.

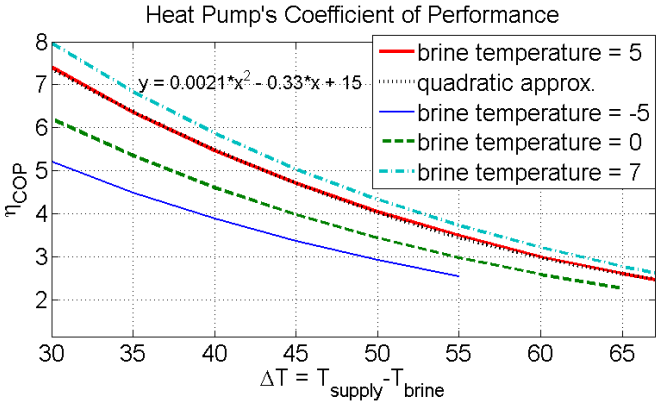

Figure 4.3: Statistical data showing the relation between $T_{for} - T_{brine}$ and the heat pump's COP. x represents the temperature lift, $T_{for} - T_{brine}$.

Assuming a geothermal heat pump with deeply buried pipes as the brine circuit, temperature at the brine side is assumed to be constant during the heating season. Presuming $T_{brine} = 5\,^{\circ}\mathrm{C}$, $\eta_{cop}(T_{for})$ is formulated by interpolation in the following:

$$\eta_{cop} \quad = 0.0021T_s^2 - 0.35T_s + 16.7 \tag{4.6}$$

4.3 Control Strategy for Optimal Cost and Energy Consumption

4.3.1 Background and Related Literature

Most commercial control solutions for heat pump-source heating systems are based on feed-forwarding the ambient temperature. The flow temperature in the building distribution pipes is adjusted based on an *a priori* known adjustment curve, see Fig. 4.4 [Dan08] which is suggested by a heat pump manufacturer. The installer of the heat pump might change the standard slope and offset according to the building specific heat demands, not to mention that a coarse conservative adjustment of the curve, which is usually the case, will deteriorate dramatically the heat pump's efficiency compared to a precise calibration. More power consumption would be the immediate result of an imprecise calibration. This is because the heat pump would not work with the potential highest efficiency which can only be maintained if it is controlled based on feedback from the real heat demand. Some vendors have made the calibration an automatic procedure as a preparatory learning phase.

Control of the heat pump using feedback of the actual heat demand is recently more addressed in the literature, [Ole01, YPLT07, CMA10, HPMJ12, CA11, KH11, ATT12]. In [YPLT07], temperature of a single room case study is controlled directly by controlling the feed flow temperature while the floor heating valve is fully opened. Several classical

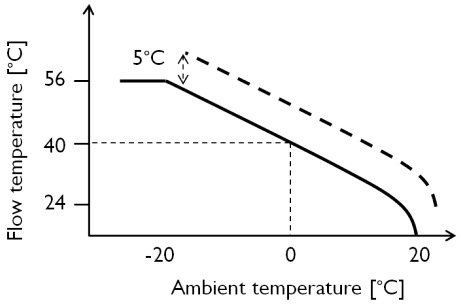

Figure 4.4: An adjustment curve showing the variations of the flow temperature against the ambient temperature. In the conventional feed-forward approach of heat pump control, an overhead might be added to the original curve by the installer, depending on the particular building heat demand (the dash).

controllers namely bang-bang, proportional integral derivative (PID)-types, PID with pre-filtering of reference input are applied to the actuator of the flow temperature regulator and the performance of the controllers are compared to each other. It turned out that PID with Pre-filtering generates the best system performance in terms of the smallest overshoot, fast response, highest transient COP, the least sensitivity to exogenous disturbances and the least power consumption. Despite of the simplicity of the controller, the proposed method is not applicable to a building with multiple temperature zones, each one bearing different heat loads.

Control of a chilled water system using model predictive controller is proposed and compared with the traditional feedback controller in [CMA10]. The developed distributed predictive controller in the context of hydronic system integration provides a novel framework as compromise between 'regulation', 'optimality', 'reliability' and 'computational complexity' [Cha10].

Minimizing the heat pump's output temperature (termed the forward temperature) and by this means the temperature lift will increase the heat pump's efficiency, mitigating the power consumption of the compressor. However, the low water temperature deteriorates the long lag of dissipated heat from the casted-in concrete floor heating pipes, resulting in more thermal dissatisfaction. However, a predictive controller can diminish the system lag by taking the future heat demands into consideration. Learning based control schemes and model-based controllers are two general control approaches which are investigated extensively in the recent studies for this application [HNF$^+$99, OPJ$^+$10, CA11, HHS$^+$12, CPSS12]. MPC facilitates tracking of set-point profile by systematically incorporating measurement and/or forecast of disturbances and future set-point signals. In the specific application of building HVAC control, the predictable disturbances include variations of ambient temperature, solar radiation and wind speed.

Energy minimizing, or in other words performance maximizing controllers of the building HVAC systems potentially contribute to consumption cost reduction. On the other hand, energy management especially for the purpose of consumption price minimization does not put force on improving performance of the system, but instead on rescheduling the consumption based on daily variations of the electricity price. As an ex-

ample, electricity price is usually higher during day than night time, therefore buffering energy in the hot water tanks or as heat in the concrete floor during night and consuming it in day time is economic. However, from the efficiency point of view, the heat pump's COP especially for AHPs is higher in daytime than night time encouraging to store heat in daytime rather than night time, that is in contradiction to the price-based energy scheduling.

Economic MPC [RA09, DAR11] can deal with this trade off systematically by incorporating both price signal from the grid utility and weather data [HEJ10, OUP+10]. In [HPMJ12], the heat pump's COP assumed to be fixed and the power cost is optimized by shifting the heat demand from peak to off-peak loads. However, the amount of power savings by optimizing COP is not negligible at all.

A heavy concrete floor heating system is an ideal heat buffer to store electricity in the form of heat when electricity is cheap and use the stored heat at pick-load times. This way, a domestic consumer can also contribute to regaining the heat balance in the smart grid, [RGZ88, ARBL11, TBS11, PAN+11, MKD12].

4.3.2 Optimization Hypothesis

In order to minimize the power consumption of the heat pump, the heat pump's COP should be optimized. COP is highly dependent on the temperature lift between evaporation and condensation sides. The evaporation temperature i.e. the temperature of the brine side is determined by uncontrollable factors i.e. under-ground or ambient air temperature. On the other hand, the condenser temperature is adjusted such that the building heat demand is satisfied. By minimizing this temperature, the gap between the two temperature is minimized and by this means the heat pump's power consumption. Condenser temperature or the forward temperature of the hot water partially depends on the heat demand of the building. It also depends on the hot water flow rate passing through the heating loops. The transferred heat to the building or equivalently the building heat demand is:

$$Q_b = c_w q_{fh}(T_{for} - T_{ret}) \tag{4.7}$$

Both q_{fh} and forward temperature of the hot water i.e.T_{for} are actuation parameters that determine the transferred heat to the building with the above relationship. The flow rate is adjusted by controlling the floor heating valve's opening and T_{for} by regulation of the heat pump's compressor . For a constant Q_b, if flow temperature decreases continuously, the flow rate increases to reach the maximum capacity of the valve. The minimum forward temperature is attained exactly at this point.

Hypothesis: In a multiple room building, the minimum forward temperature of a water-based heating system coincide with minimal saturation - just in saturation - of at least one of the flow actuators.

The above hypothesis is conceptually proved via experiments and simulations of several case studies in the thesis. This idea was first applied to a multiple-room building with both hydronic radiators and floor heating emitters in [TSR11b], the simulation results showed more than 20% improvement in energy consumption compared to the conventional method of forward temperature control. In the second study [TSR12b] open loop and closed loop tests were performed on a real-scaled uninhabited residential building as a proof of concept.

However, the above stated hypothesis is not novel in general; it has been used before in other systems especially when two actuators are available for both a regulation purpose and minimizing a performance index. Examples of such systems are building ventilation system, district heating substation and many other similar systems. In the first example, flow and temperature of the heated air are the two actuation parameters; in the second, temperature and pressure of the water. However, application of the stated hypothesis to the concerned central heating system was not addressed before in the literature.

4.3.3 A Two-Layer Hierarchical MPC

A hierarchical controller is developed in this chapter to integrate the subsystems and predicted disturbances, Fig. 1.11. Local control loops (modules in black) maintain rooms temperature set-points by adjusting the influent mass flow through the valves. At the higher level an advanced controller take the responsibility of optimizing thermal comfort, energy consumption and orchestrating the local loops by incorporating subsystems models and predicted exogenous disturbances (external loops in blue). The top level minimizes the heating cost by incorporating the electricity price profile that is provided by the electricity market a day ahead.

The block diagram of the closed loop system is depicted in Fig.4.5. We employed a model predictive controller for optimization of the flow temperature. Proportional integral controllers are employed in the single loops to regulate the corresponding room air temperature.

MPC can systematically incorporate forecast data of weather, solar radiation and other predicted disturbances in the optimization procedure. Besides constraint handling, MPC gives systematic feedforward design based on future demands [Ros03]. Therefore we designed a MPC at the top level of the control hierarchy to orchestrate function of the local controller units at the lower level.

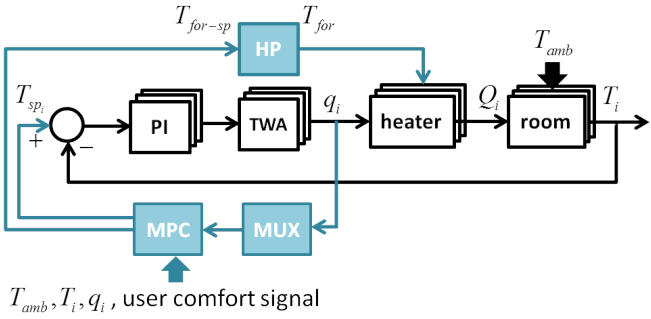

Figure 4.5: The system closed-loop block diagram.

The main role of MPC in Fig. 4.5 is to minimize forward temperature of the feed hot water. To this end, control signals of the hydronic heaters' valves are fed back to the MPC, expressing the associated room's heat demand. The largest heat deamnd is realized using a multiplexer. In the next step, MPC determines the flow temperature based on the highest heat demand in order to push the corresponding valve toward saturation. At this point, to avoid physical saturation of the valve, flow is limited to 90% by putting

hard constraints on it in the MPC design. Otherwise in the case of the valve saturation, no valve capacity is left for compensating exogenous disturbances which means loss of controllability.

4.3.4 Single-Loop Controllers

Each room is heated by only a hydronic radiator or a grid of sub-floor heating pipes. Every heater is controlled locally to maintain the corresponding room's temperature setpoint. Setpoints to the local controllers are determined by the upper level master controller based on the room's future heat demands, its specific dynamics and the weather measurements/-forecast. We designated an adaptive gain scheduled controller as the radiator regulators i.e. a PI and a lead structure as described in the Chapter 3. PI controllers are employed for regulating the floor heating valves, since the nonlinearity is not as high as the radiator. A good performance is still achievable via a simple PI controllers for this part.

Setpoint of forward temperature dictated by the MPC is easily maintained by a PI controller that adjusts the compressor speed efficiently. As the hot water temperature can be regulated much faster than rooms temperatures, we assumed a static relationship between the forward temperature and it reference.

4.3.5 Formulation of the Optimization Problem

The room with the highest heat demand determines the hot water tempearture, based on the proposed optimization hypothesis. Therefore, at every time instance, only one room's dynamics are active as the MPC internal model. Flow rate of this room should be kept at 90% by MPC as described in the control strategy. Thus the purpose is to formulate the MPC such that forward temperature is minimized and the most demanding room's flow rate is kept within some limits. The single loop controller in the internal model of MPC can appear as a PI controller for both radiators and floor heating emitters because flow rate is kept in a certain limited region, around 90%. Therefore the PI for the i^{th} room in the state space form is written as:

$$\begin{aligned} \dot{\xi} &= \frac{K_p}{T_{int}}(T_{sp_i} - T_i) \\ q_i &= K_p(T_{sp_i} - T_i) + \xi \end{aligned} \tag{4.8}$$

with ξ as the auxiliary state. The parameters of the PI controller are chosen based on the plant step response around the desired operating point which is $q = 90\% q_{max}$.

The prediction model of MPC can be formulated as a linear time invariant system in spite of the bilinear term in the system equations. In the vicinity of the desired operating point i.e. $q = 0.9 q_{max}$, the bilinear term, $Q_f = c_w q(T_{for} - T_{ret})$ is linearized. Hence the internal model of the MPC controller in a state space form is:

$$\begin{aligned} \dot{x} &= Ax + B_u u + B_d d \\ y &= Cx + D_d d \end{aligned} \tag{4.9}$$

with $x = [T_i, T_{e_i}, T_{f1_i}, T_{f2_i}, T_{w_i}, \xi]^T$, $u = [T_{for}, T_{sp_i}]^T$, $y = [T_i, q_i]^T$, and $d = [T_{amb}, T_j]$. Matrices A, B, C and D are derived based on (4.9) and (4.8). T_i is measured in each room separately and, the other states could be estimated using a Kalman

state observer and ξ is known from the local control signals. Return temperature of water is approximated with T_{f2_i} which is accurate enough for the control purposes. The step size, T_{for} for discretization is the same as the data sampling rate in the tests.

The optimal problem is formulated in the following. The prediction model is the dynamics of a single zone corresponding to the highest heat demand in the entire building.

$$\begin{aligned}
\min_{T_{for},T_{sp_i}} \quad & \sum_{k=1}^{N} \quad |T_{for}(k)| + \nu_1|\Delta T_{for}(k)| + \nu_2|T_i(k) - T_{cmf_i}(k)| + \nu_3|\Delta T_{sp_i}| \\
s.t. \quad & x(k+1) = Ax(k) + B_u u(k) + B_d d(k) \\
& y(k) = Cx(k) + D_d d(k) \\
& 0 \leq q_i(k) \leq 0.9 q_{max} \\
& T_{min} \leq T_{for}(k) \leq T_{max} \\
& -TT \leq T_{sp_i}(k) - T_{cmf_i}(k) \leq TT
\end{aligned} \tag{4.10}$$

with N as the prediction horizon. In the cost functional, $T_{cmf_i}(k)$ stands for user-defined comfort temperature at the time instant $t = k$. T_{sp_i} and T_{for} are the manipulated variables. We also penalized the manipulated variables rates of change. T_{sp_i} is the manipulated variable that must be bounded within comfort levels defined by the user. TT stands for *Thermal Tolerance*. Flow is bounded by two upper and lower hard constraints in order to avoid physical saturation of the valves. The Upper and lower limits on the flow temperature are to protect the floor surface material from thermal defects.

4.3.6 Economic MPC for Cost Minimization

Another *a priori* knowledge which is efficient to be included in the decision making process is the electricity price signal. Knowing this signal in advance would be economically desirable for domestic consumers and helpful in enhancing the electric grid balance. The main objective is to minimize the power consumption and the corresponding energy price using the extra price profile information. Power consumption by the heat pump's compressor can be formulated as:

$$W_c = \frac{c_w q(T_{for} - T_{ret})}{-aT_{for}^2 + bT_{for} + c} \tag{4.11}$$

with a, b and c defined in (4.6). W_c is positively correlated with forward temperature T_{for} of water. In the above equation, lessening T_{for} does not change the numerator because the mass flow rate will be increased in return, that corresponds with a constant building heat demand. However, denominator will increase as T_{for} decreases (the quadratic approximation function is negative definite until $T_{for} < 83.5$) which consequently leads to reduction of W_c. Therefore, the optimization problem with discretized model (4.9) is

formulated as:

$$\begin{aligned} \min_{T_{for}, T_{sp_i}} \quad & \sum_{k=1}^{N} \quad c_{for}(k)T_{for}(k) + \nu_1|\Delta T_{for}(k)| + \nu_2|T_i(k) - T_{cmf_i}(k)| + \nu_3|\Delta T_{sp_i}| \\ s.t. \quad & x(k+1) = Ax(k) + B_u u(k) + B_d d(k) \\ & y(k) = Cx(k) + D_d d(k) \\ & 0 \leq q_i(k) \leq 0.9 q_{max} \\ & T_{min} \leq T_{for}(k) \leq T_{max} \\ & -TT \leq T_{sp_i}(k) - T_{cmf_i}(k) \leq TT \end{aligned} \tag{4.12}$$

The prediction model is selected according to the dynamics of the room with the highest heat demand. N is the prediction horizon. In the cost functional, the weight $c_{for}(k)$ represents electricity price and $T_{cmf_i}(k)$ stands for user-defined temperature setpoint, both of them at time instant k. T_{sp_i} is the manipulated variable that must be bounded within comfort levels defined by the user. TT stands for *Thermal Tolerance*. We also considered constraints on the manipulated variables rate of change which is not indicated in the above formulation. Supply temperature variations rate is limited to $1\,^{\circ}\mathrm{C}$ and the setpoint temperature modification rate is limited by $0.1\,^{\circ}\mathrm{C}$, both per sample time T_{for}.

4.4 Simulation Results

Our case study is a 54 m^2 apartment which consists of three separate heat zones, i.e. rooms, shown in Fig. 4.6.

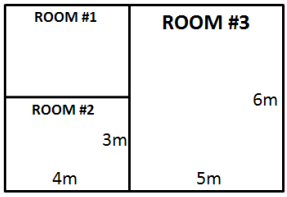

Figure 4.6: Sketch of the apartment with three separate heat zones.

Several simulation scenarios have been conducted on the same case study through the PhD study. We illustrated the results of some of them. There are a large number of parameters taken into account in our simulations which are listed at the end of chapter. It is, though, worth saying that the chosen values for all parameters are in accordance with the typical experimental and standard values.

4.4.1 Energy Minimizing MPC: Three rooms with hydronic radiator and floor heating emitters

The very first simulation results were presented in [TSR11b]. The case study consists three small rooms, see Fig.4.6; two rooms are equipped with hydronic radiators (HR) controlled by thermostatic radiator valves, and the bigger room has a serpentine floor heating (FH) system. A ground-source heat pump (GHP) supplies hot water to the hydronic heaters.

We demonstrated a situation where the house's heat demand varies during several days. While the heat demand of the southern rooms are more than the northern room initially during the cloudy day, the demand peak is shifted to the northern room when solar radiation heats up the southern rooms during the second day that is sunny.

The maximum flow rate is limited here to 90% of the valves' capacity in order not to push the valves into fully-open saturated status. Otherwise, no actuation capacity is left for compensating exogenous disturbances. The reader is referred to [TSR11b] for further details on the simulation graphs. A comparison with the conventional method of heat pump control which was explained previously by Fig. 4.4 shows a significant improvement in the electricity consumption, see table 4.1.

Table 4.1: Comparison of average electric power consumption $[KW]$ between the conventional and the proposed MPC-based controllers

	MPC	Typical	Energy saving (%)
Well insulated	32	37	13.5
Weakly insulated	33	42	21.4

We realized, during the simulations, that the conventional dimensions of radiators do not fit into the combination setup of both floor heating and radiators. Because, radiators are usually dimensioned for a higher feed temperature. They have to be redesigned in order to feed with a low temperature water feed. In the next simulations we only considered floor heating systems as the indoor heaters, however the proposed hypothesis and the designed controller can be fitted to combinations of both heaters.

4.4.2 Energy Minimizing MPC: Three rooms with floor heating

Each room in Fig. 4.6 has a separate grid of under-surface floor heating pipes. As a whole, they form the hydronic distribution circuit of the apartment. The flow of heating water in each room is controlled by a valve. Valve openings are adjustable and are controlled by local PI controllers such that room-specific temperature setpoints are followed in presence of exogenous disturbances.

The circulation pump in the distribution circuit is controlled to regulate the differential pressure across all three parallel branches of the rooms' pipe grids. Thus, the flow through each valve is assumed to be only dependent on its opening percentage.

We have selected the sampling rate of the system equal to the MPC sample time, $T_{for} = 6$min which is chosen based on the operation time of the TWAs, i.e. less than 5min.

This section investigates COP and thermal comfort improvements by including weather forecast data in the optimization process using MPC. We received real weather data recorded by Danish Meteorological Institute (DMI) for 12 days from January 20 to 31, 2012. We assumed a perfect weather forecast 6 hours in advance in the simulations where we included future weather data.

The simulation results for the three-room apartment is shown in Fig. 4.7. However, only the room with the highest heat demand at each time instant affects the results. In other words, the graph is associated with only one room.

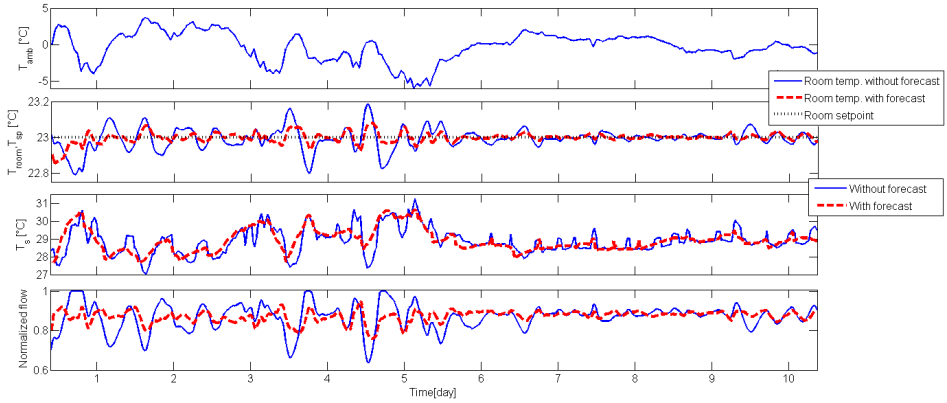

Figure 4.7: Simulation results with and without accurate weather forecast data

In order to quantify comfort improvement, the variance of error in both cases are compared using (4.13). Δt is the evaluation time horizon over which the variance is integrated.

$$\sigma = \int_{\Delta t} \frac{|T_i(t) - T_{cmf_i}(t)|}{\Delta t}\, dt \tag{4.13}$$

It turned out that in case of employing weather forecast, the variance of error was approximately 0.018, while it was around 0.04 when no forecast data was available. Thus, the comfort level is improved by almost 55%.

In order to evaluate the effect of weather forecast on the average COP values and as a result on energy savings, we calculated the average COP over 10 days using (4.6). The average COP with and without weather forecast data is 7.24 and 7.25, respectively. The COP seems degraded around 0.17% compared to the simulation without weather forecast. This does not convey any meaningful outcome in regard to power savings. On contrary, it confirms that despite having a significant positive influence on thermal comfort, weather forecast have a minor impact on the total energy consumption. This is because the effect of weather forecast was diminishing fluctuations in the water temperature; therefore the average water temperature in both simulation scenarios is quite the same which means weather forecast does not change or improve COP, nor the energy consumption.

It is worth noticing that in both scenarios we have considered zero thermal tolerance for the room temperatures. It means that the room temperatures have to be regulated as close as possible to a single temperature level. However, if occupants allow for a slight fluctuations around the desired temperature, the result would be different. This way, consumption can be shifted from night-time to day-time when the same indoor temperature can be maintained with a lower forward temperature. This hypothesis is not simulated here, but calculations show a significant amount of energy savings when the outdoor temperature variations from day to night is considerable and when the heat pump is an air-based one.

Another observation is that saturation of the valves actuators are likely to happen without weather forecast. This makes the system unresponsive to unpredicted disturbances.

This is prevented by incorporating weather data to keep the actuators within the limits.

4.4.3 Economic MPC: Three Rooms with Floor Heating

4.4.3.1 Minimizing Heating Costs

To satisfy monetary interests of end users, another mechanism is devised in this section to directly affect electricity consumption based on the instantaneous price of electrical power. In this method a list of provisional price values for the coming 24 hours is communicated through the power grid by the power utility provider. Such a price profile is designed in a way to encourage less consumption during peak hours by assigning a higher price. However, the task of the MPC controller at the end user is not to reduce the overall consumption which adversely affects user comfort. Instead, its job is to force the heat pump to consume energy when it is cheap and deprive it of energy consumption when the price is high.

To fulfill its job, the MPC modifies the setpoint of each zone according to the energy price in order to shift the heat demand from peak hours to off-peak periods, based on (4.12). Fig. 4.8 illustrates how it becomes possible to decrease the consumption cost with the same average water temperature and not sacrificing thermal comfort of residents. It shows that the average water temperature is even increased 2.2% in average compared to the scenario when energy is minimized not the cost. COP is also decreased with 1.2% which is due to the increased average water temperature. However, the cost of electricity consumption is reduced by 10% in average which is subject to the Elspot price variations shown in Fig.4.8. Higher fluctuations of the electricity price would lead to much more cost benefits. Also, it is worth mentioning that the comparison is performed against the minimum energy consumption results. Cost efficiency compared to the traditional methods would be much more significant.

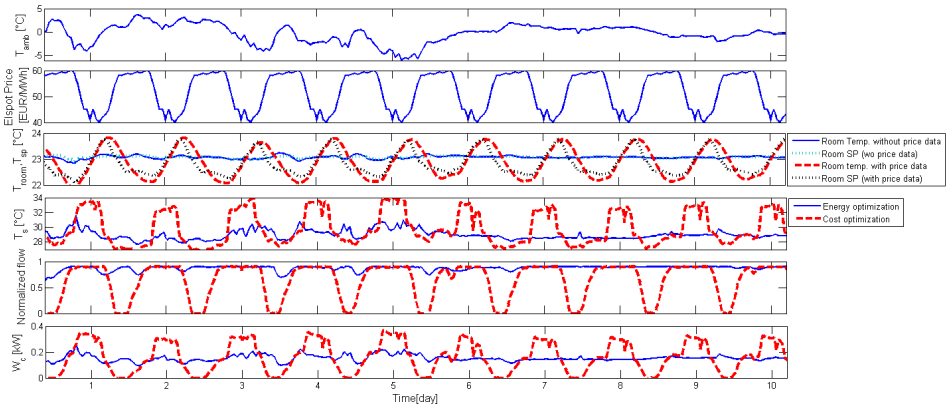

Figure 4.8: Simulation results with and without price profile data

Starting in the steady state, when the price goes down, the actual temperature setpoint in the building increases. Therefore, the valves tend to become fully open. The local PI controllers interpret this situation as saturation and impaired regulation. However, in reality the building is intentionally getting warmer than what the user had desired in order

to store energy for the next peak period. On the other hand, when the price goes up, the actual temperature setpoint in the building decreases. This will result in tightening of the valves on floor heating pipes and preventing expensive power consumption. Deviating from the user-defined setpoint is of course already permitted and approved by the user through adjustment of the thermal tolerance level.

Increase of the average water temperature and by this mean reduction of COP is due to the fact that load shifting for the purpose of cost minimization might not be in the same direction as the energy efficiency. More clearly, the two objectives could be in contradiction depending on the periodic signal of price. From the energy perspective, it is more efficient to shift the load from night to daytime when COP is usually higher. However, electricity price is normally higher in daytime due to load peaks. Therefore it is more economic to consume in night time than during the day. This contradiction has led to a deficit in the system energy efficiency, but to a lower energy cost which is the final target of the optimization problem.

It should also be noted that the constraint on flow may not be replaced with an additional term in the objective function in (4.12). The reason is that the free move of floor heating valves in a permissible interval is essential if the combination of local PI controllers and the MPC controllers should be able to function properly. It is not consistent design if the top level MPC directly regulates both the setpoint and the control signal of PI controllers. At least, one should be free and we have chosen to let PI controllers have complete control on their actuators. This is a consistent hierarchical design.

4.4.3.2 Contribution to Smart Grid Control

The case study of this part is exactly the same as the previous section. The three rooms are equipped with sub-floor heating pipes.

A simple Scenario

Fig. 4.9 shows a typical power setpoint tracking scenario, with power setpoint profile depicted in the first graph. Initial steady state value of 263 W is associated with forward temperature 36.6°C. The outdoor temperature is assumed to be 0°C. Periods of power excess/shortage are assumed to be one hour long with 30 min power surplus of as 50% much as the initial power, followed by 30 min lack of power of the same amount. Thus, the average power consumption is kept unaltered.

The third graph in Fig. 4.9 shows water flow percentage through distribution pipes of individual rooms. At steady state, control valve of room 3 is at 90% flow capacity to follow the temperature setpoint 23°C, when no exogenous disturbances are present. For rooms 1 and 2, 74% of flow range is adequate to reach the desired temperature. The temperature setpoint is assumed to be equal in all three rooms. At $t = 1$ hr, power consumption of the compressor increases. It takes some time for the forward temperature to rise, but all three valves become fully open instantly due to modification of rooms' temperature setpoints to 25°C, corresponding to a thermal tolerance level of 2°C surplus. Note that the user's desired temperature is still 23°C and this setpoint modification is merely in order to facilitate transfer of heat energy into the concrete floor.

At steady state, after approximately 10 hours, i.e. 10 surplus/shortage intervals, it is shown that the valves of rooms 1 and 2 function like on-off devices, keeping room

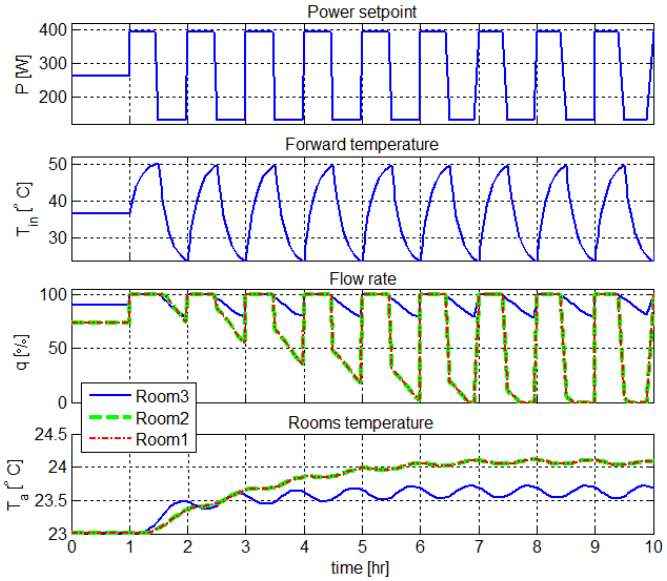

Figure 4.9: A typical power setpoint tracking scenario. 50% power surplus and shortage with duration of half an hour is tolerated by the system, provided that the thermal tolerance level of rooms are set to $+2°C$.

temperatures about 1°C higher than the original setpoint. Average temperature in room 3 is even closer to the original setpoint, but with more noticeable fluctuations. This behavior strongly depends on PI controllers selected parameters.

This simulation shows that the deviation of rooms' temperature due to a specific power setpoint profile were bounded in the permissible user-defined region. This was the consequence of applying an appropriate power setpoint profile, called *feasible* setpoint profile henceforth, combined with the corresponding suitable choice of thermal tolerance level. The power providing company could establish pricing policies to encourage users to set their thermal tolerance level at high values. Then the company can issue a feasible power setpoint profile pursuant to the user's own choice.

Generalized Results

The next question to be answered is how to prescribe a feasible power setpoint profile based on each user's thermal tolerance level. Fig. 4.10 shows a chart that can be used to predict what kind of pulses in the power setpoint profile can be accommodated by the heat pump without disrupting resident's thermal comfort, which means:

$$T_i \in [T_{sp_i} \pm TT], \qquad \forall i = 1, 2, 3 \tag{4.14}$$

in which T_i stands for room temperature, and T_{sp_i} indicates its setpoint. Index i refers to the room number.

As an example, Fig. 4.10 shows that a power surplus pulse with an amplitude of 350 W and a duration of 1 hour can be marginally accommodated by the heat storage of a 54

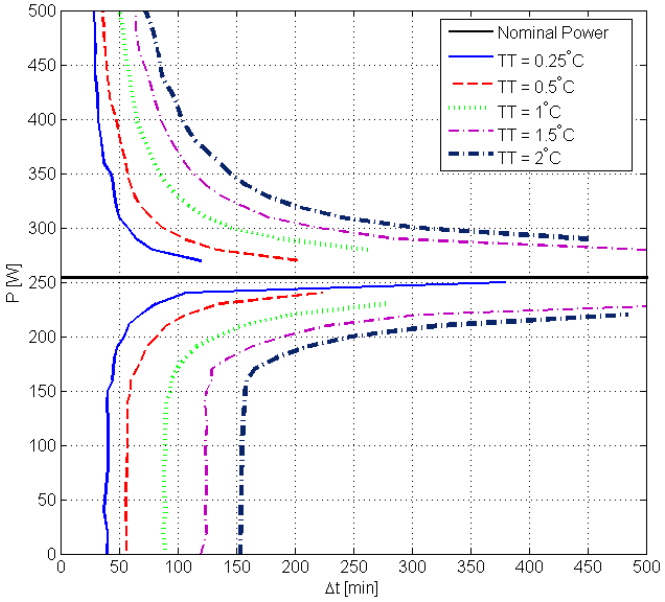

Figure 4.10: Power setpoint generation assistant chart for a 54 m^2 flat, containing several thermal tolerance (TT) levels

m^2 flat, if the temperature tolerance is set to 0.5°C. If either the amplitude or the duration is less, the excess of electrical power can be stored as heat without any difficulty. It is worth saying that the given chart in Fig. 4.10 is dependent on the following parameters:

- Ambient temperature which is assumed to be 0°C
- Local PI controller parameters

Moreover, when a different temperature setpoint is chosen for each room, the nominal heat pump power would be different, i.e. different from 263 W in this case. Thus, the chart should be shifted along the Y-axis accordingly.

4.5 Test Facilities and Experimental Results

Flex House is the test building which described earlier in Chapter 2. In this section we illustrate the results of the conducted experiments. First, a second-order model of a room in the Flex House is identified using the test data. The derived model is further used for simulation-based controller design in [TSR12b]. Two other tests are conducted in order to validate the proposed optimization hypothesis.

Each room has a separate valve controller which regulates the flow to maintain a specific room's setpoint. Thermal wax actuators adjust the valves opening/closing duration based on the Pulse Width Modulation (PWM) signal received from the local control loops. The flow temperature is regulated by another controller at a higher level receiving heat demand signal from the local control loops. Duty cycle of the valves associate with

the rooms heat demand. This is due to a constant differential pressure across the valves. A multi-speed circulation pump in the distribution circuit maintains the fairly constant differential pressure.

As of the test setup, room temperature sensors are positioned in the middle of the rooms, one meter above the floor surface. This provides us with a more accurate measurement compared to a wall-installed temperature sensor.

The hot water is supplied by a heat source, which can deliver hot water at any specified temperature to the floor heating pipes. The time response of this heat source very well simulates a heat pump dynamic i.e. around 15 minutes time constant. The heat source, in fact, consists of a boiler which provides hot water at a fixed temperature and a mixing shunt which is controlled to provide a desired flow temperature by mixing the water feed from the boiler with the return flow of the heating system.

TWAs response time is around 5 minutes to fully open/close the valve. This actuator time is negligible compared to the response time of the concrete embedded floor heating pipes which is around 30 hours. Furthermore, there is a pure time delay transferring the heat from the embedded pipes to the floor surface. We merged the actuators' response time into the system time delay which is around 30 minutes, later on in the simulations.

All the tests have been accomplished in the time interval from November 2011 until February 2012.

4.5.1 Identification of a Room Model Parameters

This section describes a second order dynamical model of a reference room in the building of concern. The model's parameters are further estimated and verified via a set of test data. The model is used later for the control design purposes.

4.5.1.1 Second-Order Model of A Room

A schematic view of the room is depicted in Fig. 2.2. The two layers of concrete floor are merged. The thermal heat capacity of the water pipes is far less than that of the concrete floor, therefore it is neglected in the simplified model. Thermal capacitance of the envelope including walls, partitions and ceiling is merged with that of the room air and furnitures; as well as the corresponding temperatures. Thus, in the thermal network of the building we considered only two nodes representing the thermal capacitances of the envelope plus air and concrete sub-floor plus water. The energy balance equations based on the two main thermal masses i.e. the air-envelope and the concrete floor are as follows:

$$\begin{aligned} C_i\dot{T}_i &= B_{ai}(T_{amb} - T_i) + B_{fi}(T_{f_i} - T_i) + B_{ji}(T_j - T_i) \\ C_{f_i}\dot{T}_{f_i} &= B_{fi}(T_i - T_{f_i}) + Q_{f_i} \end{aligned} \tag{4.15}$$

in which $i, j \in \{1, 2, 3\}$ are the corresponding room index. B represents the equivalent convection/conduction heat transfer coefficient between two connected nodes. For instance, B_{fi} is the conduction heat transfer coefficient between the concrete floor and the room#i. The heat flow is $Q_{f_i} = c_w q_i (T_{for} - T_{ret_i})$, in which temperatures' indices stand for the feed and the return flow temperatures respectively.

4.5.1.2 Parameter Estimation

The 5 parameters, B_{ji}, B_{ai}, B_{fi}, C_{f_i} and C_i of the plant model (4.15) need to be estimated. The first three parameters are obtained using two steady state points and shown in table 4.2. The other two parameters will be achieved by analyzing the transient response. The system time response to a step flow input of the amount $\frac{2}{3}q_{max}$ is depicted in Fig. 4.11 for the reference room. The mass flow temperature is about 40°C.

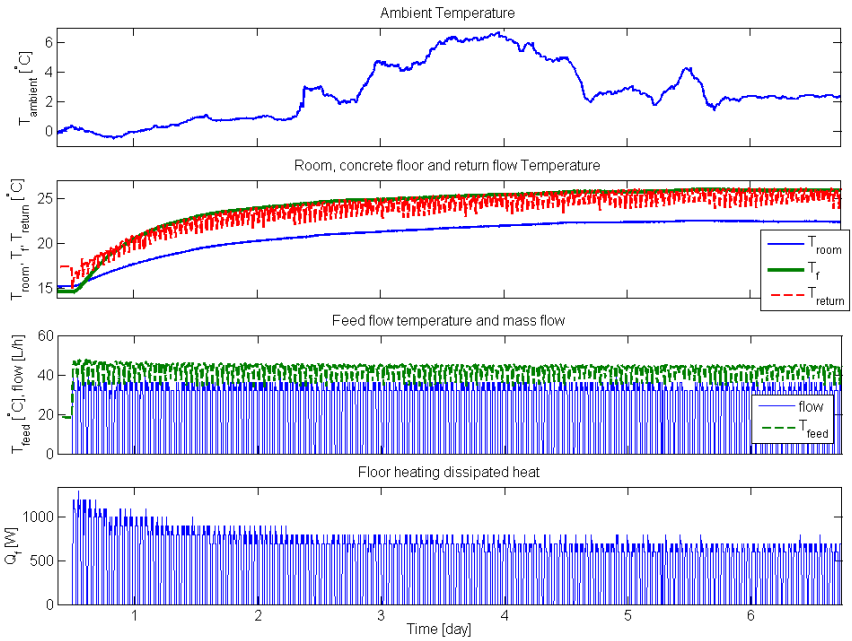

Figure 4.11: The system time response to the step flow input. The system time delay is fairly small compared to the system equivalent time constant. Two main dynamics of the system corresponds to the concrete and envelope thermal mass as considered in (4.15). The adjacent rooms temperature is about 19 °C during the course of experiments.

The concrete temperature is measured at 50 mm depth from the floor surface, in the middle of the reference room. Return and forward temperatures of water are measured immediately at the valves manifold. The fluctuations in these temperatures is correlated with the valve on/off position. When the valve is closed, flow is discontinued and the temperature falls in both feed and return path. Duty cycle of the mass flow and consequently the dissipated heat is fixed to about 67%. The latter is the system direct input which is not a step, unlike the mass flow.Therefore we can not directly extract the model dynamics by examining the room temperature response. Instead we have employed the Least Square (LS) algorithm to estimate the parameters. To this end, the plant model is discretized using backward differentiation and the chosen time step is equal to the data

sampling rate i.e. 2 minutes. The discretized model is:

$$\begin{aligned} T_i(t_k) &= \frac{1}{D_i}\left(B_{ai}T_{amb}(t_k) + B_{fi}T_{f_i}(t_k) + B_{ji}T_{ji}(t_k) + \frac{C_i}{T_{for}}T_i(t_{k-1})\right) \\ T_{f_i}(t_k) &= \frac{1}{D_{f_i}}\left(B_{fi}T_{f_i}(t_k) + \frac{C_{f_i}}{T_{for}}T_{f_i}(t_{k-1}) + Q_{f_i}(t_k)\right) \end{aligned} \tag{4.16}$$

in which, $D_i = \frac{C_i}{T_{for}} + B_{ai} + B_{fi} + B_{ji}$ and $D_{f_i}\frac{C_{f_i}}{T_{for}} + B_{fi}$. t_k is the k^{th} sampling time and $T_{for} = 2min$ is the sampling rate. Summing up the above difference equations makes it appropriate to the LS algorithm setup. The summation is:

$$\begin{aligned} C_i\frac{T_i(t_k) - T_i(t_{k-1})}{T_{for}} + C_{f_i}\frac{T_{f_i}(t_k) - T_{f_i}(t_{k-1})}{T_{for}} = \\ B_{ia}\left(T_{amb}(t_k) - T_i(t_k) + Q(t_k)\right) \end{aligned} \tag{4.17}$$

Defining new terms:

$$\begin{aligned} x(k) &= [\frac{T_i(t_k) - T_i(t_{k-1})}{T_{for}} \ \frac{T_{f_i}(t_k) - T_{f_i}(t_{k-1})}{T_{for}}] \\ y(k) &= B_{ia}\left(T_{amb}(t_k) - T_i(t_k) + Q(t_k)\right) \end{aligned}$$

equation (4.17) at the N sample points looks like:

$$\begin{pmatrix} y(1) \\ y(2) \\ \vdots \\ y(N) \end{pmatrix} = \begin{pmatrix} x_1(1) & x_2(1) \\ x_1(2) & x_2(2) \\ \vdots & \vdots \\ x_1(N) & x_2(N) \end{pmatrix} \times \begin{pmatrix} C_i \\ C_{f_i} \end{pmatrix}$$

with N as the number of total data samples. The LS solution for the parameters $[C_i \ C_{f_i}]^T$ will be $(X^TX)^{-1}(X^TY)$, in which $Y_{N\times 1}$ is the array composed of y(k) and $X_{N\times 1}$ is the matrix composed of $[x_1(k) \ x_2(k)]$ for k=1,...,N. The estimated parameters are shown in table 4.2. Fig. 4.12 compares the measurement data with both estimation and validation results for the room and concrete temperatures in three different assignments of data. Once, we picked all the data only for estimation and no validation. Second, we picked the first 2/3 portion of the data as for estimation purpose and the last 1/3 as for validation. We swapped the sets in the third test. All the results are shown in the following illustration and table 4.2.

The estimated parameters are chosen based on the set1 results which seems to be more accurate in average. The results of this section are further exploited for simulation and controller design purposes in the rest of the paper.

4.5.2 Open-Loop Test

We find the minimum required flow temperature using a bisection algorithm via an open loop test. The rooms' temperature are regulated using an on/off controller. The proportion of on-time to an interval or period of time, although not fixed, is recognized and defined as duty cycle.

Table 4.2: Estimation and Validation Results:Three sets of estimations are illustrated: (set0) all the data is used only for estimation, (set1) first 2/3 of data is used for estimation and the next third for validation, (set2) first 1/3 of data is used for validation and the next 2/3 for estimation.

	Estimated Parameters					Mean Squared Error	
	C_i	C_{f_i}	B_i	B_{fi}	B_{ji}	Estimation error	Validation error
set0:	1394	5915	9.3	115.6	62.1	0.1226	NA
set1:	1305	6137	9.3	115.6	62.1	0.1247	0.196
set2:	470	6278	9.3	115.6	62.1	0.1551	0.2591

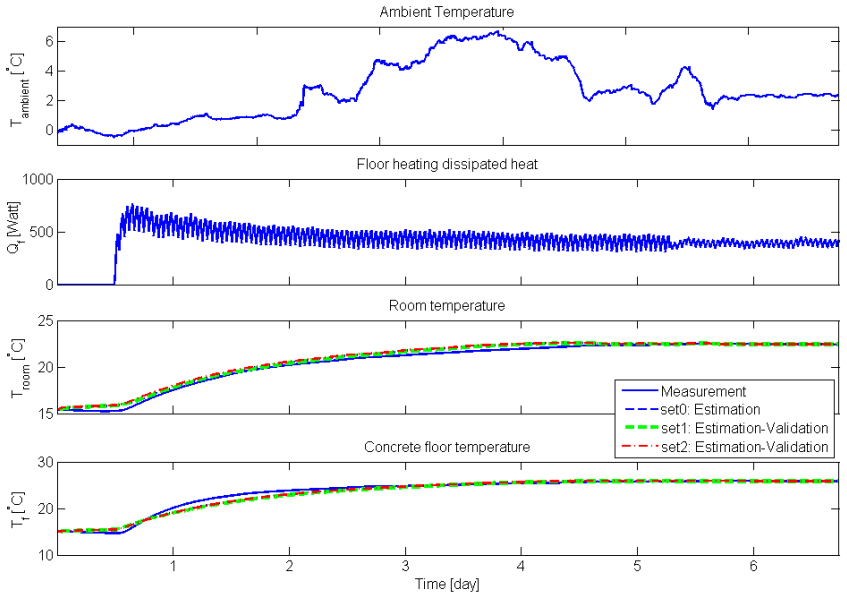

Figure 4.12: Measurement, estimation and validation results to the input heat. The mean squared estimation and validation errors of both variables for the three situations are shown in table 4.2.

First we choose a high enough feed flow temperature which corresponds to a moderate flow duty cycle, saying 60%. Then we choose a low flow temperature which gives us 100% of flow duty cycle. Next step is picking an average flow temperature between the former two flow temperatures, which correspond with a flow close enough to 90% duty cycle. The bisection algorithm is repeated such that we end up where the flow duty cycle is 90%. Each step of the algorithm took about 2 days and the whole test period lasted about 9 days. Fig. 4.13 shows the relevant experiment results.

The feed flow temperature is reduced via bisection algorithm to 31 °C where room#3's flow meets 90% of duty cycle. The other rooms have less heat demands compared to the north faced-room#3. The south-faced rooms receive solar radiation through glazing in the sunny days which are 5 days in total through the whole interval. Different intensities of the spikes corresponding with the solar radiation is due to different sensor positions in the rooms#1 and 2.

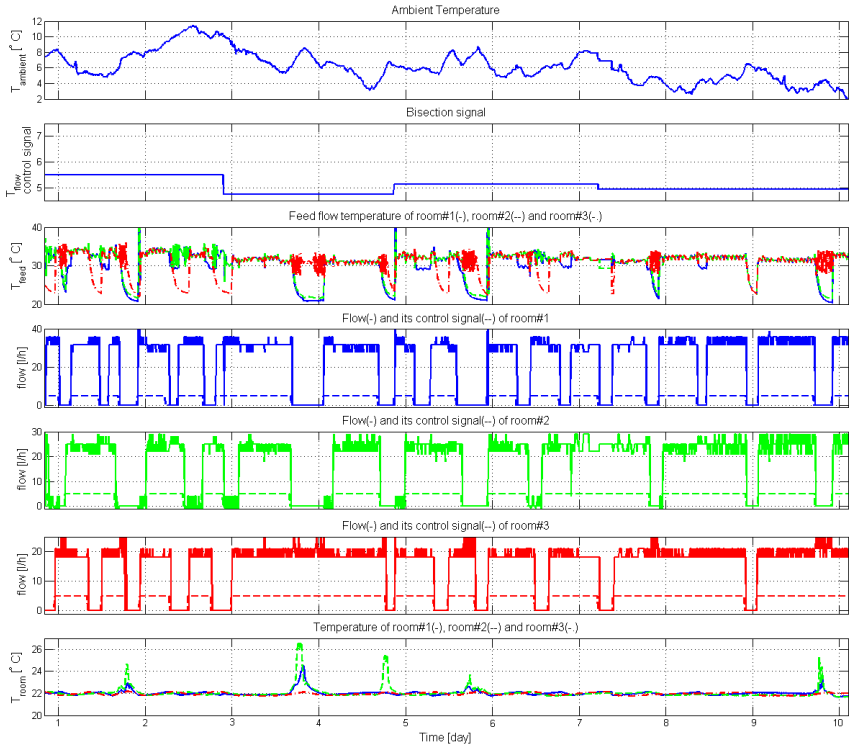

Figure 4.13: The first test results: after 3 steps or 7 days, we found the minimum feed flow temperature which is 31 °C. At this flow temperature, room#3 experience 90% duty cycle of mass flow. Rooms' temperature setpoint are very well maintained using simple relay controllers.

Fluctuations in the flow is due to the flow meters resolution. Valleys in the feed flow temperature coincide with the corresponding valve openness status It is because the feed flow temperature is measured individually for each room right after the distribution manifold, although it is the same for the whole system and vary just with the bisection signal.

It is worth noticing that a relay controller could maintain a room's temperature setpoint easily which is in part due to the large thermal mass of the concrete layer. Consequently the time constant of the heating system is much longer than its time delay. Otherwise, the pure time delay of the thick concrete layer would influence overheating of the room dramatically. On the other hand, heavy thermal insulation of the external walls filters out the ambient temperature fluctuations and transfers weather changes of a very low frequency . Therefore, the heating system with a long lag characteristic is not a burdensome when heating is required due to the weather condition changes.

4.5.3 Closed-Loop Test

Feed flow temperature in this test is regulated by feeding back the valves' control signal. The block diagram of the closed loop system is shown in Fig. 4.14. The test results are shown in Fig. 4.15.

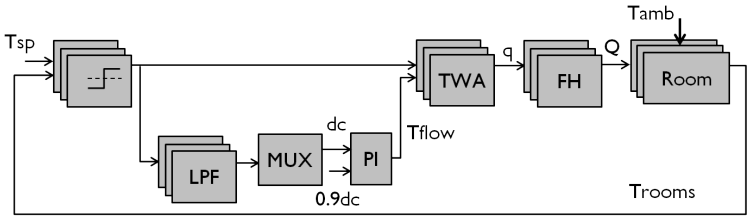

Figure 4.14: Block diagram of the closed loop test. The relay controller signals pass through a low pass filter to be compared later by the multiplexer block. This block determines the highest heat demand. The corresponding flow is regulated to 90% duty cycle by adjusting the flow temperature using a PI controller.

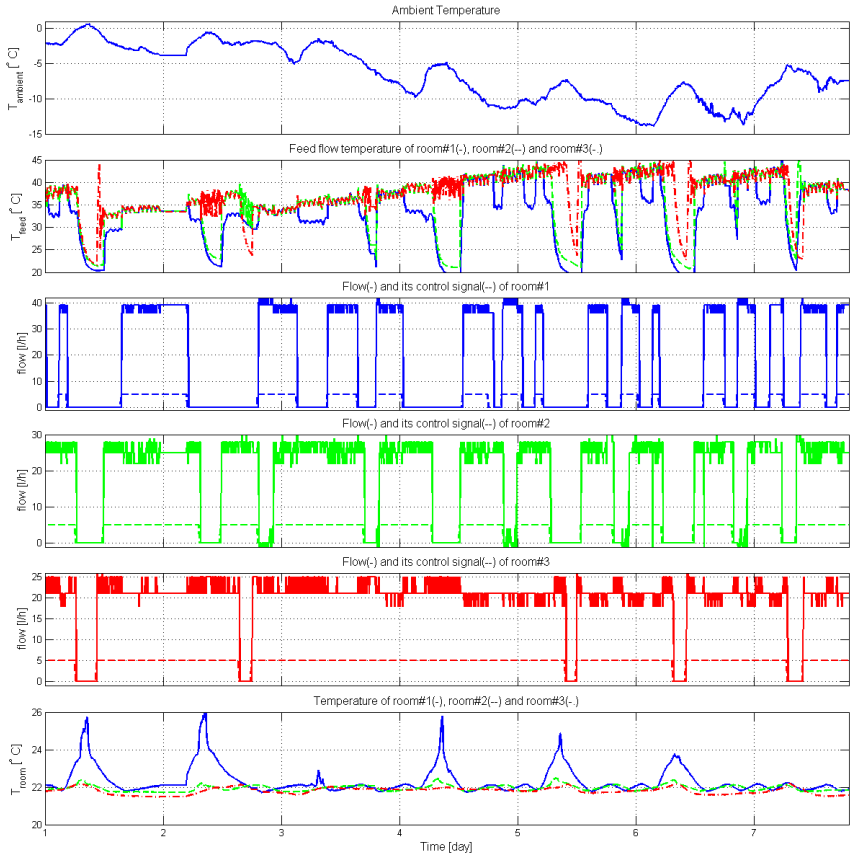

Figure 4.15: The second test results: Room#3 has the highest heat demand among the three rooms. The lower heat demand of the other rooms is mostly due to the solar radiation through glazing. While the flow duty cycle of room#3 is about 90%, Rooms# 1 and 2's flow duty cycle are about 60% and 70% respectively.

4.6 Nomenclature

Table 4.3: Symbols and Subscripts

Nomenclature	
B	heat transfer coefficient between two nodes in an electric circuit $(kJ/s°\mathrm{K})$
C	thermal capacitance $(J/kg\,°\mathrm{C})$
c_w	water specific heat $(J/kg\,°\mathrm{C})$
K	gain parameter of a first order control oriented model
L	time delay
N	total number of sections or samples in a prediction horizon
n	number of a specific element of piping
Q	dissipated heat (W)
Q_b	transferred heat to the building (W)
q	water flow rate (kg/sec)
T	temperature $(°\mathrm{C})$
TT	thermal tolerance level$(°\mathrm{C})$
τ	time constant parameter of a first order control oriented model
Subscripts	
amb	ambient
cmf	comfort (temperature)
d	delay time
e	envelope
f	floor surface
fh	floor heating
for	forward temperature of water
i	room number
int	integration time
p	proportional (gain)
ret	return temperature of water
r	radiator
s	solar
sp	setpoint

5 | Summary of Contributions

The contributions of this thesis are in two distinct areas which are: 1) dealing with the stability/performance dilemma of TRV-controlled hydronic radiators, and 2) design of an energy and cost minimizing control strategy for the entire hydronic heating circuit in a building. The rest of this chapter enumerates the contributions in both areas on a subject-based chronological order. The contributions of the relevant publications are pinpointed as well.

5.1 Dealing with Stability/Performance Dilemma of TRV-controlled Hydronic Radiators

Hydronic circuits of radiators are usually designed to fit the relative highest heat demand of a geographic region through a year. The large closed loop gain as a result of this specific design usually causes oscillations in the radiator flow and in return in the room temperature during the low heat demand season. The instability can be avoided by recalibration of thermostatic valves to reduce the closed loop gain, though in cost of an inferior performance during cold weather.

The proposed solution is a gain scheduled controller for flow regulation instead of the conventionally used proportional (P) or proportional-integral (PI) controllers with fixed design parameters. The other influencing parameters i.e. the water temperature and pressure are centrally controlled for the entire building and can not be regulated in favor of radiators, assuming that other HVAC systems might be available in the building. The gain scheduled controller is designed in a systematic fashion based on an analytically developed Linear Parameter Varying (LPV) model of the radiator's dissipated heat.

In the following the relevant publications along with the contributions are listed:

- *Thermal Analysis of an HVAC System with TRV Controlled Hydronic Radiator*. IEEE Conference on Automation Science and Engineering, August 2010.
  A control oriented model for a HVAC system is developed based on precise simulation models of the components. The HVAC system consists of a room and a hydronic radiator equipped with an electric thermostatic radiator valve that is driven by a stepper motor. We assumed that precise flow estimation is feasible by employing this type of TRV. A radiator is modeled with a series of interconnected narrow lumps that reflects water transfer delay, radiator gain and time constant very precisely. The dilemma of stability/performance is illustrated in simulations, applying simple PI-type controllers designed for either a warm or cold season.

- *Stability Performance Dilemma in Hydronic Radiators with TRV*. IEEE Conference on Control Applications, September 2011.
  The dilemma is investigated via simulation-based studies in this paper. It is shown via simulation that the instability problem arises because of a large closed loop gain and a long time constant when flow rate is small that is a low heat demand situation. A first order control-oriented model with varying parameters (LPV) model is proposed that describes the radiator dynamics very well through the entire operating region. Based on the LPV model, we designed a gain scheduled controller that facilitates radiator regulation for any heat demand. The parameters of the LPV model depend on the radiator operating point i.e. the relevant mass flow rate and room temperature. Such dependency is expressed as a look up table that is derived based on simulations.

- *Eliminating Oscillations in TRV-Controlled Hydronic Radiators*. IEEE Conference on Decision and Control, December 2011.
  We dealt with the dilemma using the same approach of the previous study [TSR11c]. However, we derived the parameters of the LPV model analytically as a function of operating point. For this purpose, the step response of a radiator that is in the form of a partial differential equation (PDE) was solved in the time domain assuming some simplifying approximations. The result is an approximation analytical expression for the radiator dissipated heat as a response to a step in flow. Simulation results show a good fit between the analytically driven LPV model and the simulation model.

- *An Analytical Solution for Stability-Performance Dilemma of TRV-Controlled Hydronic Radiators*. Submitted for Journal Publication, January 2012.
  The completely pursued objective in this paper is design of gain scheduling controller systematically, i.e. describing parameters as functions of the system operating point. Although the previous paper targeted the same goal, we derived the complete analytical expression for the radiator dissipated heat in this paper. The same PDE is solved in frequency domain without any approximation, resulting in a closed form accurate formulation for the heat step response. Analytically driven LPV model shows a perfect fit to the high-order simulation model.

5.2 Energy and Cost Minimizing Controller for a Residential Central Heating System with Hydronic Floor Heating and a Heat Pump

The research question of this part is: how to integrate the Ground-source Heat Pump (GHP) with hydronic heaters to achieve an optimal performance in terms of minimum energy consumption and associated heating cost? The proposed hypothesis is that the optimal forward temperature happens when at least one actuator works with full capacity. The rationale behind the hypothesis is heuristic: Electricity for heating purposes is mostly consumed by the heat pump's compressor. The latter would be minimized if heat pump's Coefficient of Performance (COP) increases. COP is inversely related to the temperature gap between condenser and evaporator sides. Minimizing this gap is doable by reducing the condenser temperature or equivalently the forward temperature of hot water in the

building circuit. The feed temperature can be reduced to the extent that the most demanding zone of the building can still meet the corresponding thermal comfort, in other words the relevant actuator works very close to its saturation limit; for example the floor heating valve is almost fully open. An optimization problem in a receding horizon scheme is formulated to seek the proposed optimal operating point. By incorporation of the predicted price profile for the next 24 hours, we have designed an economic MPC.

Related publications are:

- *Optimal Power Consumption in a Central Heating System with Geothermal Heat pump*. 18^{th} IFAC World Congress, September 2011.
  We evaluated the proposed optimization hypothesis for the entire integrated system with floor heating, radiator and a geothermal heat pump via simulation studies. A two level hierarchical controller were proposed for system integration. At the top level model predictive controller were formulated to minimize the forward temperature of the hot water and by this means coordinate between the heating source and the heat emitters. At the lowest level, single loop PI-type controllers were designed to meet specific temperature setpoint of individual rooms. Simulation of a multi-room house case study shows that the proposed control strategy can save considerable percentage of energy compared to the traditional control scheme.

- *Energy Minimizing Controller for a Residential Central Heating System with Hydronic Floor Heating and a Heat Pump*. Submitted for Journal Publications, September 2012.
  Results of implementing the optimization hypothesis on an actual case study are reported in this paper. The case study is a multiple room uninhabited residential house with grids of floor heating pipes in the rooms as the heat emitter. A second order model of a reference room is identified using a series of step response test data; the model was further employed in the simulations. Two open and closed loop tests were conducted that can be served as a proof of concept for the proposed optimization hypothesis.

- *Contribution of Domestic Heating Systems to Smart Grid Control*. IEEE Conference on Decision and Control. December 2011.
  How and to what extent, domestic heating systems can be helpful in regaining power balance in a smart grid, is the research question of this paper. The case study is an under-floor heating system supplied with a geothermal heat pump which is driven by electrical power from the grid. The idea is to deviate power consumption of the heat pump from its optimal value, in order to compensate power imbalances in the grid. Heating systems can be forced to consume energy, i.e. storing it in heat buffers when there is a power surplus in the grid; and be prevented from using power, in case of power shortage. We have investigated how much power imbalance could be compensated, provided that a certain, yet user adjustable, level of residents' thermal comfort is satisfied. It is shown that the large heat capacity of the concrete floor alleviates undesired temperature fluctuations. Therefore, incorporating it as an efficient heat buffer is a viable remedy for smart grid temporary imbalances.

- *Economic COP Optimization of a Heat Pump with Hierarchical Model Predictive Control*. Accepted in: IEEE Conference in Decision and Control , December 2012.

It was shown in the last paper that the the concrete floor can be treated as a heat buffer with a large storage potential which can alleviates undesired temperature fluctuations. Electricity market can adjust the energy price according to the predicted availability and provide it to end-users a day ahead as economic incentives to defer their daily power consumption and avoid high electricity bills. By this means, domestic heating systems both contribute to the grid balancing issues and reduce the consumption cost. Many factors e.g. weather conditions, occupant's thermal preferences and the building thermal mass determines the extent of this contribution and cost reduction. In this paper, we formulated a hierarchical model predictive controller that minimizes the electricity consumption price and at the same time satisfies the user thermal comfort. The proposed control strategy is a leap forward towards balanced load control in smart grids where individual heat pumps in detached houses contribute to preserve load balance through intelligent electricity pricing policies.

6 | Conclusions and Future Works

This chapter, is divided into three sections: two independent sections review the conclusions within each focus area; one section gives the remarks related to control of the integrated system.

6.1 Conclusion and Future Works on Radiator Modeling and Control

In this study, we investigated an inefficient operating conditions of TRV controlled radiators. The condition is discussed as a dilemma between stability and performance which we dealt with using a modern thermostatic radiator valves. Using this TRV, flow estimation and control becomes possible. Based on the estimated flow, we have developed a gain scheduled controller which guarantees both performance and stability for the radiator system. To this end, we derived a first-order LPV model of the radiator analytically.

All gain scheduling control approaches operate based on the basic assumption that all the system states can be measured or estimated and a generalized observability holds [ÅW08]. In this study, however, we should clarify the validity of this assumption. The parameters that we need to measure or estimate are the room temperature and the radiator flow rate. Measuring the first state is mandatory when the goal is seeking a reference for this temperature. However, radiator flow rate is not easily measurable and it have to be estimated. To have an estimation of the radiator flow rate, one possibility is to use an electric TRV in which the valve is driven by a stepper motor. Experiments show that this TRV can give a rather precise estimation of the valve opening. Knowing this fact and assuming a constant pressure drop across the radiator valve, we would be able to estimate the flow rate.

We have shown throughout the paper that using the new generation of TRVs, a gain scheduling controller would guarantee the performance of the radiator operation. In the current study, however we did not discuss the robustness of the proposed controller with respect to the model uncertainties. This task is postponed to future studies.

6.2 Conclusion and Future Works on Energy and Cost Minimizing Controller of Domestic Heating Consumers

An optimization hypothesis for minimizing the energy consumption of a domestic heating system is proposed, control strategies for fulfillment of the idea are developed, simulated

and tested on a real house. The idea was developed by design of a hierarchical controller that systematically incorporate different knowledges of the building thermal mass and disturbances to optimize the system performance with the minimum energy cost. A case study with specific heat source and emitters were considered. Nevertheless, the proposed hypothesis for optimization is general and could really contribute to reduced power consumption in almost any type of heat pump based buildings.

The proposed hierarchical controller setup compared to a central controller is more reliable due to the fact that local controller loops handle disturbances locally. Fault propagation through the entire system is less probable compared to a centralized scheme. However it is still less robust compared to a distributed controller structure. Evaluations of the degree of optimality and robustness of the system to model mismatches or measurement errors are not investigated and are subjects of future studies.

The experimental studies serve as a proof of concept. They very well reflect the feasibility of the proposed idea and confirm the principle idea of the optimal operating point. However, the amount of electricity saving compared to a conventional approach was not measurable.

The studies on the contributions of domestic buildings to smart grid control serve as a proof of concept. The most common power imbalance pulses in power systems last for less than half an hour, and are as large as $\pm 50\%$ nominal value. Our results show that, these imbalances can be well accommodated even by a small 54 m^2 apartment with a tightly selected thermal comfort level of 0.25°C in a mild cold weather with a commonplace desired indoor temperature.

In [TSMR11], we assumed that the power setpoint profile is provided by the power grid at any time instant. This assumption requires a tremendous amount of information to be transferred by the power providing company to all users. A more practical approach is to consider an intermittent communication between the grid controller and the user at equal time intervals. At the beginning of each interval, the grid controller send a message asking the user to try to increase/decrease its power consumption by $\pm \Delta P$. As a result, the burden of computing power setpoint profile is put on the heat pump control system, the design of which is not trivial anymore. An MPC is designed for this purpose later on in [TSRM12]. The MPC controller objective is to define the power setpoint in order to satisfy demands of the grid control system, subject to several constraints, which are: 1) avoid valves saturation; 2) avoid too high forward temperature in order to keep the heating system from damage; and 3) maintain the room temperature in the defined interval and last but not least optimize the heat pump's efficiency and by this mean minimize the energy consumption. It is worth saying that, the demand of the power providing company may not be completely satisfied due to probable conflicts with the above constraints.

6.3 Joint Conclusions and Future Works

We sketched the first objectives to use different heat emitters, i.e. either radiator or floor heating in individual rooms. However, the commonly used radiator panels are designed to be fed by high temperatures of water which is a limiting factor for sub-floor heating systems. Water temperature has to be restricted to avoid damage to the floor surface or the hot sensation by bare feet. Also, a high temperature is not efficient from the energy point of view because it gives a smaller COP. Therefore, to be combined with floor heating

systems, radiator panels have to be wider to work with lower water temperatures.

A future objective is to combine two hydronic heating system with different response time in the same temperature zone in order to compensate exogenous predicted or unpredicted heat demands with a proper scheduling. Combination of these sub-systems could be beneficial mostly from the sense of rejection of unpredicted disturbances like solarization through glazing and sudden heat demands for example when a door becomes open. Combination of floor heating and ventilation/cooling system is also important due to the conflicting impacts of the two systems. The combination could be beneficial in fact for diminishing the over heating conditions in rooms due to unpredicted heat inputs like solar radiation.

References

[Ada68] B. Adamson. Heat balance for rooms and buildings. Technical report, Department of Building Science, Lund Institute of Technology, Lund, Sweden, 1968.

[ÅH95] K.J. Åstrom and T. Hagglund. *PID Controllers*. ISA, North Carolina, 1995.

[AJKS+85] G.G.J. Achterbosch, P.P.G. Jong, C.E. Krist-Spit, S.K. Van Der Meulen, and J. Verberne. The development of a convenient thermal dynamic building model. *Energy and Buildings*, 8:826–38, 1985.

[ALPV08] Gregorio Andria, Anna Maria Lucia Lanzolla, Francesco Piccininni, and Gurvinder S. Virk. Design and characterization of solar-assisted heating plant in domestic houses. *IEEE Transaction on Instrumentation and Measurement*, 57(12), 2008.

[AMH98] Klaus Kaae Andersen, Henrik Madsen, and Lars H. Hansen. Modleing the heat dynamics of a building using stochastic differential equations. *Energy and Buildings*, 31(1):13–24, 1998.

[APSB04] P. Andersen, T. S. Pedersen, J. Stoustrup, and N. Bidstrup. Elimination of oscillations in a central heating system using pump control. In *IEEE American Control Conference*, pages 31–38, Chicago, Illinois, June 2004.

[ARBL11] Aivar Auvaart, Argo Rosin, Nadezhda Blonogova, and Denis Lebedev. Nordpool spot price pattern analysis for households energy management. In *7th International Conference on Compatibility and Power Electronics*, pages 103–106, Tallinn, Estonia, July 2011.

[ASH90] ASHRAE. *ASHRAE Handbook 1990, fundamentals*. ASHRAE Inc., Atlanta, 1990.

[ASS90] A. K. Athienitis, M. Stylianou, and J. Shou. Methodology for building thermal dynamics studies and control applications. *ASHRAE Trans.*, 96(2):839–848, 1990.

[ASS08] E.M.B. Aske, S. Strand, and S. Skogestad. Coordinator mpc for maximizing plant throughput. *Comput. Chem. Eng.*, 32:195–204, 2008.

[ATT12] Anil Aswani, Jay Taneja, and Claire Tomlin. Reducing transient and steady state electricity consumption in hvac using learning-based model predictive control. *proceedings of the IEEE*, 100(1):240–253, 2012.

[AU12a] Department of Civil Engineering Aalborg University. Strategic research center on zero energy buildings, 2012. Available from: http://www.en.zeb.aau.dk/about/.

[AU12b] Department of Civil Engineering Aalborg University. Strategic research center on zero energy buildings, 2012. Available from: http://www.en.zeb.aau.dk/project_descriptions/.

[ÅW08] K.J. Åstrom and B. Wittenmark. *Adaptive Controller*. DOVER Publications Inc., Mineola, New York, 2008.

[BBM00] T. Backx, O. Bosgra, and W. Marquardt. Integration of model predictive control and optimization of processes. *Advanced Control of Chemical Processes*, 2000.

[BC02] J. Braun and N. Chaturvedi. An inverse grey-box model for transient building load prediction. *HVAC Research*, 8(1):73–99, 2002.

[Bec72] P. Becher. *Varme og Ventilation, Bind 2*. Tekniksk Forlag, 1972.

[Buc89] N. A. Buckley. Application of radiant heating saves energy. *ASHRAE Journal*, 31:17–26, 1989.

[Bui12] Simon Lawrence Builders. Under floor heating, 2012. Available from: http://www.simonlawrencebuilders.co.uk.

[CA11] Jose A. Candanedo and Andreas K. Athienitis. Predictive control of radiant floor heating and solar-source heat pump operation in a solar house. *HVAC&R Research*, 17(3):235–256, 2011.

[Cal09] Caleffi. Zoning hydronic systems. Technical journal, CALEFFI North America, INC., Milwaukee, Wisconsin, USA, 2009.

[Cha10] Vikas Chandan. Modeling and control of hydronic building hvac systems. Master's thesis, University of Illinois at Urbana Champaign, Urbana, Illinois, USA, 2010.

[Che02] T.Y. Chen. Application of adaptive predictive control to afloor heating system with a thermal lag. *Energy and Buildings*, 34:45–51, 2002.

[CMA10] Vikas Chandan, Sandipan Mishra, and Andrew G. Alleyne. Predictive control of complex hydronic systems. In *American Control Conference*, Baltimore, MD, USA, June 2010.

[CP83] C.R. Cutler and R.T. Perry. Real time optimization with multivariable control is required to maximize profits. *Computers & Chemical Engineering*, 7:663–667, 1983.

[CPSS12] Chiara Corazzol, Rasmus Pedersen, John Schwensen, and Senthuran Sivabalan. Model predictive control of a refrigeration system in a smart grid. Master's thesis, Aalborg University, Denmark, Aalborg, 2012.

[CRW00] K.S. Chapman, J. Rutler, and R. Watson. Impact of heating system and wall surface temperatures on room operative temperature fields. *ASHRAE Trans.*, 106(1):506–514, 2000.

[Dan08] Danfoss. Maintenance instruction. Main report, Danfoss, Denmark, 2008.

[Dan12a] Danfoss. High capacity valve body, type ra-g. Data sheet, Danfoss, Danfoss Randall, 2012.

[Dan12b] Danfoss. Thermostatic radiator valves - mounting guide. Mounting guide, Danfoss, Danfoss Vejle, 2012.

[DAR11] Moritz Diehl, Rishi Amrit, and James B. Rawlings. A lyapunov function for economic optimization model predictive control. *IEEE Transactions on Automation Control*, 56(3):703–707, 2011.

[DC98] Jean DeGreef and K.S. Chapman. Simplified thermal comfort evaluation of mrt gradients and power consumption predicted with the bcap methodology. *ASHRAE Trans.*, 104(2):1090–1097, 1998.

[Den10] Honglian Deng. *Comfort and energy optimization control of thermal systems*. PhD thesis, Aalborg University, Aalborg, Denmark, 2010.

[Eng07] S. Engell. Feedback control for optimal process operation. *Journal of Process Control*, 17:203–219, 2007.

[FBB+80] W. Findeisen, F.N. Bailey, M. Brdys, K. Malinowski, P. Tatjowski, and A. Wozniak. *Control and Coordination in Hierarchical Systems*. Wiley and Sons, 1980.

[FM96] J.F. Forbes and T.E. Marlin. Design cost: a systematic approach to technology selection for model-based real-time optimization systems. *Computers & Chemical Engineering*, 20:717–734, 1996.

[FVLA02] G. Fraisse, C. Viardot, O. Lafabrie, and G. Achard. Developement of a simplified and accurate building model based on electrical analogy. *Energy and Buildings*, 34(10):1017–31, 2002.

[GA12] Benjamin Greening and Adisa Azapagic. Domestic heat pumps: Life cycle environmental impacts and potential implications for the uk. *Energy*, 39:205–217, 2012.

[Gam74] J. Gammelby. Heizkörperthermostate. grundsätze und eigenschaften. *Danfoss Journal*, 3, 1974.

[HAM00] A. Helbig, O. Abel, and W. Marquardt. Structural concepts for optimization based control of transient processes. *Nonlinear Model Predictive Control*, 2000.

[Han97] L. H. Hansen. *Stochastic modeling of central heating systems*. PhD thesis, Technical University of Denmark, Dep. of Mathematical Modeling, Denmark, 1997.

[Hee11] Christian Heerup. Efficiency and temperature correlation (effectivitet og temperatur sammenhng). Technical report, Denmark Technological Institute, Energi og Kilima, Gregersensvej, Taastrup, Denmark, 2011.

[HEJ10] Tobias Gybel Hovgaard, Kristian Edlund, and John Bagterp Jørgensen. The potential of economic mpc for power management. In *IEEE Conference on Decision and Control*, Atlanta, GA, USA, December 2010.

[HH00] Haruo Hanibuchi and Shuichi Hokoi. Simplified method of estimating efficiency of radiant and convective heating systems. *ASHRAE Trans.*, 106(1):487–494, 2000.

[HHK95] S. Y. Ho, R. E. Hayes, and Wood R. K. Simulation of the dynamic behavior of a hydronic floor heating system. *Heat Recovery Systems & CHP*, 15(6):505–519, 1995.

[HHS+12] Thomas Hansen, Claus Thy Henningsen, Kevin Sanchez Sancho, Ayub Tashkilot, and Dragos Adrian Urian. Iterative learning control applied on a refrigeration system. Master's thesis, Aalborg University, Denmark, Aalborg, 2012.

[HHW95] S. Y. Hu, R. E. Hayes, and R. K. Wood. Simulation of the dynamic behavior of a hydronic floor heating system. *Heat Recovery & CHP*, 15(6):505–519, 1995.

[HNF+99] Y. Hasegawa, T. Nakano, T. Fukuda, T. Komori, K. Matsumoto, and K. Shimojima. Learning predictive control for ghp (gas heat pump). In *IECON '99 Proceedings. The 25th Annual Conference of the IEEE*, pages 1277–1282, San Jose, CA, USA, November 1999.

[HPMJ12] Rasmus Halvgaard, Niels K. Poulsen, Henrik Madsen, and John B. Jrgensen. Economic model predictive control for building climate control in smart grid. In *IEEE PES Conference on Innovative Smart Grid Technologies*, Washington, USA, June 2012.

[HS94] M. Hovd and S. Skogestad. Sequential design of decentralized controllers. *Automatica*, 30:1601–1607, 1994.

[HU99] G. Hudson and C. P. Underwood. A simple building modeling procedure for matlab/simulink. *Proc. of Building Simulation*, 99(2):777–783, 1999.

[Ins] Technological Institute. Energyflexhouse - technology to the global challenge. Available from: `http://www.dti.dk/projects/energyflexhouse`.

[Jen11] Steen Kramer Jensen. Potentials and opportunities for flexible electricity consumption with special focus on individual heat pumps. Technical report, EnergiNet, Fredericia, Denmark, 31 January 2011.

[JPSØ79] J. Johansen, O. Paulsen, N. Svenningsen, and P. Øhrgaard. Vandvarmeovnens varmeydelser. Raport 2, Varme of Installationsteknik , Teknologisk Institut, Denmark, 1979.

[KH04] M. L. Kurkarni and F. Hong. Energy optimal control of residential space-conditioning system based on sensible heat transfer modeling. *Building and Environment*, 39(1):31–38, 2004.

[KH11] Henrik Karlsson and Carl-Eric Hagentoft. Application of model based predictive control for water-based floor heating in low energy residential building. *Building and Environment*, 46(3):556–569, 2011.

[KHP10] Elisabeth Kjallsson, Göran Hellström, and Bengt Perers. Optimization of systems with the combination of ground-source heat pump and solar collectors in dwellings. *Energy*, 35:2667–2673, 2010.

[KM07] J. Kadam and W. Marquardt. Integration of economical optimization and control for internationally transient process operation. *LNCIS*, 358:419–434, 2007.

[Lei91] S. B. Leigh. *An experimental approach for evaluating control strategies of hydronic radiant floor heating systems*. PhD thesis, University of Michigan, Michigan, USA, 1991.

[LPP82] K. M. Letherman, C. J. Paling, and P. M. Park. The measurement of dynamic thermal response in rooms using pseudorandom binary sequences. *Building and Environment*, 17(1), 1982.

[LZH93] Michael L'Ecuyer, Cathy Zoi, and S. John Hoffman. Space conditioning: The next frontier. Main report, Environmental Protection Agency, USA, April 1993.

[MAB04] G.L. Morrison, T. Anderson, and M. Behnia. Seasonal performance rating of heat pump water heaters. *Solar Energy*, 76:147–152, 2004.

[MDT70] M.D. Mesarovic, Macko D., and Y. Takahara. *Theory of Hierarchical Multilevel Systems*. Academic Press, New York, 1970.

[MH95] H. Madsen and J. Holst. Estimation of a continuous time model for the heat dynamics of a building. *Energy and Buildings*, 22:67–79, 1995.

[MK10] Khosrow Moslehi and Ranjit Kumar. A reliability perspective of the smart grid. *IEEE Transactions on Smart Grid*, 1(1):57–64, June 2010.

[MKD12] Yudong MA, Anthony Kelman, and Allan Daly. Predictive control for energy efficient buildings with thermal storage. *IEEE Control System Magazine*, 32(1):44–64, 2012.

[Ole83] Bjarne W. Olesen. A simplified calculation method for checking the indoor climate. *ASHRAE Trans.*, 98(2B):710–723, 1983.

[Ole01] Bjarne W. Olesen. Control of floor heating and cooling systems. In *Clima 2000/Napoli 2001 World Congress*, Napoli, September 2001.

[Ole02] Bjarne W. Olesen. Radiant floor heating in theory and practice. *ASHRAE Journal*, 44(7):19–24, 2002.

[OPJ+10] F. Oldewurtel, A. Parisio, C. N. Jones, M. Morari, D. Gyalistras, M. Gwerder, V. Stauch, B. Lehmann, and K. Wirth. Energy efficient building climate control using stochastic model predictive control and weather predictions. In *American Control Conference*, Baltimore, MD, USA, 2010.

[OUP+10] Frauke Oldewurtel, Andreas Ulbig, Alessandra Parisio, Göran Andersson, and Manfred Morari. Reducing peak electricity demand in building climate control using real-time pricing and model predictive control. In *49th IEEE Conference on Decision and Control*, Atlanta, GA, USA, 2010.

[PAN+11] Tom S. Pedersen, Palle Andersen, K. M. Nielsen, H. L. Staermose, and P. D. Pedersen. Using heat pump energy storages in the power grid. In *IEEE International Conference on Control Applications*, Denver, CO, USA, September 2011.

[PG85] O. Paulsen and S. Grundtoft. Dynamisk afprøvning af små varmecentraler. Technical report, Jydsk Teknologisk Institut, Denmark, 1985.

[QB03] S.J. Qin and T.A. Badgwell. A survey of industrial model predictive control technology. *Control Engineering Practice*, 11:733–764, 2003.

[RA09] James Rawlings and Rishi Amrit. Optimizing process economic performance using model predictive control. In *Nonlinear Model Predictive Control*, volume 384 of *Lecture Notes in Control and Information Sciences*, pages 119–138. Springer Berlin / Heidelberg, 2009.

[Rat87] P. Rathje. Modeling and simulation of a room temperature control system. In *Proceedings of SIMS87 Symposium*, pages 58–69. Scandinavian Simulation Society, 1987.

[RBJ+08] J.B. Rawlings, D. Bonnt, J.B. Jørgenste, A.N. Venkat, and S.B. Jørgensen. Unreachable setpoints in model predictive control. *IEEE Transactions on Automatic Control*, 53:2209–2215, 2008.

[RET05] RETScreen. Ground-source heat pump project analysis. Engineering and cases textbook, RETScreen International, Canada, 2005.

[RGZ88] R. E. Rink, V. Gourishankar, and M. Zaheeruddin. Optimal control of heat-pump/heat storage systems with time-of-day energy price incentive. *Journal of Optimization Theory And Applications*, 58(1), 1988.

[RM09] James B. Rawlings and David Q. Mayne. *Model Predictive Control: Theory and Design*. Nob Hill Pub, 2009.

[Ros03] J. A. Rossiter. *Model-Based Predictive Control*. CRC Press LLC, Raton, Florida, 2003.

[RR99] C.V. Rao and J.B. Rawlings. Steady states and constraints in model predictive control. *AIChE J.*, 45(6):1266–1278, 1999.

[RSIT07] Yokoyama Ryohei, Takeshi Shimizu, Koichio Ito, and Kazuhisa Takemura. Influence of ambient temperatures on performance of a co_2 heat pump water heating system. *Energy*, 32:388–398, 2007.

[Sca09] Riccardo Scattolini. Architectures for distributed and hierarchical model predictive control – a review. *Journal of Process Control*, 19:723–731, 2009.

[SEM04] D.E. Seborg, T.F. Edgar, and D.A. Mellichamp. *Process Dynamics and Control*. Wiley, New York, NY, USA, 2004.

[SGP02] E. Sequeira, M. Graells, and L. Puigjaner. Real time evolution of online optimization of continuous processes. *Industrial & Engineering Chemistry Research*, 41:1815–1825, 2002.

[SH02] E. Silberstein and J. Hohman. *Heat Pumps*. Cengage Learning, 2002.

[Sil91] Dragoslav D. Siljak. *Decentralized Control of Complex Systems*. Academic Press, Cambridge, 1991.

[Sko00] S. Skogestad. Plantwide control: the search for the self-optimizing control structure. *Journal of Process Control*, 10:487–507, 2000.

[SM01] C. A. De Swardt and J. P. Meyer. A performance comparison between an air-source and a ground-source reversible heat pump. *international Journal of Energy Research*, 25:899–910, 2001.

[SP04] V. Sakizlis and Pistikopoulos E.N. Perkins, J.D. Recent advances in optimization based simultaneous process and control design. *Comput. Chem. Eng.*, 28:2069–2086, 2004.

[sta04] The european standard en215: Thermostatic radiator valves-requirements and test methods, 2004.

[STBH05] Svend Svendsen, Henrik M. Tommerup, and Mette Beck Hansen. Energy project villa. Main report, Partners: Technical University of Denmark, Department of Civil Eng. and Rockwool, Denmark, March 2005. Downloded from DTU database.

[TBS11] Klaus Trangbaek, Jan Dimon Bendsten, and Jakob Stoustrup. Hierarchical control for smart grids. In *18^{th} IFAC World Congress*, Milan, Italy, September 2011.

[TLT07] H. Thybo, L.F.S. Larsen, and C. Thybo. Control of a water-based floor heating system. In *IEEE International Conference on Control Applications*, pages 288–294, 2007.

[TMAR05] Bourhan Tashtoush, M. Molhim, and M. Al-Rousan. Dynamic model of an hvac system for control analysis. *Energy*, 30:1729–1745, 2005.

[TSMR11] Fatemeh Tahersima, Jakob Stoustrup, Soroush A. Meybodi, and Henrik Rasmussen. Contribution of domestic heating system to smart grid control. In *Conference on Decision and Control*, Orlando, FL, USA, December 2011.

[TSR11a] Fatemeh Tahersima, Jakob Stoustrup, and Henrik Rasmussen. Eliminating oscillations in trv-controlled hydronic radiators. In *IEEE Conference on Decision and Control*, Orlando, Florida, USA, December 2011.

[TSR11b] Fatemeh Tahersima, Jakob Stoustrup, and Henrik Rasmussen. Optimal power consumption in a central heating system with geothermal heat pump. In *IFAC World Congress*, Milano, Italy, August 2011.

[TSR11c] Fatemeh Tahersima, Jakob Stoustrup, and Henrik Rasmussen. Stability-performance dilemma in trv-based hydronic radiators. In *IEEE Multi-Conference on Systems and Control*, Denver, Colorado, USA, October 2011.

[TSR12a] Fatemeh Tahersima, Jakob Stoustrup, and Henrik Rasmussen. An analytical solution for stability-performance dilemma of trv-controlled hydronic radiators, 2012. Submitted.

[TSR12b] Fatemeh Tahersima, Jakob Stoustrup, and Henrik Rasmussen. Energy minimizing controller for a residential central heating system with hydronic floor heating and a heat pump, 2012. Submitted.

[TSRM12] Fatemeh Tahersima, Jakob Stoustrup, Henrik Rasmussen, and Soroush A. Meybodi. Economic cop optimization of a heat pump with hierarchical model predictive control. IEEE Conference on Decision and Control, December 2012. to be published.

[WA03] C. Wemhöner and Th. Afjei. Seasonal performance calculation for residential heat pumps with combined space heating and hot water production (fhbb method). Final report, University of Applied Science Basel, Institute of Energy, Switzerland, October 2003.

[Web70] A. P. Weber. *Die Warmwasserheizung: Beiträge zur Berechnung und Konstruktion*. R. Oldenbourg, München, Germany, 1970.

[XFD08] B. Xu, L. Fu, and H. Di. Dynamic simulation of space heating systems with radiators controlled by trvs in buildings. *Energy and Buildings*, 40:1755–1764, 2008.

[YPLT07] Zhenyu Yang, G.K.M. Pedersen, L.F.S. Larsen, and Honglian Thybo. Modeling and control of indoor climate using a heat pump based floor heating system. In *IECON 2007 - 33rd Annual Conference of the IEEE Industrial Electronics Society*, pages 2985–2990, 2007.

[YT04] W.S: Yip and Marlin T.E. The effect of model fidelity on real-time optimization performance. *Computers and Chemical Engineering*, 28:267–280, 2004.

[ZF00] Y. Zhang and J.F. Forbes. Extended design cost: a performance criterion for real-time optimization. *Computers & Chemical Engineering*, 24:1829–1841, 2000.

[ZTdGO02] A.C. Zanin, M. Tvrzsk de Gouvea, and D. Odloak. Integration of real-time optimization into the model predictive controller of the fcc system. *Control Engineering Practice*, 10:819–831, 2002.

Contributions

Paper A

Stability Performance Dilemma in Hydronic Radiators with TRV

Fatemeh Tahersima, Jakob Stoustrup, Henrik Rasmussen

This paper is published in:
IEEE Conference on Control Applications

Abstract

Thermostatic Radiator Valves (TRV) have proved their significant contribution in energy savings for several years. However, at low heat demands, an unstable oscillatory behavior is usually observed and well known for these devices. It happens due to the nonlinear dynamics of the radiator itself which results in a high gain and a large time constant for the radiator at low flows. If the TRV is tuned in order to dampen the oscillations at low heat loads, it will suffer from poor performance and lack of comfort, i.e. late settling, when full heating capacity is needed. Based on the newly designed TRVs, which are capable of accurate flow control, this paper investigates achievable control enhancements by incorporating a gain scheduling control scheme applied to TRVs. A suitable linear parameter varying model is derived for the radiator which governs the gain scheduler. The results are verified by computer simulations.

1 INTRODUCTION

Efficient control of heating, ventilation and air conditioning (HVAC) systems has a great influence on the thermal comfort of residents. The other important objective is energy savings, mainly because of the growth of energy consumption, costs and also correlated environmental impacts.

Hydronic radiators controlled by thermostatic radiator valves (TRV) provide good comfort under normal operating conditions. Thermal analysis of the experimental results of a renovated villa in Denmark, built before 1950, has demonstrated that energy savings near 50% were achieved by mounting TRVs on all radiators and fortifying thermal envelope insulation [1].

To maintain the temperature set point in a high load situation, TRVs are usually tuned with a high controller gain.The inefficiency appears in the seasons with low heat demand especially when the water pump or radiator are over dimensioned [2]. In this situation, due to a low flow rate, loop gain increases; and as a result oscillations in room temperature may occur. Besides discomfort, oscillations decrease the life time of the actuators. This problem is addressed in [3] for a central heating system with gas-expansion based TRVs. It is proposed to control the differential pressure across the TRV to keep it in a suitable operating area using an estimate of the valve position.

In this study, we investigated the problem as a dilemma between stability and performance. The case study of the paper is a HVAC system including a room and a hydronic radiator controlled by a TRV. In this study, pressure drop across the radiator valve is maintained constant unlike what is taken as the control strategy in [3]. Instead, flow control is assumed to be feasible by the accurate adjustment of the valve opening. The valve opening is regulated by a stepper motor which allows the concrete adjustment. We have proposed control oriented models for the system components as functions of operating conditions. In this way, the nonlinear radiator model is replaced by a linear parameter varying model. Based on the proposed modeling, gain scheduling is chosen among various possible control structures to design the TRV controller.

Control oriented models are derived based on energy balance equations of the system components. Generally, there are two approaches for HVAC systems modeling, the forward approach and the data-driven (inverse) approach [4]. The first one is based on known physical characteristics and energy balance equations of the air, structural mass

and other components of the system. In this approach, three methods of heat balance, weighting factor and thermal network are addressed widely in the literature [5, 6, 7]. The alternative modeling approach is to use building measurement data with inferential and statistical methods for system identification which is addressed in [8, 9, 10]. The main drawback of this method is that it requires a significant amount of training data and may not always reflect the physical behavior of the system [11].

In this study, the control oriented model of the room is employed based on the lumped capacitance model described formerly in [12]. An extension of the *one exponent model*, addressed in [13] is proposed for describing the radiator dynamics.

The rest of the paper is organized as follows: Section II describes the system components. Control oriented model of the HVAC system is developed using the simulation models in Section III. Section IV proposes the control structure based on flow adaptation. Simulation results are illustrated in the same section. Discussion and conclusions are given finally in Sections V and VI.

2 System Description

The HVAC system is composed of a room, a radiator with thermostatic valve and a temperature sensor. Disturbances which excite the system are ambient temperature, heat from the radiator and ground temperature. The latter input affects the room temperature through thick layers of insulation and a heavy concrete. The block diagram of the system is shown in Fig. 7.1. Symbols, subscripts which are used in the paper and their corresponding amount are shown in table 7.1 and table 7.2 respectively. The parameters' value are calculated mainly based on [4].

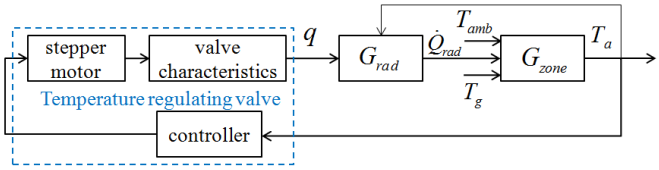

Figure 7.1: Block diagram of the room temperature control system.

Fig. 7.2 and Fig. 7.3 show a test where oscillations and low performance occur respectively. In this test the forward water temperature is at $50^{\circ}\mathrm{C}$. The proportional integral (PI) controller of TRV is tuned based on Ziegler-Nichols step response method employed from [14].

3 System Modeling

3.1 Simulation Models

A radiator is a distributed system which can be considered as N pieces in series. Using one exponent method for modeling the radiator output heat, the n^{th} section is given by,

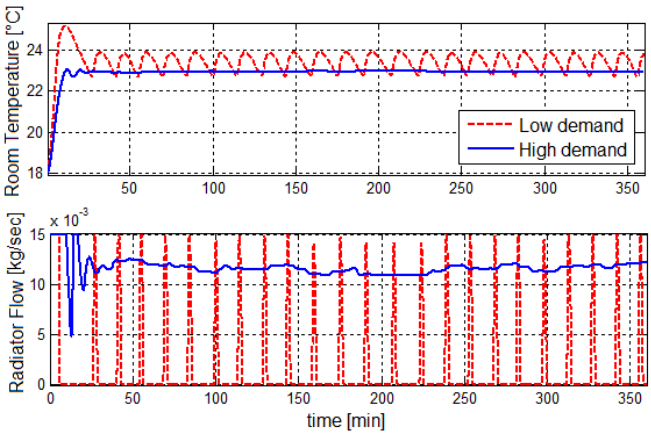

Figure 7.2: Undamped oscillations in room temperature and radiator flow which occur in low demand situation while the controller is designed for high demand condition.

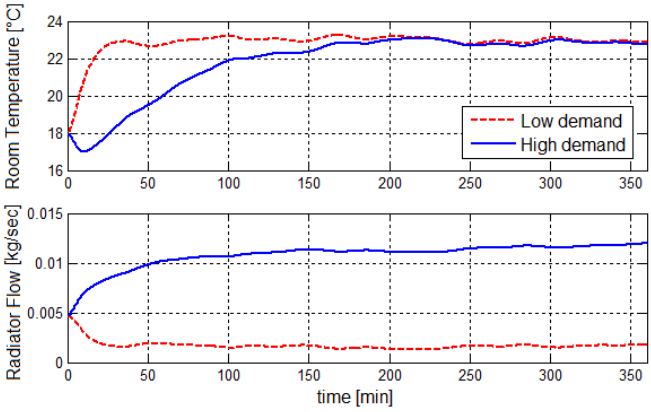

Figure 7.3: Poor performance in the cold weather condition, applying the controller designed for the low demand situation.

[13]:

$$\frac{C_{rad}}{N}\dot{T}_n \quad = \quad H_q(T_{n-1} - T_n) - \frac{\Phi_0}{N}\left(\frac{T_n - T_a}{\Delta T_{m,0}}\right)^{n_1} \tag{7.1}$$

in which C_{rad} is heat capacity of the water and the radiator material, T_n is temperature of the radiator's nth element with $n = 1, 2, \ldots, N$. Temperature of the end points are water inlet temperature $T_0 = T_{in}$ and outlet temperature $T_N = T_{out}$. $H_q = c_w q$ and Φ_0 is the nominal power of the radiator in nominal condition which is $T_{in,0} = 90\,^{\circ}\mathrm{C}$, $T_{out,0} = 70\,^{\circ}\mathrm{C}$, and $T_a = 20\,^{\circ}\mathrm{C}$. $\Delta T_{m,0}$ represents the mean temperature difference

defined as:

$$\Delta T_m \quad = \quad \frac{T_{in} - T_{out}}{2} - T_a \tag{7.2}$$

in nominal condition. n_1 in (7.1) is an exponent which varies between 1.2 and 1.4 for different radiators.

Defining the constant term $\frac{\Phi_0}{N\Delta T_{m,0}^{n_1}}$ as equivalent heat transfer coefficient, K_{rad}, (7.1) can be rewritten as:

$$\frac{C_{rad}}{N}\dot{T}_n \quad = \quad H_q(T_{n-1} - T_n) - K_{rad}(T_n - T_a)^{n_1} \tag{7.3}$$

The power transferred by the radiator to the room air can be calculated as:

$$\dot{Q}_{rad} \quad = \quad \sum_{n=1}^{N} K_{rad}(T_n - T_a)^{n_1} \tag{7.4}$$

Heat balance equations of the room is governed by the following lumped model [7]:

$$\begin{aligned} C_e\dot{T}_e &= U_eA_e(T_{amb} - T_e) + U_eA_e(T_a - T_e) \\ C_f\dot{T}_f &= U_fA_f(T_a - T_f) \\ C_a\dot{T}_a &= U_eA_e(T_e - T_a) + U_fA_f(T_f - T_a) + \dot{Q}_{rad} \end{aligned} \tag{7.5}$$

in which T_e represents the envelop temperature, T_f the temperature of the concrete floor and T_a the room air temperature. Q_{rad} is the heat power transferred to the room by radiator. Each of the envelop, floor and room air are considered as a single lump with uniform temperature distribution.

Assuming a constant pressure drop across the valve, the thermostatic valve is modeled as a static polynomial function:

$$q \quad = \quad -3.4 \times 10^{-4}\delta^2 + 0.75\delta \tag{7.6}$$

The above function is mapping the valve opening δ to the water flow through the valve.

3.2 Control Oriented Models

Step response simulations and experiments confirm a first order relationship between the radiator output heat and the input flow around a specific operating point:

$$\frac{\dot{Q}_{rad}}{q}(s) \quad = \quad \frac{K_r}{1 + \tau_r s} \tag{7.7}$$

The static gain K_r and the time constant τ_r depend on the operating point of the system i.e. corresponding flow and room temperature. In order to develop the low order model thoroughly, relationship between these parameters and the operating point will be derived based on simulation tests. Fig. 7.4 shows these relationships for a specific radiator.

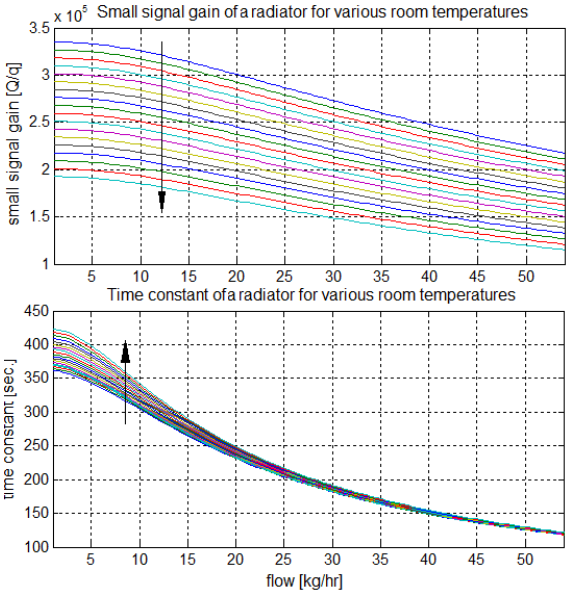

Figure 7.4: Static gain and time constant variations for various values of the radiator flow and room temperature. The arrows show the direction of room temperature increase. Room temperature is changed between $-10\,^{\circ}\mathrm{C}$ and $24\,^{\circ}\mathrm{C}$ and flow is changed between the minimum and the maximum flow

To derive the curves, radiator is simulated with small steps as the input flow. Static gain and time constant are achieved for a specific room temperature. The room temperature is then changed by $2^{\circ}\mathrm{C}$ and the procedure is repeated.

Fig. 7.4 shows that the static gain and time constant of the heat-flow transfer function are extremely dependent on the flow rate. The high gain and the long time constant in the low heat demand conditions mainly contribute to the oscillatory behavior. The model of room-radiator can be written as:

$$\frac{T_a}{q}(s) \quad = \quad \frac{K_r K_a}{(1+\tau_r s)(1+\tau_a s)} \tag{7.8}$$

Room parameters, K_a and τ_a can be estimated easily by preforming a simple step response experiment. We obtained these parameters based on [4] assuming specific materials for the components.

Estimating the flow rate and measuring the room temperature, corresponding radiator parameters can be achieved using the curves in Fig. 7.4. Consequently, the model (7.8) will be determined. These curves are approximated by two sets of polynomials using Matlab curve fitting toolbox, cftool.

4 Gain Scheduling Control Design based on Flow Adaptation

In the previous section, we developed a linear parameter varying model which approximates the radiator's nonlinearities of (7.3). In order to alleviate the effects of parameter

variations, gain scheduling control is selected among the various possible control structures which is adapted based on [15]. Therefore, the title of flow adaptation is reflecting the dependence of controller parameters to the radiator flow.

The main idea of the designed controller is to transform the primary parameter varying system model i.e. (7.8) to a system independent of the operating point. A controller would be designed based on the transformed linear time invariant (LTI) system. Block diagram of this controller is shown in Fig. 7.5.

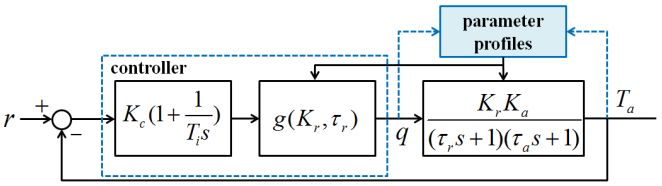

Figure 7.5: Block diagram of the controller based on linear transformation

The function g is chosen such that it cancels out the varying pole of the radiator and places a pole instead in the desired position. This position corresponds to the radiator's farthest pole in left half plane associated to the high flow rates. Therefore, the simplest candidate for the linear transfer function g is a phase-lead structure, (7.9).

$$g(K_r,\tau_r) \quad = \quad \frac{K_{r,hd}}{K_r}\frac{\tau_r s+1}{\tau_{r,hd}s+1} \tag{7.9}$$

in which $K_{r,hd}$ and $\tau_{r,hd}$ correspond to the gain and time constant of radiator in the highest demand situation when the flow rate is maximum. Consequently, the transformed system is equivalent to (7.8) at the high load operating point which corresponds to the system parameters $K_{r,hd}$ and $\tau_{r,hd}$. By choosing the high demand as the desired situation, we give the closed loop system the prospect to have the dominant poles as far as possible from the origin, and as a result as fast as possible.

The controller for the transformed LTI system is a fixed PI controller then. The parameters of this controller is calculated based on Ziegler-Nichols step response method [14]. To this end, the transformed second order system is approximated by a first-order system with a time delay, (7.10). The choice of PI controller is to track a step reference with zero steady state error.

$$\frac{T_a}{q}(s) \quad = \quad \frac{k}{1+\tau s}e^{-Ls} \tag{7.10}$$

The time delay and time constant of the above model can be found by a simple step response time analysis:

$$\begin{aligned} T_a(t) = K_{r,hd}K_a(1 &+ \frac{\tau_{r,hd}}{\tau_a-\tau_{r,hd}}e^{\frac{-t}{\tau_{r,hd}}} \\ &+ \frac{\tau_a}{\tau_{r,hd}-\tau_a}e^{\frac{-t}{\tau_a}})q(t) \end{aligned} \tag{7.11}$$

in which $q(t)=u(t)$ is the unit step input. The apparent time constant and time delay are calculated based on the time when 0.63 and 0.05 of the final value is achieved respectively.

In the following, χ is exploited as an auxiliary parameter. The positive solution of the following equation gives the time delay when $\chi = 0.95$ and the time constant when $\chi = 0.37$.

$$(\chi + 1)t^2 + 2(\tau_{r,hd} + \tau_a)(\chi - 1)t^2 + a(\chi - 1)\tau_{r,hd}\tau_a = 0 \tag{7.12}$$

Having τ and L calculated, the parameters of the regulator obtained by Ziegler-Nichols step response method would be the integration time $T_i = 3L$ and the proportional gain $K_c = \frac{0.9}{a}$ with $a = k\frac{L}{T}$ and $k = K_{r,hd} \times K_a$. k is the static gain.

4.1 Simulation Results

The proposed controller parameterized based on the radiator parameters is applied to the simulation models of the room and radiator. Parameters of the PI controller are found based on the parameter values in table 7.2 as $K_c = 0.01$ and $T_i = 400$. Ambient temperature is considered as the only source of disturbance for the system. In a partly cloudy weather condition, the effect of intermittent sunshine is modeled by a fluctuating outdoor temperature. A random binary signal is added to a sinusoid with the period of two hours to model the ambient temperature.

Simulation results with the designed controller and the corresponding ambient temperature are depicted in Fig. 7.6 and Fig. 7.7. The results are compared to the case with fixed PI controllers designed for both high and low heat demand conditions.

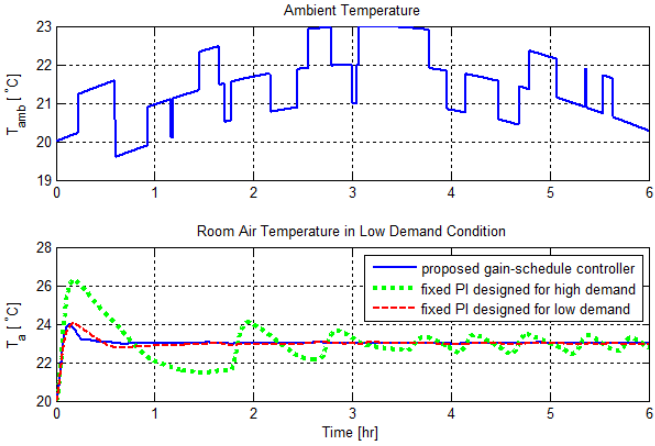

Figure 7.6: (Top) ambient temperature, (bottom) room temperature for three controllers. The results of simulation with flow adaptive controller together with two fixed PI controllers are shown. The PI controller designed for the high demand situation encounters instability in the low heat demand condition.

The simulation results of the proposed control structure show significant improvement in the system performance and stability compared to the fixed PI controller.

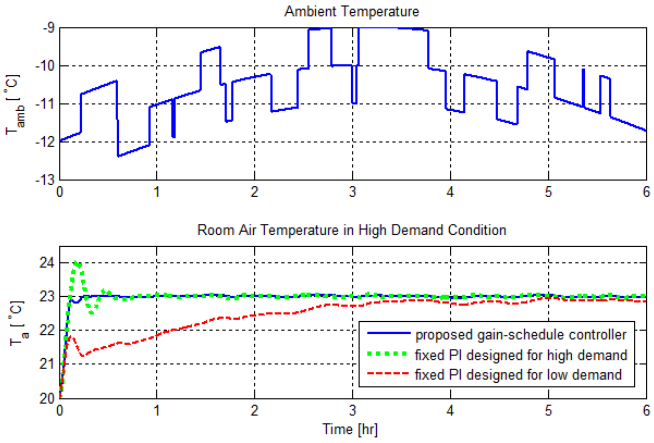

Figure 7.7: (Top) ambient temperature, (bottom) room temperature for three controllers. The results of the simulation with flow adaptive controller together with two fixed PI controllers are shown. The PI controller designed for the low demand condition is very slow for the high demand situation.

5 Discussions

All the gain scheduling control approaches are based on this assumption that all states can be measured and a generalized observability holds [15]. In this study, we also need to clarify if this assumption is valid. The parameters that we need to measure or estimate are room temperature and radiator flow rate. Measuring the first state is mandatory when the goal is seeking a reference for this temperature. However, radiator flow is not easily measurable.

To estimate the radiator's flow rate, one possibility is using a new generation of TRVs which drive the valve using a stepper motor. It is claimed that this TRV can give an estimation of the valve opening. Provided the valve opening degree, its characteristic and the pressure difference, flow rate would be estimated.

We have shown through the paper that using the new generation of TRVs, gain scheduling control would guarantee efficiency of the radiator system. However, this claim would be defensible when the flow rate estimation is done in practice through an easy, reliable method. This issue, besides robustness of the proposed controller and quantifying energy savings will be studied in the future works.

6 Conclusion

The dynamical behavior of a TRV controlled radiator is investigated. A dilemma between stability and performance for radiator control is presented. We dealt with the dilemma using a new generation of thermostatic radiator valves. With the new TRV, flow estimation and control based on energy demand would be possible. Based on the estimated flow, we have developed a gain scheduling controller which guarantees both performance and stability for the radiator system. To this end, we derived low-order models of the room-

radiator system. The model is parameterized based on the estimated operating point which is radiator flow rate. Gain scheduled controller is designed for the derived time varying model at the end.

Table 7.1: Symbols and Subscripts

Nomenclature	
A	surface area (m^2)
C	thermal capacitance $(J/kg\,^\circ\mathrm{C})$
g	linear transformation function
G	transfer function
K	static gain
K_c	controller gain
K_{rad}	equivalent heat transfer coefficient of radiator $(J/sec\,^\circ\mathrm{C})$
L	time delay $(sec.)$
N	total number of radiator distributed elements
n_1	radiator exponent
$\dot{Q}$	heat (W)
q	water flow through radiator (kg/sec)
T	temperature $(^\circ\mathrm{C})$
T_i	integration time
T_n	temperature of the radiator n^{th} element $(^\circ\mathrm{C})$
U	thermal transmittance $(kW/m^2\,^\circ\mathrm{C})$
V	volume (m^3)
ρ	density (kg/m^3)
τ	time constant $(sec.)$
Φ_0	nominal power of radiator (W)
ΔT_m	mean water temperature $(^\circ\mathrm{C})$
Subscripts	
a	room air
amb	ambient temperature (outdoor)
e	envelope
f	floor
g	ground
in	inlet (water temperature)
o	outlet (water)
out	outlet (water temperature)
p	a fraction of sun radiation heating the floor
rad, r	radiator
s	solar radiation
w	water

Table 7.2: System Parameters

Room Parameters		Radiator Parameters	
A_e	$56\ m^2$	A_r	$1.5\ m^2$
A_f	$20\ m^2$	C_{rad}	$3.1 \times 10^4\ J/kg\,^\circ\mathrm{C}$
C_a	$5.93 \times 10^4\ J/kg\,^\circ\mathrm{C}$	c_w	$4186.8\ J/kg\,^\circ\mathrm{C}$
C_e	$5 \times 10^4\ J/kg\,^\circ\mathrm{C}$	N	45
C_f	$1.1 \times 10^4\ J/kg\,^\circ\mathrm{C}$	n_1	1.3
U_e	$1.2\,kW/m^2\ ^\circ\mathrm{C}$	q_{max}	$0.015\ kg/sec$
U_f	$1.1\,kW/m^2\ ^\circ\mathrm{C}$	T_s	$70\ ^\circ\mathrm{C}$
p	neglected	V	$5\ Liter$
Q_e	neglected	Φ_0	$1700\ W$
Q_s	neglected	ρ_w	$998\ kg/m^3$

References

[1] S. Svendsen, H. M. Tommerup, and M. Beck Hansen, "Energy project villa," Partners: Technical University of Denmark, Department of Civil Eng. and Rockwool, Denmark, Main Report, March 2005, downloded from DTU database.

[2] P. Rathje, "Modeling and simulation of a room temperature control system," in *Proceedings of SIMS87 Symposium*. Scandinavian Simulation Society, 1987, pp. 58–69.

[3] K. K. Andersen, H. Madsen, and L. H. Hansen, "Modleing the heat dynamics of a building using stochastic differential equations," *Energy and Buildings*, vol. 31, no. 1, pp. 13–24, 1998.

[4] ASHRAE, *ASHRAE Handbook 1990, fundamentals*. Atlanta: ASHRAE Inc., 1990.

[5] A. K. Athienitis, M. Stylianou, and J. Shou, "Methodology for building thermal dynamics studies and control applications," *ASHRAE Trans.*, vol. 96, no. 2, pp. 839–848, 1990.

[6] M. L. Kurkarni and F. Hong, "Energy optimal control of residential space-conditioning system based on sensible heat transfer modeling," *Building and Environment*, vol. 39, no. 1, pp. 31–38, 2004.

[7] G. Hudson and C. P. Underwood, "A simple building modeling procedure for matlab/simulink," *Proc. of Building Simulation*, vol. 99, no. 2, pp. 777–783, 1999.

[8] H. Madsen and J. Holst, "Estimation of a continuous time model for the heat dynamics of a building," *Energy and Buildings*, vol. 22, pp. 67–79, 1995.

[9] K. M. Letherman, C. J. Paling, and P. M. Park, "The measurement of dynamic thermal response in rooms using pseudorandom binary sequences," *Building and Environment*, vol. 17, no. 1, 1982.

[10] J. Braun and N. Chaturvedi, "An inverse grey-box model for transient building load prediction," *HVAC Research*, vol. 8, no. 1, pp. 73–99, 2002.

[11] B. Xu, L. Fu, and H. Di, "Dynamic simulation of space heating systems with radiators controlled by trvs in buildings," *Energy and Buildings*, vol. 40, pp. 1755–1764, 2008.

[12] F. Tahersima, J. Stoustrup, H. Rasmussen, and P. Gammeljord Nielsen, "Thermal analysis of an hvac system with trv controlled hydronic radiator," in *IEEE International Conference on Automation Science and Engineering*, Toronto, Canada, August 2010, pp. 756–761.

[13] L. H. Hansen, "Stochastic modeling of central heating systems," Ph.D. dissertation, Technical University of Denmark, Dep. of Mathematical Modeling, Denmark, 1997.

[14] K. Åstrom and T. Hagglund, *PID Controllers*. North Carolina: ISA, 1995.

[15] K. Åstrom and B. Wittenmark, *Adaptive Controller*. Mineola, New York: DOVER Publications Inc., 2008.

Paper B

Eliminating Oscillations in TRV-Controlled Hydronic Radiators

Fatemeh Tahersima, Jakob Stoustrup, Henrik Rasmussen

This paper is published in:
IEEE Conference on Decision and Control ECC-CDC, December 2011,
Orlando, Florida, US

Abstract

Thermostatic Radiator Valves (TRV) have proved their significant contribution in energy savings for several years. However, at low heat demands, an unstable oscillatory behavior is usually observed and well known for these devices. This instability is due to the nonlinear dynamics of the radiator itself which result in a large time constant and high gain for radiator at low flows. A remedy to this problem is to make the controller of TRVs adaptable with the operating point instead of widely used fixed PI controllers. To this end, we have derived a linear parameter varying model of radiator, formulated based on the operating flow rate, room temperature and the radiator specifications. In order to derive such formulation, the partial differential equation of the radiator heat transfer dynamics is solved analytically. Using the model, a gain schedule controller among various possible control strategies is designed for the TRV. It is shown via simulations that the designed controller based on the proposed LPV model performs excellent and stable in the whole operating conditions.

1 INTRODUCTION

Efficient control of heating, ventilation and air conditioning (HVAC) systems has a great influence on the thermal comfort of residents. The other important objective is energy savings, mainly because of the growth of energy consumption, costs and also correlated environmental impacts.

Hydronic radiators controlled by thermostatic radiator valves (TRV) provide good comfort under normal operating conditions. Thermal analysis of the experimental results of a renovated villa in Denmark, built before 1950, has demonstrated that energy savings near 50% were achieved by mounting TRVs on all radiators and fortifying thermal envelope insulation [1].

1.1 System Description

The case study is composed of a room and a radiator with thermostatic valve. Disturbances which excite the system are ambient temperature and heat dissipated by radiator. It is assumed that heat transfer to the ground is negligible having thick layers of insulation beneath the concrete floor. Block diagram of the system is shown in Fig. 8.1. All of the symbols, subscripts and the parameters value are listed in table 8.1 and table 8.2. The chosen values for all parameters are in accordance with the typical experimental and standard values [2]. As mentioned before, the case study is adopted to the one previously studied in [3].

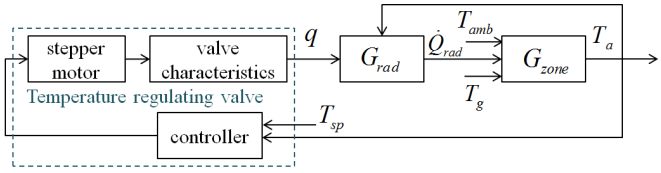

Figure 8.1: Closed loop control system of room and radiator

The TRV is driven by a batterized stepper motor. Pressure drop across the radiator valve is maintained constant unlike what is taken as the control strategy in [4]. Instead, flow control is assumed to be feasible by the accurate adjustment of the valve opening. The valve opening is regulated by the stepper motor which allows the concrete adjustment.

1.2 Problem Definition

To maintain the temperature set point in a high load situation, TRVs are usually tuned with a high controller gain.The inefficiency appears in the seasons with low heat demand especially when the water pump or radiator are over dimensioned [5]. In this situation, due to a low flow rate, loop gain increases; and as a result oscillations in room temperature may occur. Besides discomfort, oscillations decrease the life time of the actuators. This problem is addressed in [4] for a central heating system with gas-expansion based TRVs. It is proposed to control the differential pressure across the TRV to keep it in a suitable operating area using an estimate of the valve position.

The dilemma between stability and performance arises when TRV is controlled by a fixed linear controller. Designing TRV controller for high demand seasonal condition, usually leads to instability in low demand weather condition. A high loop gain and long time constant are the main reasons of this phenomenon. In contrast, selecting a smaller controller gain to handle the instability situation, will result in a poor radiator reaction while the heat demand is high.

Figures 8.2 and 8.3 show the results of a simulation where oscillations and low performance occur. In the shown simulation results, the forward water temperature is at $50°\mathrm{C}$. The proportional integral (PI) controller of TRV is tuned based on Ziegler-Nichols step response method [6].

A remedy to this dilemma is choosing an adaptive controller instead of the current fixed PI controller.

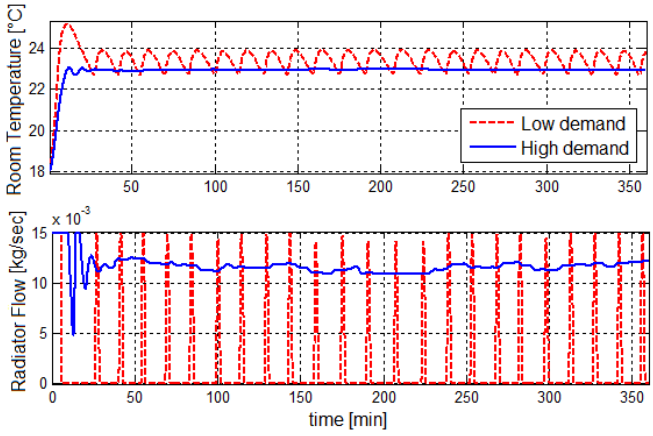

Figure 8.2: Undamped oscillations in room temperature and radiator flow which occur in low demand situation while the controller is designed for high demand condition.

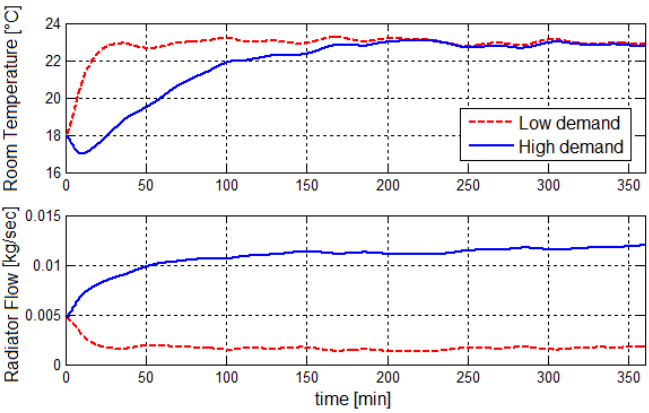

Figure 8.3: Poor performance in the cold weather condition, applying the controller designed for the low demand situation

It is, also, worth mentioning that the same problem was investigated via simulation based studies in [3]. The LPV control oriented model of radiator was, however, developed based on simulations.

In order to validate the controller performance, we utilized simulation models of the HVAC components. Two approaches for HVAC systems modeling are the forward, [7, 8, 9] and the data-driven methods [10, 11, 12] indicated by [2].

In this paper, we adopted heat balance equations of the room model in accordance to the analogous electric circuit, described formerly in [13]. Radiator dynamics are formulated as a distributed system in order to analyze the radiator transferred heat.

Rest of the paper is organized as follows: In section II, the radiator transferred heat is derived analytically. Based on the result, control oriented models are developed in section III. Utilizing the models, the control structure based on flow adaptation is proposed in the same section. A simulation-based test is conducted in section IV. Discussion and conclusions are given finally in Sections V.

2 System Modeling

2.1 Heat Balance Equations

Radiator is modeled as a lumped system with N elements in series. The nth section temperature is given by, [14]:

$$\frac{C_{rad}}{N}\dot{T}_n = c_w q(T_{n-1} - T_n) - \frac{K_r}{N}(T_n - T_a) \tag{8.1}$$

in which C_{rad} is the heat capacity of the water and radiator material, T_n is the temperature of the radiator's nth element and $n = 1, 2, \ldots, N$. The temperature of the radiator ending points are inlet temperature: $T_0 = T_{in}$, and return temperature: $T_N = T_{out}$. In this formulation, we assumed the same temperature of the radiator surface as the water inside radiator. Besides, heat transfer only via convection is considered. K_r represents

the radiator equivalent heat transfer coefficient which is defined based on one exponent formula, [14] in the following:

$$K_r = \frac{\Phi_0}{{\Delta T_{m,0}}^{n_1}} (T_n - T_a)^{n_1 - 1} \tag{8.2}$$

in which Φ_0 is the radiator nominal power in nominal condition which is $T_{in,0} = 90°C$, $T_{out,0} = 70°C$ and $T_a = 20°C$. $\Delta T_{m,0}$ expresses the mean temperature difference which is defined as $\Delta T_m = \frac{T_{in} - T_{out}}{2} - T_a$ in nominal condition. n_1 is the radiator exponent which varies between 1.2 and 1.4, but 1.3 is the value of the exponent for most radiators. In such case, we can approximate the non fixed, nonlinear term in K_r with a constant between 2.5 and 3.2 for a wide enough range of temperature values. Picking 2.8 as the approximation value, $K_r = 2.8 \times \frac{\Phi_0}{{\Delta T_{m,0}}^{1.3}}$.

The power transferred to the room can be described as:

$$Q_r = \sum_{n=1}^{N} K_r (T_n - T_a) \tag{8.3}$$

Heat balance equations of the room is governed by the following lumped model [9]:

$$\begin{aligned} C_e \dot{T}_e &= U_e A_e (T_{amb} - T_e) + U_e A_e (T_a - T_e) \\ C_f \dot{T}_f &= U_f A_f (T_a - T_f) \\ C_a \dot{T}_a &= U_e A_e (T_e - T_a) + U_f A_f (T_f - T_a) + Q_r \end{aligned} \tag{8.4}$$

in which T_e represents the envelop temperature, T_f the temperature of the concrete floor and T_a the room air temperature. Q_r is the heat power transferred to the room by radiator. Each of the envelop, floor and room air are considered as a single lump with uniform temperature distribution.

Assuming a constant pressure drop across the valve, the thermostatic valve is modeled with a static polynomial function mapping the valve opening δ to the flow rate q:

$$q = -3.4 \times 10^{-4} \delta^2 + 0.75\delta \tag{8.5}$$

The above presented radiator model is highly nonlinear and not suitable for design of controller; thus a simplified control oriented LPV model is developed in the next section.

2.2 Control Oriented Models

The relationship between room air temperature and radiator output heat can be well approximated by a 1^{st} order transfer function.

$$\frac{T_a}{Q_{rad}}(s) = \frac{K_a}{1 + \tau_a s} \tag{8.6}$$

The above model parameters can be identified simply via a step response test as well.

Step response simulations and experiments confirm a first order transfer function between the radiator output heat and input flow rate at a specific operating point as

$$\frac{Q_r}{q}(s) = \frac{K_{rad}}{1 + \tau_{rad} s} \tag{8.7}$$

In the next section, parameters of the above model are formulated based on the closed-form solution of the radiator output heat, $Q_r(t, q, T_a)$.

2.3 Radiator Dynamical Analysis

In this paper, unlike [3], we found the closed-form map between the radiator heat and operating point which is corresponding flow rate q, and room temperature T_a. We, previously, derived this dependency via a simulative study in the form of two profile curves, [3].

To develop $Q(t, q, T_a)$, a step flow is applied to the radiator, i.e. changing the flow rate from q_0 to q_1, at a constant differential pressure across the valve. Propagating with the speed of sound, the flow shift is seen in a fraction of second all along the radiator. Hence, flow is regarded as a static parameter for $t > 0$, rather than temperature distribution along radiator.

Consider a small radiator section Δx with depth d and hight h as shown in Fig. 8.4. The temperature of incoming flow to this section is $T(x)$, while the outgoing flow is at $T(x + \Delta x)°C$. Temperature is considered to be constant $T(x)$ in a single partition.

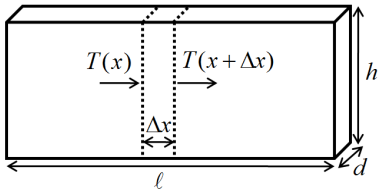

Figure 8.4: A radiator section area with the heat transfer equation governed by (8.8)

The corresponding heat balance equation of this section is given as follows.

$$qc_w\left(T(x) - T(x+\Delta x)\right) + K_r\frac{\Delta x}{\ell}\left(T_a - T(x)\right) = = C_r\frac{\Delta x}{\ell}\frac{\partial T}{\partial t} \tag{8.8}$$

in which flow rate is q_0 at $t = 0$ and q_1 for $t > 0$. C_r is the heat capacity of water and the radiator material defined as: $C_r = c_w\rho_w V_w$. Dividing both sides by Δx and approaching $\Delta x \to 0$, we have:

$$-qc_w\frac{\partial T(x,t)}{\partial x} + \frac{K_r}{\ell}\left(T_a - T(x,t)\right) = \frac{C_r}{\ell}\frac{\partial T(x,t)}{\partial t} \tag{8.9}$$

with boundary condition $T(0,t) = T_{in}$, $T(\ell, 0^-) = T_{out,0}$ and $T(\ell,\infty) = T_{out,1}$. If there exists a separable solution, it would be like $T(x,t) = T(t) \times X(x)$. Substituting it into (8.9), we achieve:

$$T(0,t) = c_1 e^{k_1 t} + c_2 \tag{8.10}$$

which implies a contradiction.

Before proceed to solve the full PDE (8.9), we need to find the two boundary conditions $T_{out,0}$ and $T_{out,1}$. For this purpose, take the steady state form of (8.9) as follows.

$$-qc_w\frac{dT}{dx} + \frac{K_r}{\ell}\left(T_a - T(x)\right) = 0 \tag{8.11}$$

which can be written as:

$$\frac{dT}{dx} + \frac{\beta}{\gamma} T(x) = T_a \tag{8.12}$$

with constants $\beta = \frac{K_r}{C_r}$ and $\gamma = \frac{qc_w\ell}{C_r}$. We will be using the two definitions throughout the paper frequently.

Therefore, the steady state temperature, $T(x,t)|_{t\to\infty}$ will be achieved as:

$$T(x) = c_1 e^{-\frac{\beta}{\gamma}x} + c_0 \tag{8.13}$$

at the specific flow rate q. Substituting the above equation in (8.12) gives $c_0 = T_a$. Knowing $T(0) = T_{in}$, c_1 is also found. Finally $T(x)$ looks like:

$$T(x) = (T_{in} - T_a)e^{-\frac{\beta}{\gamma}x} + T_a \tag{8.14}$$

Therefor the two boundary conditions are: $T_{out,0} = (T_{in} - T_a)e^{-\frac{\beta}{\gamma_0}x} + T_a$ and $T_{out,1} = (T_{in} - T_a)e^{-\frac{\beta}{\gamma_1}x} + T_a$ corresponding to the flow rates q_0 and q_1.

Generally solving the full PDE (8.9) in time domain is a difficult task. However we are interested in the radiator transferred heat to the room rather than temperature distribution along the radiator. Instead of $T(x,t)$, therefore, we will find $Q(t)$ which is independent of x. $Q(t)$ can be formulated as:

$$Q(t) = \int_0^\ell \frac{K_r}{\ell} \left(T(x,t) - T_a\right) \, dx \tag{8.15}$$

Taking time derivative of the above equation and using (8.9):

$$\frac{dQ}{dt} = \int_0^\ell \frac{K_r}{C_r} \left(-qc_w \frac{\partial T}{\partial x} + \frac{K_r}{\ell} \left(T_a - T(x,t)\right) \right) \, dx \tag{8.16}$$

with $\beta = \frac{K_r}{C_r}$. The above equation can be rewritten as:

$$\frac{dQ}{dt} + \beta Q = \beta q c_w \left(T_{in} - T_{out}\right) \tag{8.17}$$

in which T_{in} is the constant forward temperature. However T_{out} in the above equation is a function of time. Therefor we need an expression for $T_{out}(t)$ which is attained in the following.

To develop $T_{out}(t)$, consider (8.9) at $x = \ell$:

$$-qc_w \frac{\partial T}{\partial x} \mid_\ell + \frac{K_r}{\ell} \left(T_a - T(\ell,t)\right) = \frac{C_r}{\ell} \frac{dT(\ell,t)}{dt} \tag{8.18}$$

The first term in the left side of the above equation is an unknown function of time which we call it $f(t)$. Thus the above equation can be rewritten as:

$$\dot{T}_{out} + \beta T_{out} = \beta T_a - \gamma f(t) \tag{8.19}$$

with $\beta = \frac{K_r}{C_r}$ and $\gamma = \frac{qc_w\ell}{C_r}$. In order to estimate $f(t)$ we take a look at the simulation result for this function which is a position derivative of $T(x,t)$ at the end of radiator.

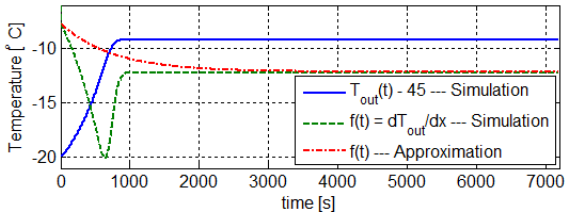

Figure 8.5: Simulation results for scaled $T_{out}(t)$, its first position derivative and its approximation are shown. The first position derivative i.e. $f(t)$ is approximated with an exponential function.

It turns out we can approximate $f(t)$ with an exponential function roughly as shown in Fig.8.5

We know the initial and final value of $f(t)$. Also, the minimum of $f(t)$ occurs at the transportation time of flow to the end of radiator i.e. $\frac{\rho_w V_w}{q}$. Therefore, we approximate $f(t)$ as bellow:

$$f(t) = (f_0 - f_1)e^{-\tau t} + f_1 \tag{8.20}$$

with $f_0 = -\frac{\beta}{\gamma_0}(T_{in} - T_a)e^{-\frac{\beta}{\gamma_0}\ell}$, $f_1 = -\frac{\beta}{\gamma_1}(T_{in} - T_a)e^{-\frac{\beta}{\gamma_1}\ell}$ and $\tau = \frac{q}{\rho_w V_w}$.

Substituting $f(t)$ in (8.18), the return temperature is obtained as follows:

$$T_{out}(t) = c_1 e^{-\beta t} + c_2 e^{-\tau t} + c_0 \tag{8.21}$$

with $c_0 = T_a - \frac{\gamma_1}{\beta}$, $c_2 = \frac{\gamma_1(f_0 - f_1)}{\tau}$ and $c_1 = T_{out,0} - c_0 - c_2$.

Back to (8.17), we substitute $T_{out}(t)$ in the equation. $Q(t)$ becomes:

$$\begin{aligned} Q(t) &= (k_1 t + k_0)e^{-\beta t} + k_2 e^{-\tau t} + k_3 \\ k_1 &= -\beta q c_w c_1 \\ k_2 &= \frac{\beta q c_w c_2}{\tau - \beta} \\ k_3 &= q c_w (T_{in} - c_0) \\ k_0 &= c_w q_0 (T_{in} - T_{out,0}) - k_2 - k_3 \end{aligned} \tag{8.22}$$

The result is not a precise solution because we have made an approximation while deriving $T_{out}(t)$. But it is still enough for us to extract useful information regarding the time constant and gain. The analytic solution and simulation for a specific flow rate is shown in Fig.8.6.

The overshoot in the analytic solution compared to the simulation is due to neglecting an undershoot in $T_{out}(t)$ calculations.

In the next section, we utilize the derived formula to extract the required gain and time constant for the control oriented LPV model.

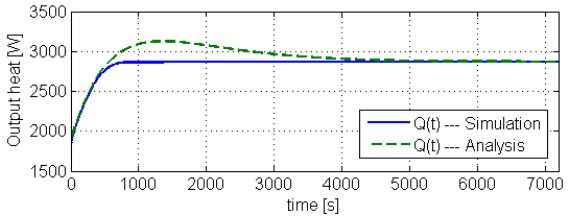

Figure 8.6: Simulation and analysis results for Q(t). The analytic solution gives us a good enough approximation of the transient and final behavior of the radiator output heat. We utilize this analytic solution to extract the parameters of a first order approximation of $Q(t)$ step response.

2.4 Radiator LPV Model

Parameters K_{rad} and τ_{rad} of the radiator LPV model (8.7) are derived based on first order approximation of the radiator power step response (8.22). The steady state gain is:

$$K_{rad} \quad = c_w(T_{in} - T_{out,1}) \tag{8.23}$$

with $T_{out,1}$ corresponding to the flow rate q_1. Using the tangent to $Q(t)$ at $t = 0$ we can obtain the time constant. The slope of the tangent would be equivalent to the first derivative of $Q_{final} + (Q_0 - Q_{finale})e^{-\frac{t}{\tau_{rad}}}$ at $t = 0$ which gives:

$$\tau_{rad} = \frac{Q_{final} - Q_0}{k_1 - \beta k_0 - \tau k_2} \tag{8.24}$$

Therefore, at a specific operating point, the radiator gain and time constant can be obtained via (8.24) and (8.23). For a set of operating points these parameters are shown as two profile of curves in Fig. 8.7.

Fig. 8.7 shows that the radiator gain and time constant of the heat-flow transfer function significantly depend on the flow rate. The high gain and the long time constant in the low heat demand conditions mainly contribute to the oscillatory behavior. The control oriented model of room-radiator can be written as:

$$\frac{T_a}{q}(s) = \frac{K_{rad}K_a}{(1 + \tau_{rad}s)(1 + \tau_a s)} \tag{8.25}$$

Room parameters, K_a and τ_a can be estimated easily by preforming a simple step response experiment. We obtained these parameters based on [2] assuming specif materials for the components.

3 Gain Scheduling Control Design based on Flow Adaptation

In the previous section, we developed a linear parameter varying model for radiator instead of the high-order nonlinear model (8.1). To control this system, among various possible control structures, gain scheduling approach is selected which is a very useful technique for reducing the effects of parameter variations [15]. Therefore, the name of

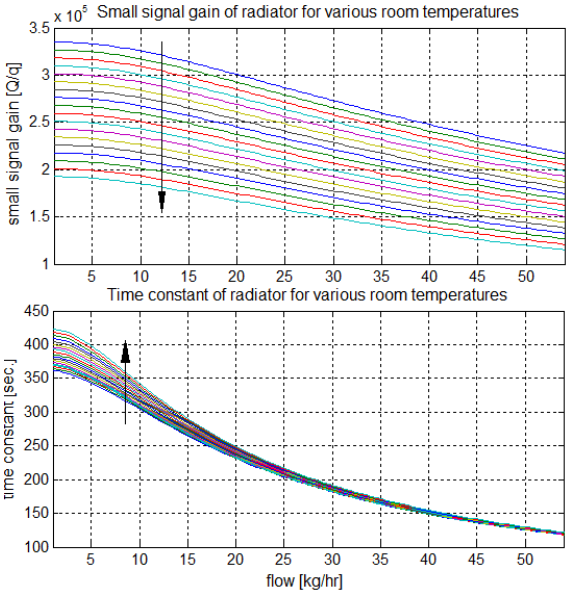

Figure 8.7: Steady state gain and time constant variations for various values of the radiator flow and room temperature. The arrows show the direction of room temperature increase. Room temperature is changed between $-10\,^{\circ}\mathrm{C}$ and $24\,^{\circ}\mathrm{C}$ and flow is changed between the minimum and maximum flow

flow adaptation indicates to this fact that controller parameters are dependent on the estimated radiator flow.

The main idea for design of adaptive controller is to transform the system model (8.25) to a system independent of the operating point. Then, the controller would be designed based on the transformed linear time invariant (LTI) system. The block diagram of this controller is shown in Fig. 8.8.

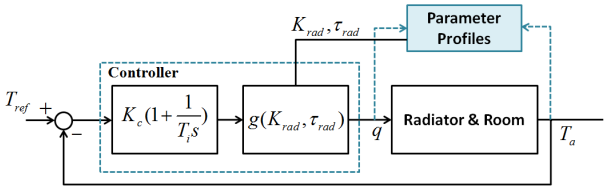

Figure 8.8: Block diagram of the closed loop system with linear transformation

Function g is chosen such that to cancel out the moving pole of the radiator and places a pole instead in the desired position. This position corresponds to the farthest position of the radiator pole which happens in high flows or high demand condition. Therefore, the

simplest candidate for the linear transfer function g is a phase-lead structure, (8.26).

$$g(K_{rad}, \tau_{rad}) = \frac{K_{hd}}{K_{rad}} \frac{\tau_{rad} s + 1}{\tau_{hd} s + 1} \tag{8.26}$$

in which K_{hd} and τ_{hd} correspond to the gain and time constant of radiator in the high demand situation when the flow rate is maximum. Consequently, the transformed system would behave always similar to the high demand situation. By choosing the high demand as the desired situation, we give the closed loop system the prospect to have the dominant poles as far as possible from the origin, and as a result as fast as possible.

The controller for the transformed LTI system is a fixed PI controller then. The parameters of this controller is calculated based on Ziegler-Nichols step response method [6]. To this end, the transformed second order system is approximated by a first-order system with a time delay, (8.27). The choice of PI controller is to track a step reference with zero steady state error.

$$\frac{T_a}{q}(s) \quad = \quad \frac{k}{1 + \tau s} e^{-Ls} \tag{8.27}$$

The time delay and time constant of the above model can be found by a simple step response time analysis of the transformed second-order model:

$$\begin{aligned} T_a(t) = K_{hd} K_a (1 + \frac{\tau_{hd}}{\tau_a - \tau_{hd}} e^{\frac{-t}{\tau_{hd}}} \\ + \frac{\tau_a}{\tau_{hd} - \tau_a} e^{\frac{-t}{\tau_a}}) q(t) \end{aligned} \tag{8.28}$$

in which $q(t) = u(t)$ is the unit step input. The apparent time constant and time delay are calculated based on the time when 0.63 and 0.05 of final T_a is achieved, respectively. The positive solution of the following equation gives the time delay when $\chi = 0.95$ and the time constant when $\chi = 0.37$.

$$(\chi + 1)t^2 + 2(\tau_{hd} + \tau_a)(\chi - 1)t^2 + a(\chi - 1)\tau_{hd}\tau_a = 0 \tag{8.29}$$

Having τ and L calculated, the parameters of the regulator obtained by Ziegler-Nichols step response method would be the integration time $T_i = 3L$ and proportional gain $K_c = \frac{0.9}{a}$ with $a = k\frac{L}{T}$ and $k = K_{hd} \times K_a$ which is the static gain.

3.1 Simulation Results

The proposed controller parameterized based on radiator parameters, is applied to the simulation models of room and radiator. Parameters of the PI controller are found based on the parameter values in table 8.2 as $K_c = 0.01$ and $T_i = 400$. Ambient temperature is considered as the only source of disturbance for the system. In a partly cloudy weather condition, the effect of intermittent sunshine is modeled by a fluctuating outdoor temperature. A random binary signal is added to a sinusoid with the period of two hours to model the ambient temperature.

Simulation results with the designed controller and the corresponding ambient temperature are depicted in Fig. 8.9 and Fig. 8.10. The results are compared to the case with fixed PI controllers designed for both high and low heat demand conditions.

The simulation results of the proposed control structure show significant improvement in the system performance and stability compared to the fixed PI controller.

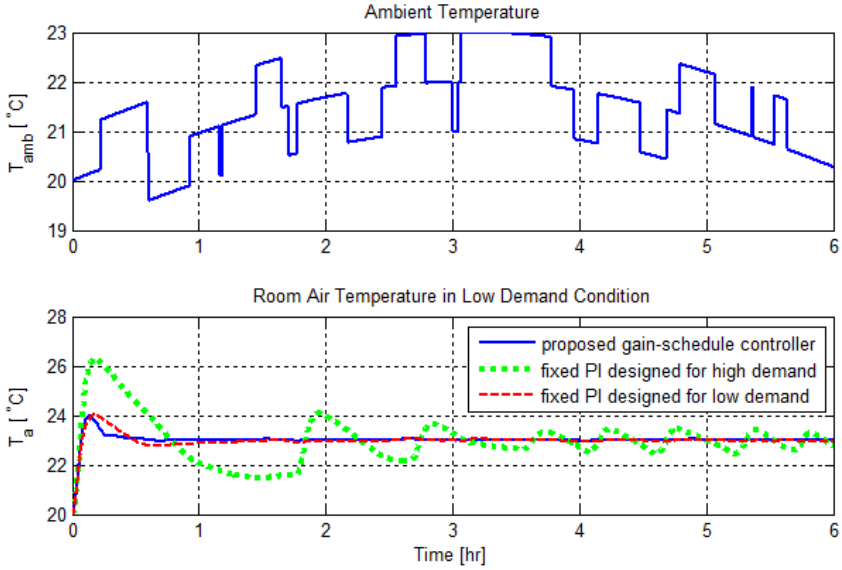

Figure 8.9: (Top) ambient temperature, (bottom) room temperature for three controllers. The results of simulation with flow adaptive controller together with two fixed PI controllers are shown. The PI controller designed for the high demand situation encounters instability in the low heat demand condition.

4 Discussions

All the gain scheduling control approaches are based on this assumption that all states can be measured and a generalized observability holds [15]. In this study, we also need to clarify if this assumption is valid. The parameters that we need to measure or estimate are room temperature and radiator flow rate. Measuring the first state is mandatory when the goal is seeking a reference for this temperature. However, radiator flow is not easily measurable.

To have an estimation of the radiator flow rate, one possibility is using a new generation of TRVs which drive the valve with a step motor. It is claimed that this TRV can give an estimation of the valve opening. Knowing this fact and assuming a constant pressure drop across the radiator valve, we would be able to estimate the flow rate.

We have shown through the paper that using the new generation of TRVs, gain scheduling control would guarantee the efficiency of the radiator system.

5 Conclusion

The dynamical behavior of a TRV controlled radiator is investigated. A dilemma between stability and performance for radiator control is presented. We dealt with the dilemma using a new generation of thermostatic radiator valves. With the new TRV, flow estimation and control would be possible. Based on the estimated flow, we have developed a gain schedule controller which guarantees both performance and stability for the radiator sys-

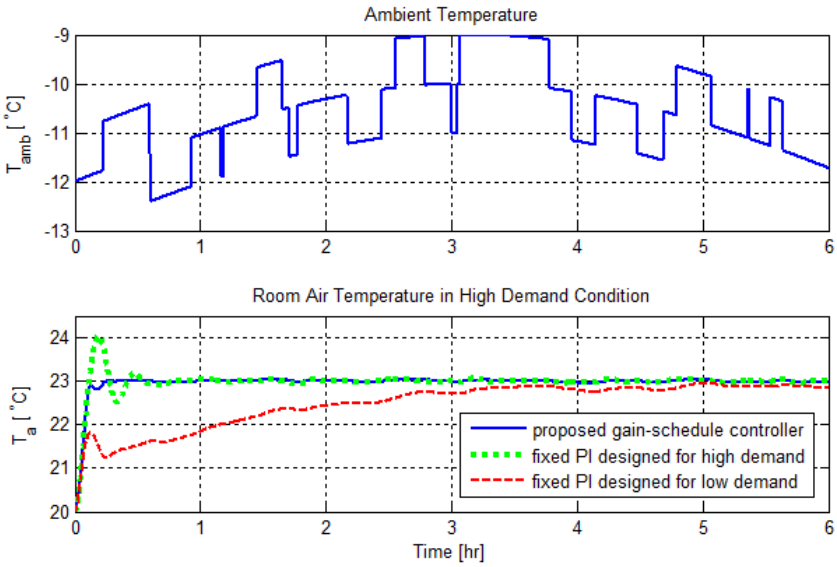

Figure 8.10: (Top) ambient temperature, (bottom) room temperature for three controllers. The results of the simulation with flow adaptive controller together with two fixed PI controllers are shown. The PI controller designed for the low demand condition is very slow for the high demand situation.

tem. To this end, we derived low-order models of the room-radiator system. The model is parameterized based on the estimated operating point which is radiator flow rate. Gain schedule controller is designed for the resulted time varying model.

References

[1] S. Svendsen, H. M. Tommerup, and M. Beck Hansen, "Energy project villa," Partners: Technical University of Denmark, Department of Civil Eng. and Rockwool, Denmark, Main Report, March 2005, downloded from DTU database.

[2] ASHRAE, *ASHRAE Handbook 1990, fundamentals*. Atlanta: ASHRAE Inc., 1990.

[3] F. Tahersima, J. Stoustrup, and H. Rasmussen, "Stability-performance dilemma in trv-based hydronic radiators," in *IEEE Multi-Conference on Systems and Control*, Denver, Colorado, USA, October 2011.

[4] K. K. Andersen, H. Madsen, and L. H. Hansen, "Modleing the heat dynamics of a building using stochastic differential equations," *Energy and Buildings*, vol. 31, no. 1, pp. 13–24, 1998.

[5] P. Rathje, "Modeling and simulation of a room temperature control system," in *Proceedings of SIMS87 Symposium*. Scandinavian Simulation Society, 1987, pp. 58–69.

[6] K. Åstrom and T. Hagglund, *PID Controllers*. North Carolina: ISA, 1995.

[7] A. K. Athienitis, M. Stylianou, and J. Shou, "Methodology for building thermal dynamics studies and control applications," *ASHRAE Trans.*, vol. 96, no. 2, pp. 839–848, 1990.

[8] M. L. Kurkarni and F. Hong, "Energy optimal control of residential space-conditioning system based on sensible heat transfer modeling," *Building and Environment*, vol. 39, no. 1, pp. 31–38, 2004.

[9] G. Hudson and C. P. Underwood, "A simple building modeling procedure for matlab/simulink," *Proc. of Building Simulation*, vol. 99, no. 2, pp. 777–783, 1999.

[10] H. Madsen and J. Holst, "Estimation of a continuous time model for the heat dynamics of a building," *Energy and Buildings*, vol. 22, pp. 67–79, 1995.

[11] K. M. Letherman, C. J. Paling, and P. M. Park, "The measurement of dynamic thermal response in rooms using pseudorandom binary sequences," *Building and Environment*, vol. 17, no. 1, 1982.

[12] J. Braun and N. Chaturvedi, "An inverse grey-box model for transient building load prediction," *HVAC Research*, vol. 8, no. 1, pp. 73–99, 2002.

[13] F. Tahersima, J. Stoustrup, H. Rasmussen, and P. Gammeljord Nielsen, "Thermal analysis of an hvac system with trv controlled hydronic radiator," in *IEEE International Conference on Automation Science and Engineering*, Toronto, Canada, August 2010, pp. 756–761.

[14] L. H. Hansen, "Stochastic modeling of central heating systems," Ph.D. dissertation, Technical University of Denmark, Dep. of Mathematical Modeling, Denmark, 1997.

[15] K. Åstrom and B. Wittenmark, *Adaptive Controller*. Mineola, New York: DOVER Publications Inc., 2008.

Table 8.1: Symbols and Subscripts

Nomenclature	
A	surface area (m^2)
C	thermal capacitance $(J/kg\,^\circ\mathrm{C})$
c_w	thermal capacitance of both water and radiator material
d	depth of radiator
g	linear transformation function
G	transfer function
h	height of radiator (m)
h_a	air convective heat transfer coefficient
K	DC gain
K_c	controller gain
K_r	equivalent heat transfer coefficient of radiator $(J/sec\,^\circ\mathrm{C})$
L	time delay $(sec.)$
N	total number of radiator distributed elements
n_1	radiator exponent
Q	heat (W)
q	water flow through radiator (kg/sec)
T	temperature $(^\circ\mathrm{C})$
T_i	integration time
T_{in}	inlet water temperature
T_n	temperature of the radiator n^{th} element $(^\circ\mathrm{C})$
T_{out}	outlet water temperature
T^i_{out}	steady state T_{out} corresponding to flow rate q_i
U	thermal transmittance $(kW/m^2\,^\circ\mathrm{C})$
V_w	water capacity of radiator (m^3)
ρ	density (kg/m^3)
τ	time constant $(sec.)$
δ	valve opening
ℓ	length of radiator
Subscripts	
a	room air
amb	ambient temperature (outdoor)
e	envelop
f	floor
hd	high demand
rad	radiator
ref	reference temperature of room

Table 8.2: System Parameters

Room Parameters		Radiator Parameters	
A_e	$56\ m^2$	A_r	$1.5\ m^2$
A_f	$20\ m^2$	C_{rad}	$3.1 \times 10^4\ J/kg\,°\mathrm{C}$
C_a	$5.93 \times 10^4\ J/kg\,°\mathrm{C}$	c_w	$4186.8\ J/kg\,°\mathrm{C}$
C_e	$5 \times 10^4\ J/kg\,°\mathrm{C}$	N	45
C_f	$1.1 \times 10^4\ J/kg\,°\mathrm{C}$	n_1	1.3
U_e	$1.2\,kW/m^2\ °\mathrm{C}$	q_{max}	$0.015\ kg/sec$
U_f	$1.1\,kW/m^2\ °\mathrm{C}$	T_s	$70\ °\mathrm{C}$
		V	$5\ Liter$

Paper C

An Analytical Solution for Stability-Performance Dilemma of TRV-Controlled Hydronic Radiators

Fatemeh Tahersima, Jakob Stoustrup, Henrik Rasmussen

This paper is submitted in:
Energy and Buildings

The layout has been revised

Abstract

Thermostatic radiator valves (TRV) have proved their significant contribution in energy savings for several years. However, at low heat demands, an unstable oscillatory behavior is usually observed and well known for these devices. This closed-loop instability is due to the nonlinear dynamics of the radiator which result in a large time constant and high gain for the radiator at low flows. In order to alleviate the caused discomfort, one way is to replace the fixed PI controller of TRV with an adaptive controller. this paper presents a gain scheduling controller based on a proposed linear parameter varying model of radiator dynamics. The model is parameterized based on the operating flow rate, room temperature and radiator specifications. The parameters are derived according to the proposed analytic solution for the heat dissipated by the radiator. It is shown via simulations that the designed controller based on the proposed linear parameter varying (LPV) model performs excellent and remains stable in the whole operating conditions.

keywords:*Hydronic radiator, Modeling, Dynamical analysis, Thermal comfort, Gain-scheduling control*

1 Introduction

Efficient control of heating, ventilation and air conditioning (HVAC)[1] systems has a great influence on the thermal comfort of residents. The other important objective is energy savings, mainly because of the growth of energy consumption, costs and also correlated environmental impacts. A thermostatic radiator valve (TRV)[2] mounted on a hydronic radiator is an excellent example of such energy efficient controller. It cuts down the heating energy consumption up to 20% while improving comfort [1].

Hydronic radiators controlled by TRVs provide good comfort under normal operating conditions. Thermal analysis of the experimental results of a renovated villa in Denmark, built before 1950, has demonstrated that energy savings near 50% were achieved by mounting TRVs on all radiators and fortifying thermal envelope insulation [2]. Also, various studies are conducted worldwide to conclude that radiant heating consumes less energy compared to that used by a forced air heating system [3, 4, 5].

However, less studies are conducted around a very well-know inefficient radiator operation condition. To maintain the room temperature set point in a high load situation, the TRV is usually tuned with a high controller gain.The inefficiency appears in the seasons with low heat demand especially when the water pump or radiator are over dimensioned [6]. In this situation, due to a low flow rate, loop gain increases; and as a result oscillations in room temperature may occur. Besides discomfort, oscillations decrease the life time of the actuators. This problem is addressed in [7] for a central heating system with gas-expansion based TRVs. It is proposed to control the differential pressure across the TRV to keep it in a suitable operating area by estimating the valve position.

In this study, however, we dealt with a TRV, driven by a battery-based stepper motor. It has been investigated via simulations that a fixed proportional integral (PI)[3] controller

[1] HVAC stands for heating, ventilation and air conditioning systems

[2] TRV represents for thermostatic radiator valve

[3] PI stands for proportional integral.

controller would also fail to guarantee both performance and stability for a radiator in the whole operating conditions. We investigated this problem as a dilemma between stability and performance. In this study, pressure drop across the radiator valve is maintained constant unlike what is taken as the control strategy in [7]. Instead, flow control is assumed to be feasible by the accurate adjustment of the valve opening. The valve opening is regulated by the stepper motor which allows the concrete adjustment. The control strategy is adapted based on the proposed radiator linear parameter varying (LPV)[4] model. According to the derived analytic expression of the radiator dissipated heat, the LPV model is parameterized systematically. Based on the proposed modeling, gain scheduling is chosen among various possible control structures to design the TRV controller.

It is, also, worth mentioning that the same problem was investigated via simulation based studies in [8] and also via approximation analysis in [9].

In order to validate the controller performance, we utilized simulation models of the HVAC components in Matlab/Simulink. Two approaches for HVAC systems modeling are the forward and the data-driven methods [10]. The first one is based on known physical characteristics and energy balance equations of the air, structural mass and other components of the system, addressed widely in the literature [11, 12, 13]. The alternative modeling approach is to use building measurement data with inferential and statistical methods for system identification which is addressed in [14, 15, 16]. The latter method requires a significant amount of data and may not always reflect the physical behavior of the system [17].

In this paper, we adopted heat balance equations of the room model in accordance to the analogous electric circuit, described formerly in [18]. Radiator dynamics are formulated in two ways. Once, it has been treated as a distributed system in order to analyze the radiator transferred heat. Secondly, it is approximated by a lumped system while simulating in Matlab. This way, the computational costs are cut down by solving an ODE[5] at a few points rather than a full PDE[6].

The remainder of the paper is organized as follows: Section II defines the problem. In Section III, the radiator dissipated heat is derived analytically. Based on the result, control oriented models are developed in Section IV. Utilizing the models, the control structure based on flow adaptation is proposed in the same section. A simulation-based test is conducted in Section V, exploiting the ODEs of the room and radiator. Discussion and conclusions are given finally in Section VI.

2 Stability-Performance Dilemma

The case study is composed of a room, a radiator with thermostatic valve and a room temperature sensor. The only disturbance which excites the system is the ambient temperature. It is assumed that heat transfer to the ground is negligible having thick layers of insulation beneath the concrete floor. A block diagram of the system is shown in Fig. 9.1. All symbols, subscripts and parameter values are listed in Table 9.1 and Table 9.2. It is, though, worth stating that the chosen values of all parameters are in accordance with the

[4]LPV represents linear parameter varying
[5]ODE stands for ordinary differential equation
[6]ODE represents partial differential equation

typical experimental and standard values. As mentioned before, the case study is adopted to the one previously studied in [8].

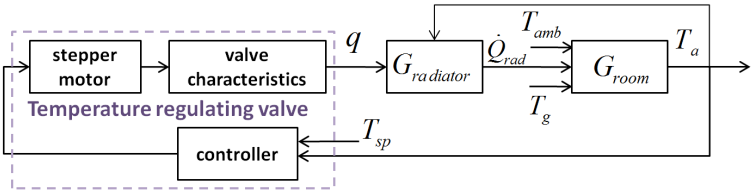

Figure 9.1: Closed loop control system of room and radiator

The dilemma between stability and performance arises when the TRV is controlled by a fixed linear controller. Designing a TRV controller for high demand seasonal condition, usually leads to instability in low demand weather condition. A high loop gain and long time constant are the main reasons of this phenomenon. In contrast, selecting a smaller controller gain to handle the instability situation, will result in a poor radiator reaction while the heat demand is high.

Figures 9.2 and 9.3 show the results of a simulation where oscillations and low performance occur. In the shown simulation results, the forward water temperature is at $50°C$. The proportional integral (PI) controller of TRV is tuned based on Ziegler-Nichols step response method [19].

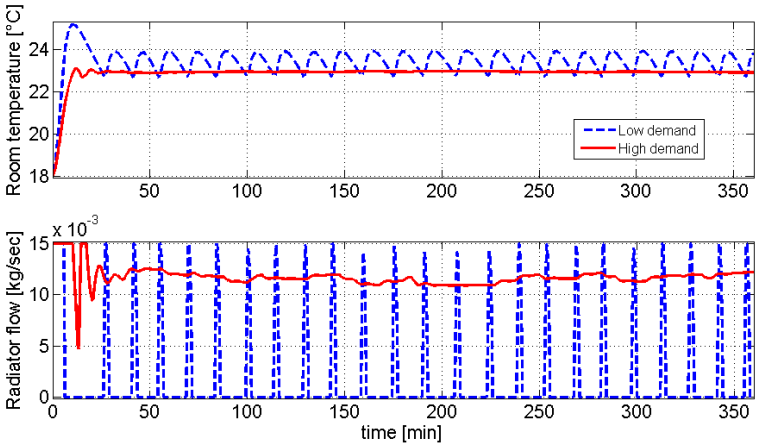

Figure 9.2: Undamped oscillations in room temperature and radiator flow which occur in low demand situation while the controller is designed for a high demand condition.

A remedy to this dilemma is choosing an adaptive controller instead of the current fixed PI controller.

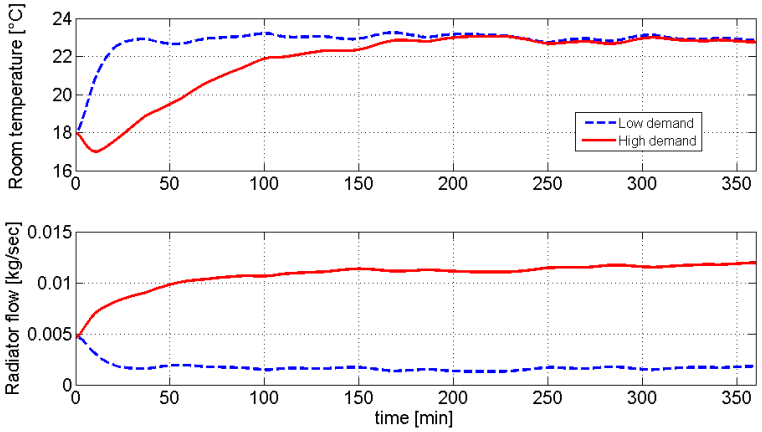

Figure 9.3: Poor performance in the cold weather condition, applying the controller designed for the low demand situation

3 System Modeling

3.1 Heat Balance Equations

Radiator is modeled as a lumped system with N elements in series. The nth section temperature is given by, [20]:

$$\frac{C_r}{N}\dot{T}_n = c_w q(T_{n-1} - T_n) - \frac{K_r}{N}(T_n - T_a) \tag{9.1}$$

in which C_r is the heat capacity of water and radiator material, T_n is the temperature of the radiator's nth section area and $n = 1, 2, \ldots, N$. The temperature of the radiator ending points are inlet temperature: $T_0 = T_{in}$, and return temperature: $T_N = T_{out}$. In this formulation, we assumed the same temperature of the radiator surface as the water inside radiator. Besides, heat transfer from radiator surface only via convection is considered. We have also assumed that heat is transferred between two sections only by mass transport, implying that convective heat transfer is neglected. K_r represents the radiator equivalent heat transfer coefficient which is defined based on one exponent formula, [20] in the following:

$$K_r = \frac{\Phi_0}{\Delta T_{m,0}{}^{n_1}}(T_n - T_a)^{n_1 - 1} \tag{9.2}$$

in which Φ_0 is the radiator nominal power in nominal condition which is $T_{in,0} = 90°C$, $T_{out,0} = 70°C$ and $T_a = 20°C$. $\Delta T_{m,0}$ expresses the mean temperature difference which is defined as follows:

$$\Delta T_m = \frac{T_{in} - T_{out}}{2} - T_a \tag{9.3}$$

in nominal condition. The exponent n_1 is usually around 1.3, [20]. In such a case, we can approximate the non-fixed, nonlinear term in K_r with a constant between 2.5 and 3.2

for a wide enough range of temperature values. Picking 2.8 as the approximation value would result in:

$$K_r = 2.8 \times \frac{\Phi_0}{{\Delta T_{m,0}}^{1.3}} \tag{9.4}$$

The heat dissipated to the room by the radiator can be described as:

$$Q = \sum_{n=1}^{N} K_r (T_n - T_a) \tag{9.5}$$

Heat balance equations of the room is governed by the following lumped model [13], which is shown in Fig. 9.4:

$$\begin{aligned} C_e \dot{T}_e &= U_e A_e (T_{amb} - T_e) + U_e A_e (T_a - T_e) \\ C_f \dot{T}_f &= U_f A_f (T_a - T_f) \\ C_a \dot{T}_a &= U_e A_e (T_e - T_a) + U_f A_f (T_f - T_a) + Q \end{aligned}$$

in which T_e represents the envelop temperature, T_f the temperature of the concrete floor and T_a the room air temperature. Q is the heat dissipated to the room by the radiator. Each of the envelop, floor and room air subsystems are considered as a single lump with uniform temperature distribution.

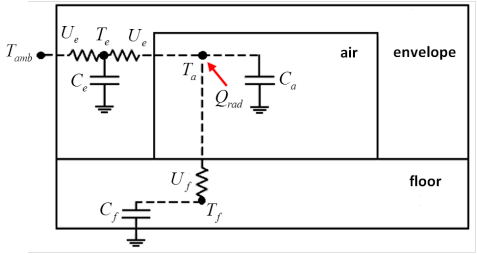

Figure 9.4: Analogous electrical circuit to the room thermal model

Assuming a constant pressure drop across the valve, the thermostatic valve is modeled with a static polynomial function mapping the valve opening δ to the flow rate q:

$$q = -3.4 \times 10^{-4} \delta^2 + 0.75\delta \tag{9.6}$$

The above presented radiator model is highly nonlinear and not suitable for design of a controller; thus a simplified control oriented LPV model is developed in the next section.

3.2 Control Oriented Models

For our purposes, the relationship between room air temperature and radiator output heat can be well approximated by a 1^{st} order transfer function as follows:

$$\frac{T_a}{Q}(s) = \frac{K_a}{1 + \tau_a s} \tag{9.7}$$

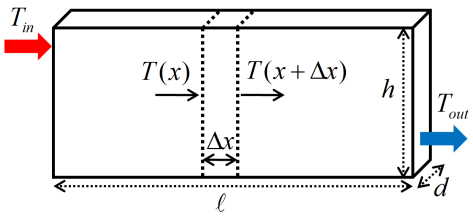

Figure 9.5: A radiator section area with the heat transfer equation governed by (9). Entering flow to the section is at the temperature $T(x)$ and the leaving flow is at $T(x+\Delta x)$.

Parameters τ_a and K_a can be identified simply via a step response test.

Step response simulations and experiments confirm a first order transfer function between the radiator output heat and input flow rate at a specific operating point as:

$$\frac{Q}{q}(s) = \frac{K_{rad}}{1+\tau_{rad}s} \tag{9.8}$$

Parameters of the above model are formulated in the next section based on the closed-form solution of the radiator dissipated heat, $Q(t,q,T_a)$.

3.3 Radiator Dynamical Analysis

In this paper, unlike [8] and [9], we found the precise closed-form map from the operating point to the radiator dissipated heat i.e. $Q(t,q,T_a)$. q and T_a are respectively the hot water flow rate through the radiator and the room temperature. We, previously, derived this map via a simulation study in the form of two profile curves in [8].

To develop the map, $Q(t,q,T_a)$, a step flow is applied to the radiator, i.e. changing the flow rate from q_0 to q_1, at a constant differential pressure across the valve. Propagating with the speed of sound, the flow shift is seen in a fraction of a second all along the radiator. Hence, flow is regarded as a static parameter for $t>0$, rather than a temperature distribution along the radiator.

Consider a small radiator section Δx with depth d and height h as shown in Fig. 9.5. The temperature of incoming flow to this section is $T(x)$, while the outgoing flow is at $T(x+\Delta x)^\circ C$. The temperature is considered to be the same as $T(x)$ throughout a single partition.

The corresponding heat balance equation of this section is given as follows:

$$qc_w\left(T(x)-T(x+\Delta x)\right)+K_r\frac{\Delta x}{\ell}\left(T_a-T(x)\right)=C_r\frac{\Delta x}{\ell}\frac{\partial T}{\partial t} \tag{9.9}$$

in which flow rate is q_0 at $t=0$ and q_1 for $t>0$. C_r is the heat capacity of water and the radiator material defined as: $C_r=c_w\rho_w V_w$. Dividing both sides of (9.9) by Δx and letting $\Delta x\to 0$, we have:

$$-qc_w\frac{\partial T(x,t)}{\partial x}+\frac{K_r}{\ell}\left(T_a-T(x,t)\right)=\frac{C_r}{\ell}\frac{\partial T(x,t)}{\partial t} \tag{9.10}$$

with boundary conditions:

$$T(0,t)=T_{in} \tag{9.11a}$$

$$T(\ell, 0^-) = T_{out,0} \tag{9.11b}$$

$$T(\ell, \infty) = T_{out,1} \tag{9.11c}$$

in which T_{in} is the constant temperature of supply water, $T_{out,0}$ and $T_{out,1}$ are return water temperatures corresponding to q_0 and q_1 respectively. The first solution candidate would be a separable solution like $T(x,t) = T(t) \times X(x)$. Substituting it into (9.10), gives:

$$T(0,t) = c_1 e^{k_1 t} + c_2 \tag{9.12}$$

which implies a contradiction according to 9.11a.

Before proceeding to solve the full PDE (9.10), we need to find the two boundary conditions $T_{out,0}$ and $T_{out,1}$. For this purpose, take the steady state form of (9.10):

$$-qc_w \frac{dT}{dx} + \frac{K_r}{\ell}\left(T_a - T(x)\right) = 0 \tag{9.13}$$

which can be written as:

$$\frac{dT}{dx} + \frac{\beta}{\gamma} T(x) = T_a \tag{9.14}$$

with constants $\beta = \frac{K_r}{C_r}$ and $\gamma = \frac{qc_w\ell}{C_r}$.
Therefore, the steady state temperature, $T(x,t)|_{t\to\infty}$ will be achieved as:

$$T(x) = c_1 e^{-\frac{\beta}{\gamma}x} + c_0 \tag{9.15}$$

at a specific flow rate q. Substituting the above equation in (9.14) gives $c_0 = T_a$. Knowing $T(0) = T_{in}$, c_1 is also found. Finally $T(x)$ looks like:

$$T(x) = (T_{in} - T_a)e^{-\frac{\beta}{\gamma}x} + T_a \tag{9.16}$$

Therefor the two boundary conditions are:

$$T_{out,0} = (T_{in} - T_a)e^{-\frac{\beta}{\gamma_0}x} + T_a \tag{9.17a}$$

$$T_{out,1} = (T_{in} - T_a)e^{-\frac{\beta}{\gamma_1}x} + T_a \tag{9.17b}$$

corresponding to the flow rates q_0 and q_1.

Next, we solve (9.10) for $T(x,t)$ in frequency domain. Taking Laplace transform of this equation will give:

$$-qc_w \frac{\partial \tilde{T}(x,s)}{\partial x} + \frac{K_r}{\ell}\left(\frac{T_a}{s} - \tilde{T}(x,s)\right) = \frac{C_r}{\ell}\left(s\tilde{T}(x,s) - T(x,0)\right) \tag{9.18}$$

which is simplified to:

$$\frac{\partial \tilde{T}(x,t)}{\partial x} + \frac{s+\beta}{\gamma}\tilde{T}(x,s) = \frac{\beta}{\gamma}\frac{T_a}{s} + \frac{1}{\gamma}T(x,0) \tag{9.19a}$$

$$T(x,0) = (T_{in} - T_a)e^{-\frac{\beta}{\gamma_0}x} + T_a \tag{9.19b}$$

$$Boundary\ Condition : \tilde{T}(0,s) = \frac{T_{in}}{s} \tag{9.19c}$$

with $\beta = \frac{K_r}{C_r}$, $\gamma_0 = \frac{q_0 c_w \ell}{C_r}$ and $\gamma_1 = \frac{q_1 c_w \ell}{C_r}$. The initial condition, $T(x,0)$ is obtained using (9.16). The solution to the above differential equation comes out of inspection as follows:

$$\tilde{T}(x,s) = c_1 e^{-\frac{\beta}{\gamma_0}x} + c_2 e^{-\frac{s+\beta}{\gamma_1}x} + c_0 \tag{9.20}$$

$$\begin{aligned} c_0 &= \frac{T_a}{s} \\ c_1 &= \frac{T_{in} - T_a}{s + \beta(1 - \frac{\gamma_1}{\gamma_0})} \\ c_2 &= \frac{T_{in}}{s} - c_0 - c_1 \end{aligned} \tag{9.21}$$

The time response is obtained via taking inverse Laplace transform of the above frequency response. It is shown in the following:

$$\begin{aligned} T(x,t) = (T_{in} - T_a)e^{-\beta t - \frac{\beta}{\gamma_0}(x - \gamma_1 t)} \left(u(t) - u(t - \frac{x}{\gamma_1}) \right) \\ + (T_{in} - T_a)e^{-\frac{\beta}{\gamma_1}x} u(t - \frac{x}{\gamma_1}) \end{aligned} \tag{9.22}$$

in which $u(t)$ is a *unit step function*.

We, however, are interested in the radiator output heat $Q(t)$ to find K_{rad} and τ_{rad} in (9.8). It is defined as:

$$Q(t) = \int_0^\ell \frac{K_r}{\ell} \left(T(x,t) - T_a \right) \, dx \tag{9.23}$$

Taking time derivative of the above equation gives:

$$\frac{dQ}{dt} = \int_0^\ell \frac{K_r}{\ell} \frac{\partial T(x,t)}{\partial t} \, dx \tag{9.24}$$

and rewriting the result using (9.10):

$$\begin{aligned} \frac{dQ}{dt} &= \int_0^\ell \beta \left(-q c_w \frac{\partial T}{\partial x} + \frac{K_r}{\ell} \left(T_a - T(x,t) \right) \right) \, dx \\ &= \beta q c_w (T_{in} - T_{out}(t)) - \beta Q \end{aligned} \tag{9.25}$$

which turns into the following differential equation:

$$\frac{dQ}{dt} + \beta Q = \beta q c_w \left(T_{in} - T_{out}(t) \right) \tag{9.26a}$$

$$T_{out}(t) = T(\ell, t) \tag{9.26b}$$

in which $T(\ell, t)$ is obtained using (9.23). The solution to the above first order differential equation via inspection is:

$$\begin{aligned} Q(t) = Q(0)e^{-\beta t} + c_w q(T_{in} - T_a)(1 - e^{-\beta t}) + \\ + \frac{c_w q(T_{in} - T_a)\gamma_0}{\gamma_1} e^{-\beta t}\left(e^{-\frac{\beta}{\gamma_0}\ell} - e^{-\frac{\beta}{\gamma_0}(\ell - \gamma_1 t)}\right) - \\ - c_w q(T_{in} - T_a)e^{-\beta t}\left(\frac{\gamma_0}{\gamma_1}(1 - e^{-\frac{\beta}{\gamma_0}(\ell-\gamma_1 t)}) - (1 - e^{-\frac{\beta}{\gamma_1}(\ell-\gamma_1 t)})\right) u(t - \frac{\ell}{\gamma_1}) \end{aligned} \tag{9.27}$$

In the next section, we utilize the derived formula to extract the required gain and time constant for the approximation LPV model.

3.4 Radiator LPV Model

Parameters K_{rad} and τ_{rad} of the radiator LPV model (9.8), are derived based on the best first order fit to the step response of the radiator dissipated heat (9.27). Using the tangent to $Q(t)$ at $t = 0^+$, we obtain the time constant. The slope of the tangent at $t = 0^+$ is made equal to the first derivative of

$$Q_{final} + (Q_0 - Q_{final})e^{-\frac{t}{\tau_{rad}}} \tag{9.28}$$

i.e. the first order approximation of $Q(t)$. It gives:

$$\tau_{rad} = \frac{Q_{final} - Q_0}{q_1 c_w \beta (T_{in} - T_a)(\frac{\gamma_0}{\gamma_1} - 1)} \tag{9.29}$$

Steady state gain is also obtained as follows:

$$K_{rad} = \frac{Q_{final} - Q_0}{q_1}$$

in which Q_{final} and Q_0 are the dissipated heat by the radiator in steady state corresponding to flow rates q_1 and q_0 respectively.

These two parameters depend also on room temperature and supply water temperature. However, we have assumed a constant feed water temperature for the heating system. Therefore, variations of K_{rad} and τ_{rad} against a number of flow rates and room temperatures are shown in the following figure. Room temperature varies between 5 and 25 $^\circ C$ and flow rate changes between the minimum and the maximum flow rates i.e. 0 and 360 $\frac{kg}{h}$.

In Fig.9.6, no variation of time constant against room temperature is recognized. However, the small signal gain decreases with an increase in the room temperature which seems rational. There is also a slight difference between the simulation and the analytic results with respect to the time constant. This is due to employing different methods in τ_{rad} calculations. In simulation, the time constant is taken as the time when 0.63 of the final value is met while in calculations, this is derived based on the tangent to $Q(t)$ and its first order approximation.

In the next section, we will design a gain scheduling controller based on the developed radiator LPV model.

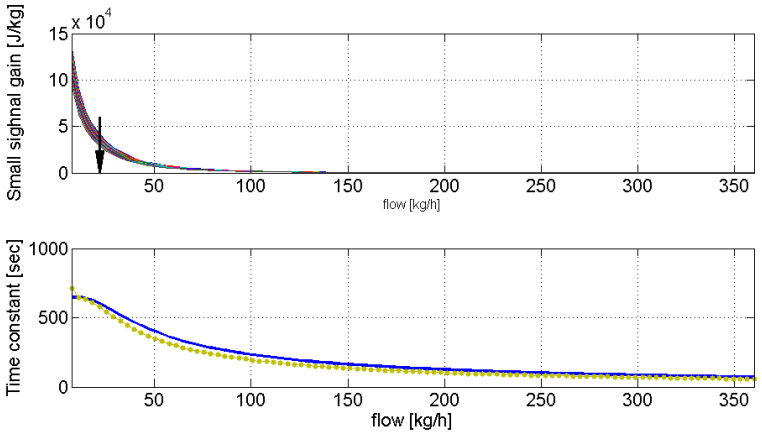

Figure 9.6: K_{rad} and τ_{rad} deviations against flow rate and room temperature variations. The direction of air temperature increase is shown via an arrow. The results are shown for both simulation (dotted) and analytic (solid) results. Comparing the result of analytic solution with simulation, the system gain is the same throughout all operating points, however there is marginal variations in the system time constant. This is due to employing the best 1^{st} order fit of $Q(t)$.

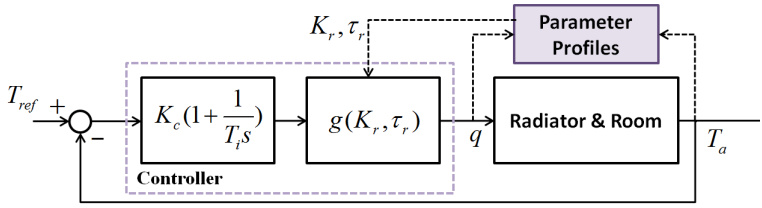

Figure 9.7: Block diagram of the closed loop system with linear transformation

4 Gain Scheduling Controller Design based on Flow Adaptation

In the previous section, we developed a linear parameter varying model of the radiator instead of the high-order nonlinear model (9.1). To control the system, among various possible control structures, a gain scheduling approach is selected which is a very useful technique for reducing the effects of parameter variations [21].

The term of flow adaptation, here, is chosen to further emphasize on the operating point-dependent controller. The main idea of designing an adaptive controller is to transform the system (9.8) to one which is independent of the operating point. The controller, subsequently, would be designed for the new transformed system which is a linear time invariant (LTI) system. The block diagram of this controller is shown in Fig. 9.7.

The function g is chosen in a way to cancel out the variable dynamics of the radiator and to place a pole instead in a desired position. The desired position corresponds to the high flow rate or high demand condition. In this situation, the radiator has the fastest dynamic. Therefore, the simplest candidate for the linear transfer function g is a phase-

lead structure, as follows:

$$g(K_{rad}, \tau_{rad}) = \frac{K_{hd}}{K_{rad}} \frac{\tau_{rad} s + 1}{\tau_{hd} s + 1} \tag{9.30}$$

in which K_{hd} and τ_{hd} correspond to the gain and time constant of radiator in the high demand situation when the flow rate is maximum. Consequently, the transformed system would behave always similar to the high demand situation. By choosing high demand as the desired situation, we give the closed loop system the incentive to place the dominant poles as far as possible from the imaginary axis, and as a result as fast as possible.

The controller of the transformed linear time invariant (LTI)[7] system is, therefore, a fixed PI controller. The rationale for choosing a PI controller is to track a step reference with zero steady state error. Parameters of this controller is calculated based on the Ziegler-Nichols step response method [19]. To this end, the transformed second order control-oriented model i.e.

$$\frac{T_a}{q} = \frac{K_a K_r}{(1 + \tau_a s)(1 + \tau_r s)} \tag{9.31}$$

is approximated by a first-order system with a time delay as follows:

$$\frac{T_a}{q}(s) \quad = \quad \frac{k}{1 + \tau s} e^{-Ls} \tag{9.32}$$

The time delay and time constant of the above model can be found easily by looking into the time response of the second-order model (9.31) to a unit step input q. The step response is derived and shown in the following:

$$T_a(t) = K_{hd} K_a (1 + \frac{\tau_{hd}}{\tau_a - \tau_{hd}} e^{\frac{-t}{\tau_{hd}}} + \frac{\tau_a}{\tau_{hd} - \tau_a} e^{\frac{-t}{\tau_a}}) q(t) \tag{9.33}$$

in which $q(t) = u(t)$ is the unit step input.

The apparent time constant and time delay are calculated based on the time when 0.63 and 0.05 of the final value of T_a is achieved, respectively. The positive solution of the following equation gives the time delay when $\chi = 0.05$ and the time constant when $\chi = 0.63$.

$$(2 - \chi) t^2 - 2\chi(\tau_{hd} + \tau_a) t^2 - 4\chi \tau_{hd} \tau_a = 0 \tag{9.34}$$

Solving the above equation for τ and L, the PI parameters comes out of the Ziegler-Nichols step response method. The parameters are the integration time $T_i = 3L$ and proportional gain $K_c = \frac{0.9}{a}$ with $a = k\frac{L}{T}$ and DC gain $k = K_{hd} \times K_a$.

5 Simulation Results

The proposed flow adaptive controller is designed for the paper case study which is described earlier in Sec. 2. The controller is applied to simulation models of room and radiator. Parameter values used in simulation are listed in Table 9.2. PI controller parameters are obtained as $K_c = 0.01$ and $T_i = 400$. Ambient temperature is considered as

[7] LTI stands for linear time invariant

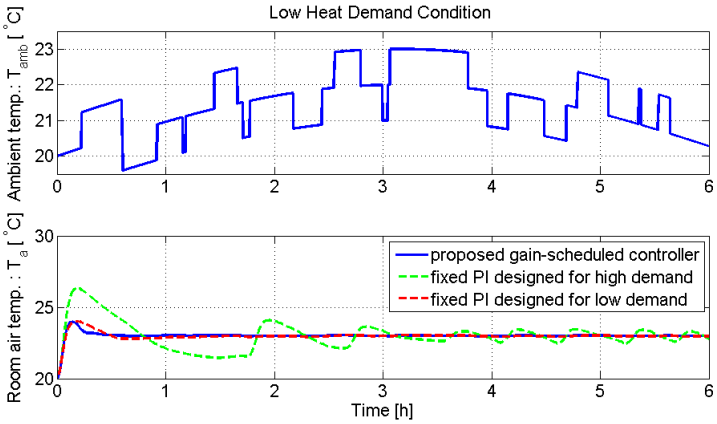

Figure 9.8: (Top) ambient temperature, (bottom) room temperature for three controllers. The results of simulation with flow adaptive controller together with two fixed PI controllers are shown. The PI controller designed for the high demand situation encounters instability in the low heat demand condition.

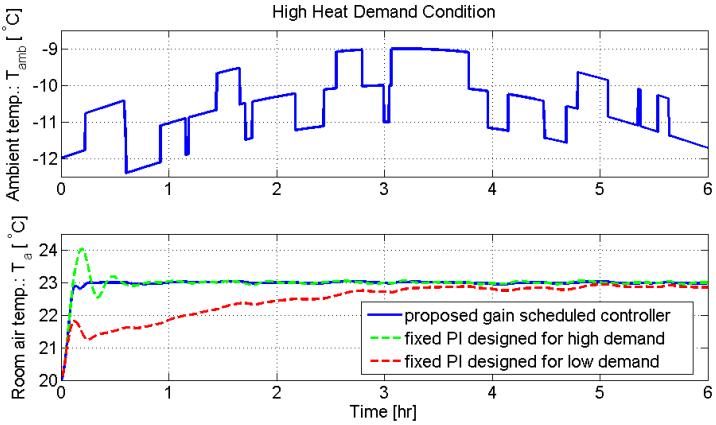

Figure 9.9: (Top) ambient temperature, (bottom) room temperature for three controllers. The results of the simulation with flow adaptive controller together with two fixed PI controllers are shown. The PI controller designed for the low demand condition is very slow for the high demand situation.

the only source of disturbance for the system. In a partly cloudy weather condition, the effect of intermittent sunshine is modeled by a fluctuating outdoor temperature. A random binary signal is added to a sinusoid with the period of 12 hours to model the ambient temperature.

Simulation results with the designed controller and the corresponding ambient temperature are depicted in Fig. 9.8 and Fig.9.9. The results are compared to the case with fixed PI controllers designed for both high and low heat demand conditions.

The simulation results of the proposed control structure show significant improvement in the system performance and stability compared to the fixed PI controller.

6 Discussions and Conclusions

In this study, we investigated an inefficient operating conditions of TRV controlled radiators. The condition is discussed as a dilemma between stability and performance which we dealt with using a new generation of thermostatic radiator valves. Using the new TRV, flow estimation and control becomes possible. Based on the estimated flow, we have developed a gain scheduled controller which guarantees both performance and stability for the radiator system. To this end, we derived analytically, low-order models of the room-radiator system parameterized based on the estimated operating point.

All gain scheduling control approaches operate based on the basic assumption that all system states can be measured or estimated and a generalized observability holds [21]. In this study, however, we should clarify the validity of this assumption. The parameters that we need to measure or estimate are room temperatures and radiator flow rates. Measuring the first state is mandatory when the goal is seeking a reference for this temperature. However, radiator flow rate is not easily measurable.

To have an estimation of the radiator flow rate, one possibility is to use a new generation of TRVs in which the valve is driven by a stepper motor. Experiments show that this TRV can give a rather precise estimation of the valve opening. Knowing this fact and assuming a constant pressure drop across the radiator valve, we would be able to estimate the flow rate.

We have shown throughout the paper that using the new generation of TRVs, a gain scheduling controller would guarantee the performance of the radiator operation. In the current study, however we did not discuss the robustness of the proposed controller with respect to the model uncertainties. This task is postponed to be studied in future studies.

References

[1] Danfoss, “Thermostatic radiator valves: Benefits,” 2011. [Online]. Available: http://www.radiatorcontrol.com/benefits.aspx

[2] S. Svendsen, H. M. Tommerup, and M. Beck Hansen, “Energy project villa,” Partners: Technical University of Denmark, Department of Civil Eng. and Rockwool, Denmark, Main Report, March 2005, downloded from DTU database.

[3] J. DeGreef and K. Chapman, “Simplified thermal comfort evaluation of mrt gradients and power consumption predicted with the bcap methodology,” *ASHRAE Trans.*, vol. 104, no. 2, pp. 1090–1097, 1998.

[4] K. Chapman, J. Rutler, and R. Watson, “Impact of heating system and wall surface temperatures on room operative temperature fields,” *ASHRAE Trans.*, vol. 106, no. 1, pp. 506–514, 2000.

[5] H. Hanibuchi and S. Hokoi, “Simplified method of estimating efficiency of radiant and convective heating systems,” *ASHRAE Trans.*, vol. 106, no. 1, pp. 487–494, 2000.

Table 9.1: Symbols and Subscripts

Nomenclature	
A	surface area (m^2)
C	thermal capacitance $(\frac{J}{^\circ\mathrm{C}})$
C_r	heat capacity of water and the radiator material $(\frac{J}{^\circ\mathrm{C}})$
c_w	specific heat capacity of water $(\frac{J}{kg^\circ\mathrm{C}})$
d	depth of radiator (m)
h	height of radiator (m)
K	DC gain
K_c	controller gain
K_r	equivalent heat transfer coefficient of radiator $(\frac{J}{s^\circ\mathrm{C}})$
L	time delay (s)
N	total number of radiator distributed elements
Q	dissipated heat by the radiator (W)
q	flow rate of the hot water through radiator $(\frac{kg}{s})$
T	temperature $(^\circ\mathrm{C})$
T_i	integration time
T_{in}	inlet water temperature
T_n	temperature of the radiator n^{th} element $(^\circ\mathrm{C})$
T_{out}	outlet water temperature
T^i_{out}	steady state T_{out} corresponding to flow rate q_i
U	thermal transmittance $(\frac{W}{m^{2\,\circ}\mathrm{C}})$
V_w	water capacity of radiator (m^3)
ρ	density $(\frac{kg}{m^3})$
τ	time constant (s)
δ	valve opening
ℓ	length of radiator (m)
Subscripts	
a	room air
amb	ambient temperature (outdoor)
e	envelope
f	floor
hd	high demand
n_1	radiator exponent
rad	radiator
ref	reference temperature of room

[6] P. Rathje, "Modeling and simulation of a room temperature control system," in *Proceedings of SIMS87 Symposium*. Scandinavian Simulation Society, 1987, pp. 58–69.

[7] P. Andersen, T. S. Pedersen, J. Stoustrup, and N. Bidstrup, "Elimination of oscillations in a central heating system using pump control," in *IEEE American Control Conference*, Chicago, Illinois, June 2004, pp. 31–38.

Table 9.2: System Parameters

Room Parameters		Radiator Parameters	
A_e	$56\ m^2$	A_r	$1.5\ m^2$
A_f	$20\ m^2$	C_r	$3.1 \times 10^4\ \frac{J}{^\circ\mathrm{C}}$
C_a	$5.93 \times 10^4\ \frac{J}{^\circ\mathrm{C}}$	c_w	$4186.8\ \frac{J}{kg\,^\circ\mathrm{C}}$
C_e	$5 \times 10^4\ \frac{J}{^\circ\mathrm{C}}$	N	45
C_f	$1.1 \times 10^4\ \frac{J}{^\circ\mathrm{C}}$	n_1	1.3
U_e	$1.2\ \frac{W}{m^2\,^\circ\mathrm{C}}$	q_{max}	$0.015\ \frac{kg}{s}$
U_f	$1.1\ \frac{W}{m^2\,^\circ\mathrm{C}}$	T_s	$70\ ^\circ\mathrm{C}$
		V	$5\ \ell$

[8] F. Tahersima, J. Stoustrup, and H. Rasmussen, "Stability-performance dilemma in trv-based hydronic radiators," in *IEEE Multi-Conference on Systems and Control*, Denver, Colorado, USA, October 2011.

[9] ——, "Eliminating oscillations in trv-controlled hydronic radiators," in *IEEE Conference on Decision and Control*, Orlando, Florida, USA, December 2011.

[10] ASHRAE, *ASHRAE Handbook 1990, fundamentals*. Atlanta: ASHRAE Inc., 1990.

[11] A. K. Athienitis, M. Stylianou, and J. Shou, "Methodology for building thermal dynamics studies and control applications," *ASHRAE Trans.*, vol. 96, no. 2, pp. 839–848, 1990.

[12] M. L. Kurkarni and F. Hong, "Energy optimal control of residential space-conditioning system based on sensible heat transfer modeling," *Building and Environment*, vol. 39, no. 1, pp. 31–38, 2004.

[13] G. Hudson and C. P. Underwood, "A simple building modeling procedure for matlab/simulink," *Proc. of Building Simulation*, vol. 99, no. 2, pp. 777–783, 1999.

[14] H. Madsen and J. Holst, "Estimation of a continuous time model for the heat dynamics of a building," *Energy and Buildings*, vol. 22, pp. 67–79, 1995.

[15] K. M. Letherman, C. J. Paling, and P. M. Park, "The measurement of dynamic thermal response in rooms using pseudorandom binary sequences," *Building and Environment*, vol. 17, no. 1, 1982.

[16] J. Braun and N. Chaturvedi, "An inverse grey-box model for transient building load prediction," *HVAC Research*, vol. 8, no. 1, pp. 73–99, 2002.

[17] B. Xu, L. Fu, and H. Di, "Dynamic simulation of space heating systems with radiators controlled by trvs in buildings," *Energy and Buildings*, vol. 40, pp. 1755–1764, 2008.

[18] F. Tahersima, J. Stoustrup, H. Rasmussen, and P. Gammeljord Nielsen, "Thermal analysis of an hvac system with trv controlled hydronic radiator," in *IEEE International Conference on Automation Science and Engineering*, Toronto, Canada, August 2010, pp. 756–761.

[19] K. Åstrom and T. Hagglund, *PID Controllers*. North Carolina: ISA, 1995.

[20] L. H. Hansen, "Stochastic modeling of central heating systems," Ph.D. dissertation, Technical University of Denmark, Dep. of Mathematical Modeling, Denmark, 1997.

[21] K. Åstrom and B. Wittenmark, *Adaptive Controller*. Mineola, New York: DOVER Publications Inc., 2008.

Paper D

Optimal Power Consumption in a Central Heating System with Geothermal Heat pump

Fatemeh Tahersima, Jakob Stoustrup, Henrik Rasmussen

This paper is published in:
IFAC World Congress, IFAC2011, September 2011, Milan, Italy

Abstract

A ground source heat pump connected to a domestic hydronic heating network is studied to be driven with the minimum electric power. The hypothesis is to decrease the forward temperature to the extent that one of the hydronic heaters work at full capacity. A less forward temperature would result in a dramatic temperature drop in the room with saturated actuator. The optimization hypothesis is inspired by the fact that, the consumed electric power by the heat pump has a strong positive correlation with the generated forward temperature. A model predictive control scheme is proposed in the current study to achieve the optimal forward temperature. At the lower hierarchy level, local PI controllers seek the corresponding room temperature setpoint. Simulation results for a multi-room house case study show considerable energy savings compared to the heat pump's traditional control scheme.

keywords:*Hydronic heating system, Heat pump, Building energy efficiency, Hierarchical model predictive control*

1 Introduction

In recent years, there has been a growing interest in energy saving concepts and thermal comfort analysis within the building sector. Efficient control of heating, ventilation and air conditioning (HVAC) systems has a great influence on the thermal comfort sensation of the residents. The other important objective of a well designed control strategy is energy savings, mainly due to the growth of energy consumption, costs and also correlated environmental impacts.

1.1 Motivations and background

Heat pumps are drawing more attentions nowadays due to a surge for energy savings and the quest for mitigation of global warming. The most important benefit of utilizing heat pump systems is that they use 25% to 50% less electrical power than conventional heating or cooling systems. According to EPA, emissions of the ground-source heat pumps (GHP) are up to 44% less than air-source heat pumps (AHP) and up to 72% less than electric resistance heating with standard air-conditioning equipments [1]. The other advantage of GHP compared to AHP is the fact that, at depth, the earth has a relatively constant temperature, warmer than the air in winter and cooler than the air in summer.

Here, we are specifically interested in geothermal heat pumps. However the achieved controller scheme can be generalized to AHPs as well. Heat pumps act like refrigerators in reverse and can generate up to 3-4 kWh of heat from 1 kWh of electricity. They transfer heat energy from the underground soil to residential buildings via a network of pipes. See Fig. 10.1. There are typically two hydronic and one refrigerant circuits interconnected through two heat exchangers. These are: 1) the underground buried brine-filled – mixture of water and anti-freeze – pipes with a small circulating pump; 2) the refrigerant-filled circuit, equipped with an expansion valve and driven by a compressor which is called heat pump; and 3) the indoor under-surface grid of pipes with another small circulating pump which distributes heat to the concrete floor of the building or to the hydronic radiators through a different network of pipes.

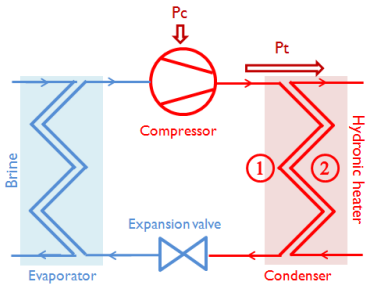

Figure 10.1: Fluid circuits of a heat pump.

Traditional heat pump control scheme relies on the direct feedback from outdoor temperature. The objective of the heat pump controller is to seek the water temperature setpoint which is specified based on a prescribed curve, see Fig.10.2. This curve is suggested by the producer company and is adjusted manually by the heat pump installer. The installer changes the standard slope and offset according to dimensions of the building. Off peak loads easily might happen as a result of a coarse adjustment of such curve. The other inefficiency in power usage occurs because of a bypass stream of the return cooler water.

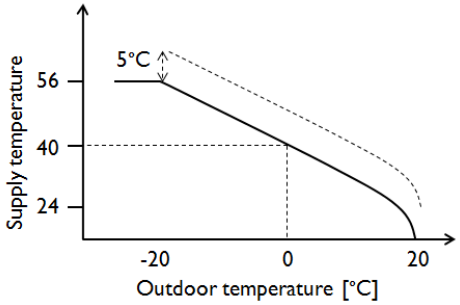

Figure 10.2: Graph showing the supply water temperature setpoint against ambient temperature in a conventional heat pump control. The dash shows an overhead above the standard curve due to the more heat demand in a specific construction

There has been little attention in the literature to GHPs optimal control in the sense of electric power consumption while it is connected to the system. Some control methods, P, PI and PID with pre-filtering have been tested and compared in [2] for heat pump control integrated with a floor heating system. In that paper, the water flow rate is fixed to the maximum value (full valve opening with constant differential pressure) and the heat pump is controlled directly based on the feedback from room temperature. This control scheme for a single room is simple and requires little information (room temperature only) to track the room temperature setpoint profile. Undoubtedly, this control method can not be applied to the multiple rooms case, due to the specific heat demand of each single room. Therefore, having local controllers combined with a master controller is inevitable.

In the similar area of chillers liquid-loop control, a new principle called *chilled water temperature reset* (CWTR) has been advocated in recent years, see [3]. In this method, the chilled water set-point is adjusted during the course of the day based on the net energy requirements of the building. Model predictive control in both centralized and distributed schemes is proposed in [4] to find the optimal outlet water temperature of chiller.

1.2 Main Contribution

In this study, we employed a simple idea – new in the field of concern – to optimally control the GHP integrated with a domestic hydronic heating network. Suppose we have several rooms in a building, each of which equipped with floor heating (FH) or hydronic radiator (HR) with GHP as hot water supplier. If the forward temperature is lowered to the extent that one of the hydronic valves works at high capacity, the heat pump is absorbing the minimum electric power. The inspiration behind this hypothesis is: the less the forward temperature is the less electric power would be consumed by the heat pump's compressor. The intuition behind the hypothesis is simple: if all the hydronic valves work at partial loads, then the forward temperature is still allowed to be lower, hence the consumed power can be lowered. The optimal point will be attained at the point where at lease one of the heaters goes to saturation.

The main objective of the current work is to present the above-stated principle as the unique optimal solution for driving the GHP integrated into the central heating system. Although, the idea is similar to the one proposed in [4], we have proposed a different scheme for designing the distributed model predictive control.

To facilitate the understanding, models of the system components are chosen deliberately simple. A central controller in collaboration with several local controllers is employed to achieve the optimal operating point of all subsystems. Simulation based test compares the new control system efficiency against the traditional one.

1.3 Paper Structure

The paper is organized as follows: Section II introduces the case study which is further investigated through the paper. Section III comes with the models of the system components. Section IV presents a hierarchical control structure which consists of local PI controllers and an MPC as the central controller. The developed control framework is tested by simulations and evaluated in Section V. Final conclusions are given in section VI. All the symbols and subscripts are listed in table 10.1.

2 Central Heating System

2.1 Case Study

A single-family detached house is considered as the case study, see Fig. 10.3. The two small rooms are equipped with hydronic radiators (HR) controlled by thermostatic radiator valves, one in each room. The bigger room has a serpentine floor heating (FH) system. The GHP provides hot water for the hydronic heaters in the building. Rooms number 1 and 3 have south faced glazings; hence they receive more sun.

Table 10.1: Symbols and Subscripts

Nomenclature	
A	surface area (m^2)
C	thermal capacitance $(J/kg\,^\circ\mathrm{C})$
K_r	equivalent heat transfer coefficient of HR$(J/sec\,^\circ\mathrm{C})$
K_{fh}	equivalent heat transfer coefficient of FH$(J/sec\,^\circ\mathrm{C})$
N, M	total number of HR and FH distributed elements
n_1	radiator exponent
P_c	consumed power by compressor
P_t	transferred power to the secondary side
Q	heat (W)
q	water flow in hydronic heater (kg/sec)
R_i	room number i
T	temperature $(^\circ\mathrm{C})$
T_i, T_j	temperature of the i, j^{th} element (HR,FH) $(^\circ\mathrm{C})$
U	thermal transmittance $(kW/m^2\,^\circ\mathrm{C})$
V	volume (m^3)
τ	time constant
τ_d	time delay of floor heating
Subscripts	
a	air
e	envelop
f	floor
fh	floor heating
hp	heat pump
s	supply water
out	outlet (water)
amb	ambient (temperature)
r	radiator
Ref	reference
w	water

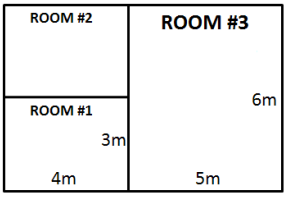

Figure 10.3: Sketch of the apartment with three separate heat zones

2.2 Hierarchical Control Structure

Schematic of the hierarchical model predictive controller is depicted in Fig. 10.4. Local proportional integral (PI) controllers are designed for each hydronic heater based on

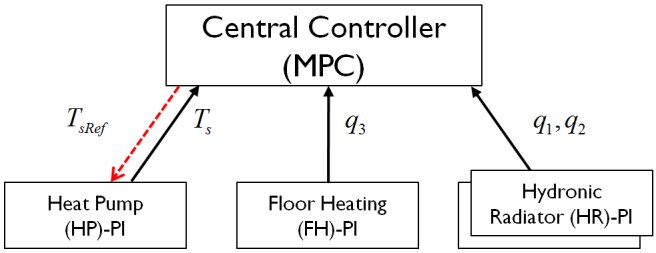

Figure 10.4: Schematic of the hierarchical control structure: setponit signal (dashed) and measurements (continuous). Signals' indices correspond to the respective room number.

Ziegler Nichols step response method, ([5]). PI controllers seek the respective room temperature setpoint, adjusting the valve opening of HRs and duty cycle of FH's on/off valve. Heat pump's PI controller adjusts the compressor duty cycle to seek the specified temperature setpoint provided by the central controller.

Model predictive controller receives all the operating points i.e. all flow rates. Based on that, it specifies the supply water temperature for GHP. The minimum supply temperature occurs at a point where at least one of the valves is almost entirely open.

Some of the main assumptions are: 1) An circulating pump in the water circuit is seeking a constant head gain; 2) Maximum valve opening corresponds to the highest capacity in both FH and HRs; 3) Flow rate of HRs are estimated, having TRVs driven by a stepper motor.

3 System Modeling

This section is devoted to modeling details of the components and subsystems which are employed in the simulations.

3.1 Simulation Models

Energy balance equations of a single room based on the analogy between thermal systems and electrical circuits are as following:

$$\begin{aligned} C_e\dot{T}_e &= UA_e(T_{amb} - T_e) + UA_e(T_a - T_e) \\ C_f\dot{T}_f &= UA_f(T_a - T_f) + Q_{fh}(t - \tau_d) \\ C_a\dot{T}_a &= UA_e(T_e - T_a) + UA_f(T_f - T_a) + Q_r \end{aligned} \tag{10.1}$$

The above equations are developed mainly based on [6]. More details regarding the parameters can be found in table 10.1 and furthermore in [7]. Envelope, room air and concrete floor are assumed to be at uniform temperature, i.e. no temperature gradient is considered in any of them. Heat flux via partition walls between the rooms is neglected, provided that temperature differences among the rooms are not noticeable.

Radiator is modeled as a lumped system with N elements in series. The ith section temperature is given by [8]:

$$\frac{C_r}{N}\dot{T}_i = c_w q_r (T_{i-1} - T_i) - \frac{K_r}{N}(T_i - T_a)^{n_1} \tag{10.2}$$

in which T_i is the radiator's ith element temperature and $i = 1, 2, ..., N$. For details of K_r and the assumptions made in the above formulation, the reader is directed to section 6.3.1 of [8].

Assuming a constant pressure drop across the valve, a specific thermostatic valve is modeled with a static polynomial function mapping the valve opening δ to the flow through valve.

$$q = -3.4^{-4}\delta^2 + 0.75\delta \tag{10.3}$$

The specific TRV has a stepper motor to adjust the valve opening. This is a new type of TRV of which the valve position can be estimated and consequently the flow rate.

The considered floor heating has a serpentine piping embedded into a heavy concrete. Heat flux from pipes exterior is considered only upward. Employing a similar modeling as radiator, the distributed lump model is governed by:

$$\frac{C_{fh}}{M}\dot{T}_j = c_w q_{fh} (T_{j-1} - T_j) - \frac{K_{fh}}{M}(T_j - T_a) \tag{10.4}$$

in which T_j represents the jth element temperature with $j = 1, 2, ..., M$. Distribution of lumped elements are considered to be along the pipe. We have also assumed that heat is transferred between two sections only by mass transfer, implying that convective heat transfer is neglected. Constants C_{fh} and K_{fh} depend on the floor and pipes material. For more details, please see [9].

Floor heating valve has an on-off thermal wax actuator. This actuator is controlled by pulse width modulation signal in practice. However, without loss of generality, we designed FH controller in continuous time.

3.2 Control Oriented Models

We have presented low-order models for control design purposes based on the relatively sophisticated simulation models of previous section.

Each room temperature pertains to the heat of radiator or floor heating via a 3^{rd} order transfer function which can be approximated with a first order transfer function. The model parameters are derived for each room separately.

The relationship between radiator output heat and influent water flow around a specific operating point can be approximated by a first order transfer function. The approximation precision suffices for the control purposes.

$$\frac{Q_r}{q_r}(s) = \frac{k_r}{1 + \tau_r s} \tag{10.5}$$

Parameters can be found via linearizion around an operating point, via simulation or experiment. These parameters are found previously in [10] composing a linear parameter

varying (LPV) model. In that paper, parameters were found by linearizion around operating points and were presented as some profile curves.

The transfer function between output heat and flow through FH:

$$\frac{Q_{fh}}{q_{fh}}(s) = \frac{k_{fh}}{1+\tau_{fh}s}e^{-\tau_d s} \tag{10.6}$$

Constants k_{fh} and τ_{fh} depend on the floor heating operating point, i.e. the flow and inlet water temperature. These parameters are estimated by linearization around specific operating points.

Closed loop transfer function of the heat pump system is approximated by its dominant dynamic between the supply water temperature and its setpoint as following:

$$\frac{T_s}{T_{sRef}}(s) = \frac{1}{1+\tau_{hp}s} \tag{10.7}$$

4 Hierarchical Control Design

Local control units in cooperation with a central controller is considered as shown in Fig. 10.4. A local unit is a FH or HR system controlled by a PI controller. With a single unit in each room, PI is tuned based on the specific room's dynamic. Both flow rate and influent water temperature are manipulated variables of a single heating unit. While flow rate is controlled in the local unit, the forward temperature is adjusted in the central controller. Central controller receives valve opening as the status signal from all other units. Connection between the valve opening and the flow rate is via the fixed polynomial (10.3), independent of the pressure drop across the valve. A circulating pump seeks a constant differential pressure across all units. Henceforth, we use flow rate instead of valve opening in the central controller unit.

4.1 PI based Local Controllers

We presented LPV models of the system local units in the modeling section. In spite of the variable model parameters, we designed fixed PI controllers for each unit. It means satisfying performance measures and stability margins coarsely. Although, a gain schedule controller could handle variable parameters to maintain high performance measures, a simple PI controller is granted to simplify the proof of concept. Such gain schedule controller is designed in [10].

PI controllers are designed for each FH and HR unit integrated with the corresponding room. The integrated models are:

$$\begin{aligned}\frac{T_a}{q_r} &= \frac{k_1}{(1+\tau_1 s)(1+\tau_r s)} \\ \frac{T_a}{q_{fh}} &= \frac{k_2}{(1+\tau_2 s)(1+\tau_{fh} s)}e^{-\tau_d s}\end{aligned} \tag{10.8}$$

PI controller is designed based on Ziegler Nichols step response method. The time delay of floor heating is not taken into consideration for local controller design. However, it is considered in the model predictive control design.

4.2 MPC based Central Controller

Central controller (CC) determines the reference forward temperature of heat pump based on the operating point of other local units. CC decreases forward water temperature until one of the heating units works at full capacity. The resulted minimum forward temperature based on the house heat demand corresponds to the minimum electric power consumption by the heat pump.

Model predictive control (MPC) is chosen as CC. Features like handling constraints, disturbances and setpoint profile tracking in a systematic way, have made MPC a very popular tool in many process applications [11]. We, specifically, count on the constraint handling specification of MPC in this paper. However, MPC is chosen as to fulfill other future targets in this specific case study, i.e. disturbance rejection.

We did not take the whole integrated state space model (Fig. 10.4) into consideration as MPC model. Instead we relied on the relationship between flow rates and forward temperature of each unit. Such linear relationship is $\dot{q} = -\alpha q - \beta T_s(t - \tau_d)$. A pure delay term should only be considered in association with floor heating unit. We need to derive the parameters of this dynamical equation first. The corresponding transfer function looks like:

$$\frac{q}{T_s} = \frac{-\beta}{s + \alpha} \tag{10.9}$$

The DC gain is found by equating the outgoing heat in one situation with the new situation in steady state. Suppose supply water temperature is changed from T_s^1 to T_s^2. Then, the steady state flow would change from q_1 to q_2. The new flow rate can be achieved from:

$$c_w q_1 (T_s^1 - T_{out}) = c_w q_2 (T_s^2 - T_{out}) \tag{10.10}$$

In both sides of the above equation, T_{out} is the same, provided that the flow rate is limited by a balancing task initially at installation phase. Therefore, the DC gain is:

$$\frac{\beta}{\alpha} = -q_1 \times \frac{T_s^1 - T_{out}}{T_s^2 - T_{out}} \tag{10.11}$$

To find α, we take a look to the channel through which q is influenced by T_s. The dominant pole in this channel belongs to the room air dynamic together with a pure time delay connected to the concrete floor. Therefore, $\alpha = \frac{1}{\tau_a}$ and $\beta = \alpha \times DCgain$.

The applied model to predict the influence of forward temperature on flow rate is as following:

$$\begin{aligned} R_i : \dot{q_i} &= -\alpha q_i + \beta T_s \quad i = 1, 2 \\ R_3 : \dot{q_3} &= -\alpha q_3 + \beta T_s(t - \tau_d) \\ HP : \dot{T_s} &= -\frac{1}{\tau_{hp}} T_s + \frac{1}{\tau_{hp}} T_{sRef} \end{aligned} \tag{10.12}$$

The presented MPC minimizes the following cost functional:

$$\begin{aligned} J : \min_{T_{sRef}} \ & \theta T_s^2 + \phi \Delta T_{sRef}^2 \\ & s.t.\ 0 \leq q_i \leq q_{iMax} \end{aligned} \tag{10.13}$$

The objective function is a summation of two terms with weights θ and ϕ that can be tuned. The first term seeks minimization of electric power consumption. The second term prevents abrupt changes in actuation signal. This online optimization problem can be solved using standard solvers e.g. MATLAB. We selected the prediction horizon such that it includes all significant dynamics i.e. room air plus time delay of concrete floor. Control interval is chosen based on the operation time of the slowest actuators which are on-off thermal wax actuators. We chose the control horizon not to be less than the fastest control loop settling time.

5 Simulation Results

The potential energy saving with the proposed control scheme is investigated via a simulation test. The case study shown in Fig. 10.3 is simulated employing the accurate nonlinear models described in Section 3.1.

5.1 Simulation

We demonstrated a situation where the house heat demand varies during a day. While heat demand is more in the first room initially, the demand peak is shifted to the second room when solar radiation heats up the first and third rooms.

Ambient temperature is an unmeasured disturbance input for the system. A sinusoid with the period of 24 hours models the ambient temperature. In this simulation, behavior of the system in a period of two days is simulated.

The maximum flow through FH is $0.1 Lit/sec$ and through each HR is $0.015 Lit/sec$. In Fig. 10.6 the flow of FH is scaled.

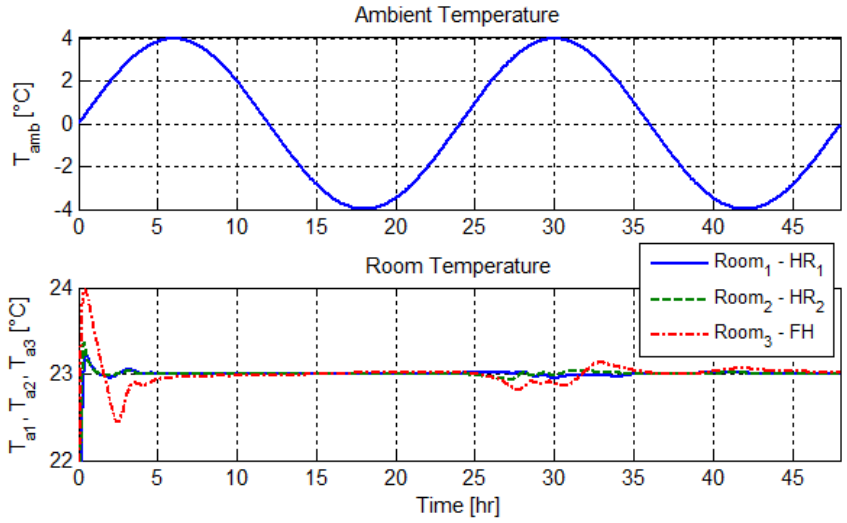

Figure 10.5: Top: Ambient temperature variations during 48 hours. Bottom: Temperature variations of the three rooms. At the earlier times of the second day, solar radiation through glazing causes a temperature increase in the southern rooms.

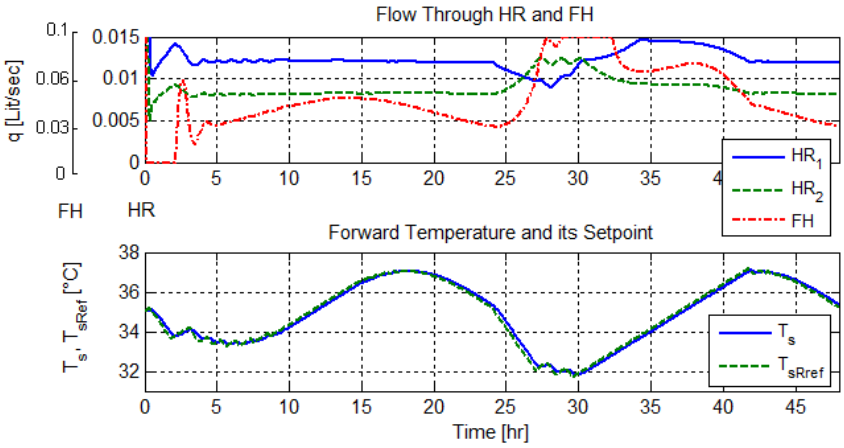

Figure 10.6: Top: Flow through radiators and floor heating. FH's flow is scaled. Bottom: Forward temperature of GHP and the reference of this temperature. Due to the solar radiation at the earlier times of the second day, the flow through the first radiator starts to fall and consequently the forward temperature of GHP. This causes that the other radiator in the northern room and the FH demand for more flow and start to increase and works around 90% capacity. The slow response of the FH system is due to the delay imposed by the heavy floor.

As shown in Fig. 10.6, the temperature of the forward water decreases from $34°\mathrm{C}$ at the day-time of the first day to $32°\mathrm{C}$ in the day-time during the second day due to the solar radiation. This decrease in the demanded forward temperature is translated to a shorter compressor operation time and consequently to a lower power consumption.

The maximum flow rate is limited here to 90% of maximum flow in order not to push the valves into fully-open saturated status. Otherwise, no actuation capacity is left for compensating exogenous disturbances.

5.2 Evaluation of the Results

In this section, we have compared the energy consumption by the heat pump against the conventional heat pump control. Currently, the dominant method of heat pump control is based on a feed-forward approach. The supply water temperature is specified via a predefined map as shown in Fig. 10.2 which has been employed from [12]. The offset and the slop of this curve is usually adjusted manually by the installer. If, with the standard settings of heat pump, the demanded heat can not be provided due to the large dimensions of the building or a poor thermal insulation, an overhead would be considered by the installer.

The comparison is performed on the same case study with the same disturbance model and setpoints. The forward temperature is calculated based on two methods. Relation ship between electric power consumption and the house's heat demand is

$$P_c = \frac{P_t}{COP} \tag{10.14}$$

in which COP is the heat exchanger's coefficient of Performance and P_t is the transferred heat to the house. Since energy loss of the building is the same independent of the forward temperature, P_t is the same in both methods. But, a lower forward temperature resulted from our control scheme means a higher COP and thus a lower P_c. A COP curve is shown in Fig. 10.7 which is the result of an investigation over 100 models of heat pumps [13].

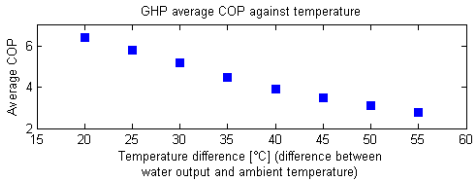

Figure 10.7: Average COP of around 100 heat pump models against the temperature rise across the heat pump

Relying on the curve in Fig. 10.7, the COP corresponding to the forward temperatures are calculated for both methods which is shown in Fig. 10.8. Integrating the inverse of COP multiplied by P_t over the period of two days, we calculated the electric power consumption. The percent of energy saving with the proposed MPC method and the conventional control scheme is shown in table 10.2.

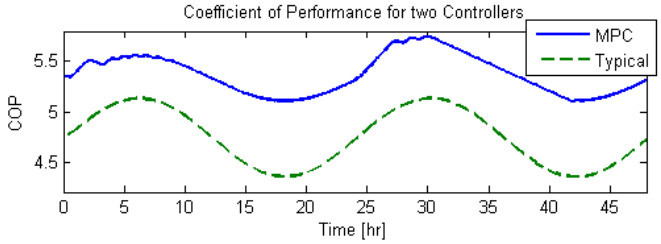

Figure 10.8: Heat pump coefficient of performance for two methods, the proposed MPC controller and a typical heat pump controller.

Table 10.2: Comparison of average electric power consumption $[KW]$

	MPC	Typical	Energy saving (%)
Well insulated	32	37	13.5
Weakly insulated	33	42	21.4

6 Conclusion

A hypothesis for heat pump energy optimization is proposed. Heat pump consumes the least electric power when at least one of the hydronic heaters in the house work at full load. The proposition relies on the fact that the power consumed by heat pump has a

strong positive correlation with the water forward temperature. Employing simplified low order models and simple local controllers, this paper serves as the proof of concept. Nevertheless, the proposed hypothesis for optimization is general and could really contribute to reduced power consumption in almost any type of heat pump based building. More detailed simulations and real life experiments are subjects of future works. Besides, energy measurements at the compressor end would be presented to evaluate the efficiency improvement.

References

[1] B. Rakhesh, G. Venkatarathnam, and S. Srinivasa Murthy, "Experimental studies on a heat pump operating with r22, r407c and r407a: Comparison from an exergy point of view," *Journal of Energy Resources Technology, Transactions of the ASME*, vol. 125, no. 2, pp. 101–112, 2003.

[2] Z. Yang, G. Pedersen, L. Larsen, and H. Thybo, "Modeling and control of indoor climate using a heat pump based floor heating system," in *IECON 2007 - 33rd Annual Conference of the IEEE Industrial Electronics Society*, 2007, pp. 2985–2990.

[3] J. Piper, *Operations and maintenance manual for energy management*. ME Sharpe, 1999.

[4] V. Chandan, S. Mishra, and A. G. Alleyne, "Predictive control of complex hydronic systems," in *American Control Conference*, Baltimore, MD, USA, June 2010.

[5] K. Åstrom and T. Hagglund, *PID Controllers*. North Carolina: ISA, 1995.

[6] G. Hudson and C. P. Underwood, "A simple building modeling procedure for matlab/simulink," *Proc. of Building Simulation*, vol. 99, no. 2, pp. 777–783, 1999.

[7] F. Tahersima, J. Stoustrup, H. Rasmussen, and P. Gammeljord Nielsen, "Thermal analysis of an hvac system with trv controlled hydronic radiator," in *IEEE International Conference on Automation Science and Engineering*, Toronto, Canada, August 2010, pp. 756–761.

[8] L. H. Hansen, "Stochastic modeling of central heating systems," Ph.D. dissertation, Technical University of Denmark, Dep. of Mathematical Modeling, Denmark, 1997.

[9] S. Y. Hu, R. E. Hayes, and R. K. Wood, "Simulation of the dynamic behavior of a hydronic floor heating system," *Heat Recovery & CHP*, vol. 15, no. 6, pp. 505–519, 1995.

[10] F. Tahersima, J. Stoustrup, and H. Rasmussen, "Stability-performance dilemma in trv-based hydronic radiators," in *IEEE Multi-Conference on Systems and Control*, Denver, Colorado, USA, October 2011.

[11] J. M. Maciejowski, *Predictive Control with Constraints*. Harlow, England: Prentice Hall, 2002.

[12] Danfoss, "Maintenance instructions dhp-h opti pro," Danfoss," Maintenance Instruction, 2008.

[13] I. Staffell, “A review of domestic heat pump coefficient of performance, Technical Report,” 2009.

Paper E

Energy Minimizing Controller for a Residential Central Heating System with Hydronic Floor Heating and a Heat Pump

Fatemeh Tahersima, Jakob Stoustrup, and Henrik Rasmussen

This paper is submitted in:
Energy

Abstract

An optimization hypothesis for minimizing power consumption of a heat pump is developed and implemented on a real detached house. Heat pump's coefficient of performance has to be maximized in order to minimize the electricity consumption. To this aim, fundamentally, we minimize the flow temperature using feedback of the building real-time heat demand; Because heat pump's efficiency is inversely dependent on the flow temperature.

Individual room's temperature is regulated by a separate floor heating valve controller, similar to the conventional methods. In principle, a new level of control hierarchy is added on top of the existing floor heating thermostats in order to regulate the flow temperature based on the real heat demand. Experimental results are intended to serve as a proof of concept for the proposed optimization idea. We also estimated the parameters of a second order lumped model of a reference room for controller design purposes. Both simulation and experimental results confirm an outstanding performance and remarkable energy savings compared to the conventional methods.

keywords:*Heat pump, Floor heating, Indoor climate control, Minimizing power consumption, Model predictive controller, Hierarchical controller, Real-time heat demand control*

1 Introduction

Low-temperature heating systems with renewable energy sources have become more popular due to the growing public attention to environmental issues. A hydronic under floor heating system is an example of such systems which offers a profitable heating solution mainly in suburban areas by utilizing a ground/air-source heat pump.

1.1 Motivation and Background

Hydronic radiant floor heating systems have been used in Europe for decades in domestic, commercial and industrial applications [1]. Its popularity in Europe increased by standardizing the plastic pipes for floor heating in late 1970s, especially in Switzerland, Austria, Germany and Scandinavian countries [2]. The mainly used plastic pipes are PEX-types, today. Its popularity is partly due to the higher level of comfort that such systems provide compared to conventional 100% forced air heating systems, not to mention in a noise-free operation. Much of the interest in hydronic floor heating systems stems from the reduced energy consumption [3] to be about 30% as suggested by [4]. According to [5] a floor heating system can reach the same level of operative temperature at a lower air temperature compared to the air-forced heating system. This will result in a lower ventilation heat loss in buildings with high ventilation rates.

A heat pump is an ideal heat source for radiant floor heating systems as they are intrinsically low-temperature and potentially high performance sources. They are drawing more attention today due to a surge for energy savings and the quest for mitigation of global warming. According to the Environmental Protection Agency (EPA), Ground-source Heat Pump (GHP) systems are one of the most energy efficient, environmentally clean, and cost-effective space conditioning systems available. About 70% of the energy used by a GHP system is from a renewable energy source i.e. the ground. High efficiency

GHP systems are on average 48% more efficient than gas furnaces, 75% more efficient than oil furnaces, and 43% more efficient when in the cooling mode [6].

A heat pump acts like a refrigerator and transfers the heat from a colder medium, e.g. the ambient air, shallow ground or water to the building which is at a higher temperature. An electrically driven heat pump can generate 3-4 kWh of heat from 1 kWh of electricity for driving the heat pump's compressor. A geothermal heat pump system is shown in Fig. 11.1. There are typically two hydronic and one refrigerant circuits interconnected through two heat exchangers. These are: 1) the underground buried brine-filled – mixture of water and anti-freeze – pipes with a small circulating pump; 2) the refrigerant-filled circuit, equipped with an expansion valve and driven by a compressor which is called heat pump; and 3) the indoor under-surface grid of pipes with another small circulating pump which distributes heat to the concrete floor of the building [7].

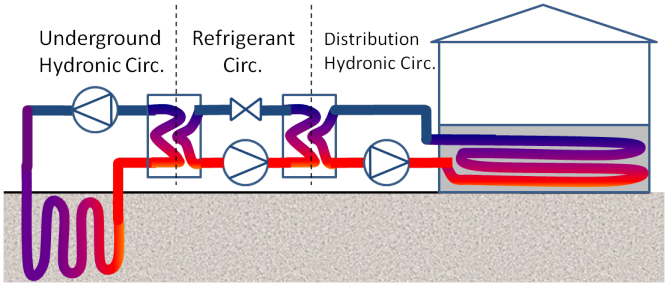

Figure 11.1: An under-floor heating system with a geothermal heat pump.

The underground temperature is fairly constant during several days and slowly varies with an annual pattern. This slow dynamic is due to the huge capacity of the ground and is an advantage to the air-source heat pump with the brine pipes exposed to the ambient air. The higher temperature at the evaporator side of the refrigerant circuit potentially increases the heat pump's Coefficient of Performance (COP) in the cold season. It is also an advantage in the warm season when heat pump works in reverse to cool down the building; because underground temperature is cooler than the ambient air in summer. Therefore, we specifically focus on geothermal heat pumps and assume a constant brine temperature all over the cold season.

Most commercial control solutions for heat pumps are based on feed-forwarding the ambient temperature. The flow temperature in the building distribution pipes is adjusted based on an *a priori* known adjustment curve, see Fig. 11.2 [8]. The curve is suggested by the heat pump's manufacturer. The installer of the heat pump might change the standard slope and offset according to the building specific heat demands. Off-peak loads might usually happen as the result of a coarse adjustment of the curve. Therefore, the heat pump is not usually working with the potential highest efficiency which can only be maintained if feedback from the real heat demand is provided.

1.2 Main Contribution

We investigated the feedback control of heat pumps for minimizing the feed flow temperature which is called the feed temperature henceforth through the paper. The minimum

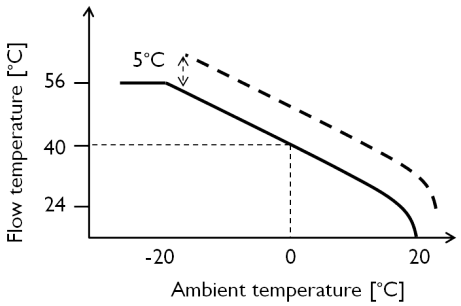

Figure 11.2: An adjustment curve showing the variations of the flow temperature against the ambient temperature. In the conventional feedforward approach of heat pump control, an overhead might be added to the original curve by the installer, depending on the particular building heat demand (the dash).

feed temperature corresponds with the maximum COP and as a result the minimum power consumption by the compressor. Feedback control of heat pump based on the building specific heat demand was formerly studied in [9]. In the latter work, the rooms' temperature are controlled individually to maintain their specific setpoint temperatures, like the conventional setup by a relay/PI controller. The advantage compared to the old setup is that an outer loop minimizes the flow temperature without pushing any of the valves into fully-open saturated status, otherwise no actuation capacity is left for compensating exogenous disturbances. The lower feed temperature reduces the gap with respect to the brine temperature, eventually ending to a higher COP. On the other hand, rooms are less prone to overheating due to the uniformly lower flow temperature.

We, in the current paper, presented the experimental results of implementing the proposed heat pump controller on a real detached house. The results are served as a proof of concept and are further used for parameter estimation and model validation purposes. We have exploited the validated model in simulation studies to compare the proposed controller with the conventional approach of heat pump control from the energy savings perspective and the thermal comfort. The results, from energy savings perspective, greatly depend on the building type and the envelope insulations. For our case study, this is about 12.8% of electric power reduction comparing to a fairly designed conventional controller. A new result show that the ambient temperature measurement can be neglected when the insulation of the building is good enough. In this case, feedback control of the building heat demand would suffices. For a poor insulated building, however, it is not the case. In contrary, it worth to have a forecast of the ambient temperature when the building insulation is poor.

1.3 State of the Art

Feedback control of similar heating/cooling systems are investigated in several recent studies, [10, 11, 12, 13, 14, 15]. The flow temperature is controlled by feeding back a single room's temperature in [10]. The room's floor heat valve is fully opened and the corresponding flow temperature is controlled by several control methods, Proportional

(P), P-Integral (PI), PI-Derivative (PID) and relay controllers. The performance of these controllers are compared with each other. This method obviously is not appropriate for a building with multiple rooms, rather is possible only for a single room. In [11] a distributed model predictive controller is introduced for a residential building where different zones' temperature are controlled by semi-independent MPCs. The adjacent rooms communicate their instantaneous temperature setpoint with each other. In [12] the heat pump's COP is fixed and the power cost is optimized by shifting the heat demand from peak to off-peak loads. However, the amount of power savings by optimizing COP is not negligible at all. In this study we showed via experimental and simulation study that the amount of energy saving by minimizing COP will be 12.8% for the paper case study which is a low energy building. This percentage would be different for buildings with different insulation degrees.

The main contribution of this study, however, is not optimization of heat pump performance by centralizing the system controller like many recent studies [11, 13, 16]. It proposes a new framework which can also be applied to the existing thermostatic based space controllers. The contribution is a new level of control hierarchy on the top which integrate local loops with the heat source such that the power consumption is minimized. It stems from the novel method by that the minimum feed temperature is reached i.e. lowering the feed temperature up to the point where at least a local controller reaches saturation. All the subsequent proposal of controller hierarchy and formulations are based on this fundamental optimal point.

The paper is organized as follows: Section II presents the system setup and the test building. Section III gives the subsystems dynamical models. Experimental results which serve as the proof of concept are illustrated and discussed in Section IV. Also, parameter estimation and model validation for the controller design purposes come in this section. Using the verified model, the simulations are conducted to make a quantitative assessment of the energy savings in Section V. Conclusions and Discussions are given consecutively in the last Section.

2 Case Study

The case study is a low energy demonstration building located in Copenhagen, Denmark. The building is built to provide possibilities for testing energy efficient constructional solutions and components and comprises test facilities [17]. Built in 2009, Energy Flex House Lab is an uninhabited test facility examining the interplay of various floor types, outer walls and technical installations, Fig. 11.3.

2.1 Central Heating System

The system consists of three separate heat zones i.e. rooms. Each room has a separate grid of sub-floor pipes embedded into a thick layer of concrete, in a serpentine pattern with a center-to-center distance of 100 mm. The mass flow rate through the three parallel pipe branches corresponding to each room is not the same due to different adjustments. It is regulated by a multiple-rate circulating pump to around 32, 22 and 20 l/h through the pipes of the rooms#1,2 and 3 respectively. The average U-value of the building envelope of the reference room, including 1.6 m^2 of windows, is $0.2W/m^2/K$. A Schematic diagram of the closed loop piping system is shown in Fig. 11.4.

Figure 11.3: Energy Flex House: a low energy building for testing, developing and demonstrating innovative energy efficient solutions

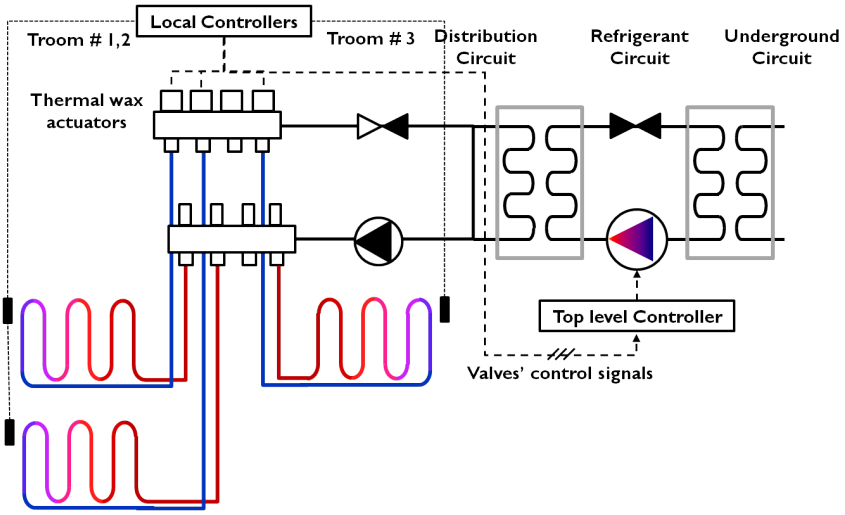

Figure 11.4: A schematic diagram of the piping system

The three rooms in the above schematic are of the same size, each having a triple-glazed window which faces south in rooms#1 and 2, and faces north in room#3. Being in the north hemisphere, rooms#1 and 2 receive solar radiation through windows and have high solar heat gains.

There are other spaces adjacent to the aforementioned rooms i.e. a room adjacent to room#3, a corridor between southern and northern rooms and two bathrooms. Each space has its own sub-floor heating pipe grid that was disconnected from the main manifold in the course of experiments. The building has two floors with the lab located in the ground floor. The measurement and control are limited to the three separated rooms in the ground floor that receive negligible heat gain from the adjacent and above spaces. It is because, those spaces were disconnected from the heat source.

2.2 Control System Structure

Each room has a separate valve controller which regulates the flow to maintain a specific room's setpoint. Thermal wax actuators adjust the valves opening/closing duration based on the Pulse Width Modulation (PWM) signal received from the local control loops.

The flow temperature is regulated by another controller at a higher level receiving heat demand signal from the local control loops. Duty cycle of the valves associate with the rooms heat demand. This is due to a constant differential pressure across the valves. A multi-speed circulation pump in the distribution circuit maintains the fairly constant differential pressure.

As of the refrigerant circuit, the expansion valve has a built-in mechanical feedback mechanism to marginally prevent flow of condensed refrigerant into the compressor, i.e. the heat pump. The heat pump could be continuously controlled. We employed a MPC in a simulation study,[9], to reduce the heat pump's power consumption as much as possible which was fulfilled by minimizing the mass flow temperature in the distribution circuit.

3 Simplified System Model

This section describes a second order dynamical model of a reference room in the building of concern. The model's parameters are further estimated and verified via a set of test data. The model is used later for the control design purposes. All symbols, subscripts and parameter values are given later in table 11.3.

The state space equations which govern a single room's dynamics are derived based on the analogy between thermal systems and electrical circuits [18]. A schematic view of the room with two analogous electrical circuit are shown in Fig. 11.5. The right circuit that is precise enough for control design purposes, is the reduced order model of the left one . In the figure, T_e, T_a, T_f, T_w, Q_f and T_{amb} represent respectively associated temperature of the room envelope, indoor air, concrete floor, hot water through the pipes, dissipated heat through the pipes and the ambient. Resistors and capacitors symbolize the conduction/convection heat transfer coefficient and heat storage capacity accordingly.

The energy balance equations based on the two main thermal masses i.e. the air-envelope and the concrete floor are as follows:

$$\begin{aligned} C_i\dot{T}_i &= B_{ai}(T_{amb} - T_i) + B_{fi}(T_{f_i} - T_i) + B_{ji}(T_j - T_i) \\ C_{f_i}\dot{T}_{f_i} &= B_{fi}(T_i - T_{f_i}) + Q_{f_i} \end{aligned} \tag{11.1}$$

in which $i, j \in \{1, 2, 3\}$ are the corresponding room index. B represents the equivalent convection/conduction heat transfer coefficient between two connected nodes. For instance, B_{fi} is the conduction heat transfer coefficient between the concrete floor and the room#i. The second equation which describes the heat flow through the concrete floor is a simplified version of a more accurate simulation model presented in [19]. The heat flow is $Q_{f_i} = c_w q_i(T_{feed} - T_{return_i})$, in which temperatures' indices stand for the feed and the return flow temperatures respectively.

The heat pump dynamic is much faster than the fastest dynamic of the building. Therefore, we consider a static relationship between the transferred heat to the building, Q_b, and the heat pump's electrical work done by its compressor, W_c, which is given

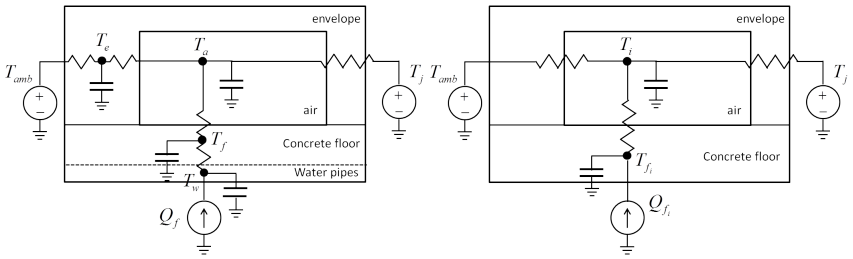

(a) Model#1: 4^{th} order model (b) Model#2: Reduced order model

Figure 11.5: Analogous electrical circuit to the room thermal model; Fig. a shows a 4^{th} order model and Fig. b illustrates the reduced order model. The thermal heat capacity of the water pipes is far less than that of the concrete floor, therefore it is neglected in the simplified model. Thermal capacitance of the envelope including walls, partitions and ceiling is merged with that of the room air and furnitures; as well as the corresponding temperatures.

as:

$$W_c = \frac{Q_b}{\eta_{cop}} \tag{11.2}$$

with η_{COP} representing the heat pump coefficient of performance (COP). This term inversely depends on the temperature difference between the evaporator i.e. the brine temperature, and the condenser i.e. the feed flow temperature. This dependency is usually indicated by the manufacturer in the heat pump data sheet. The COP curve that we used in our simulations is based on the statistical data reported in [20], see Fig. 11.6.

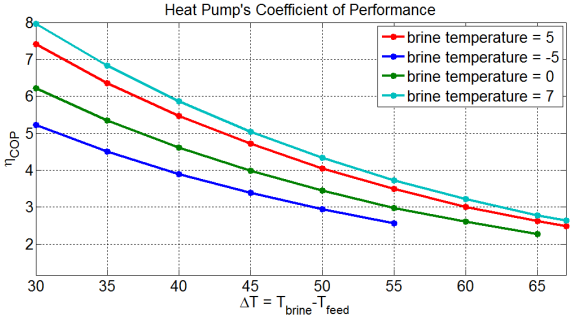

Figure 11.6: Statistical data showing the relevance between $T_{brine} - T_{feed}$ and the COP

With buried pipes in deep underground, the brine temperature of a geothermal heat pump is assumed to be constant allover the high demand season. Presuming $T_{brine} = 2\,^{\circ}\mathrm{C}$, $\eta_{cop}(T_{feed})$ is formulated by interpolation:

$$\eta_{cop} = -0.13 T_{feed} + 11 \tag{11.3}$$

4 Experimental Results

As of the test setup, room temperature sensors are positioned in the middle of the rooms, one meter above the floor surface. This provides us with a more accurate measurement compared to a wall-installed temperature sensor.

The hot water is supplied by a heat source, which can deliver hot water at any specified temperature to the floor heating pipes. The time response of this heat source very well simulates a heat pump dynamic i.e. around 15 minutes time constant. The heat source, in fact, consists of a boiler which provides hot water at a fixed temperature and a mixing shunt. The mixing shunt is controlled to provide a desired flow temperature by mixing the feed flow of the boiler with the return flow of the heating system.

TWAs response time is around 5 minutes to fully open/close the valve. This actuator time is negligible compared to the response time of the concrete embedded floor heating pipes which is around 30 hours. Furthermore, there is a pure time delay transferring the heat from the embedded pipes to the floor surface. We merged the actuators' response time into the system time delay which is around 30 minutes, later on in the simulations.

Three sets of tests are implemented on the aforementioned test setup. The first set is simple steady state and step response experiments conducted to estimate and verify the parameters of the plant model (11.1). The second and the third tests in this section are served as a proof of the optimization hypothesis for the central heating system.

All the tests have been accomplished in the interval from November 2011 until February 2012.

4.1 Parameter Estimation and Model Validation

The 5 parameters, B_{ji}, B_{ai}, B_{fi}, C_{f_i} and C_i of the plant model (11.1) need to be estimated. The first three parameters are obtained using two steady state points and shown in table 11.1. The other two parameters will be achieved by analyzing the transient response. The system time response to a step flow input of the amount $\frac{2}{3}q_{max}$ is depicted in Fig. 11.7 for the reference room. The mass flow temperature is about 40°C.

The concrete temperature is measured at 50 mm depth from the floor surface, in the middle of the reference room. The return and feed flow temperatures are measured immediately after the valves manifold. The fluctuations in these temperatures is correlated with the valve on/off position. When the valve is closed, flow is discontinued and the temperature falls in both feed and return path. Duty cycle of the mass flow and consequently the dissipated heat is fixed to about 67%. The latter is the system direct input which is not a step, unlike the mass flow.Therefore we can not directly extract the model dynamics by examining the room temperature response. Instead we have employed the Least Square (LS) algorithm to estimate the parameters. To this aim, the plant model is discretized using backward differentiation and the chosen time step is equal to the data sampling rate i.e. 2 minutes. The discretized model is:

$$\begin{aligned} T_i(t_k) &= \frac{1}{\frac{C_i}{t_s} + B_{ai} + B_{fi} + B_{ji}} \left(B_{ai}T_{amb}(t_k) + B_{fi}T_{f_i}(t_k) + B_{ji}T_{ji}(t_k) + \frac{C_i}{t_s}T_i(t_{k-1}) \right) \\ T_{f_i}(t_k) &= \frac{1}{\frac{C_{f_i}}{t_s} + B_{fi}} \left(B_{fi}T_{f_i}(t_k) + \frac{C_{f_i}}{t_s}T_{f_i}(t_{k-1}) + Q_{f_i}(t_k) \right) \end{aligned} \tag{11.4}$$

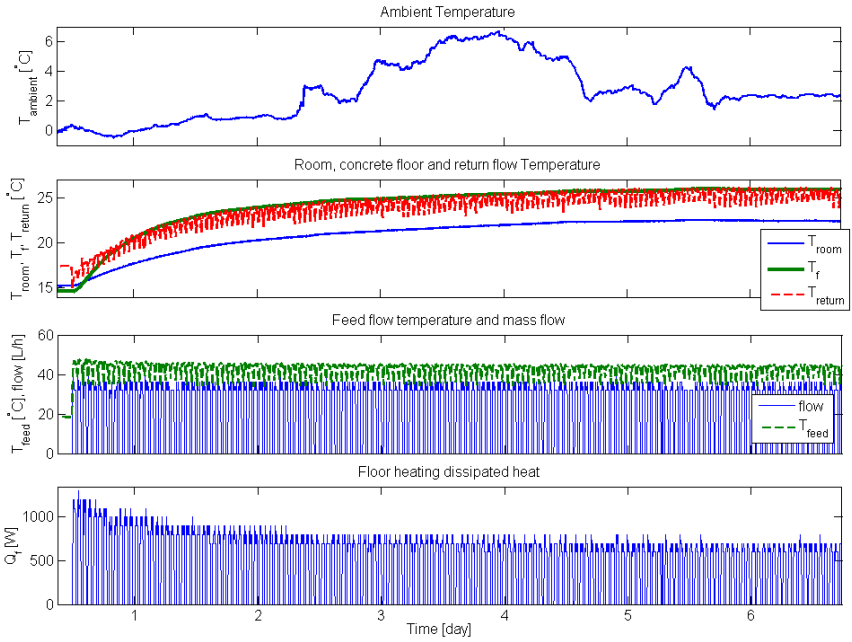

Figure 11.7: The system time response to the step flow input. The system time delay is fairly small compared to the system equivalent time constant. Two main dynamics of the system corresponds to the concrete and envelope thermal mass as considered in (11.1). The adjacent rooms temperature is about 19 °C during the course of experiments.

in which, t_k is the k^{th} sampling time and $t_s = 2min$ is the sampling rate. Summing the above difference equations makes it appropriate to the LS algorithm setup. The summation is:

$$C_i \frac{T_i(t_k) - T_i(t_{k-1})}{t_s} + C_{f_i} \frac{T_{f_i}(t_k) - T_{f_i}(t_{k-1})}{t_s} = B_{ia} \left(T_{amb}(t_k) - T_i(t_k) + Q(t_k)\right) \tag{11.5}$$

Defining new terms:

$$x(k) = [\frac{T_i(t_k) - T_i(t_{k-1})}{t_s} \ \frac{T_{f_i}(t_k) - T_{f_i}(t_{k-1})}{t_s}]$$
$$y(k) = B_{ia} \left(T_{amb}(t_k) - T_i(t_k) + Q(t_k)\right)$$

equation (11.5) at the N sample points looks like:

$$\begin{pmatrix} y(1) \\ y(2) \\ \vdots \\ y(N) \end{pmatrix} = \begin{pmatrix} x_1(1) & x_2(1) \\ x_1(2) & x_2(2) \\ \vdots & \vdots \\ x_1(N) & x_2(N) \end{pmatrix} \times \begin{pmatrix} C_i \\ C_{f_i} \end{pmatrix}$$

with N as the number of total data samples. The LS solution for the parameters $[C_i\ C_{f_i}]^T$ will be $(X^TX)^{-1}(X^TY)$, in which $Y_{N\times1}$ is the array composed of y(k) and $X_{N\times1}$ is the matrix composed of $[x_1(k)\ x_2(k)]$ for k=1,...,N. The estimated parameters are shown in table 11.1. Fig. 11.8 compares the measurement data with both estimation and validation results for the room and concrete temperatures in three different assignments of data. Once, we picked all the data only for estimation and no validation. Second, we picked the first 2/3 portion of the data as for estimation purpose and the last 1/3 as for validation. We swapped the sets in the third test. All the results are shown in the following illustration and table 11.1.

Table 11.1: Estimation and Validation Results:Three sets of estimations are illustrated: (set0) all the data is used only for estimation, (set1) first 2/3 of data is used for estimation and the next third for validation, (set2) first 1/3 of data is used for validation and the next 2/3 for estimation.

	Estimated Parameters					Mean Squared Error	
	C_i	C_{f_i}	B_i	B_{fi}	B_{ji}	Estimation error	Validation error
set0:	1394	5915	9.3	115.6	62.1	0.1226	NA
set1:	1305	6137	9.3	115.6	62.1	0.1247	0.196
set2:	470	6278	9.3	115.6	62.1	0.1551	0.2591

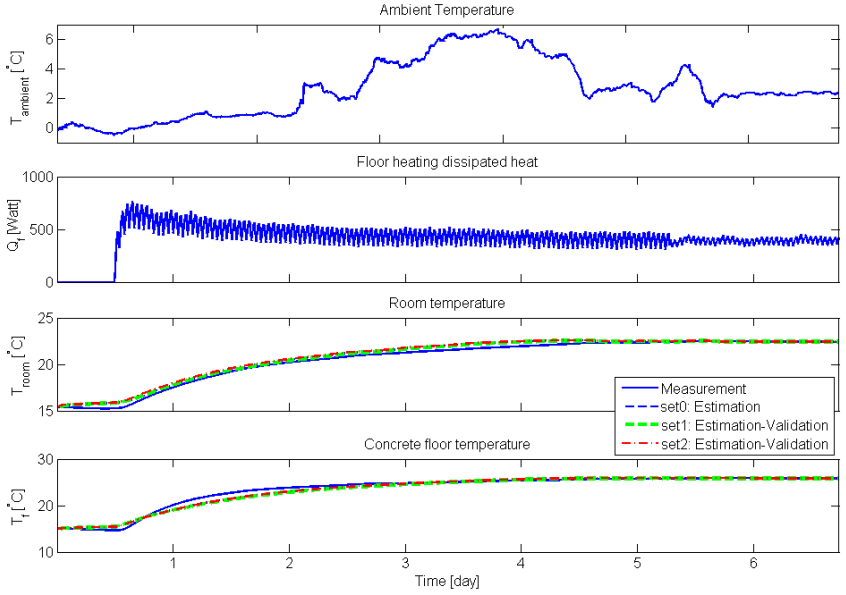

Figure 11.8: Measurement, estimation and validation results to the input heat. The mean squared estimation and validation errors of both variables for the three situations are shown in table 11.1.

The estimated parameters are chosen based on the set1 results which seems to be

more accurate in average. The results of this section are further exploited for simulation and controller design purposes in the rest of the paper. The other rooms' corresponding parameters are estimated through separate experiments and are listed in table 11.3.

4.2 Open-Loop Test Results

We find the minimum required flow temperature using a bisection algorithm in an open loop test. The rooms' temperature are regulated using an on/off controller. The proportion of on-time to an interval or period of time, although not fixed, is recognized and defined as duty cycle.

First we choose a high enough feed flow temperature which corresponds to a moderate flow duty cycle, saying 60%. Then we choose a low flow temperature which gives us 100% of flow duty cycle. Next step is picking an average flow temperature between the former two flow temperatures, which correspond with a flow close enough to 90% duty cycle. The bisection algorithm is repeated such that we end up where the flow duty cycle is 90%. Each step of the algorithm took about 2 days and the whole test period lasted about 9 days. Fig. 11.9 shows the relevant experiment results.

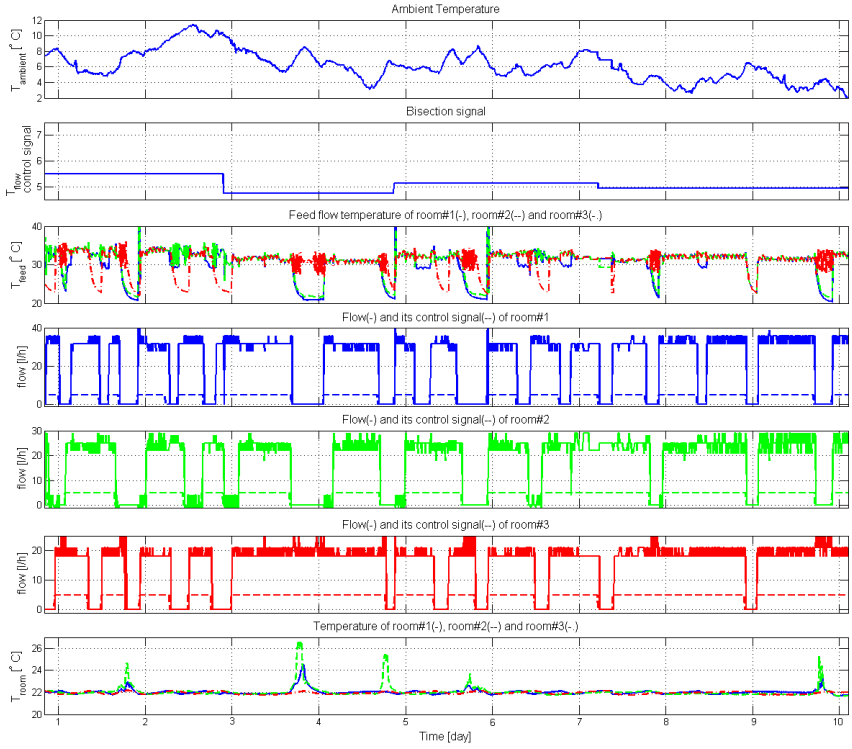

Figure 11.9: The first test results: after 3 steps or 7 days, we found the minimum feed flow temperature which is 31 °C. At this flow temperature, room#3 experience 90% duty cycle of mass flow. Rooms' temperature setpoint are very well maintained using simple relay controllers.

The feed flow temperature is reduced via bisection algorithm to 31 °C where room#3's flow meets 90% of duty cycle. The other rooms have less heat demands compared to the north faced-room#3. The south-faced rooms receive solar radiation through glazing in the sunny days which are 5 days in total through the whole interval. Different intensities of the spikes corresponding with the solar radiation is due to different sensor positions in the rooms#1 and 2.

Fluctuations in the flow is due to the flow meters resolution. Valleys in the feed flow temperature coincide with the corresponding valve openness status It is because the feed flow temperature is measured individually for each room right after the distribution manifold, although it is the same for the whole system and vary just with the bisection signal.

It is worth noticing that a relay controller could maintain a room's temperature set-point easily which is in part due to the large thermal mass of the concrete layer. Consequently the time constant of the heating system is much longer than its time delay. Otherwise, the pure time delay of the thick concrete layer would influence overheating of the room dramatically. On the other hand, heavy thermal insulation of the external walls filters out the ambient temperature fluctuations and transfers weather changes of a very low frequency . Therefore, the heating system with a long lag characteristic is not a burdensome when heating is required due to the weather condition changes.

4.3 Closed-Loop Test Results

Feed flow temperature in this test is regulated by feeding back the valves' control signal. The block diagram of the closed loop system is shown in Fig. 11.10. The test results are shown in Fig. 11.11.

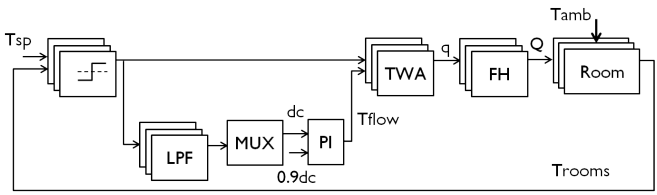

Figure 11.10: Block diagram of the closed loop test. The relay controller signals pass through a low pass filter to be compared later by the multiplexer block. This block determines the highest heat demand. The corresponding flow is regulated to 90% duty cycle by adjusting the flow temperature using a PI controller.

5 Optimal Problem Formulation

In the simulation section we have conducted the same aforementioned hierarchical control structure, except that we employed a model predictive controller for optimization of the flow temperature. Also, proportional integral controllers are employed in the local controller loops which is more appropriate when the energy class of the building is lower compared to our case study. Block diagram of the closed loop system is shown in Fig. 11.12.

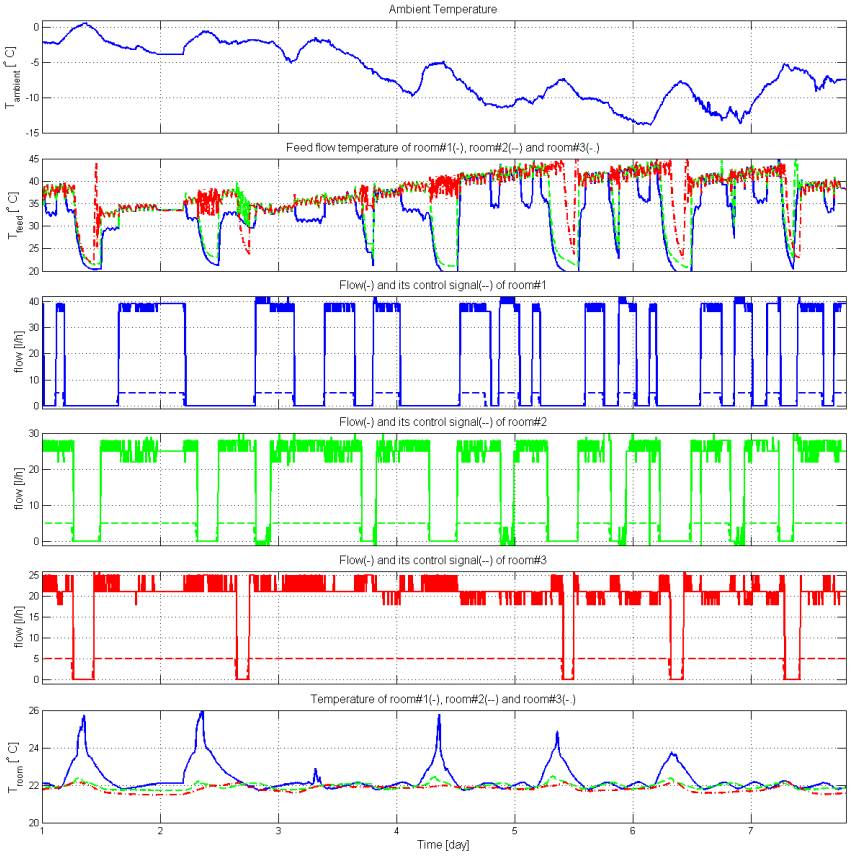

Figure 11.11: The second test results: Room#3 has the highest heat demand among the three rooms. The lower heat demand of the other rooms is mostly due to the solar radiation through glazing. While the flow duty cycle of room#3 is about 90%, Rooms# 1 and 2's flow duty cycle are about 60% and 70% respectively.

MPC can systematically incorporate forecast data of weather, solar radiation and electricity price signals in the optimization procedure. Besides constraint handling, MPC gives systematic feedforward design based on future demands [21]. Therefore we designed a MPC at the top level of the control hierarchy to orchestrate function of the local controller units at the lower level. The block diagram of the closed loop hierarchical controller is shown in Fig. 11.12.

In order to minimize the power consumption of the heat pump, the heat pump's COP should be increased. A solution to this is to reduce the flow temperature in the distribution circuit in order to decrease the gap between the brine and the distribution circuit temperature. Hence, regardless the thermal demand, electricity consumption by the heat pump's compressor is lessened.

The main role of MPC in Fig. 11.12 is to minimize the feed flow temperature. To this end, control signals of the floor heating valves are fed back to the MPC, expressing

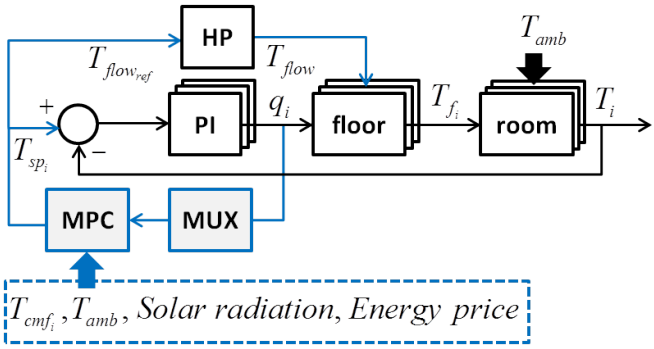

Figure 11.12: The system closed-loop block diagram

the associated room's heat demand. The largest one is selected using a multiplexer as the highest heat demand. MPC determines the flow temperature based on the highest heat demand in order to push the corresponding valve toward saturation. At this point, to avoid physical saturation of the valve, flow is limited to 90% by putting hard constraints on it in the MPC prediction model. Otherwise, no valve capacity is left for compensating exogenous disturbances.

On the other hand, MPC systematically facilitates minimizing the adverse impact of abrupt system disturbances e.g. solar radiation through glazing or an unforeseen user defined comfort temperature alteration [21]. Another *a priori* knowledge which is efficient to be included in the decision making process is the electricity price signal. Knowing this signal in advance would be profitable for domestic consumers and helpful in enhancing the electric grid balance. However, we only focus on the primary task of MPC in the following simulations and postpone the other possibilities of integrating the unforeseen heat demands to future.

5.1 Controller Design

The local PI controller for the i^{th} room in state space form is:

$$\begin{aligned} \dot{\xi} &= \frac{K_p}{T_{int}}(T_{sp_i} - T_i) \\ q_i &= K_p(T_{sp_i} - T_i) + \xi \end{aligned} \tag{11.6}$$

with ξ as the auxiliary state. The parameters of the PI controller are chosen based on the plant step response around the desired operating point which is $q = 90\% q_{max}$.

The prediction model of MPC can be formulated as a linear time invariant system in spite of the bilinear term in the system equations. In the vicinity of the desired operating point i.e. $q = 0.9 q_{max}$, the bilinear term, $Q_f = c_w q(T_{feed} - T_{return})$ is linearized. Hence the internal model of the MPC controller in a state space form is:

$$\begin{aligned} \dot{x} &= Ax + B_u u + B_d d \\ y &= Cx + D_d d \end{aligned} \tag{11.7}$$

with $x = [T_i, T_{f_i}, \xi]^T$, $u = [T_{feed}, T_{sp_i}]^T$, $y = [T_i, q_i]^T$, and $d = [T_{amb}, T_j]$. Matrices A, B, C and D are derived based on (11.1) and (11.6). T_i is measured in each room separately and, T_{f_i} is estimated using a Kalman state observer and ξ is known from the local control signals. Return temperature of water is approximated with T_{f_i} which seems to be appropriate enough for the control purposes. The step size, t_s for discretization is the same as the data sampling rate of the test results.

The optimal problem is formulated via (11.7). The prediction model is the dynamics of the corresponding room with the highest heat demand.

$$\begin{aligned} \min_{T_{feed}, T_{sp_i}} \quad & \sum_{k=1}^{N} |T_s(k)| + \nu_1 |\Delta T_s(k)| + \nu_2 |T_i(k) - T_{cmf_i}(k)| + \nu_3 |\Delta T_{sp_i}| \\ s.t. \quad & x(k+1) = Ax(k) + B_u u(k) + B_d d(k) \\ & y(k) = Cx(k) + D_d d(k) \\ & 0 \leq q_i(k) \leq 0.9 q_{max} \\ & T_{min} \leq T_{feed}(k) \leq T_{max} \end{aligned} \tag{11.8}$$

with N as the prediction horizon. In the cost functional, $T_{cmf_i}(k)$ stands for user-defined comfort temperature at the time instant $t = k$. T_{sp_i} and T_{feed} are the manipulated variables. We also penalized the manipulated variables rate of changes. Flow is bounded by two upper and lower hard constraints in order to avoid physical saturation of the valves. The Upper and lower limits on the flow temperature are to protect the floor surface material form distortion.

6 Simulation Results

In this section, we conducted two sets of simulations for demonstration of different purposes. We have employed the estimated parameters of the reference room listed in table 11.1 corresponding to the set1 estimation and validation results.

6.1 Scenario 1: Variable Heat Demands

Heat demand in one room might vary in the course of season depending on the demanded thermal comfort, solar radiation through glazing or other sources of heat gains. That will cause competing heat demand among the rooms in a building.

Fig. 11.13 shows a situation when room#2 has the highest heat demand i.e. corresponding with $0.9q_{max}$. After a few days, the heat demand of the rooms#1 and 2 decreases due to solar radiation through glazing, causing a decrease in flow temperature. Consequently, room#3' flow starts to increase until $90\%q_{max}$. An increase in the flow temperature keeps the flow of the most demanding room at 90% and prevents it from saturation.

A comparison with the conventional method shows that, potentially 12.8% of electricity would be saved if we regulate the feed temperature based on the real-time heat demand rather than feed forwarding the ambient temperature (conventional method). The configuration of the heat pump controller in the conventional method is $T_{feed} = -T_{amb} + 45$. This is adjusted such that the most demanding room's flow is 70% duty cycle to maintain the room temperature at 22°C.

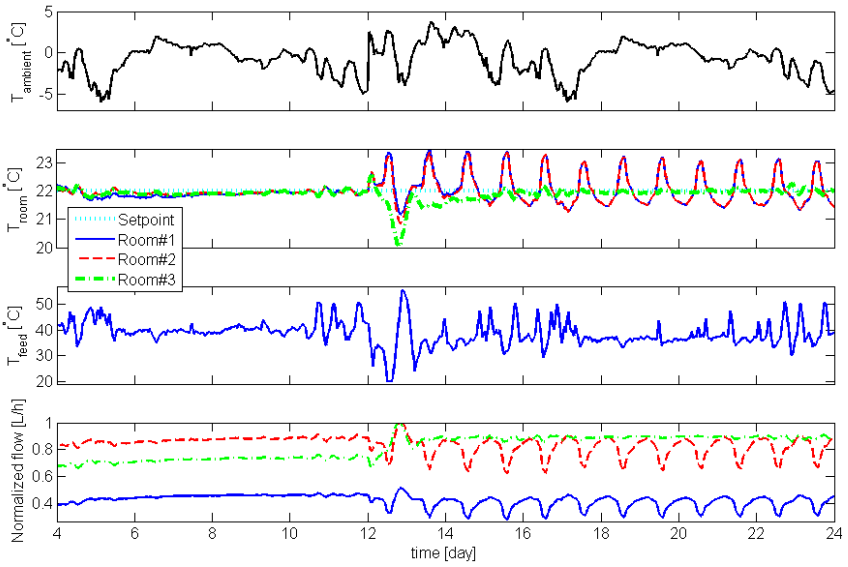

Figure 11.13: Heat demand of room#2 which is dominant in the first 12 days, falls down in the last 12 days due to solarization through glazing. Room#3 becomes dominant in the heat demand among the three rooms. The disturbance measurement i.e. the ambient temperature is available at every time instant.

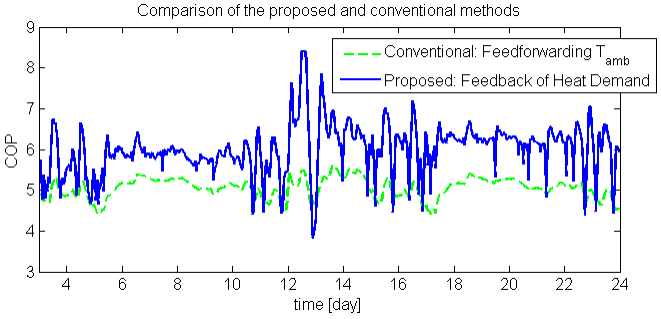

Figure 11.14: Comparison of COP with the proposed and conventional methods. 12.8% of electricity could be saved by the proposed method compared to the conventional feedforward approach.

6.2 Scenario 2: Disturbance Measurement

In this section we demonstrated different performances of the proposed controller when disturbance is perfectly foreseen, only instantaneously measured and not measured. The graph corresponding to the three situations is shown in Fig. 11.15.

A quantitative comparison is shown in table 11.2. Although the results of the case with perfect forecast is the best from both comfort and energy saving perspectives, it is not far different from practical point of view.

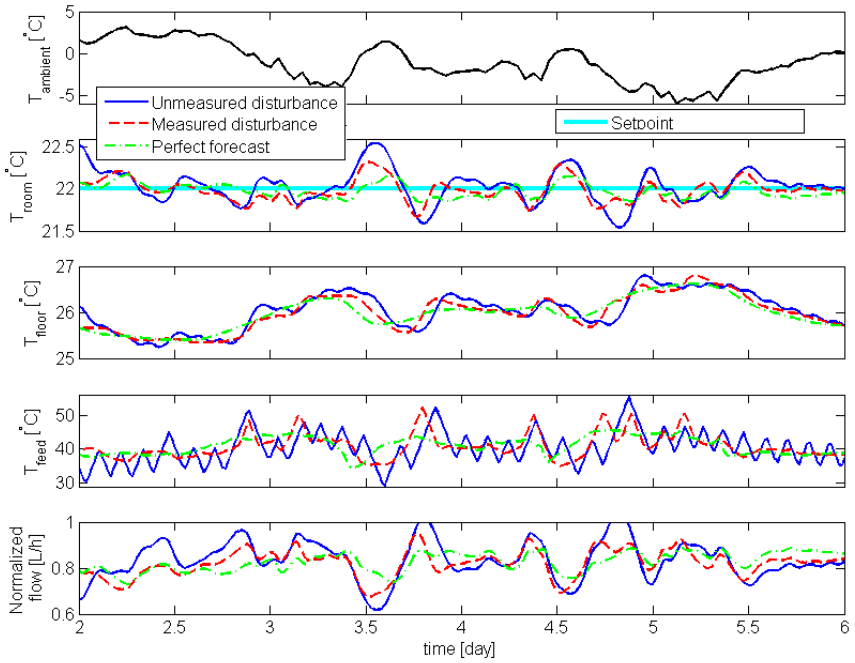

Figure 11.15: Performance of the proposed controller in 3 scenarios are compared. The disturbance i.e. the ambient temperature is forecasted perfectly 5 hours in advance and shown with green dash. The other graphs show the results for the measured and unmeasured disturbance, respectively with red dash and blue line. The results of perfect forecast is the best, however not outstanding in our case with a low energy building.

Table 11.2: Quantitative Comparison for Fig.11.15

	Unmeasured disturbance	Measured disturbance	Perfect forecast
Thermal comfort MSE (Mean Squared Error)	0.0273	0.0129	0.0047
Average Power Consumption [W]	82.1	82	80.5

7 Discussions and Conclusions

Integration of a hydronic radiant floor heating with a heat source is investigated. heat pump's operation is optimized in the sense of power consumption and the thermal comfort of residents. For this purpose, subsystems models are derived, estimated and further used for the purpose of controller design. However, the contribution is not only designing an MPC controller which potentially handles disturbances and setpoint profiles in a systematic way, but mainly includes a hypothesis of the optimal operating point of the whole system. Based on the idea, a hierarchical controller is proposed which intrinsically embeds the existing local room thermostats.

The proposed hierarchical controller setup compared to a central controller is more reliable due to the fact that local controller loops handle disturbances locally. However it is still less robust compared to a distributed controller structure.

Table 11.3: Symbols and Subscripts

Nomenclature	
B_{ji}	heat transfer coefficient between two adjacent rooms $(W/^{\circ}\mathrm{K})$
B_{fi}	heat transfer coefficient between room#i air and the concrete floor $(W/^{\circ}\mathrm{K})$
B_{ai}	heat transfer coefficient between ambient air and room#i $(W/^{\circ}\mathrm{K})$
C	thermal capacitance $(KJ/^{\circ}\mathrm{C})$
K_p	proportional gain
Q_f	dissipated heat to the room by floor heating pipes(W)
Q_b	transferred power to the building
q	mass flow rate (l/h)
T_{cmf}	comfort temperature set by the user $(^{\circ}\mathrm{C})$
T_{int}	integration time of the PI controller
T_{feed}	Feed flow temperature $(^{\circ}\mathrm{C})$
T_{return}	Return flow temperature $(^{\circ}\mathrm{C})$
T_{min}	minimum feed temperature $(^{\circ}\mathrm{C})$
T_{max}	maximum feed temperature $(^{\circ}\mathrm{C})$
W_c	Power consumption of the compressor
ξ	auxiliary state
η_{cop}	coefficient of performance
Subscripts	
a	room air
amb	ambient
cmf	comfort
e	envelope
f	floor
f_i	floor of the ith room
i	room number
k	time instant (s)
sp	setpoint
w	water

References

[1] S. B. Leigh, "An experimental approach for evaluating control strategies of hydronic radiant floor heating systems," Ph.D. dissertation, University of Michigan, Michi-

gan, USA, 1991.

[2] B. W. Olesen, "Radiant floor heating in theory and practice," *ASHRAE Journal*, vol. 44, no. 7, pp. 19–24, 2002.

[3] S. Y. Hu, R. E. Hayes, and R. K. Wood, "Simulation of the dynamic behavior of a hydronic floor heating system," *Heat Recovery & CHP*, vol. 15, no. 6, pp. 505–519, 1995.

[4] N. A. Buckley, "Application of radiant heating saves energy," *ASHRAE Journal*, vol. 31, pp. 17–26, 1989.

[5] B. W. Olesen, "A simplified calculation method for checking the indoor climate," *ASHRAE Trans.*, vol. 98, no. 2B, pp. 710–723, 1983.

[6] M. L'Ecuyer, C. Zoi, and S. J. Hoffman, "Space conditioning: The next frontier," Environmental Protection Agency, USA, Main Report, April 1993.

[7] E. Silberstein and J. Hohman, *Heat Pumps*. Cengage Learning, 2002.

[8] Danfoss, "Maintenance instruction," Danfoss, Denmark, Main Report, 2008.

[9] F. Tahersima, J. Stoustrup, and H. Rasmussen, "Optimal power consumption in a central heating system with geothermal heat pump," in *IFAC World Congress*, Milano, Italy, August 2011.

[10] Z. Yang, G. Pedersen, L. Larsen, and H. Thybo, "Modeling and control of indoor climate using a heat pump based floor heating system," in *IECON 2007 - 33rd Annual Conference of the IEEE Industrial Electronics Society*, 2007, pp. 2985–2990.

[11] V. Chandan, S. Mishra, and A. G. Alleyne, "Predictive control of complex hydronic systems," in *American Control Conference*, Baltimore, MD, USA, June 2010.

[12] R. Halvgaard, N. K. Poulsen, H. Madsen, and J. B. Jrgensen, "Economic model predictive control for building climate control in smart grid," in *IEEE PES Conference on Innovative Smart Grid Technologies*, Washington, USA, June 2012.

[13] J. A. Candanedo and A. K. Athienitis, "Predictive control of radiant floor heating and solar-source heat pump operation in a solar house," *HVAC&R Research*, vol. 17, no. 3, pp. 235–256, 2011.

[14] B. W. Olesen, "Control of floor heating and cooling systems," in *Clima 2000/Napoli 2001 World Congress*, Napoli, September 2001.

[15] H. Karlsson and C.-E. Hagentoft, "Application of model based predictive control for water-based floor heating in low energy residential building," *Building and Environment*, vol. 46, no. 3, pp. 556–569, 2011.

[16] A. Aswani, J. Taneja, and C. Tomlin, "Reducing transient and steady state electricity consumption in hvac using learning-based model predictive control," *proceedings of the IEEE*, vol. 100, no. 1, pp. 240–253, 2012.

[17] T. Institute, "Energyflexhouse - technology to the global challenge." [Online]. Available: http://www.dti.dk/projects/energyflexhouse

[18] G. Hudson and C. P. Underwood, "A simple building modeling procedure for matlab/simulink," *Proc. of Building Simulation*, vol. 99, no. 2, pp. 777–783, 1999.

[19] F. Tahersima, J. Stoustrup, S. A. Meybodi, and H. Rasmussen, "Contribution of domestic heating system to smart grid control," in *Conference on Decision and Control*, Orlando, FL, USA, December 2011.

[20] C. Heerup, "Efficiency and temperature correlation (effectivitet og temperatur sammenhng)," Denmark Technological Institute, Energi og Kilima, Gregersensvej, Taastrup, Denmark, Tech. Rep., 2011.

[21] J. A. Rossiter, *Model-Based Predictive Control*. Raton, Florida: CRC Press LLC, 2003.

Paper F

Controbution of Domestic Heating Systems to Smart Grid Control

Fatemeh Tahersima, Jakob Stoustrup, Soroush A. Meybodi, Henrik Rasmussen

This paper is published in:
IEEE Conference on Decision and Control, CDC-ECC, December 2011,
Orlando, Florida, US

Abstract

How and to what extent, domestic heating systems can be helpful in regaining power balance in a smart grid, is the question to be answered in this paper. Our case study is an under-floor heating system supplied with a geothermal heat pump which is driven by electrical power from the grid. The idea is to deviate power consumption of the heat pump from its optimal value, in order to compensate power imbalances in the grid. Heating systems could be forced to consume energy, i.e. storing it in heat buffers when there is a power surplus in the grid; and be prevented from using power, in case of power shortage. We have investigated how much power imbalance could be compensated, provided that a certain, yet user adjustable, level of residents' thermal comfort is satisfied. It is shown that the large heat capacity of the concrete floor alleviates undesired temperature fluctuations. Therefore, incorporating it as an efficient heat buffer is a viable remedy for smart grid temporary imbalances.

1 Introduction

Unprecedented advances in communication technologies have created vision for large scale and very complex interconnected systems. It has also heated the control community in many aspects. Smart Grid, with a large number of electrical power producers and consumers of various types is a state of the art example of such gigantic systems. It is an Intelligent power system that can integrate all connected users' behavior and actions, all those that produce electricity, those who consume electricity, and those who do both, to effectively deliver a sustainable, economical and safe energy [1].

The presence of so many producers and consumers in interconnected sectors makes them prone to power imbalances. At the same time, it provides a chance to compensate irregularities by modifying individual power requirements of some consumers which can use power in a flexible pattern.

Electrically driven domestic heating systems form a class of such smart grid loads. Here, we are specifically interested in geothermal heat pumps which act like refrigerators in reverse and can generate up to 3-4 kWh of heat from 1 kWh of electricity. They transfer heat energy from the underground soil to residential buildings via a network of pipes. See Fig. 12.1. There are typically two hydronic and one refrigerant circuits interconnected through two heat exchangers. These are: 1) the underground buried brine-filled – mixture of water and anti-freeze – pipes with a small circulating pump; 2) the refrigerant-filled circuit, equipped with an expansion valve and driven by a compressor which is called heat pump; and 3) the indoor under-surface grid of pipes with another small circulating pump which distributes heat to the concrete floor of the building.

The underground temperature is fairly constant during several days and slowly varies with an annual pattern. This is due to the huge heat capacity of the ground. The heat is transferred from this heat buffer to the surface, into floor concrete, when needed. Why not using the same idea in a system that has a different time scale? The concrete floor could be used as a huge electrical energy buffer, to be stored in form of heat, when there is a power excess in the grid. On the contrary, when there is a power shortage, no or a little power should be drawn from the grid into the heating system. This can also be embedded in electricity pricing policies.

From residents perspective, they can avoid high electricity bills by deferring their daily power consumption. According to [1], approximately half of the economic potential

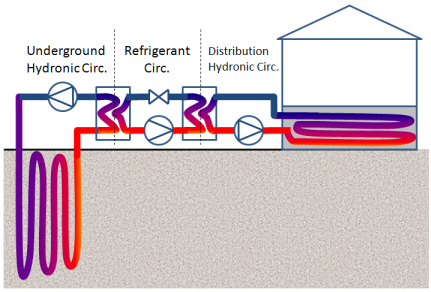

Figure 12.1: Under-floor heating system with a geothermal heat pump

for saving in annual electricity bills, can be achieved by postponing power consumption in each day.

This paper studies another perspective of the problem, i.e. maintaining electrical power balance of the grid. It investigates how much power imbalance could be compensated without sacrificing residents' thermal comfort which is the primary objective of heating systems. The idea of utilizing flexible loads to regain balance in a smart grid is not novel. It is also known that hydro and pumped devices are the most typical type of storage devices which can turn electrical power into heat to be stored in previously installed infrastructure [2]. However, we are going to incorporate concrete floor instead of a hot water reservoir. Moreover, this research is motivated by the fact that heating systems are used almost year around in countries like Denmark and could be thought of as an invariable part of the grid. The potential compensator could be numerous, as many as houses, and distributed geographically. Therefore, it is of importance and value, if the amount of possible compensating action is quantified. This is the task that we have accomplished and verified in this paper via simulations with real parameters.

As the first detailed step, our control strategy for the heating system for a specific apartment is given in Section II. Presentation of the results start in Section III by reconstructing a typical scenario of power setpoint tracking. It is assumed that the power providing company, suggests a setpoint profile for power consumption of the heat pump. This section is concluded by generalizing the sample simulation to the extreme cases to see how much, and for how long, power imbalances can be compensated by employing the above mentioned method. This helps the power providing company to produce a feasible setpoint profile. Section IV concludes the paper by offering a discussion on future works.

2 Strategy of Control

Our case study is a 54 m^2 apartment which consists of three separate heat zones, i.e. rooms, shown in Fig. 12.2.

There are a large number of parameters taken into account in our simulations which we do not mean to list in the main body of the paper. An introduction to the model and the parameter values are given as an appendix instead. It is, though, worth saying that the chosen values for all parameters are in accordance with the typical experimental and standard values.

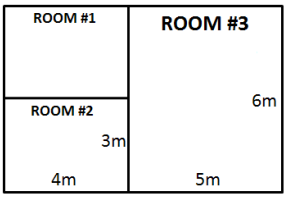

Figure 12.2: Sketch of the apartment with three separate heat zones

Each room in Fig. 12.2 has a separate grid of under-surface floor heating pipes. As a whole, they form the hydronic distribution circuit of the apartment. The flow of heating water in each room is controlled by a valve. The valve opening is adjustable and is controlled by a local PI controller such that the room-specific temperature setpoint is followed in presence of exogenous disturbances.

The circulation pump in the distribution circuit is controlled such that to regulate the differential pressure across all three parallel branches of the rooms' pipe grids. Thus, the flow through each valve only varies by its opening position.

As of the refrigerant circuit, the expansion valve has a built-in mechanical feedback mechanism to marginally prevent flow of condensed refrigerant into the compressor, i.e. the heat pump. The heat pump could be continuously controlled. In one of our recent works [3], we have employed a Model Predictive Controller (MPC) to reduce heat pump's power consumption as much as possible. It is achieved when the *forward temperature* has its minimum allowable value, described as follows. Forward temperature is the temperature of water at inlet of the distribution piping grid; and it should be high enough in order to facilitate room temperature control by local PI controllers without pushing any of the valves into fully-open saturated status, otherwise no actuation capacity is left for compensating exogenous disturbances.

Nonetheless, in this research, we are going to drive the heat pump, by directly exploiting the power consumption setpoint that is prescribed by the power providing company. Therefore, no specific control algorithm is required for the heat pump. The only constraint to satisfy is to restrict the highest permissible forward temperature which is hardly reachable in practice, as well.

In case of power surplus, forward temperature is increased which will eventually result in lessening rooms' valves openings. In order to let heat be stored in the concrete as much as possible, temperature setpoint of the rooms should be increased by a certain amount, defined as *thermal tolerance* (TT) level. TT is user adjustable in the interval TT $\in [TT_{min}, TT_{Max}]$. However, this does not guarantee that the room temperature remains bounded by its original setpoint plus TT.

In case of lack of power, no room temperature setpoint modification is required. The above mentioned strategy is very simple to implement and clearly not optimal in terms of energy efficiency of the individual heating system. However, it facilitates integration of the domestic heating into the power grid control system.

3 Case Study Results

3.1 A simple Scenario

Fig. 12.3 shows a typical power setpoint tracking scenario, with power setpoint profile depicted in the first graph. Initial steady state value of 263 W is associated with forward temperature 36.6°C. The outdoor temperature is assumed to be 0°C. Periods of power excess/shortage are assumed to be one hour long with 30 min power surplus of as 50% much as the initial power, followed by 30 min lack of power of the same amount. Thus, the average power consumption is kept unaltered.

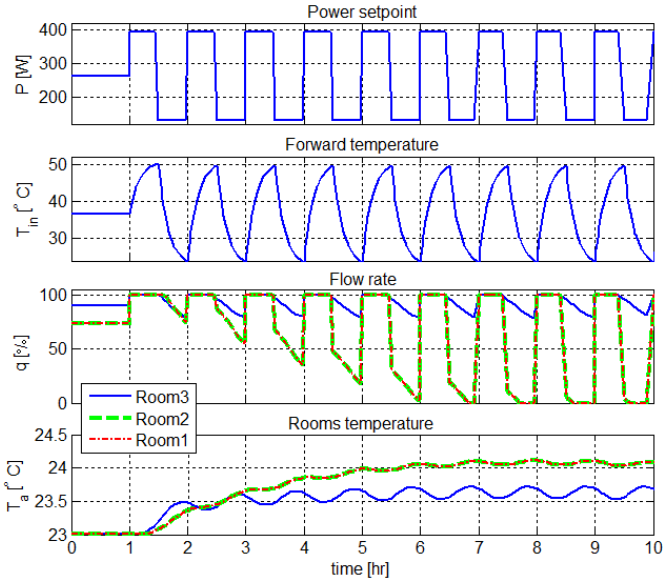

Figure 12.3: A typical power setpoint tracking scenario. 50% power surplus and shortage with duration of half an hour is tolerated by the system, provided that the thermal tolerance level of rooms are set to $+2°C$.

The third graph in Fig. 12.3 shows water flow percentage through distribution pipes of individual rooms. At steady state, control valve of room 3 is at 90% flow capacity to follow the temperature setpoint 23°C, when no exogenous disturbances are present. For rooms 1 and 2, 74% of flow range is adequate to reach the desired temperature. The temperature setpoint is assumed to be equal in all three rooms. At $t = 1$ hr, power consumption of the compressor increases. It takes some time for the forward temperature to rise, but all three valves become fully open instantly due to modification of rooms' temperature setpoints to 25°C, corresponding to a thermal tolerance level of 2°C surplus. Note that the user's desired temperature is still 23°C and this setpoint modification is merely in order to facilitate transfer of heat energy into the concrete floor.

At steady state, after approximately 10 hours, i.e. 10 surplus/shortage intervals, it is shown that the valves of rooms 1 and 2 function like on-off devices, keeping room temperatures about 1°C higher than the original setpoint. Average temperature in room 3

is even closer to the original setpoint, but with more noticeable fluctuations. This behavior strongly depends on PI controllers selected parameters.

This simulation shows that the deviation of rooms' temperature due to a specific power setpoint profile were bounded in the permissible user-defined region. This was the consequence of applying an appropriate power setpoint profile, called *feasible* setpoint profile henceforth, combined with the corresponding suitable choice of thermal tolerance level. The power providing company could establish pricing policies to encourage users to set their thermal tolerance level at high values. Then the company can issue a feasible power setpoint profile pursuant to the user's own choice.

3.2 Generalized Results

The next question to be answered is how to prescribe a feasible power setpoint profile based on each user's thermal tolerance level. Fig. 12.4 shows a chart that can be used to predict what kind of pulses in the power setpoint profile can be accommodated by the heat pump without disrupting resident's thermal comfort, which means:

$$T_{r_i} \in [T_{r_i Ref} \pm TT], \qquad \forall i = 1, 2, 3 \tag{12.1}$$

in which T_r stands for room temperature, and T_{rRef} indicates its setpoint. Index i refers to the room number.

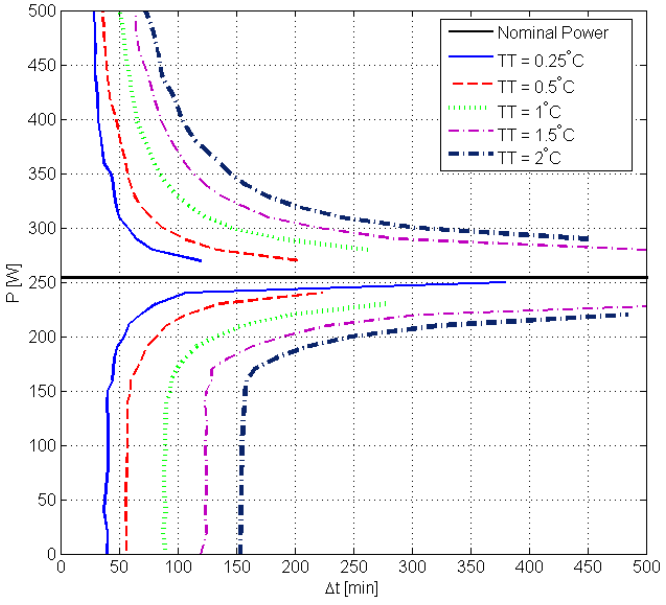

Figure 12.4: Power setpoint generation assistant chart for a 54 m^2 flat, containing several thermal tolerance (TT) levels

As an example, Fig. 12.4 shows that a power surplus pulse with an amplitude of 350 W and a duration of 1 hour can be marginally accommodated by the heat storage of a 54 m^2 flat, if the temperature tolerance is set to 0.5°C. If either the amplitude or the duration

is less, the excess of electrical power can be stored as heat without any difficulty. It is worth saying that the given chart in Fig. 12.4 is dependent on the following parameters:

- Ambient temperature which is assumed to be 0°C
- Local PI controller parameters

Moreover, when a different temperature setpoint is chosen for each room, the nominal heat pump power would be different, i.e. different from 263 W in this case. Thus, the chart should be shifted along the Y-axis accordingly.

4 Disscusion and Future Works

This paper serves as a proof of concept. The most common power imbalance pulses in power systems last for less than half an hour, and are as large as $\pm 50\%$ nominal value. Our results show that, these imbalances can be well accommodated even by a small 54 m^2 apartment with a tightly selected thermal comfort level of 0.25°C in a mild cold weather with a commonplace desired indoor temperature.

Throughout the paper, we have assumed that the power setpoint profile is provided by the power grid at any time instant. This assumption requires a tremendous amount of information to be transferred by the power providing company to all users. A more practical approach is to consider an intermittent communication between the grid controller and the user at equal time intervals. At the beginning of each interval, the grid controller send a message asking the user to try to increase/decrease its power consumption by $\pm\Delta P$. As a result, the burden of computing power setpoint profile is put on heat pump control system which its design is not trivial anymore. An ongoing optimizing mechanism should be exploited which suggests a MPC design. The MPC controller objective is to define the power setpoint in order to satisfy demands of the grid control system, subject to several constraints, which are: 1) avoid valve saturation when the room temperature is not higher than its setpoint; 2) avoid too high forward temperature in order to keep the heating system from damage; and 3) maintain the room temperature in the interval defined by (12.1) . It is worth saying that, the demand of the power providing company may not be completely satisfied due to probable conflicts with the above constraints.

Design of such a MPC controller makes use of the chart in Fig. 12.4 and is amongst our recent future works.

References

[1] S. K. Jensen, "Potentials and opportunities for flexible electricity consumption with special focus on individual heat pumps," EnergiNet, Fredericia, Denmark, Tech. Rep., 31 January 2011.

[2] K. Moslehi and R. Kumar, "A reliability perspective of the smart grid," *IEEE Transactions on Smart Grid*, vol. 1, no. 1, pp. 57–64, June 2010.

[3] F. Tahersima, J. Stoustrup, and H. Rasmussen, "Optimal power consumption in a central heating system with geothermal heat pump," in *IFAC World Congress*, Milano, Italy, August 2011.

[4] G. Hudson and C. P. Underwood, "A simple building modeling procedure for matlab/simulink," *Proc. of Building Simulation*, vol. 99, no. 2, pp. 777–783, 1999.

[5] ASHRAE, *ASHRAE Handbook 1990, fundamentals*. Atlanta: ASHRAE Inc., 1990.

[6] L. H. Hansen, "Stochastic modeling of central heating systems," Ph.D. dissertation, Technical University of Denmark, Dep. of Mathematical Modeling, Denmark, 1997.

[7] S. Y. Hu, R. E. Hayes, and R. K. Wood, "Simulation of the dynamic behavior of a hydronic floor heating system," *Heat Recovery & CHP*, vol. 15, no. 6, pp. 505–519, 1995.

This amendment is devoted to modeling details of the components and subsystems which are employed in our simulations. All of the used symbols and subscripts henceforth, are listed in table .1.

Table .1: Symbols and Subscripts

Nomenclature	
A	surface area (m^2)
C	thermal capacitance $(J/kg\,^\circ\mathrm{C})$
K	equivalent heat transfer coefficient of pipes and concrete
P_c	consumed power by compressor
P_t	transferred power to the house
Q	heat (W)
q	water flow rate in floor heating (kg/sec)
T	temperature $(^\circ\mathrm{C})$
U	thermal transmittance $(W/m^2\,^\circ\mathrm{C})$
τ	time constant
Subscripts	
amb	ambient
e	envelop
f	floor (with 1 and 2 indices corresponding to the first and second layer of concrete floor)
FH	floor heating
i	room number
in	forward water into floor heating system
n	n^{th} lump section of the floor heating pipe
out	return water from floor heating system
r	room
ref	reference
w	water

0.1 Zone Model

Energy balance equations of each single room are derived based on the analogy between thermal systems and electrical circuits mainly based on [4]. Fig. .5 shows a schematic

view of the room with its analogous electrical circuit. Energy balance equations at the envelop, floor, and air nodes are as follows:

$$
\begin{aligned}
C_e\dot{T}_e &= U_eA_e(T_{amb} - T_e) + U_eA_e(T_r - T_e) \\
C_{f_1}\dot{T}_{f_1} &= U_{f_2}A_f(T_{f_2} - T_{f_1}) + U_{f_1}A_f(T_r - T_{f_1}) \\
C_{f_2}\dot{T}_{f_2} &= U_{f_2}A_f(T_{f_1} - T_{f_2}) + Q_{FH} \\
C_r\dot{T}_r &= U_eA_e(T_e - T_r) + U_{f_1}A_f(T_{f_1} - T_r)
\end{aligned}
\tag{2}
$$

in which T_e represents the envelop temperature, T_{f_1} and T_{f_2} are the concrete floor's first layer and second layer temperatures, respectively; and T_r represents room temperature. Exogenous inputs include ambient temperature T_{amb}, and heat from floor heating Q_{FH}.

Envelops, room air and each layer of concrete floor are assumed to be at uniform temperature, i.e. no temperature gradient is considered in any of them. Heat flux via partition walls between the rooms is neglected, provided that temperature differences among the rooms are not noticeable.

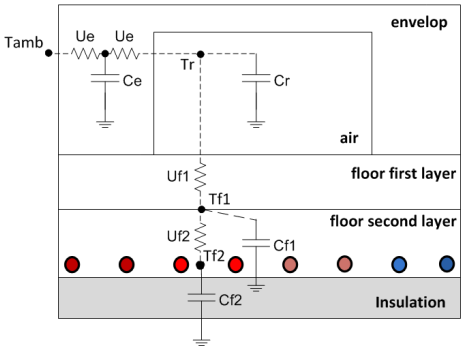

Figure .5: Analogous electrical circuit to the room thermal model

0.2 Hydronic Floor Heating

The considered floor heating has a serpentine piping with the pipes embedded into a heavy concrete as shown in Fig. .5. As a typical assumption, water flow is limited to a specific rate by balancing the total opening of the pipes. To guarantee the highest possible floor heating efficiency, the diameter of the pipes is adjusted at the point of branching from manifold. Since the distribution circulating pump provides a constant differential pressure across the valves, maximum flow rate would be limited by such a balancing task.

Floor heating is modeled as distributed lumped elements governed by:

$$
C_n\dot{T}_n = c_wq(T_{n-1} - T_n) + K_n(T_{f_2} - T_n) \tag{3}
$$

with T_n as the nth section temperature. Distribution of lumped elements are considered to be along the pipe. Heat propagation from the pipes exterior surface is considered to be only upwards toward the floor surface. We have also assumed that heat is transferred between two sections only by mass transport, implying that convective heat transfer is

neglected. Another assumption is that the pipes material and water are at the same temperature. Neglecting the thermal resistance of the pipe, heat transfer coefficient, K would only depend on thermal conductivity of concrete, i.e. $K_n = U_{f_2} A_n$ in which A_n is the effective area of the nth section. U values are selected based on thickness and composition of concrete floor layers, [5].

Heat transferred to the second layer of concrete floor is computed as:

$$Q_{FH} = \sum_{n=1}^{N} K_n (T_n - T_{f_2}) \tag{4}$$

The employed simulation model for floor heating is inspired by a similar radiator model addressed in [6]. The distributed lump model is derived based on the analogy to floor heating, proposed in [7].

0.3 Geothermal Heat Pump

Heat pump is a device which applies external work to extract heat from a cold reservoir and deliver it to a hot reservoir. Three separate fluid circuits are required for a heat pump to retrieve heat energy from heat source and transfer it to the heating system of a house. These circuits are already shown in Fig. 12.1.

Two heat exchangers are exploited in these circuits. Coefficient of performance (COP) is defined for the refrigerant circuit and two adjacent heat exchangers. It indicates the relationship between the amount of produced heat and consumed electricity by the heat pump. COP has a strong positive correlation with differential temperature between the influent brine of the primary heat exchanger and the influent water of the house. Given a constant brine temperature, COP is determined by referring to the manual of the heating system vendor.

Given COP value, the consumed power by the compressor in the refrigerant circuit (primary side) can be described as:

$$P_c = \frac{P_t}{COP} \tag{5}$$

in which P_t is the transferred heat to the secondary side, i.e. house and P_c is the consumed power by the compressor.

Conventional heat pump control takes action based on outdoor temperature. Forward water temperature setpoint is determined based on the ambient temperature, which can be regarded as a feedforward control approach. A PI controller adjusts the absorbed power by the compressor in order to maintain the target forward temperature. Normally, it takes a few minutes for the heat pump to reach the new forward temperature.

In the present study, however, compressor is driven by the power setpoint profile provided by the power company. Hence, to find the forward temperature corresponding to a specific P_c we have utilized (5). Both P_t and COP are functions of the forward temperature T_{in}. P_t can be described as energy loss of the building:

$$P_t = c_w q (T_{in} - T_{out}) \tag{6}$$

with T_{out} as return water temperature. In an efficiently balanced floor heating system, as implied before, the return temperature would always be 1 to 2°C higher than room

temperature. Hence, it can be regarded as constant being at a specific room temperature, i.e. 23°C in simulations. In this case $T_{out} = 25°C$.

COP of a specific heat pump is borrowed from the manufacturer's datasheet and is shown as data points in Fig. .6.

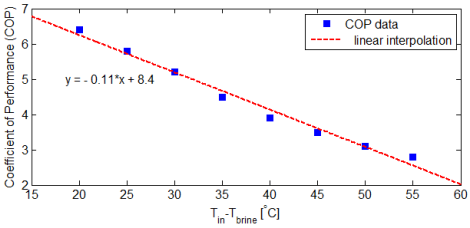

Figure .6: COP against temperature difference between forward and brine water

An interpolating line is fitted to the points. The linear approximation is used to find T_{in} corresponding to the compressor consumed power. Therefore, (5) turnes into:

$$P_c = \frac{c_w q(T_{in} - T_{out})}{aT_{in} + b} \tag{7}$$

with a and b as constants of the approximated affine map in Fig. .6. At a specific T_{out} and P_c, forward temperature can be found with no difficulty based on (7). Calling this temperature T_{inRef}, it takes a few minutes for the heat pump to transfer heat to the secondary side and maintain this temperature:

$$\frac{T_{in}}{T_{inRef}}(s) \quad = \quad \frac{1}{1 + \tau s} \tag{8}$$

To summarize this section:

- room dynamics, i.e. the dynamics between room temperature and temperature of the envelop, ambient, and floor, are governed by (2)
- floor heating dynamics, i.e. the dynamics between concrete temperature and forward temperature, are governed by (3)
- heat pump dynamics, i.e. the dynamics between forward temperature and consumed electrical power, are governed by (7) and (8). Note that, (7) is used to find T_{inRef}.

Paper G

Economic COP Optimization of a Heat Pump with Hierarchical Model Predictive Control

Fatemeh Tahersima, Jakob Stoustrup, Henrik Rasmussen, Soroush A. Meybodi

This paper is accepted for publication in:
IEEE Conference in Decision and Control, CDC, December 2012, Maui, Hawaii, US

Abstract

A low-temperature heating system is studied in this paper. It consists of hydronic under-floor heating pipes and an air/ground source heat pump. The heat pump in such a setup is conventionally controlled only by feed-forwarding the ambient temperature. Having shown >10% cut-down on electricity bills by involving feedback control in a previous study, this paper has continued the same line of argument and has investigated effects of *a priori* knowledge on weather forecast and electricity price profile to alleviate the total electricity cost subject to constraints on resident's thermal comfort. A two level hierarchical control structure is chosen for this purpose. While local PI controllers at the bottom level maintain individual temperature set-points of the rooms, a model predictive controller at the top level minimizes water supply temperature, and hence maximizes the heat pump's coefficient of performance. At the same time, it determines the actual temperature set-points of the rooms by deviating from the user-defined set-points within a thermal tolerance zone. Simulations results confirm significant cut-down on electricity bills without sacrificing resident thermal comfort. The proposed control strategy is a leap forward towards balanced load control in Smart Grids where individual heat pumps in detached houses contribute to preserve load balance through intelligent electricity pricing policies.

1 Introduction

Low-temperature heating systems with renewable energy sources have become more popular due to growing public attention to the environmental issues. Hydronic under-floor heating system is an example of such systems which offers a profitable heating solution in suburban areas by utilizing a ground/air-source heat pump. A heat pump acts like a refrigerator and transfers heat from a colder medium, e.g. ambient air, shallow ground or water to the building which is at a higher temperature. An electrically driven heat pump can generate 3-4 kWh of heat from 1 kWh of electricity for driving the heat pump's compressor. A geothermal heat pump system is shown in Fig. A.1. There are typically two hydronic and one refrigerant circuits interconnected through two heat exchangers. These are: 1) the underground buried brine-filled – mixture of water and anti-freeze – pipes with a small circulating pump; 2) the refrigerant-filled circuit, equipped with an expansion valve and driven by a compressor which is called heat pump; and 3) the indoor under-surface grid of pipes with another small circulating pump which distributes heat to the concrete floor of the building.

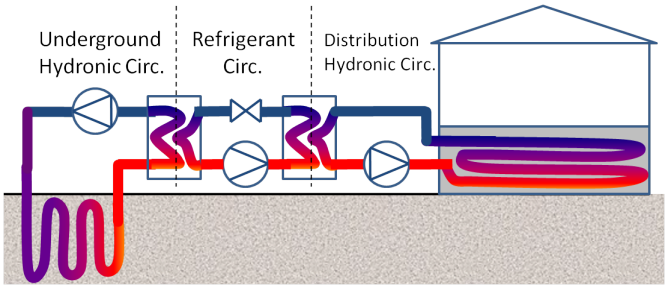

Figure A.1: An under-floor heating system with a geothermal heat pump

The underground temperature is fairly constant during several days and slowly varies with an annual pattern. This slow dynamic is due to the huge capacity of the ground and is an advantage to the air-source heat pump with the brine pipes exposed to the ambient air. The higher temperature at the evaporator side of the refrigerant circuit potentially increases the heat pump's Coefficient of Performance (COP) in the cold season. It is also an advantage in the warm season when heat pump works in reverse to cool down the building; because underground temperature is cooler than the ambient air in summer. Therefore, we specifically focus on geothermal heat pumps and assume a constant brine temperature.

Most commercial control solutions for heat pumps are based on feed-forwarding the ambient temperature. The forward temperature of water in the distribution hydronic circuit is adjusted based on *a priori* known adjustment curves. This method is further explained in one of our recent works [1]. In that paper, we investigated feedback control of heat pumps based on specific heat demands of individual houses. Effects of calculating the minimum heat demand of a building that handles all system constraints systematically were studied using a model predictive controller (MPC). It turned out that approximately 13% saving can be achieved in electricity consumption compared to pure feed-forward control.

Feedback control for a similar heating/cooling system is investigated in several other references too. Reference [2] conducts a comparison study among proportional (P), P-integral (PI), PI-derivative (PID) and relay controllers with a fixed control strategy. The approach is to lock the floor heating valve at fully-open position and control the forward temperature based on feedback from the room temperature. This method is practically efficient for a single-temperature zone. Multiple-temperature zones with different heat demands in a residential/office building can not be controlled by this control scheme. Reference [3] presents an MPC controller for both cooling and heating purposes. It focuses on a distributed model predictive control (DMPC) where different zones are controlled by semi-separated MPCs that only communicate their temperature setpoints with the adjacent zones. In another approach [4], the main simplifying assumption is to choose a constant COP for the heat pump. However, the amount of electricity saving by controlling a heat pumps' varying COP is considerable and should not be neglected at all.

This paper presents an integrated framework for COP and cost optimization of the specified hydronic heating system. We optimized COP by minimizing the supply temperature and shifting power consumption according to variations of the ambient temperature. The principal idea for this optimization method is developed in our previous work [1]. Optimization of electricity price is also feasible by load shifting, [5]. This is maintained by incorporating the concrete floor as a heat reservoir to store heat. By deferring daily power consumption from price-peak times to off-peak periods, residents can cut down electricity bills. According to [6], approximately half of the economic potential for saving in annual electricity bills, can be achieved by postponing power consumption in each day for a couple of hours.

The rest of this paper is structured as follows. As the first detailed step, our control strategy for the heating system of a specific apartment is given in Section II. Section III presents problem formulation by describing the plant model and introducing an optimization problem. The optimization problem is tackled by the control strategy and the results are presented in Section IV. Section V concludes the paper by offering a discussion on results and a road map to future works.

2 Control System Structure

Our case study is a 54 m^2 apartment which consists of three separate heat zones, i.e. rooms, shown in Fig. A.2.

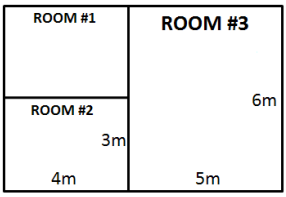

Figure A.2: Sketch of the apartment with three separate heat zones

Each room in Fig. A.2 has a separate grid of under-surface floor heating pipes. As a whole, they form the hydronic distribution circuit of the apartment. The flow of heating water in each room is controlled by a valve. Valve openings are adjustable and are controlled by local PI controllers such that room-specific temperature setpoints are followed in presence of exogenous disturbances.

The circulation pump in the distribution circuit is controlled to regulate the differential pressure across all three parallel branches of the rooms' pipe grids. Thus, the flow through each valve is assumed to be only dependent on its opening percentage.

As of the refrigerant circuit, the expansion valve has a built-in mechanical feedback mechanism to marginally prevent flow of condensed refrigerant into the compressor, i.e. the heat pump. The heat pump could be continuously controlled. In [1], we have employed a Model Predictive Controller (MPC) to reduce heat pump's power consumption as much as possible. This goal was achieved by minimizing the *forward temperature*. Forward temperature is the temperature of water at inlet of the distribution piping grid; and it should be high enough in order to facilitate room temperature control by local PI controllers without driving any of the room valves into the fully-open saturated status, otherwise no actuation capacity is left for compensating exogenous disturbances that may hit the system at any time.

In the aforementioned paper, however, we did not consider the influence of a priori known disturbances like the ambient temperature and electricity price. Knowledge about the ambient temperature in advance could help to improve thermal comfort and result in a higher daily COP. A higher COP means less electricity consumption and a cut down in energy costs. The control strategy which lead us toward this objective is deferring heat load from nighttime to daytime. We can store heat in the concrete floor during day when the demanded forward temperature is lower than in night, or in the other words, COP is higher. The buffered heat can then be used in night time when COP is normally higher.

A priori knowledge about price of electricity could be provided by the grid utility 24 hours in advance. Two types of electricity tariffs are considered: daily and hourly prices. Deferring the load can be well accommodated by daily price variations, however hourly variations do not influence the pattern of daily load shifting. The concrete floor, as a low-pass filter, can be cooperated to diminish the influence of slow disturbances. A similar control strategy is envisioned for this purpose like the one employed in [5]. The difference with the latter study, however, is that the grid utility provides users with

the electricity price profile instead of a power setpoint for the heat pump. Besides, we proposed a MPC in order to systematically reduce daily energy prices of the heating, by including future disturbances in the optimization process.

MPC can systematically incorporate forecast data of weather and price along with other system constraints in the optimization procedure. Besides constraint handling, MPC gives systematic feedforward design based on future demands [7]. Therefore, we designed a MPC in the top level of control hierarchy to orchestrate functioning of local controller units at the lower level.

The closed loop hierarchical control system is shown in Fig. A.3. There are as many internal loops as the number of rooms and an outer loop with a multiplexer and a MPC. In the inner loops, each PI regulates a specific room's temperature to the setpoint value received from the MPC. In the outer loop, the room with highest heat demand is selected. The MPC controller then minimizes the supply temperature based on the dynamics of that room.

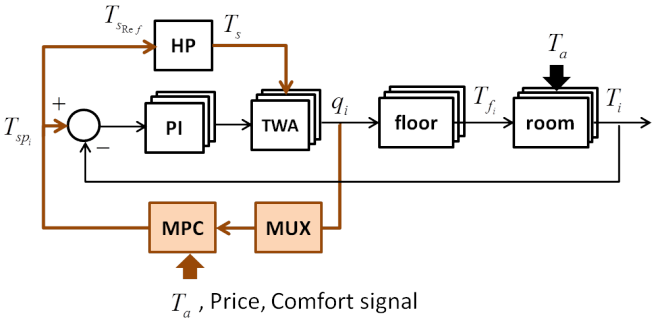

Figure A.3: Block diagram of the closed loop system consisting of three individual rooms with under-floor heating pipes. Temperature of the rooms are controlled by local PI controllers which give signal to the Thermal Wax Actuators (TWA) to adjust the flow rate. The MPC controller specifies temperature setpoints of supply, $T_{s_{Ref}}$, and each room, T_{sp}, based on the actual heat demand of individual rooms.

In the real case, a PI's signal to a thermal wax actuator (TWA) is a two-level Pulse Width Modulation (PWM) signal which is translated into a continuous signal in simulations. Thus, the corresponding control signal determines the valves opening percentage.

3 Problem Formulation and Method

3.1 Plant Model

This section gives an introduction to the model of the plant and control model that is used in simulations. A description of all symbols, subscripts and parameter values are given later in table A.1. The chosen values for all parameters are in accordance with experimental data. Some experiments have been conducted on a low-energy building in Copenhagen for the purpose of model verification and testing designated control solutions.

The state space equations which govern a single room's dynamics are derived based on the analogy between thermal systems and electrical circuits [8]. The energy balance

equations based on three main thermal masses: air, concrete floor, and water are as follows:

$$\begin{aligned} C_i\dot{T}_i &= B_a(T_a - T_i) + B_{ij}(T_j - T_i) + B_{if}(T_{f_i} - T_i) \\ C_{f_i}\dot{T}_{f_i} &= B_{if}(T_i - T_{f_i}) + B_{fw}(T_{w_i} - T_{f_i}) \\ C_{w_i}\dot{T}_{w_i} &= B_{fw}(T_{f_i} - T_{w_i}) + c_w q_i(T_s - T_{f_i}) \end{aligned} \tag{A.1}$$

in which i and j are indices of two adjacent rooms, $i, j \in \{1, 2, 3\}$. B represents the equivalent convection/conduction heat transfer coefficient between two connected nodes. For instance, B_{fw} is the conduction heat transfer coefficient between the concrete layer and floor heating pipes that are at temperature T_w. The third equation which models heat flow to the concrete floor through a network of pipes is the simplified version of a more accurate simulation model which is presented in [5].

The local PI controller for the i^{th} room in state space form is:

$$\begin{aligned} \dot{\xi} &= \frac{K_p}{T_{int}}(T_{sp_i} - T_i) \\ q_i &= K_p(T_{sp_i} - T_i) + \xi \end{aligned} \tag{A.2}$$

with ξ as the auxiliary state. The parameters of the PI controller are chosen based on the plant step response around the desired operating point which is $q = 90\%q_{max}$. The choice of the operating point is originated from the fact that water supply temperature should be high enough not to drive floor heating valves to the fully open position.

The heat pump dynamics is much faster than the fastest dynamic in the building. Therefore, we consider it as a static gain. Relation between the transferred heat from the condenser to water in the distribution circuit, Q_c, and the heat pump's electrical work, W_c, is given by:

$$W_c = \frac{Q_c}{\eta_{cop}} \tag{A.3}$$

with η_{COP} representing the coefficient of performance. This term depends on the temperature difference between the evaporator i.e. brine water temperature, and the condenser i.e. floor heating supply temperature. COP as a manufacturer parameter is usually documented in the heat pump data sheet. We have used a COP curve, see Fig. A.4 based on the statistical data given in [9]. The aforementioned models comprise the plant's simulation model.

Assuming a geothermal heat pump with deeply buried pipes in brine side, the brine temperature is assumed to be constant during heating season. Presuming $T_{brine} = 5\,^{\circ}\mathrm{C}$, $\eta_{cop}(T_s)$ is formulated by interpolation in the following:

$$\eta_{cop} = 0.0021T_s^2 - 0.35T_s + 16.7 \tag{A.4}$$

The prediction model for MPC controller can be formulated as a linear time invariant system in spite of a bilinear term in the last row of A.1. In the vicinity of the desired operating point which is $q = 0.9q_{max}$, the bilinear term can be linearized. Hence the internal model of the MPC controller can be written in a state space form as:

$$\begin{aligned} \dot{x} &= Ax + B_u u + B_d d \\ y &= Cx + D_u u + D_d d \end{aligned} \tag{A.5}$$

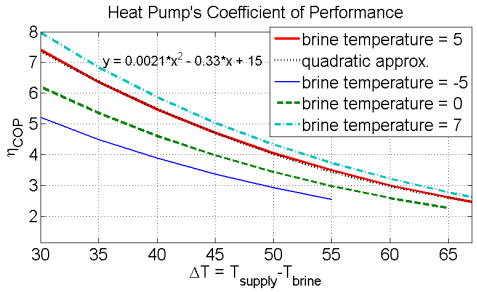

Figure A.4: Statistical data showing the relation between $T_s - T_{brine}$ and the heat pump's COP. x represents the temperature lift, $T_s - T_{brine}$.

with $x = [T_i, T_{f_i}, T_{w_i}, \xi]^T$, $u = [T_s, T_{sp_i}]^T$, $y = [T_i, q_i]^T$, and $d = T_a$. Matrices A, B, C and D are derived based on (A.1) and (A.2). Room temperatures are measured and the flow rate is estimated by knowing the valve opening degree and the differential pressure across the valve. The other state variables, ξ, T_{w_i} and T_{f_i} are estimated using a Kalman state observer. The above model is discretized using a sampling time, t_s which is chosen based on the fastest dynamic of the system.

3.2 The Optimization Problem

The main objective is to minimize power consumption and the corresponding energy price. Power consumption, as mentioned earlier in A.3, is:

$$W_c = \frac{c_w q(T_s - T_f)}{-aT_s^2 + bT_s + c} \tag{A.6}$$

with a, b and c defined in (A.4). W_c is positively correlated with supply temperature T_s for a constant transferred heat to the building. In the above equation, lessening T_s does not change the numerator because the mass flow rate will be increased in return. Denominator will increase as T_s decreases (the quadratic approximation function is negative definite until $T_s < 83.5$) which consequently leads to reduction of W_c. Therefore, the optimization problem with discretized model (A.5) is formulated as:

$$\begin{aligned} \min_{T_s, T_{sp_i}} & \sum_{k=1}^{N} c_s(k) T_s(k) + |T_i(k) - T_{cmf_i}(k)| \\ s.t.\ & x(k+1) = Ax(k) + B_u u(k) + B_d d(k) \\ & y(k) = Cx(k) + D_d d(k) \\ & 0 \le q_i(k) \le 0.9 q_{max} \\ & T_{s,min} \le T_s(k) \le T_{s,max} \\ & -TT \le T_{sp_i}(k) - T_{cmf_i}(k) \le TT \end{aligned} \tag{A.7}$$

The prediction model is selected according to the dynamics of the room with the highest heat demand. N is the prediction horizon. In the cost functional, the weight $c_s(k)$ represents electricity price and $T_{cmf_i}(k)$ stands for user-defined temperature setpoint,

both of them at time instant k. T_{sp_i} is the manipulated variable that must be bounded within comfort levels defined by the user. TT stands for *Thermal Tolerance*. We also considered constraints on the manipulated variables rate of change which is not indicated in the above formulation. Supply temperature variations rate is limited to $1\,^{\circ}\mathrm{C}$ and the setpoint temperature modification rate is limited by $0.1\,^{\circ}\mathrm{C}$, both per sample time t_s.

4 Simulation Results

We have selected discretization sampling rate of the system equal to the MPC sample time, $t_s = 6min$ which is chosen based on the operation time of the TWAs, i.e. less than $5min$.

4.1 Weather Forecast Data

This section investigates the improvement achieved for COP optimization by exploiting weather forecast data. Recorded weather data was provided by the Danish Meteorological Institute (DMI) for 12 days from January 20 to 31, 2012. In the simulations where weather forecast is involved, we assumed that a perfect forecast was available 6 hours in advance. The coefficient $c_s(k)$ and the Thermal Tolerance level (TT) in (A.7) are zero indicating that price of energy does not influence the optimization. Also, T_{sp_i} is not a control input in this simulation scenario, but it is equivalent to the user specified comfort temperature, T_{comf_i}.

The simulation results for the three-room apartment is shown in Fig. A.5. However, only the room with the highest heat demand at each time instant affects the results. In other words, the graph is associated with only one room.

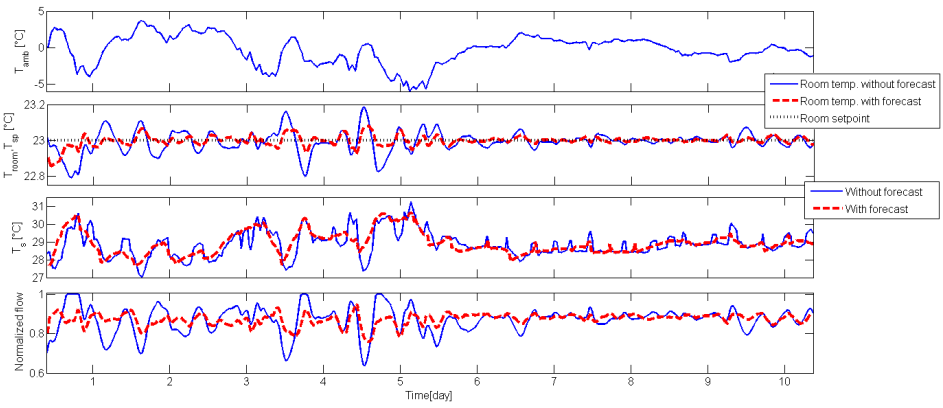

Figure A.5: Simulation results with and without accurate weather forecast data

Both comfort and energy costs are improved compared to the case without weather forecast data. In order to quantify comfort improvement, the variance of error in both cases are compared using (A.8). ΔT is the evaluation time horizon over which the vari-

ance is integrated.

$$\sigma = \int_{\Delta T} \frac{|T_i(t) - T_{cmf_i}(t)|}{\Delta T}\, dt \tag{A.8}$$

It turned out that in case of employing weather forecast, the variance of error was approximately 0.018, while it was around 0.04 when no forecast data was available. Thus, the comfort level is improved by almost 55%.

In order to evaluate the effect of weather forecast on the average COP values, we calculated the average COP over 10 days using (A.4). The average COP with and without weather forecast data is 7.24 and 7.25, respectively. The COP is degraded around 0.17% compared to the situation without weather forecast involvement. This does not convey any meaningful outcome in regard to power savings. In the contrary, it confirms that despite having a significant positive influence on thermal comfort, weather forecast have a minor negative impact on the total energy consumption cost. The effect of weather forecast was diminishing fluctuations in the water temperature, therefore the average water temperature in both simulation scenarios is quite the same which means weather forecast does not change or improve COP, nor the energy consumption cost.

4.2 Price Profile

To satisfy monetary interests of end users, another mechanism is devised in this section to directly affect electricity consumption based on the instantaneous price of electrical power. In this method a list of provisional price values for the coming 24 hours is communicated through the power grid by the power utility provider. Such a price profile is designed in a way to encourage less consumption during peak hours by assigning a higher price. However, the task of the MPC controller at the end user is not to reduce the overall consumption which adversely affects user comfort. Instead, its job is to force the heat pump to consume energy when it is cheap and deprive it of energy consumption when the price is high.

To fulfill its job, the MPC modifies the setpoint of each zone according to the energy price in order to shift the heat demand from peak hours to off-peak periods, based on (A.7). Fig. A.6 illustrates how it becomes possible to decrease the consumption cost with the same average water temperature and not sacrificing thermal comfort of residents. It shows that the average water temperature is even increased 2.2% in average compared to the scenario when energy is minimized not the energy cost. COP is also increased 1.2% which is due to the increased average water temperature. However, the cost of electricity consumption is reduced by 10% in average which is subject to the Elspot price variations shown in Fig.A.6. Higher fluctuations of the electricity price would lead to much more cost benefits.

Increase of the average water temperature and by this mean reduction of COP is due to the fact that load shifting for the purpose of cost minimization might not be in the same direction as the energy efficiency. More clearly, the two objectives could be in contradiction depending on the periodic signal of price. From the energy perspective, it is more efficient to shift the load from night to daytime when COP is usually higher. However, electricity price is normally higher in daytime due to peak load. Therefore it is more economic to consume in night time than during the day. This contradiction has led

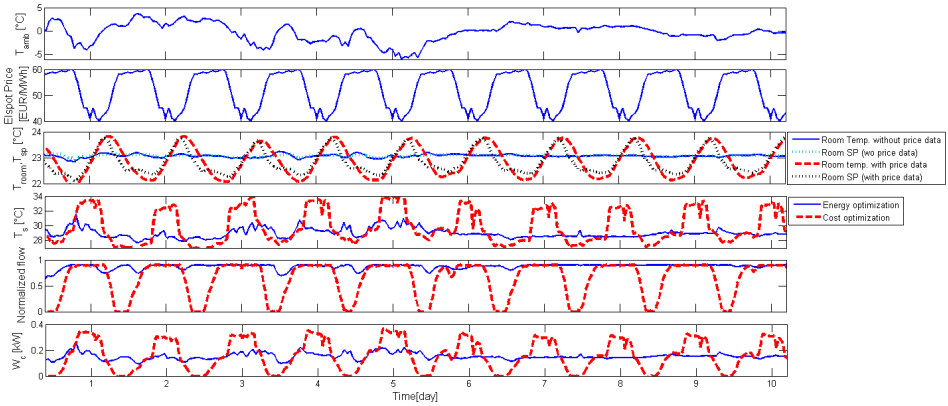

Figure A.6: Simulation results with and without price profile data

to a deficit in the system energy efficiency, but to a lower energy cost which is the final target of the optimization problem.

Starting in the steady state, when the price goes down, the actual temperature setpoint in the building increases. Therefore, the valves tend to become fully open. The local PI controllers interpret this situation as saturation and impaired regulation. However, in reality the building is intentionally getting warmer than what the user had desired in order to store energy for the next peak period. On the other hand, when the price goes up, the actual temperature setpoint in the building decreases. This will result in tightening of the valves on floor heating pipes and preventing expensive power consumption. Deviating from the user-defined setpoint is of course already permitted and approved by the user through adjustment of the thermal tolerance level.

It should also be noted that the constraint on flow may not be replaced with an additional term in the objective function in (A.7). The reason is that the free move of floor heating valves in a permissible interval is essential if the combination of local PI controllers and the MPC controllers should be able to function properly. It is not consistent design if the top level MPC directly regulates both the setpoint and the control signal of PI controllers. At least, one should be free and we have chosen to let PI controllers have complete control on their actuators. This is a consistent hierarchical design.

In summary, it can be stated that the main contribution of the paper is to formulate objectives and constraints in the optimization problem in (A.7) such that a consistent hierarchical structure is created.

5 Conclusion

In this paper we studied the effects of: 1) weather forecast data, 2) electricity price profile, and 3) the indirectly found heat demand, on control of a heat pump. This was done by employing a two level control system structure. The lower level consisted of local PI controllers which were used to regulate temperature setpoints of individual heat zones in a building. The size of the control signal in each of the heat zones was interpreted as an indication of the heat demand in that zone and was taken into account as the basis for

selection of the zone with the highest heat demand. Afterwards, the weather forecast data and electricity price profile were involved in an optimization problem by the top level MPC controller. An interesting result was that a priori knowledge on weather conditions proved to have negligible effects on saving money despite its significant role in improving user's comfort and improving temperature regulation capability of the control system. On the contrary, a priori knowledge on electricity price profile turned out to have a vast potential for providing monetary savings in electricity bills. At the end, it is the user who adjusts his desired thermal tolerance, and hence determines the constraints that must be satisfied by the control system. It is a deal between end users and the power utility company. Should the company send out inexpensive bills, it requires to affect control of users' heat pumps via their pricing policies.

References

[1] F. Tahersima, J. Stoustrup, and H. Rasmussen, "Optimal power consumption in a central heating system with geothermal heat pump," in *IFAC World Congress*, Milano, Italy, August 2011.

[2] Z. Yang, G. Pedersen, L. Larsen, and H. Thybo, "Modeling and control of indoor climate using a heat pump based floor heating system," in *IECON 2007 - 33rd Annual Conference of the IEEE Industrial Electronics Society*, 2007, pp. 2985–2990.

[3] V. Chandan, S. Mishra, and A. G. Alleyne, "Predictive control of complex hydronic systems," in *American Control Conference*, Baltimore, MD, USA, June 2010.

[4] R. Halvgaard, N. K. Poulsen, H. Madsen, and J. B. Jrgensen, "Economic model predictive control for building climate control in smart grid," in *IEEE PES Conference on Innovative Smart Grid Technologies*, Washington, USA, June 2012.

[5] F. Tahersima, J. Stoustrup, S. A. Meybodi, and H. Rasmussen, "Contribution of domestic heating system to smart grid control," in *Conference on Decision and Control*, Orlando, FL, USA, December 2011.

[6] S. K. Jensen, "Potentials and opportunities for flexible electricity consumption with special focus on individual heat pumps," EnergiNet, Fredericia, Denmark, Tech. Rep., 31 January 2011.

[7] J. A. Rossiter, *Model-Based Predictive Control*. Raton, Florida: CRC Press LLC, 2003.

[8] G. Hudson and C. P. Underwood, "A simple building modeling procedure for matlab/simulink," *Proc. of Building Simulation*, vol. 99, no. 2, pp. 777–783, 1999.

[9] C. Heerup, "Efficiency and temperature correlation (effectivitet og temperatur sammenhng)," Denmark Technological Institute, Energi og Kilima, Gregersensvej, Taastrup, Denmark, Tech. Rep., 2011.

Table A.1: Symbols and Subscripts

Nomenclature	
B	heat transfer coefficient between two nodes in an electric circuit $(kJ/s^{\circ}\mathrm{K})$
B_{if}	heat transfer coefficient between a room air and the layer of concrete floor$(kJ/s^{\circ}\mathrm{K})$
B_{ij}	heat transfer coefficient between two adjacent rooms $(kJ/s^{\circ}\mathrm{K})$
B_{fw}	heat transfer coefficient between influent water and concrete floor $(kJ/s^{\circ}\mathrm{K})$
C	thermal capacitance $(J/kg\,^{\circ}\mathrm{C})$
c_s	electric power price
K_p	proportional gain
Q_c	transferred power to the house
Q	heat (W)
q	water flow rate in floor heating (kg/sec)
q_{max}	maximum water flow rate in floor heating pipes (kg/sec)
T	temperature $(^{\circ}\mathrm{C})$
T_{cmf}	comfort temperature set by the user $(^{\circ}\mathrm{C})$
T_{int}	integration time
T_s	supply temperature (also called forward temperature) $(^{\circ}\mathrm{C})$
$T_{s,min}$	minimum supply temperature $(^{\circ}\mathrm{C})$
$T_{s,max}$	maximum supply temperature $(^{\circ}\mathrm{C})$
TT	Thermal Tolerance $(^{\circ}\mathrm{C})$
W_c	consumed power by compressor
ξ	auxiliary state
η_{cop}	coefficient of performance
Subscripts	
a	ambient
cmf	comfort
f	floor (with i index corresponding to the ith room concrete floor)
f_i	floor of the ith room
i, j	room number
k	time instant (s)
s	supply temperature
sp	setpoint
w	water